uOttawa

L'Université canadienne
Canada's university

FACULTÉ DES ÉTUDES SUPÉRIEURES ET POSTOCTORALES

uOttawa

L'Université canadienne
Canada's university

FACULTY OF GRADUATE AND POSDOCTORAL STUDIES

Karim Mekhail

AUTEUR DE LA THÈSE / AUTHOR OF THESIS

Ph.D. (Cellular and Molecular Medicine)

GRADE / DEGREE

Department of Cellular and Molecular Medicine

FACULTÉ, ÉCOLE, DÉPARTEMENT / FACULTY, SCHOOL, DEPARTMENT

H± Driven Remodeling of Molecular Networks by the Nucleolar Architecture

TITRE DE LA THÈSE / TITLE OF THESIS

Stephen Lee

DIRECTEUR (DIRECTRICE) DE LA THÈSE / THESIS SUPERVISOR

CO-DIRECTEUR (CO-DIRECTRICE) DE LA THÈSE / THESIS CO-SUPERVISOR

EXAMINATEURS (EXAMINATRICES) DE LA THÈSE / THESIS EXAMINERS

Jocelyn Côté

Ruth Slack

Douglas Gray

Arnim Pause

Gary W. Slater

Le Doyen de la Faculté des études supérieures et postdoctorales / Dean of the Faculty of Graduate and Postdoctoral Studies

H^+-Driven Remodeling of Molecular Networks by the Nucleolar Architecture

Karim Mekhail

Thesis submitted to the

Faculty of Graduate and Postdoctoral Studies

in partial fulfillment of the requirements for the degree of

Ph.D. in Cellular and Molecular Medicine

Department of Cellular and Molecular Medicine

Faculty of Medicine

University of Ottawa

Your file Votre référence
ISBN: 978-0-494-25887-3
Our file Notre référence
ISBN: 978-0-494-25887-3

Abstract

Acidosis protects cells facing low oxygen tension (hypoxia) in various physiological and pathological settings that include muscle exercise, tumor development, and ischemic disorders. A central element in the adaptive response to low oxygen tension is HIF (hypoxia-inducible factor), a transcription factor that activates an array of genes implicated in oxygen homeostasis, tumour vascularization and ischemic preconditioning. HIF is activated by hypoxia, but undergoes degradation by the VHL (von Hippel-Lindau) tumour suppressor ubiquitin ligase complex in the presence of oxygen. Here, we uncover a gene-regulatory and energy homeostasis process that relies on the cooperation between acidosis, VHL, and the nucleolus. Cellular sensing of increased environmental hydrogen ion (H^+) concentration, triggered by Pasteur or Warburg hyperglycolytic effects, allows the nucleolar architecture, or more specifically the intergenic spacers (IGS) of rRNA genes (rDNA), to capture and confine VHL to nucleoli by converting the protein from a dynamic to a static state. This phenomenon is reverted following the re-instatement of neutral pH conditions. A protein surface region of VHL was identified as a discrete H^+-responsive nucleolar detention signal. More importantly, nucleolar sequestration of VHL enables HIF to evade destruction in the presence of oxygen and activate its target genes. Strikingly, H^+-dependent trapping of VHL to IGS restricts rDNA transcription limiting ribosomal biogenesis, the most energy-demanding cellular process. rDNA silencing harmonizes ATP demand with limited anaerobic supply to preserve energy equilibrium and viability under hypoxia. These findings reveal that H^+ controls gene expression and cellular energy demand, and provide an explanation for the protective effect of acidosis in ischemic settings such as development, stroke, and cancer.

Table of Contents

List of Figures

List of Tables

List of Abbreviations

AcCoA	acetyl coenzyme-A
ActD	actinomycin D
AP	acidification-permissive media
B23	rRNA processing factor nucleophosmin
BFP	blue fluorescent protein
CBP	cycli-AMP-reponse-element-binding protein (CREB)-binding protein
CAIX	carbonic anhydrase IX
CAC	citric acid cycle
CIHR	Canadian Institutes of Health Research
CMV	cytomegalovirus
CTAD	carboxy-terminal transactivation domain
d	day
DMEM	Dubelcco's modified Eagle's medium
DNHIF	dominant negative hypoxia-inducible factor
DNVHL	dominant negative VHL
6-DOG	6-deoxyglucose
E3	ubiquitin ligase
EGFR	epidermal growth factor receptor
ETC	electron transfer chain
ETS	external transcribed spacer
EPO	erythropoietin
$FADH_2$	reduced flavin adenine dinucleotide

FBS	fetal bovine serum
FCs	nucleolar fibrillar centers
FDA	fluorescein diacetate
FIB	rRNA processing factor fibrillarin
FLIP	fluorescence loss in photobleaching
GFP	green fluorescent protein
Glut-1	glucose transporter 1
GTP	guanosine triphosphate
h	hour
H^+	hydogen ions
H1	histone H1
H2	histone H2
H3	histone H3
H4	histone H4
HECT	homologous to E6-AP carboxyl terminus ubiquitin ligase
HIF	hypoxia-inducible factor
HIV-1	human immunodeficiency virus 1
HRE	hypoxia-response element
HRP	horse radish peroxidase
IAP	inhibitors of apoptosis
iFRAP	inverse fluorescence recovery after photobleaching
IGS	intergenic spacer
ITS	internal transcribed spacer

La^-	lactate
La^-H^+	lactic acid
LOH	loss of heterozygosity
MDM2	murine double minute protein
min	minute or minutes
mRNA	messenger RNA
NAD^+	nicotinamide adenine dinucleotide
NCIC	National Cancer Institute of Canada
NES	nuclear export signal
NLS	nuclear localization signal
$NoDS^{H+}$	$[H^+]$-regulated nucleolar detention signal
NoLS	nucleolar localization signal
NoRS	nucleolar retention signal
NSERC	Natural Sciences and Engineering Research Council of Canada
NTAD	amino-terminal transactivation domain
ODDD	Oxygen-dependent degradation domain
OH	hydroxyl
PBS	phosphate buffer saline
PCR	polymerase chain reaction
PDH	pyruvate dehydrogenase
PDK-1	pyruvate dehydrogenase kinase 1
PEG	polyethylene glycol
pH	extracellular concentration of hydrogen ions

PI	propidium iodide
PHD	prolyl hydroxylase
Pre-rRNA	precursor for messenger RNA of rDNA
RCC	clear cell renal cell carcinoma
rDNA	ribosomal RNA genes
RRE	REV response element
rRNA	ribosomal RNA
RS	ribosomal stress
ROS	reactive oxygen species
RT	room temperature
RT-PCR	reverse transcriptase polymerase chain reaction
SD	standard acidification-blocking media
SDS-PAGE	sodium dodecyl sulphate-polyacrylamide gel electrophoresis
SEM	standard error of the mean
snoRNA	small nucleolar RNA
siRNA	small interfering RNA
TGFα	transforming growth factor alpha
tRNA	transfer RNA
UBF1	RNA polymerase I preinitation factor upstream binding factor 1
VEGF	vascular endothelial growth factor
VHL	von Hippel-Lindau

List of Publications

First-Author Publications (see Appendix B for Published Highlights)

V. **Mekhail, K.***, Rivero-Lopez, L.*, Brandon, C., Al-Masri, A., Payette, J., and Lee, S. (2006) Identification of general pH-dependent nucleolar localization and detention signals. (*in preparation*, *equal contribution, paper not included in thesis)

IV. **Mekhail, K.**, Rivero-Lopez, L., and Lee, S. (2006) Restriction of ribosomal biogenesis by pH-dependent interactions between VHL and the nucleolus: A possible mechanism for the protective effect of acidosis under hypoxia. **Cell Cycle** 5:2401-2413.

- See "MEETING REPORT" Static for Silencing. (2006) J. Cell Biol. 174:478-479.

III. **Mekhail, K.**, Khacho, M., Carrigan, A., Hache, R. J., Gunaratnam, L., and Lee, S. (2005) Regulation of ubiquitin ligase dynamics by the nucleolus. **J. Cell Biol.** 170:733-744.

- See "IN THIS ISSUE" Hiding proteins in the nucleolus. (2005) J. Cell Biol. 170:696.

- See "RESEARCH HIGHLIGHTS" Bound and gagged. (2005) Nature 437:298.

- Paper is cited in the Faculty of 1000 where it was included into the Top Ten Hidden Jewels List (October 2005).

- Second most read citation in the Faculty of 1000 Neuroscience (October 2005).

II. **Mekhail, K.**, Khacho, M., Gunaratnam, L., and Lee, S. (2004) Oxygen sensing by H^+: implications for HIF and hypoxic cell memory. **Cell Cycle** 3:1027-1029.

I. **Mekhail, K.**, Gunaratnam, L., Bonicalzi, M. E., and Lee, S. (2004) HIF activation by pH-dependent nucleolar sequestration of VHL. **Nature Cell Biol.** 6:642-647.

- Paper is cited *four* times in the Faculty of 1000.

Collaborative Publications (see appendix C)

III. Khacho, M., **Mekhail, K.**, and Lee, S. (2006) EDNA exploits the translational apparatus to export molecules from the nucleus. (*in preparation*, paper not included in thesis)

II. Smith, K., Gunaratnam, L., Morley, M., Franovic, A., **Mekhail, K.**, and Lee, S. (2005) Silencing of epidermal growth factor receptor suppresses hypoxia-inducible factor-2-driven VHL-/- renal cancer. **Cancer Res.** 65:5221-5230.

I. Gunaratnam, L., Morley, M., Franovic, A., de Paulsen, N., **Mekhail, K.**, Parolin, D. A., Nakamura, E., Lorimer, I. A., and Lee, S. (2003) HIF activates the TGFα/EGFR growth stimulatory pathway in VHL-/- renal cell carcinoma cells. **J. Biol. Chem.** 278:44966-44974.

Authorizations for the Use of Published Material

Nature Cell Biology (one article)

Cell Cycle (two articles)

The Journal of Cell Biology (one article)

Acknowledgements

I was once told by my parents that as you go through life, you will meet a small number of special people who will make an everlasting impression on you as a person. I guess that would make Dr. Stephen Lee a very special person. I will forever be indebted to Dr. Lee for being a great mentor and a dear friend. We shared several eureka moments and countless out-of-the-box philosophical brainstorms that I will strive to experience with my colleagues and students in the future. Dr. Lee's laboratory is built on a group of very good hearted and intelligent people who never hesitate to help each other. I sincerely thank my colleagues Luis Rivero-Lopez, Mireille Khacho, and Amanda Carrigan, and my summer students Caroline Brandon and Ahmad Al-Masri for conducting or assisting with some of the experiments presented here. I would also like to thank Aleksandra Franovic, Karlene Smith, Josianne Payette, Isabelle Robert, Erica Sanger, David Patten, Karine Pilon-Larose and Christine Lavigne for their help, support, insightful suggestions, or technical expertise. A special thank you to my dear friend Dr. Lakshman Gunaratnam for jump starting my scientific inquisition. A big thank you to the members of my graduate committee, Dr. Robert Hache, Dr. David Park, and Dr. Doug Gray, for their time, input, and assistance. Thank you to the Natural Sciences and Engineering Research Council of Canada (NSERC) for providing me with generous salary support through the Doctoral Canada Graduate Scholarship (CGS-D) and to the Canadian Institutes of Health Research (CIHR) for grant support to Dr. Lee.

The biggest thank you has to go to my family for unconditional love and support. My dad, my mom, and my sister have always been the biggest fans of my work and have

sacrificed so much for me to complete my Ph.D. To Christine, I cannot imagine having done this without your immeasurable love and support.

Chapter 1. General Introduction

Chapter 1. General Introduction

1.1. Cancer

1.1.1. The dynamics of cancer

Increases in human longevity over the last century have steered the Western world into unchartered territory. According to the National Cancer Institute of Canada (NCIC), the rising incidence of cancer in Canada is primarily due to an aging population. During their lifetime, 38% of Canadian women and 43% of men will develop cancer, and approximately one out of every four Canadians will die of this disease (National Cancer Institute of Canada: Canadian Cancer Statistics 2004). Cancer is a disease involving dynamic changes in the genome. Tumor development proceeds via a process formally analogous to Darwinian evolution in which a succession of genetic changes, each conferring one or another type of growth advantage, leads to the progressive conversion of normal human cells into cancer cells (Hanahan and Weinberg, 2000). Deciphering the cancer code on genetic and molecular fronts holds great promise for stopping this disease.

1.1.2. Cancer susceptibility genes

The concept that genetic mutations can produce oncogenes, such as myc and ras, with dominant gain of function or inactivate tumor suppressor genes such as BRCA1 and p53, with recessive loss of function is supported by a rich body of evidence acquired over the last 30 years (Hanahan and Weinberg, 2000). Two different types of tumor suppressor genes do exist. Genes that directly restrict proliferation, such as retinoblastoma (Rb), are known as "gatekeepers" as their biallelic inactivation directly initiates neoplasia (Figure 1.1). Genes that maintain the stability of the genome, such as BRCA1 and BRCA2 do

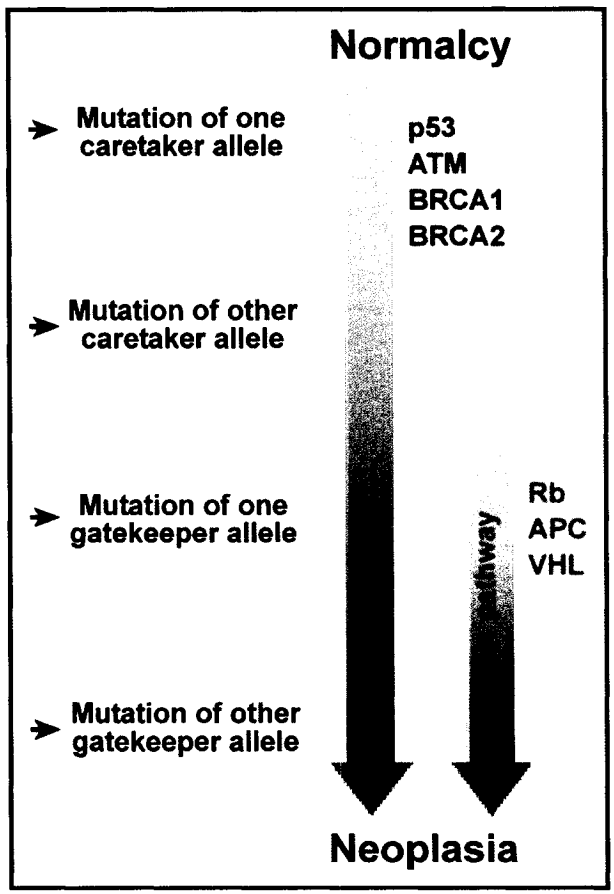
Normalcy
Mutation of one caretaker allele
Mutation of other caretaker allele
Mutation of one gatekeeper allele
Mutation of other gatekeeper allele
p53
ATM
BRCA1
BRCA2
Rb
APC
VHL
Neoplasia

Figure 1.1

Figure 1.1. Comparison of the genetic pathophysiology of gatekeeper and caretaker tumor suppressor genes. Functional inactivation of both alleles of a gatekeeper gene initiates tumorigenesis. Functional inactivation of both alleles of a caretaker gene does not directly initiate neoplastic growth but increases the chance of occurrence of other mutagenic events such as the loss of function of a gatekeeper gene. Therefore, at least four genetic alterations are believed to occur in caretaker-dependent tumorigenesis. Figure adapted from (Kinzler and Vogelstein, 1997).

through DNA repair, are called "caretakers" as their inactivation increases the probability of acquiring mutations in all genes, including gatekeeper tumor suppressor genes (Kinzler and Vogelstein, 1997; Levitt and Hickson, 2002). Thus, more genetic aberrations have to occur after the loss of caretakers than in the case of gatekeepers before neoplastic growth is initiated (Figure 1.1).

1.1.3 Knudson's "two-hit" hypothesis

It was actually in 1971, that Knudson noted that the differences between hereditary and sporadic retinoblastoma, with respect to age-specific incidence and propensity for multifocality, could be accounted for if the development of retinoblastoma required two rate-limiting mutations ("hits") and if one of these hits had already occurred in the germ line of the hereditary patients (Knudson, 1971). Later, he speculated that the two hits might consist of the inactivation of the maternal and paternal copies of a tumor suppressor gene – a prediction later proved to be correct for retinoblastoma and other cancers (Figure 1.1) (Knudson, 1985).

1.2 Kidney Cancer

1.2.1. Kidney Cancer: Worldwide and in Canada

Kidney cancer affects approximately 150,000 people worldwide each year, resulting in 78,000 deaths annually, and its incidence is rising (Pavlovich and Schmidt, 2004). Canada's share of these unfortunate statistics is substantial. According to the NCIC, 12'000 Canadians suffer from this disease and close to 1'350 patients die each year due to complications arising from primary kidney tumors. 1 in 80 Canadians will develop this disease during his or her lifetime and about 1 in 90 Canadians will die from this

disease, which now accounts for 3% of all cancers diagnosed in Canada (NCIC).

1.2.2. Kidney cancer in the clinic

Clinically, kidney cancer is not a single entity but rather comprises a class of tumors the majority of which are of renal epithelial origin. Although the largest proportion of cases of this cancer seems to follow a sporadic occurrence, an inherited predisposition to renal neoplasia accounts for about 4% of cases and often involves the same genes implicated in sporadic renal cancer. Extensive histological and molecular evaluation has resulted in the classification of kidney cancer into different subtypes (Pavlovich and Schmidt, 2004), the most common of which is conventional or clear cell renal cell carcinoma (CRCC, hereafter referred to as RCC for the sake of simplicity), which accounts for over 75% of all renal neoplasms (Linehan et al., 2003). Unfortunately, there are no effective treatments for kidney cancer. The situation is especially bleak for individuals diagnosed with advanced metastatic disease, which is the case of most patients (Bukowski and Novick, 2000). An incomplete understanding of the molecular programs at the core of this disease makes surgery the prevalent clinical approach. Interferon-α and interleukin-2-based therapies improve the median time of disease progression (MTDP) from 4 months (historical control data) to five months only and kidney cancer patients unfortunately have a five-year survival rate of less than 10% (Motzer et al., 1996). However, the results of two recent and separate clinical trials indicate that the anti-angiogenic drugs sunitinib (Sutent®) and temsirolimus increase the MTDP to almost eleven month (National Cancer Institute, National Institutes of Health).

1.2.3. Kidney cancer is associated with the von Hippel-Lindau gene

1.2.3.1. von Hippel-Lindau disease

The first reports in the medical literature of families afflicted with the hereditary cancer syndrome known as von Hippel-Lindau (VHL) disease were published by Treacher Collins, Eugene von Hippel and Arvid Lindau (Collins, 1894; Lindau, 1927; von Hippel, 1904). Individuals afflicted with this disease are predisposed for the development of multiple highly vascularized tumors including retinal angioma, cerebral haemangioblastoma, phaeochromocytoma, and clear cell renal cell carcinoma (Figure 1.2). VHL disease is a rare disorder with a 1 in 35,000 incidence (Kaelin, 2002). Symptoms typically develop in the second to fourth decades of life and patients usually succumb to the disease in the forties due to unresectable hemangioblastomas or complications caused by primary renal tumors (Maher and Kaelin, 1997).

1.2.3.2. The VHL tumor suppressor gene in hereditary and sporadic kidney cancer

In 1993, the VHL tumor suppressor gene was identified by studying affected members of VHL kindreds (Latif et al., 1993). The VHL gene resides on the short arm of chromosome 3 (3p25) (Latif et al., 1993; Tory et al., 1989). Loss of heterozygosity (LOH) at chromosome 3p is observed in both familial VHL disease as well as sporadic RCC, and loss of the remaining VHL allele was attributed to mutations or epigenetic inactivation by hypermethylation of the remaining VHL allele (Gnarra et al., 1994; Herman et al., 1994; Latif et al., 1993). Clinically, VHL disease is inherited in an autosomal dominant fashion (Figure 1.3) (Maher *et al.,* 1991), and genetically VHL behaves as a typical tumor suppressor, as defined by Knudson's two hit hypothesis (Figure 1.4). Patients who have inherited a germ-line mutation of the VHL gene are

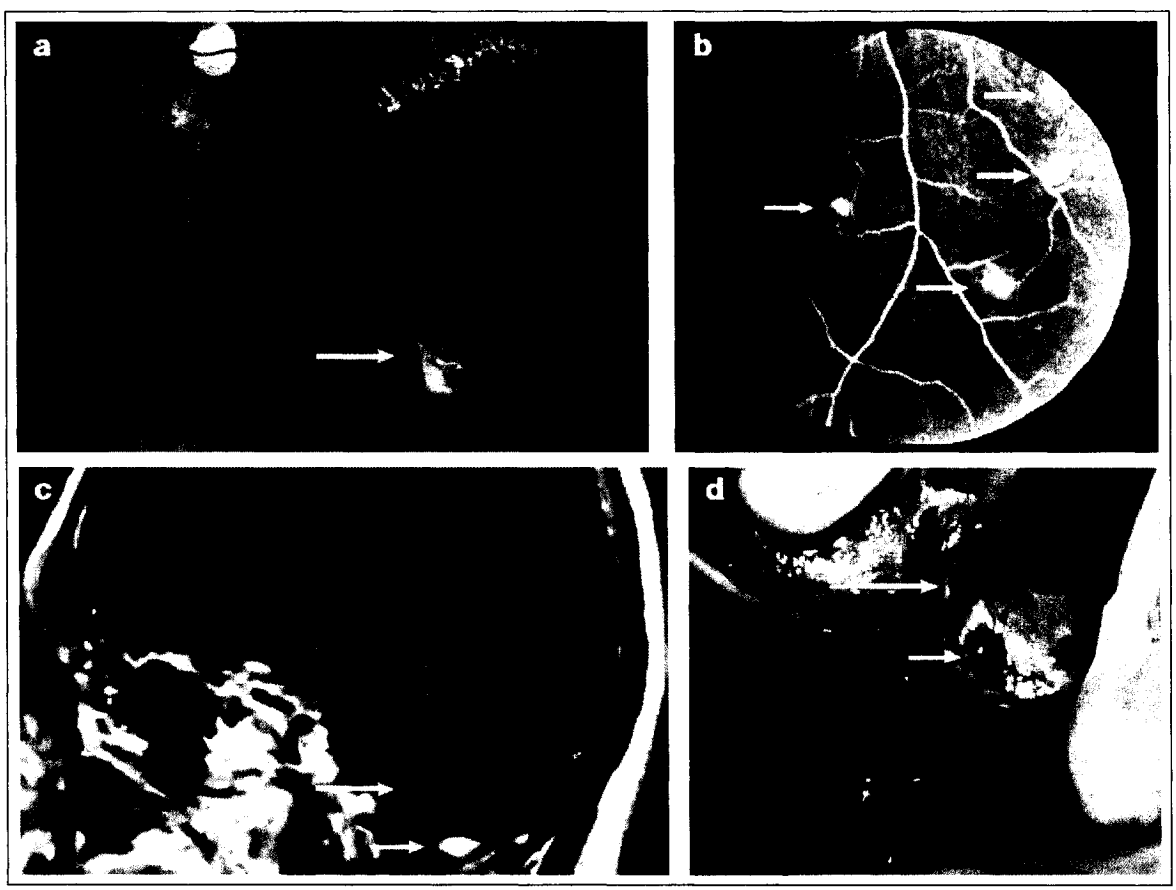

Figure 1.2

Figure 1.2. von Hippel–Lindau-associated tumors. (**a**) Fundoscopic view of a retinal haemangioblastoma (arrow). The optic nerve is seen on the upper left. (**b**) Fluorescein angiogram showing multiple retinal haemangioblastomas (arrows). (**c**) Sagittal magnetic resonance image of a large cystic cerebellar haemangioblastoma (white arrow). Magnetic resonance imaging shows the solid component of the tumour as an enhancing (bright) lesion (yellow arrow). (**d**) Renal carcinoma (yellow arrow) arising in a large renal cyst (white arrow) (Kaelin, 2002).

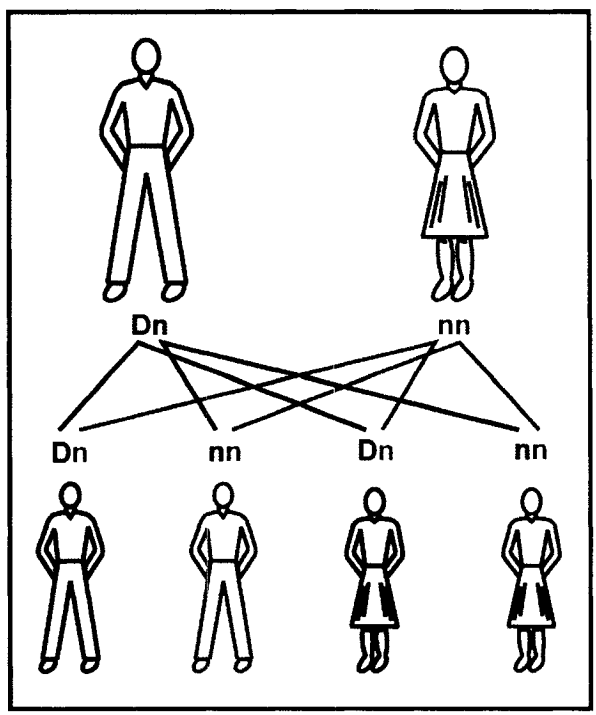

Figure 1.3

Figure 1.3. Dominance in the inheritance of VHL disease. D (dominance) symbolizes the mutated allele and n (normal) signifies the normal allele.

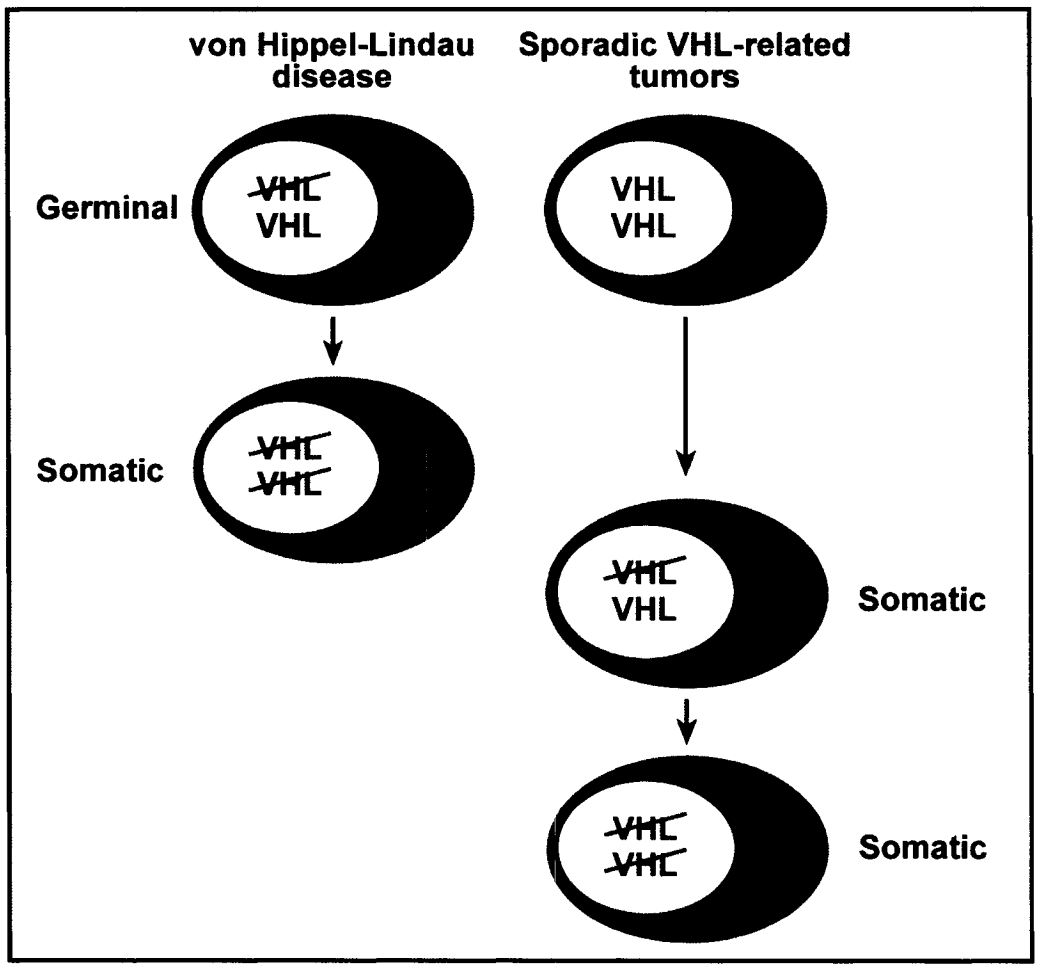
von Hippel-Lindau disease
Sporadic VHL-related tumors
Germinal
VHL
VHL
VHL
VHL
Somatic
VHL
VHL
VHL
VHL
Somatic
VHL
VHL
Somatic

Figure 1.4

Figure 1.4. VHL loss follows Knudson's two-hit hypothesis. Inactivation of both alleles of the VHL tumor suppressor gene, within the same cell, is required for neoplastic transformation (blue to red). In addition, loss of the first VHL allele increases the chances (shorter arrows) of acquiring a mutation within the second allele.

predisposed to the development of the above-mentioned tumors. In the affected tissues, tumor formation arises from cells following somatic loss of function of the remaining wild-type copy of the VHL gene. Biallelic loss of VHL function is also found in the majority of sporadic RCCs (Gnarra et al., 1994; Motzer et al., 1996). The VHL gene is categorized as a gatekeeper tumor suppressor gene, as its biallelic inactivation ($VHL^{-/-}$) is associated with a significant increased probability of tumorigenesis (Kaelin and Maher, 1998). Consistent with this classification, reintroduction of wild type VHL into VHL-deficient RCC cells is sufficient to prevent tumor formation in nude mice (Iliopoulos et al., 1995).

1.2.3.3. VHL loss is associated with several hallmarks of cancer

Douglas Hanahan and Robert Weinberg presented a paradigm-breaking concept to the field of cancer research as a whole by highlighting evidence supporting their now famous hallmarks of cancer theory (Hanahan and Weinberg, 2000). They suggested that most, if not all, cancers acquire the same set of functional capabilities during their development: (1) limitless replicative potential, (2) self-sufficiency in growth signals, (3) sustained angiogenesis, (4) tissue invasion and metastasis, (5) insensitivity to anti-growth signals, (6) evasion of apoptosis. VHL-deficient RCC cells form tumors in nude mice (Iliopoulos et al., 1995), grow in the absence of exogenous growth factors (Herlyn et al., 1990; Pause et al., 1998), overproduce angiogenic factors (Gnarra et al., 1996b; Iliopoulos et al., 1996), and fail to deposit an extracellular matrix promoting metastasis and evasion of cellular differentiation (Davidowitz et al., 2001; Hanahan and Weinberg, 2000; Kurban et al., 2006; Lieubeau-Teillet et al., 1998; Ohh et al., 1998; Ruoslahti, 1984; Stickle et al., 2004; Sutherland, 1988). Reintroduction of VHL into cells abolishes all these

tumorigenic features (Davidowitz et al., 2001; Gnarra et al., 1996b; Hanahan and Weinberg, 2000; Herlyn et al., 1990; Iliopoulos et al., 1995; Iliopoulos et al., 1996; Kaelin, 2002; Kurban et al., 2006; Lieubeau-Teillet et al., 1998; Ohh et al., 1998; Pause et al., 1998; Ruoslahti, 1984; Stickle et al., 2004; Sutherland, 1988).

1.3. The VHL tumor suppressor gene: early clues to function

1.3.1. VHL: gene to protein

The VHL gene contains three exons and is transcribed into a 4.4 Kb mRNA. The VHL messenger harbors two in-frame start codons generating two proteins composed of 213 (p30) and 160 (p19) amino acids (Blankenship et al., 1999; Iliopoulos et al., 1995; Iliopoulos et al., 1998; Schoenfeld et al., 1998). Both protein forms display similar biochemical characteristics and will hereafter be referred to as VHL. Crystal structure analysis revealed that VHL contains a β-sheet domain and a α-helical domain spanning residues 63 to 154 and 155-189, respectively (Stebbins et al., 1999). The α- and β-domains are 'hot spots' for cancer causing mutations observed in patients with VHL disease and sporadic RCC, respectively (Figure 1.5) (Gnarra et al., 1996a).

1.3.2. The VBC/Cul-2 complex links VHL to ubiquitylation networks

VHL associates with at least four other partners: elongin B, elongin C, Cullin-2, and Rbx1 forming the VBC/Cul-2 complex (Figure 1.6) (Rbx is excluded from complex schematics for simplicity) (Duan et al., 1995a; Duan et al., 1995b; Kamura et al., 1999; Kibel et al., 1995; Lonergan et al., 1998; Pause et al., 1997). The original suggestion that VHL might be inhibiting the transcriptional complex SIII by binding its essential subunits elongins B and C, was rapidly dismissed by the fact that all SIII subunits are in excess

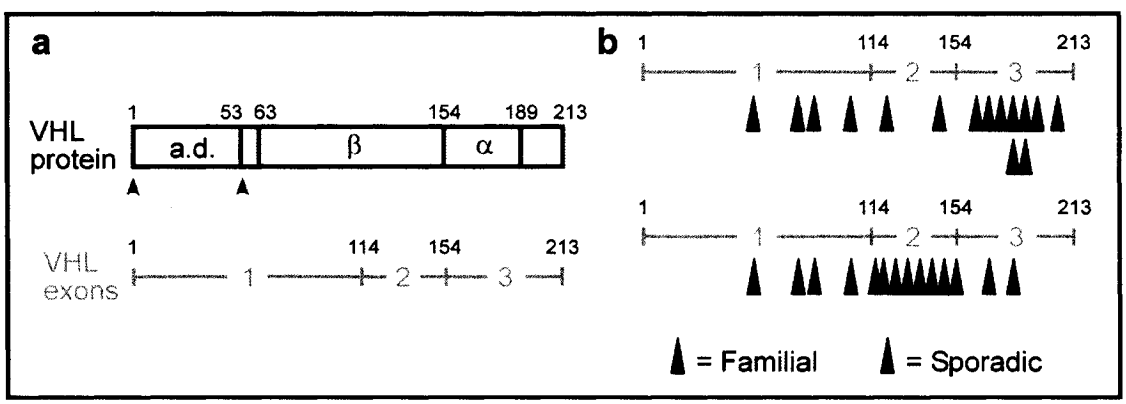
a
VHL protein
1
53 63
154
189 213
a.d.
β
α
VHL exons
1
114
154
213
1
2
3
b
1
114
154
213
1
2
3
1
114
154
213
1
2
3
= Familial
= Sporadic

Figure 1.5

Figure 1.5. VHL: gene and protein. Structure of the VHL protein (**a**) and mutational hotspots (**b**) in familial and sporadic RCC. Amino acid positions within the VHL protein and exon numbers are indicated. Transcriptional start sites are marked by small arrowheads in (a). a.d., acidic domain; β, β-sheet domain; α, α-helical domain. Note that exon-2-encoded β-domain and exon-3-encoded α-domain contain several mutational hotspots in sporadic and familial RCC, respectively.

relative to VHL on the basis of molarity. However, the observation of a high structural homology of elongin C and Cullin-2 with the SKP1 and CDC53 members of the SCF^{CDC4} yeast ubiquitin-ligase complex, respectively, suggested a role for VBC/Cul-2 in protein ubiquitylation (Figure 1.6) (Gorospe et al., 1999; Kibel et al., 1995; Pause et al., 1997; Pause et al., 1999). This was confirmed by several other studies that will be discussed further in section 1.4.4.

1.3.3. Molecular features of ubiquitylation networks

Ubiquitylation is a post-translational modification consisting of the conjugation of a 76 amino-acid polypeptide called ubiquitin to proteins destining them for very different fates in the cell (Ciechanover, 2005; Muratani and Tansey, 2003; Weissman, 2001). Although targeting proteins for degradation via the 26S proteasome is the best-studied role of ubiquitylation, this modification is integral to several biochemical pathways including receptor internalization (Terrell et al., 1998), chromatin maintenance (Muratani and Tansey, 2003) and DNA repair (Gillette et al., 2001; Russell et al., 1999). The ubiquitin system is sustained by the interaction of multiple dynamic molecular networks that begin with ATP-dependent loading of ubiquitin onto an ubiquitin-activating enzyme (E1) via a thioester bond (Figure 1.7). The ubiquitin moiety is then transferred to an ubiquitin-conjugating enzyme (E2) forming a second thioester bond; and finally, an ubiquitin protein ligase (E3) catalyzes the transfer of ubiquitin from E2 to the lysine residue of a specific substrate through a peptidic bond, thereby altering its cellular fate. There are many more E3s in the cell than there are E1s and E2s combined and it is thought that E3s determine the specificity of substrate recognition within the ubiquitin system. The

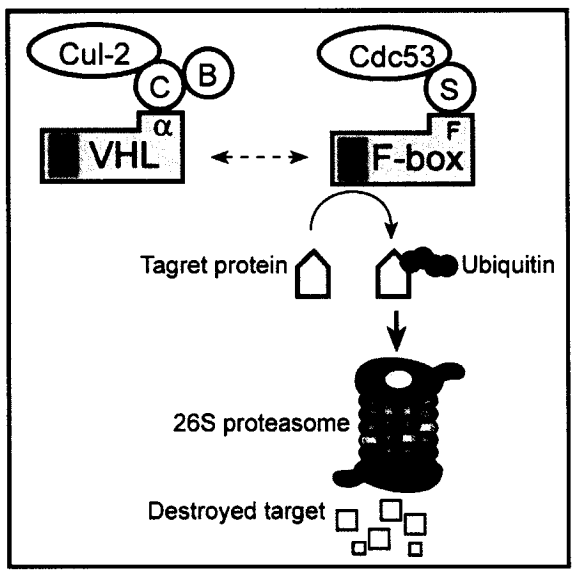
Cul-2
C
B
α
VHL
Cdc53
S
F
F-box
Tagret protein
Ubiquitin
26S proteasome
Destroyed target

Figure 1.6

Figure 1.6. The VBC/Cul-2 complex structurally resembles the SCF (Skp1-Cdc53-Fbox protein) yeast ubiquitin ligase complex. SCF targets proteins for ubiquitylation and degradation. The α and β domains of VHL display structural similarities with the F-box motif and the substrate (yellow)-docking site of the F-box protein. Adapted from (Kaelin, 2002)

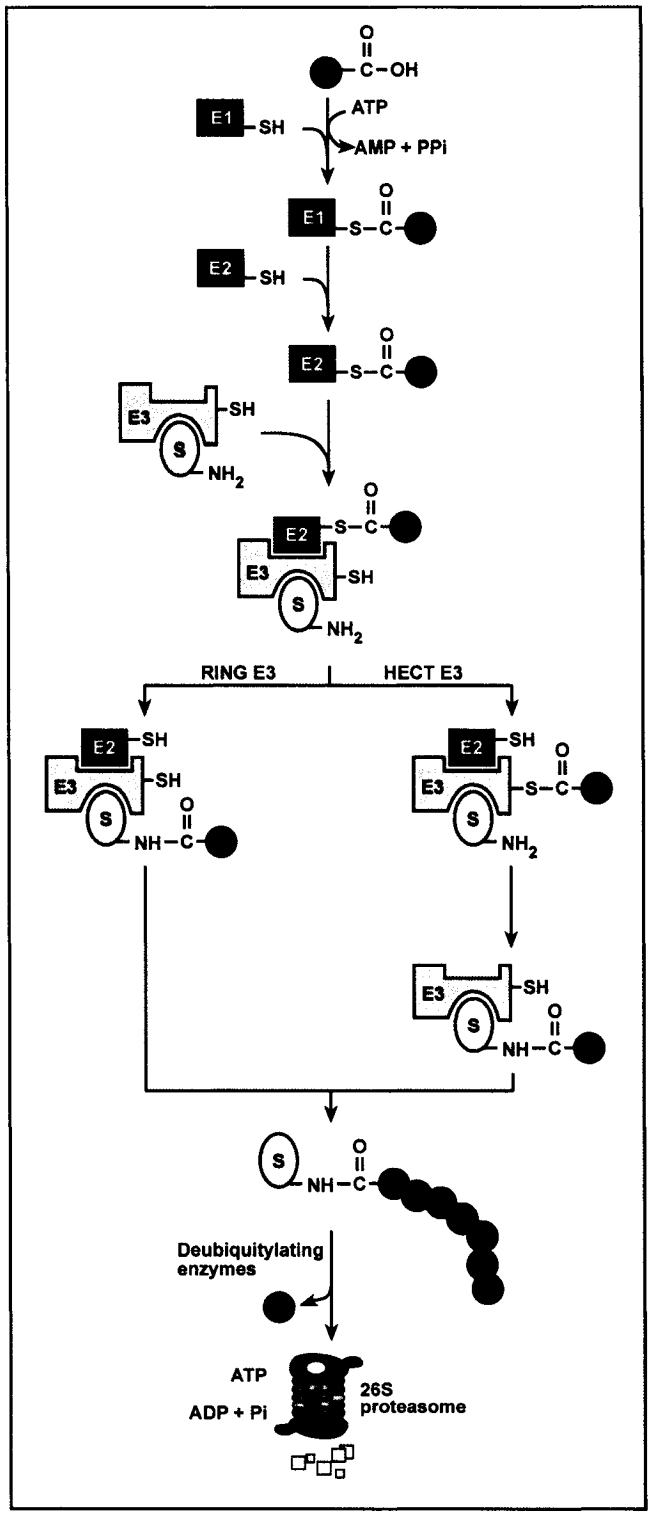
C–OH
E1
SH
ATP
AMP + PPi
E1
S–C
E2
SH
E2
S–C
E3
SH
S
NH2
E2
S–C
E3
SH
S
NH2
RING E3
HECT E3
E2
SH
E3
SH
S
NH–C
E2
SH
E3
S–C
S
NH2
E3
SH
S
NH–C
S
NH–C
Deubiquitylating enzymes
ATP
ADP + Pi
26S proteasome

Figure 1.7

Figure 1.7. Details of the energy dependent process of the ubiquitin-proteasome system. Please note that deubiquitylating enzymes have been shown to be implicated in the control of the level of ubiquitylation of several substrates. Adapted from (Ciechanover, 2005; Weissman, 2001).

function of an ubiquitin ligase can be regulated by controlling the ligase or its substrate at various levels such as post-translational modifications, interactions with regulatory factors or subcellular localization (Petroski and Deshaies, 2005). Two main families of E3s have been defined based on their conserved protein domains. The first is called after the conserved ~350-amino-acid HECT (homologous to E6-AP carboxyl terminus, E6-AP being the founder member of this family) domain and the other is known as RING finger ubiquitin ligase family (Huibregtse et al., 1995; Joazeiro and Weissman, 2000; Scheffner et al., 1990). RING finger E3s are defined structurally by two interleaved zinc ion-coordinating sites and consist of a consensus sequence ($CX_2CX_{(9-39)}CX_{(1-3)}HX_{(2-3)}C/HX_2CX_{(4-48)}CX_2C$) where cysteines and histidines are metal-binding sites where the first, second, fifth and sixth of these recognizing one zinc ion and the third, fourth, seventh and eighth binding the second (Weissman, 2001). While HECT E3s form thiol-ester intermediates with ubiquitin as part of the ubiquitylation process, most RING finger E3s mediate the direct transfer of ubiquitin from E2 to substrate (Figure 1.17). Single subunit RING finger E3s include MDM2, which ubiquitylates p53, the proto-oncoprotein c-Cbl, which ubiquitylates growth factor receptors, and the inhibitors of apoptosis (IAPs) (Weissman, 2001). Multisubunit E3s include the anaphase promoting complex (APC) and the SCF^{CDC4} yeast ubiquitin-ligase complex. Some E3s follow what is now known as the N-end rule, which defines a category of enzymes that have a marked selectivity for substrates bearing basic or large hydrophobic N-terminal amino-acids (Bachmair and Varshavsky, 1989; Koegl et al., 1999; Xie and Varshavsky, 1999). It was suggested that the half life of a mature protein substrate could be partially determined by its N-terminal residue when degraded by an E3 that follows the N-end rule. For example, while

methionine and serine confer stability ($t_{1/2}$ > 20 h), phenylalanine and tryptophane are strongly destabilizing ($t_{1/2}$ ~ 3 min) (Bachmair and Varshavsky, 1989).

1.3.4. The Proteasome: a protein shredder

Cellular proteins can be targeted for degradation via the vacuolar system, which incorporates the action of lysosomes, endosomes, and the endoplasmic reticulum, or via a large 2000 kDa dumbbell-shaped multi-protein complex, the 26S proteasome (Ciechanover, 2005; Hershko et al., 1984; Hough et al., 1986; Hough et al., 1987; Waxman et al., 1987). The latter is composed of a 20S core particle (CP) that carries at least five different peptidase activities and one (or two) 19S regulatory particle (RP) conferring proteasomal selectivity to polyubiquitylated proteins (Figure 1.8) (Ciechanover, 2005; Eytan et al., 1989; Glickman et al., 1998). The 20S CP is a barrel-shaped structure composed of four stacked rings, two identical outer α rings and two identical inner β rings. In eukaryotes, each of these rings is composed of seven distinct subunits, giving the CP the general structure of $\alpha_{1\text{-}7}\beta_{1\text{-}7}\beta_{1\text{-}7}\alpha_{1\text{-}7}$. Catalytic sites are localized to the β subunits. One or both ends of the 20S barrel is usually capped by a 19S RP, which is composed of two subcomplexes consisting of a nine subunit base and an eight subunit lid (Hoffman et al., 1992). The 19S RP selectively unfolds polyubiquitylated proteins and opens an orifice in the α ring through which it can insert the substrate into the 20S CP. Peptide fragments are then released and ubiquitin molecules are recycled.

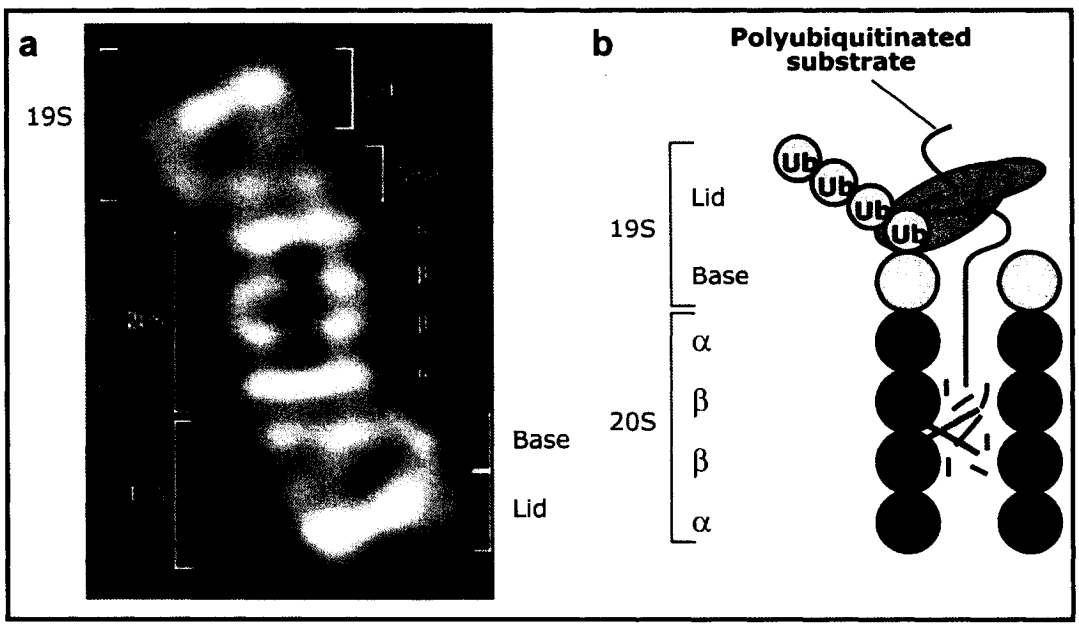
a
19S
Base
Lid
b
Polyubiquitinated substrate
Ub
Ub
Ub
Ub
19S
Lid
Base
20S
α
β
β
α

Figure 1.8

Figure 1.8. The 26S proteasome. (**a**) Electron microscopy of the 26S proteasome. (**b**) Schematic representation of the proteasome and its subunits. The 26S proteasome is composed of a 20S core particle (CP) carrying the protease activity and at least five different peptidase activities and a 19S regulatory particle (RP) providing specificity to polyubiquitylated proteins. The CP is a barrel-shaped structure composed of four stacked rings (two α rings constituting a tight passage to two β rings containing catalytic sites). The RP selectively unfolds polyubiquitylated proteins and opens an orifice in the α ring through which it can insert the substrate into the 20S CP. Peptide fragments are then released and ubiquitin molecules are recycled. Adapted from (Ciechanover, 2005; Glickman et al., 1998).

1.4. VHL targets the hypoxia-inducible factor transcription factor for oxygen-dependent degradation via the ubiquitin proteasome pathway

1.4.1. Early observation: VHL-loss uncouples hypoxia-inducible gene expression from oxygen levels

VHL-related tumors are highly vascularized. VHL-deficient RCC cells overproduce mRNAs and proteins of angiogenic factors such as vascular endothelial growth factor (VEGF) and erythropoietin (EPO), a phenomenon that usually occurs in non-malignant cells only under low oxygen tension (hypoxia) (Gnarra et al., 1996a; Golde et al., 1981; Iliopoulos et al., 1996; Krieg et al., 2000; Siemeister et al., 1996; Wizigmann-Voos et al., 1995). Reintroduction of VHL into VHL-deficient RCC cells restores oxygen-dependent expression of these angiogenic factors in a manner requiring formation of the VBC/Cul-2 complex, suggesting a role for the latter in cellular oxygen homeostasis (Gnarra et al., 1996b; Iliopoulos et al., 1996; Lonergan et al., 1998).

1.4.2. Role of the hypoxia-inducible factor in oxygen homeostasis

Hypoxia-inducible factor (HIF) is a heterodimeric transcription factor that activates hypoxia-inducible genes involved in processes such as glucose uptake (glucose transporter 1, Glut-1), iron transport (transferrin), pH regulation (carbonic anhydrase IX, CAIX), angiogenesis (VEGF), and erythrogenesis (EPO) in response to reductions in environmental oxygen tension (Table 1.1) (Forsythe et al., 1996; Harris, 2002; Semenza, 1998; Semenza, 2003; Wenger, 2002). HIF is composed of an α subunit (HIFα) and a β subunit (HIFβ), also called aryl hydrocarbon receptor nuclear translocator or ARNT,

Oxygen Transport: Erythropoiesis and Iron Metabolism	
Erythropoietin (EPO)	Erythropoiesis
Transferrin	Iron transport
Transferrin receptor	Iron uptake
Ceruloplasmin	Iron oxidation
Oxygen Transport: Vascular Regulation	
Vascular endothelial growth factor (VEGF)	Angiogenesis
Flt-1	VEGF receptor 1
Endocrine-gland-derived (EG)-VEGF	Angiogenesis
Plamsminogen activator inhibitor-1 (PAI-1)	Angiogenesis
Nitric oxide synthase (NOS)	NO production
Heme oxygenase 1	CO production
Adrenomedullin	Vascular tone
α1B-adrenergic receptor	Vascular tone
Endothelin-1	Vascular tone
Anaerobic Energy: Glucose Uptake and Glycolysis	
Glucose transporters 1 and 3 (Glut-1 and -3)	Glucose uptake
PFKFB3	Glycolysis regulation
Phosphofructokinase L (PFKL)	Glycolysis
Aldolase A and C	Glycolysis
Glyceraldehyde-3-phosphate dehydrogenase (GAPDH)	Glycolysis
Phosphoglycerate kinase 1 (PGK1)	Glycolysis
Enolase 1	Glycolysis
Lactate dehydrogenase A (LDHA)	Glycolysis
Other	
p35srj	HIF-1 feedback regulation
Collagen prolyl-4-hydroxylase α1	Collagen matrix formation
Intestinal trefoil factor	Growth factor
ETS-1	Transcription factor
Insulin-like growth factor 2 (IGF-2)	Growth factor
Insulin-like growth factor binding proteins (IGFBP) 1, 2 and 3	Transcription factors
Platelet derived growth factor (PDGF)-β	Growth factors/Angiogenesis
Transforming growth factor (TGF)-β	Growth factors/Angiogenesis

Table 1.1

Table 1.1. Identified HIF target genes. Genes are grouped according to the general cellular processes in which they are implicated and more specific functional categorizations are indicated on the right hand side.

which are differentially regulated (Huang et al., 1996; Kallio et al., 1999; Salceda and Caro, 1997; Semenza, 1999). In the presence of oxygen (normoxia), HIFα is expressed but rapidly degraded. Following a shift to hypoxia, HIFα is stabilized allowing it to bind through its basic helix-loop-helix (bHLH) domain (Figure 1.9) to the constitutively expressed HIFβ, forming the active transcription factor HIF (Wang and Semenza, 1995). Stabilized HIF recognizes a particular DNA region known as hypoxia response element (HRE) consisting of a CGTG box in the promoter region of hypoxia-inducible genes (Semenza, 1999). When this DNA sequence was introduced into a heterologous reporter gene and transfected into cultured cells, there was a dramatic increase in reporter gene transcription following the transfer of cells to hypoxia (Beck et al., 1991; Blanchard et al., 1992; Pugh et al., 1991; Semenza et al., 1991; Semenza and Wang, 1992). Recruitment of transcriptional co-activators such as cAMP-response element-binding (CREB) binding protein (CBP), as well as the histone acetyl transferases p300, SRC1 and TIF2 via the N and C terminal transactivation domains (NTAD and CTAD) of HIFα allow it to mediate target gene expression (Figure 1.9 and Table 1.1) (Arany et al., 1996; Carrero et al., 2000; Ema et al., 1997; Gu et al., 2001; Kallio et al., 1999; Kung et al., 2000; Kvietikova et al., 1995). HIFα contains a PAS (Per ARNT Sim) motif and is therefore classified under the family of transcription factors named after this domain. An inhibitory domain (ID) within HIFα negatively regulates its transactivation domains.

There are three members of the HIFα family – HIF-1α, HIF-2α, and HIF-3α. HIF-3α lacks the transactivation domain and is suggested to act as a dominant negative to compete with HIF-1α and HIF-2α mediated gene expression in certain settings (Maynard et al., 2005; Maynard et al., 2003). While HIF-1α is more ubiquitously expressed,

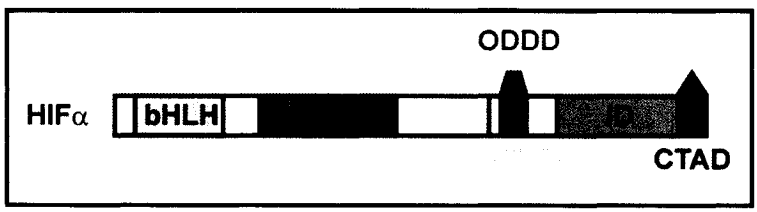

Figure 1.9

Figure 1.9. Features of the alpha subunit of the hypoxia-inducible factor.

Following a shift to hypoxia, HIFα is stabilized allowing it to bind through its basic helix-loop-helix (bHLH) domain to the constitutively expressed HIFβ, forming the active transcription factor HIF. Recruitment of transcriptional co-activators such as cAMP-response element-binding (CREB) binding protein (CBP), as well as the histone acetyl transferases p300, SRC1 and TIF2 via the N and C terminal transactivation domains (NTAD and CTAD) of HIFα allow it to mediate target gene expression. HIFα contains a PAS (Per ARNT Sim) motif and is therefore classified under the family of transcription factors named after this domain. An inhibitory domain (ID) within HIFα negatively regulates its transactivation domains.

HIF-2α displays a cell-type specific expression pattern (Kaelin, 2002). HIF-2α is more abundantly produced in highly vascularized tissues such as the heart, lung and liver (Ema et al., 1997). HIF-1α and HIF-2α activate shared as well as specific targets. The different transcriptional activity of the different HIF-α isoforms may be due to differential recruitment of co-factors. The NF-κB Essential Modulator (NEMO) could be such a factor as it was recently reported that the specific interaction of HIF-2α, but not HIF-1α, with NEMO specifically aids it in the recruitment of the CBP and p300 transcriptional co-activators (Bracken et al., 2005). The above-mentioned findings exemplify a growing body of evidence demonstrating distinct differences between HIF-1 and HIF-2 function. That HIF-1α and HIF-2α are not redundant proteins is supported by *in vivo* analyses of knockout mice. The knockout of either one is embryonically lethal but yields mice with different developmental defects. While HIF-1α knockout generates mice with severe defects in vascularization (Iyer et al., 1998; Kotch et al., 1999), HIF-2α$^{-/-}$ mice exhibit abnormal lung maturation, bradycardia, and diminished catecholamine levels in addition to blood vessel defects (Tian *et al.,* 1998).

1.4.3. VHL targets HIFα for proteasomal degradation

The fact that HIFα is regulated primarily at the protein level was suggested by the insensitivity of its transcript to fluctuations in oxygen concentration (Wenger et al., 1997). In 1999, Maxwell and colleagues discovered that VHL mediates proteasomal degradation of HIFα in the presence of oxygen (Maxwell et al., 1999). They reported that this mechanism requires direct or indirect VHL/HIF interactions, which were abrogated by exposure to iron chelation or cobaltous ions. This explained the

hyperactivation phenotype of hypoxia-inducible genes in VHL-deficient cells and provided a new focus for understanding cellular oxygen sensing.

1.4.4. VHL/HIFα interaction is regulated by oxygen-sensitive proline hydroxylation

Identification of VHL's HIF regulatory function (Maxwell et al., 1999) was followed by a series of publications that deciphered this intricate process. It is now well accepted that VHL acts as the particle recognition motif of the VBC/Cul-2 RING finger ubiquitin ligase complex to target HIFα for oxygen-dependent degradation (Table 1.2) (Iwai et al., 1999; Kamura et al., 1999; Kamura et al., 2000; Kibel et al., 1995; Lisztwan et al., 1999; Lonergan et al., 1998; Maxwell et al., 1999; Ohh et al., 2000; Pause et al., 1997; Pause et al., 1999). In the presence of oxygen, HIFα is post-translationally modified at two key proline residues within its oxygen-dependent degradation (ODD) domain by enzymes known as prolyl hydroxylases (PHDs) (Figure 1.10 and Table 1.2) (Bruick and McKnight, 2001; Epstein et al., 2001; Ivan et al., 2001; Jaakkola et al., 2001; Yu et al., 2001). This allows VHL to recognize HIFα and target it for Cullin-2-mediated ubiquitylation and degradation via the 26S proteasome (Kaelin, 2002). Abrogation of VHL-HIFα interactions by hypoxia stabilizes HIF, which then activates genes that mediate the oxygen homeostatic response.

PHDs modify prolyl residues and the best-studied of these enzymes are the collagen prolyl hydroxylases, which reside in the endoplasmic reticulum and are necessary for collagen maturation (Myllyharju, 2003). However, HIFα hydroxylation is carried out by members of the EGLN family of PHDs, which require several cofactors such as 2-oxoglutarate, ascorbate (or vitamin C) and iron in addition to oxygen (Figure 1.10) (Kaelin, 2002). The enzymatic reaction is coupled to the decarboxylation of

O_2 Status	PHD Status	Recognition Status	HIF Status
Normoxia	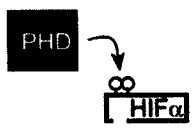	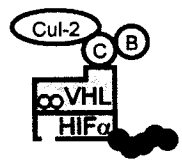	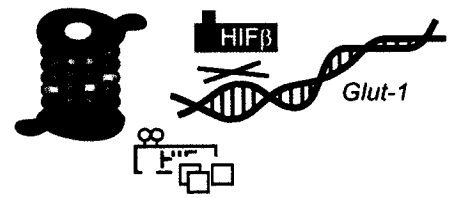
Hypoxia		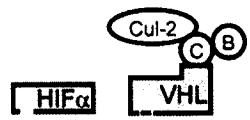	

Table 1.2

Table 1.2. Oxygen-dependent regulation of HIFα by VHL. In the presence of oxygen, VHL targets hydroxylated HIFα for Cul-2-mediated ubiquitylation and subsequent proteasomal degradation. Hypoxia inactivates PHDs allowing HIFα to evade degradation. Stabilized HIF then activates its target genes to remodel the cellular gene expression profile and adapt cells to low oxygen tension.

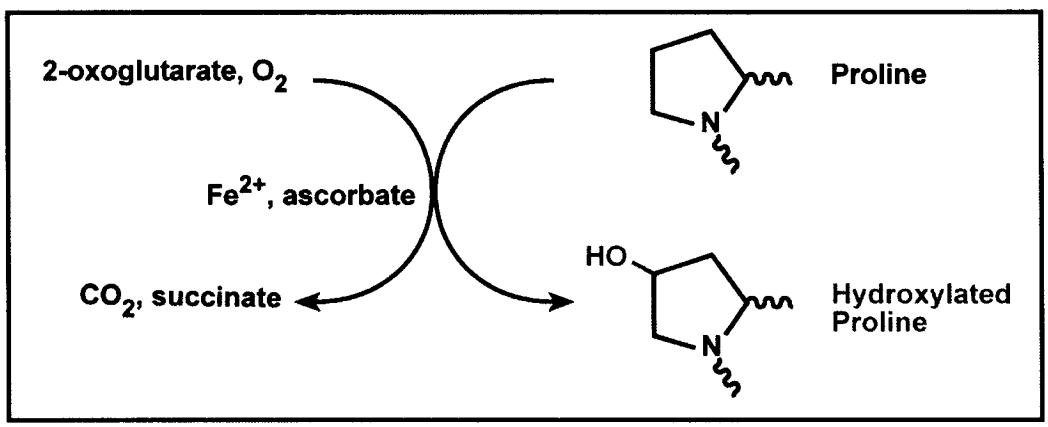
2-oxoglutarate, O_2
Fe^{2+}, ascorbate
CO_2, succinate
Proline
HO
Hydroxylated Proline

Figure 1.10

Figure 1.10. Schematic of proline residue hydroxylation. Prolyl hydroxylases require several cofactors, including 2-oxoglutarate, iron and ascorbate, in addition to molecular oxygen. It is important to note that the oxygen atom that is incorporated into the hydroxyl group is derived from molecular oxygen. Adapted from (Kaelin, 2002).

2-oxoglutarate to succinate and relies on ascorbate to prevent enzyme auto-oxidation. The oxygen atom incorporated into the hydroxyl group is derived from molecular oxygen, providing a molecular explanation for the known effects of oxygen scarcity on HIF stability.

1.4.5. Insights into intersubunit and E3/substrate interactions of the VBC/Cul-2 complex revealed by crystal structure analyses

1.4.5.1. Intersubunit interactions

Crystal structure of the VCB ternary complex at 2.7 angstrom (Å) resolution (Stebbins et al., 1999) revealed the intricate interactions of elongin C with elongin B and VHL through two distinct interfaces and that VHL does not directly interact with elongin B (Figure 1.11A). Each interface consists of a total surface area of about 2000 Å. Three α helices (VHL H1, H2, and H3) of the α domain of VHL are packed with an α helix from elongin C into a four-helix cluster where two pairs of helices are positioned at a perpendicular angle. The β domain of VHL consists of a seven-stranded β sheet sandwich and an α helix (VHL H4) that packs against one of the beta sheets through hydrophobic interactions. The α and β domains are connected by two short polypeptide linkers and a polar interface stabilized by hydrogen-bond networks from the H1 helix, the beta sandwich, and elongin C. Several of the residues at the interdomain interface have been found mutated in tumors (Stebbins et al., 1999). The VHL-elongin C interface is mainly hydrophobic but contains a few hydrogen bonds. The elongin C-elongin B interface is similar in extent to the elongin C-VHL interface but is less hydrophobic.

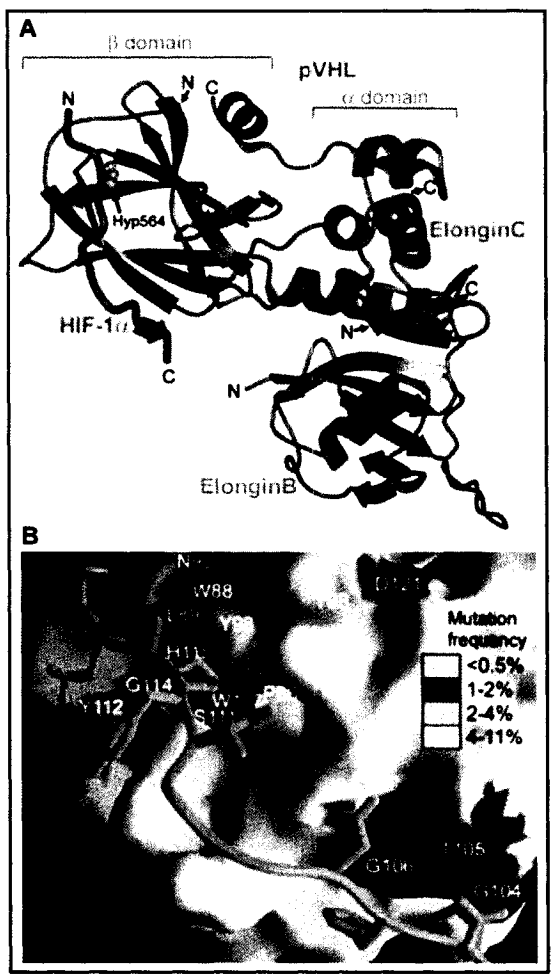
A
β domain
pVHL
α domain
N
N
C
Hyp564
ElonginC
C
HIF-1α
C
N
N
ElonginB
B
W88
Mutation
frequency
<0.5%
1-2%
2-4%
4-11%
G114
112

Figure 1.11

Figure 1.11. The HIF-1α destruction sequence binds the β domain of VHL in an extended β-strand-like conformation. (**a**) Schematic representation of the 15-residue portion of the HIF-1α destruction sequence bound to the β domain of VHL in the VBC complex. The portion of HIF-1α that adopts a continuous β-strand conformation is indicated by a wide arrow. HIF-1α is in blue, hydroxylated proline 564 (Hyp^{564}) in yellow, VHL in red, elongin B in magenta, and elongin C in green. C, COOH-terminus; N, NH2-terminus. (**b**) The Hyp^{564} binding site is a hotspot of tumorigenic VHL mutations. Surface representation of the VHL β domain colored according to the frequency of tumorigenic missense mutations. The universal VHL-mutation database contains 363 tumor-derived missense mutations, 210 of which map to the β domain residues 60 to 153. Mutation frequencies > 4% are shown in yellow, < 4% and > 2% in orange, < 2% and > 1% in red. Adapted from (Min et al., 2002).

1.4.5.2. Complex/HIFα interactions

The 1.85 Å structure of a 20-residue HIF-1α peptide-VBC complex revealed that HIF-1α binds to VHL in an extended β-strand-like conformation (Figure 1.11A) (Hon et al., 2002; Min et al., 2002). The hydroxyproline inserts into a gap in the VHL hydrophobic core, at a site that is a hotspot for tumorigenic mutations (Figure 1.11B), with its hydroxyl group recognized by buried serine and histidine residues. Although the β-sheet-like interactions contribute to the stability of the complex, the hydroxyproline contacts are central to the strict specificity characteristic of signaling (Min et al., 2002).

1.4.6. HIFα/co-activator interactions are regulated by asparagine hydroxylation

Prolyl hydroxylation is not the only hydroxyl-based post-translational modification to which HIFα is subjected. In the presence of oxygen, enzymes known as factor inhibiting HIF (FIH) hydroxylate a key asparagine residue within the CTAD of HIFα, thereby preventing recruitment of the co-activators p300 and CBP (Figure 1.12) (Lando et al., 2002a; Lando et al., 2002b). Thus, HIF is regulated through prolyl hydroxylation-dependent recruitment by VHL at the level of protein turnover and through asparaginyl hydroxylation-dependent binding of co-activators at the level of transcriptional activity. While these findings first seemed to be at odds with the well-documented normoxic activation of hypoxia-inducible genes in VHL loss settings (Maxwell et al., 1999), one possibility, suggested by the work of Greg Semenza, is that VHL might be required for asparagine hydroxylation (Wykoff et al., 2000). It is also possible that an unidentified protein that is not expressed in renal cell carcinoma cells recognizes and binds the hydroxylated CTAD to actively or physically prevent recruitment of transcriptional co-activators independent of VHL. Therefore, the gene encoding such a protein would be

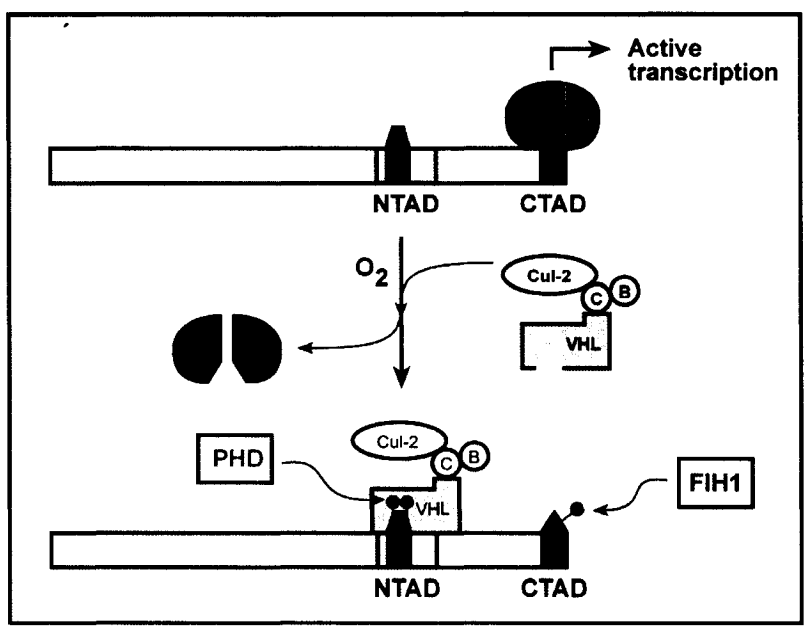
Active
transcription
NTAD
CTAD
O_2
Cul-2
C
B
VHL
PHD
Cul-2
C
B
VHL
FIH1
NTAD
CTAD

Figure 1.12

Figure 1.12. Regulation of HIF stability and activity by oxygen-dependent post-translational modifications. In the presence of oxygen, enzymes known as factor inhibiting HIF (FIH) hydroxylate a key asparagine residue within the CTAD of HIFα, thereby preventing recruitment of the co-activators p300 and CBP. In light of the role of oxygen-dependent PHDs in VHL/HIF interactions, HIF is thus regulated through prolyl hydroxylation-dependent recruitment by VHL at the level of protein turnover and through asparaginyl hydroxylation-dependent binding of co-activators at the level of transcriptional activity.

classified as a tumor suppressor for renal cell carcinoma. A recent study identified Nore1A and LSAMP as candidate tumor suppressors whose expression is lost due to the epigenetic event of promoter hypermethylation (Chen et al., 2003). It would be interesting to test whether the reintroduction of these tumor suppressor genes into VHL-deficient RCC cells abolishes normoxic HIF activation.

1.5. Subcellular dynamics of the VHL/HIF system

1.5.1. HIF degradation requires nuclear-cytoplasmic shuttling of VHL

VHL localizes predominantly to the cytoplasmic compartment but engages in a dynamic nuclear-cytoplasmic shuttle (Lee et al., 1996; Lee et al., 1999). *In vitro* studies revealed that nuclear export of VHL requires ATP hydrolysis and is Ran-dependent (see Figure 1.13 for details of Ran-dependent shuttling) (Fahrenkrog and Aebi, 2003; Groulx et al., 2000). Nuclear export of VHL does not rely on a classical nuclear export signal (NES) since it is insensitive to leptomycin B (LMB) treatment but was found to require ongoing RNA polymerase-II (RNAPII) activity as treatment with actinomycin D (ActD) or 5,6-dichlorobenzimidazole riboside (DRB) abolishes export (Lee et al., 1999). This led to the investigation of the relationship between VHL shuttling and its HIF-regulatory function in living cells (Groulx and Lee, 2002). In the presence of oxygen, HIFα molecules translated in the cytoplasm are imported in the nucleus where it is hydroxylated by PHDs. This allows VHL to recruit HIFα for nuclear ubiquitylation. VHL-mediated nuclear export of the substrate then targets it for degradation via the 26S proteasome in the cytoplasm (Figure 1.14) (Groulx and Lee, 2002). In hypoxia, loss of PHD activity allows HIFα to evade degradation activating its target genes and the VBC/Cul-2 complex

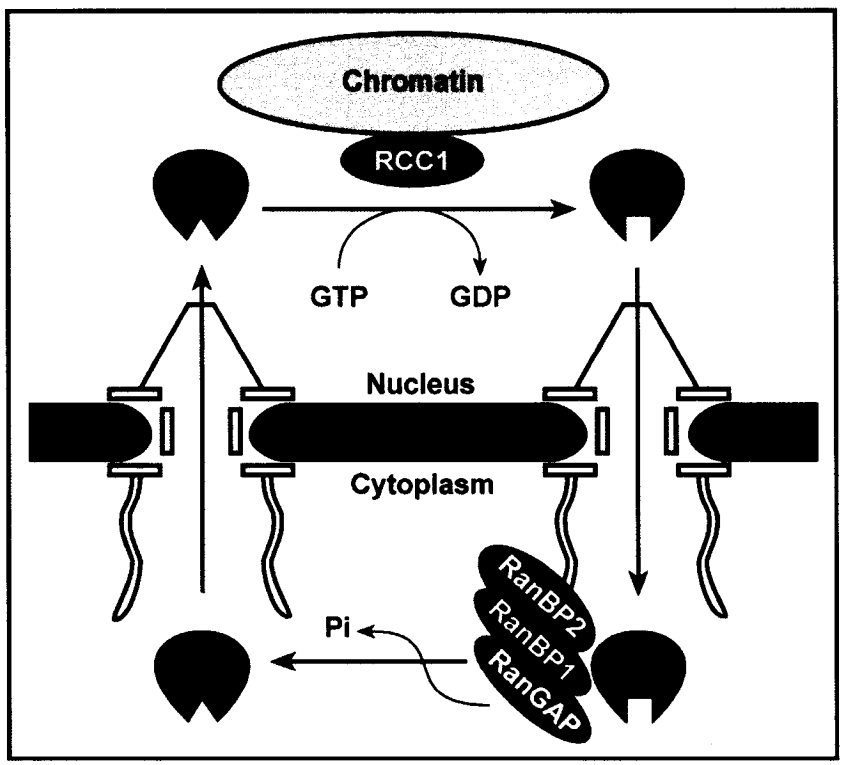
Chromatin
RCC1
GTP
GDP
Nucleus
Cytoplasm
RanBP2
RanBP1
RanGAP
Pi

Figure 1.13

Figure 1.13. The RanGTPase cycle. The RanGTPase cycle regulates the binding and release of a signal-bearing cargo from its transport receptor, and therefore gives directionality to nucleo-cytoplasmic transport. The binding of RanGTP to an import cargo–receptor complex in the nuclear near-field of a nuclear pore complex (NPC) 'throws a switch' in the receptor that lowers its affinity for the cargo, so that the cargo is released into the nucleus. An export receptor, in turn, can only escort its cargo out of the nucleus in a heterotrimeric complex with RanGTP. The Ran gradient in the cell is achieved by an asymmetric distribution of the Ran regulators, which determines the nucleotide-bound state of Ran. RCC1 — the Ran guanine-nucleotide exchange factor — is bound to chromatin in the nucleus and promotes the dissociation of GDP from Ran and allows the binding of GTP. Ran in the nucleus is therefore predominantly in its GTP-bound form. If RanGTP leaves the nucleus, the RanGTPase-activating protein (RanGAP) induces GTP hydrolysis by Ran in cooperation with two RanGTP-binding proteins (RanBP1 and RanBP2) at the cytoplasmic filaments of the NPC. In the cytoplasm, the RanGTP concentration is therefore low, whereas the RanGDP concentration is high. Pi, inorganic phosphate. (Figure adapted from (Fahrenkrog and Aebi, 2003))

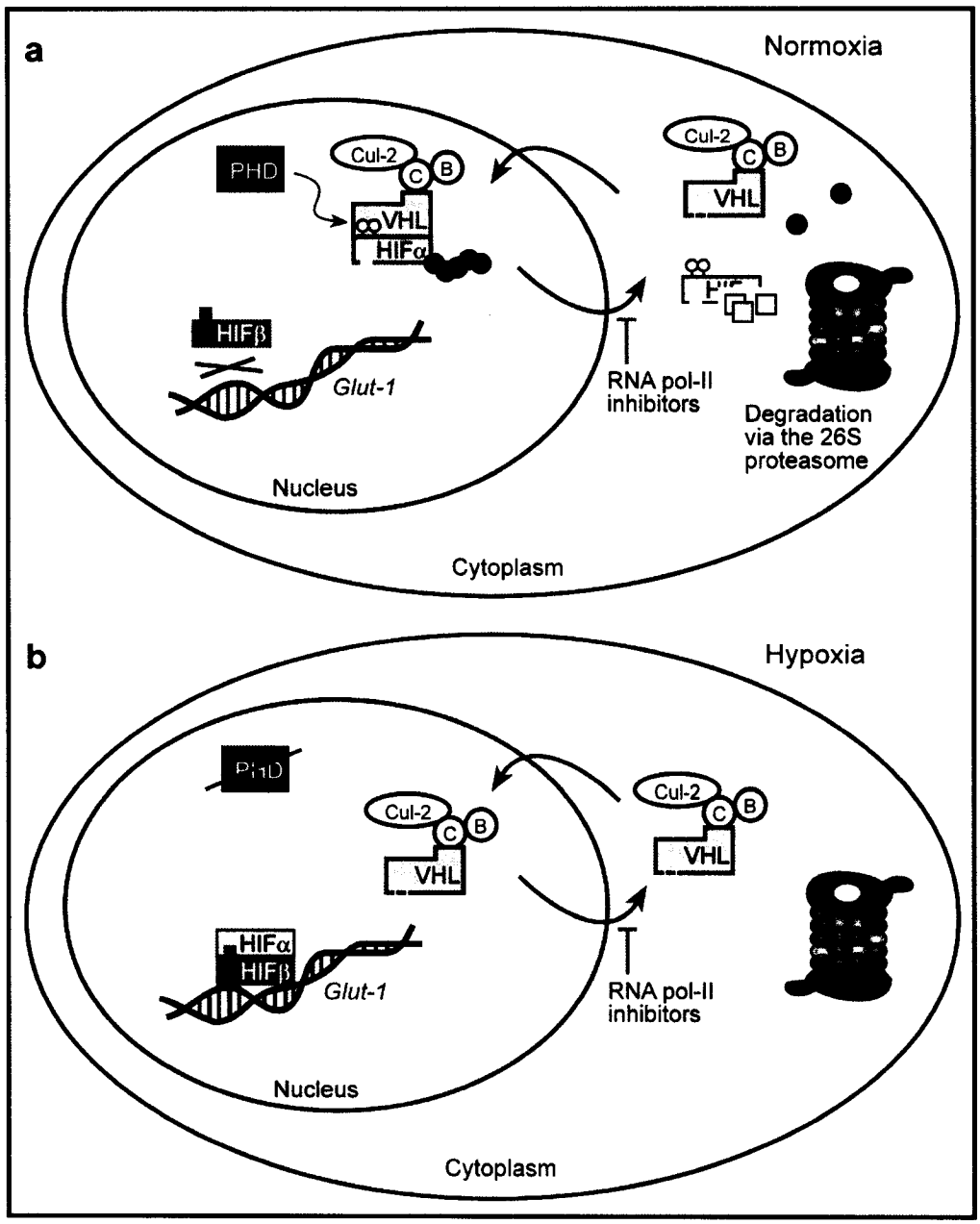
a
Normoxia
PHD
Cul-2
C
B
VHL
HIFα
HIFβ
Glut-1
RNA pol-II
inhibitors
Degradation
via the 26S
proteasome
Nucleus
Cytoplasm
b
Hypoxia
PHD
Cul-2
C
B
VHL
HIFα
HIFβ
Glut-1
RNA pol-II
inhibitors
Nucleus
Cytoplasm

Figure 1.14

Figure 1.14. Oxygen-dependent degradation of VHL requires nuclear-cytoplasmic shuttling of the VHL ubiquitin ligase. (**a**) In the presence of oxygen, PHDs hydroxylate key proline residues within HIFα allowing VHL to recruit it for cullin-2-mediated ubiquitylation. VHL-dependent nuclear export of the complex then targets HIFα for degradation via the 26S proteasome. (**b**) Inactivation of PHDs in hypoxia allows HIF to evade recognition by VHL. Stabilized HIF-α then heterodimerizes with the constitutively expressed HIF-β forming the complete transcription factor HIF, which can then activate its target genes. RNA polymerase II inhibitors such as Act-D or DRB disrupt VHL's HIF-regulatory function by blocking VHL-mediated nuclear export.

continues to shuttle between the nucleus and cytoplasm without its substrate.

1.5.2. Discrete motif allows VHL to exit the nucleus by exploiting the translational machinery

The most studied type of nuclear export signal (NES) is contained within a short peptide sequence with closely spaced large hydrophobic amino acids, especially leucines and isoleucines ($LX_{1-3}LX_{2-4}LXL$). The first classical NES sequence was identified in the human immunodeficiency virus 1 (HIV-1) Rev protein, which directs nuclear export of viral pre-mRNAs and mRNAs containing its binding site, the Rev response element (RRE) (Fischer et al., 1995). NES-containing proteins exit the nucleus via interaction with the CRM1 export receptor (Fornerod et al., 1997; Ossareh-Nazari et al., 1997; Stade et al., 1997). Until recently, the NES/CRM1 nuclear export pathway was thought to be the major route for proteins to exit the nucleus. Recently, VHL was found to interact with the elongation factor 1A (EF1A) through its now dubbed EF1A-dependent nuclear export adaptor (EDNA) domain, encoded into amino acids 121 to 129 of VHL ($DXGX_2DX_2L$), in a transcription-dependent manner (Figure 1.15) (Khacho et al., 2006). This interaction allows EF1A to mediate the egression of VHL from the nucleus. Interestingly, similar EDNA sequences were found in hundreds of proteins and have been confirmed to be required for the nuclear export of all proteins tested so far, which include the RNA metabolism factor poly(A)-binding protein 1 (PABP1), the proapoptotic protein BAX, and the cell cycle regulator Cyclin C (Khacho et al., 2006). Future work should focus on the exact role of EDNA in the functional regulation of these and other proteins.

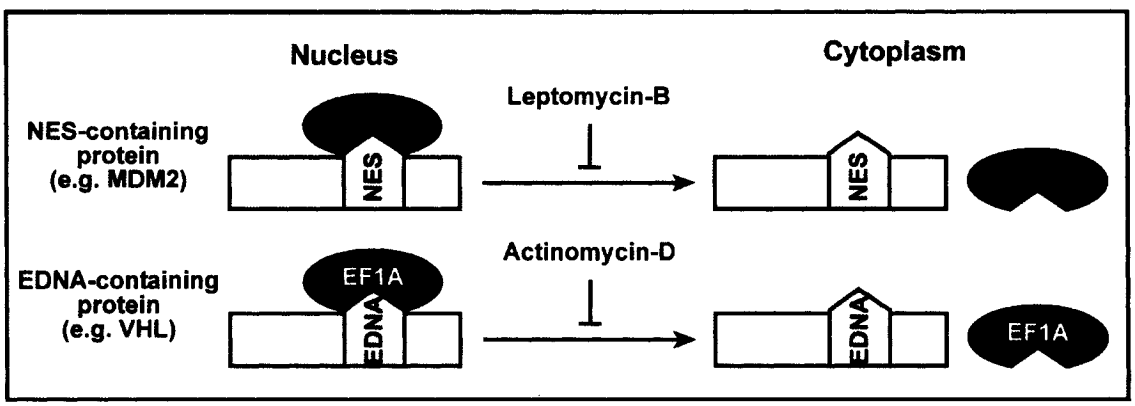
Nucleus
Cytoplasm
Leptomycin-B
NES-containing
protein
(e.g. MDM2)
NES
NES
Actinomycin-D
EDNA-containing
protein
(e.g. VHL)
EF1A
EDNA
EDNA
EF1A

Figure 1.15

Figure 1.15. Comparison of NES and EDNA nuclear export pathways. Two main nuclear export pathways seem to be present in the cell. In the first, CRM1 recognizes NES-bearing proteins. In the second, EF1A recognizes EDNA-containing proteins. Leptomycin-B inhibits CRM1, whereas EF1A/EDNA interactions are negatively regulated by Actinomycin-D treatment.

1.5.3. VHL utilizes a bipartite NLS for nuclear import

The classical nuclear localization signals (NLS) are short stretches of basic positively charged amino acid sequences capable of mediating nuclear import of proteins. The first classical NLS sequences were first identified in SV40 large T antigen and nucleoplasmin. VHL, similar to the p53 tumor suppressor, contains another type of NLS, a bipartite NLS ($PRRX_{53}RPRPV$) (Lee et al., 1996), which are usually comprised of two basic clusters separated by a variable number of different types of amino acids. All NLS sequences are recognized by a heterodimeric complex called the NLS receptor, which is composed of importins α and β. This complex facilitates the nuclear import of VHL driven by cycling of GTP hydrolysis involving the small GTPase, Ran.

1.5.4. Nuclear-cytoplasmic trafficking of ligases, substrates and tumor suppressors is commonly observed in ubiquitin proteasome degradation systems

It is becoming increasingly evident that the degradation of several nuclear proteins requires nuclear-cytoplasmic shuttling of the substrate proteins, as well as the E3 ubiquitin ligase (Figure 1.16). For example, similar to the VHL/HIF system, the murine double minute oncoprotein (MDM2) and anaphase promoting complex (APC) ubiquitin ligases target the p53 tumor suppressor protein and β-catenin for ubiquitylation in the nucleus followed by nuclear export for degradation by the cytoplasmic 26S proteasome, respectively (Freedman and Levine, 1998; Michael and Oren, 2003; Momand et al., 1992; Oliner et al., 1993; Roth et al., 1998). Similarly, proteasomal degradation of TGF-β-induced transcription factor Smad3 and the nuclear cyclin-dependent kinase inhibitor $p27^{kip1}$ requires nuclear export by SCF^{Fbw1a} and Jab1, respectively

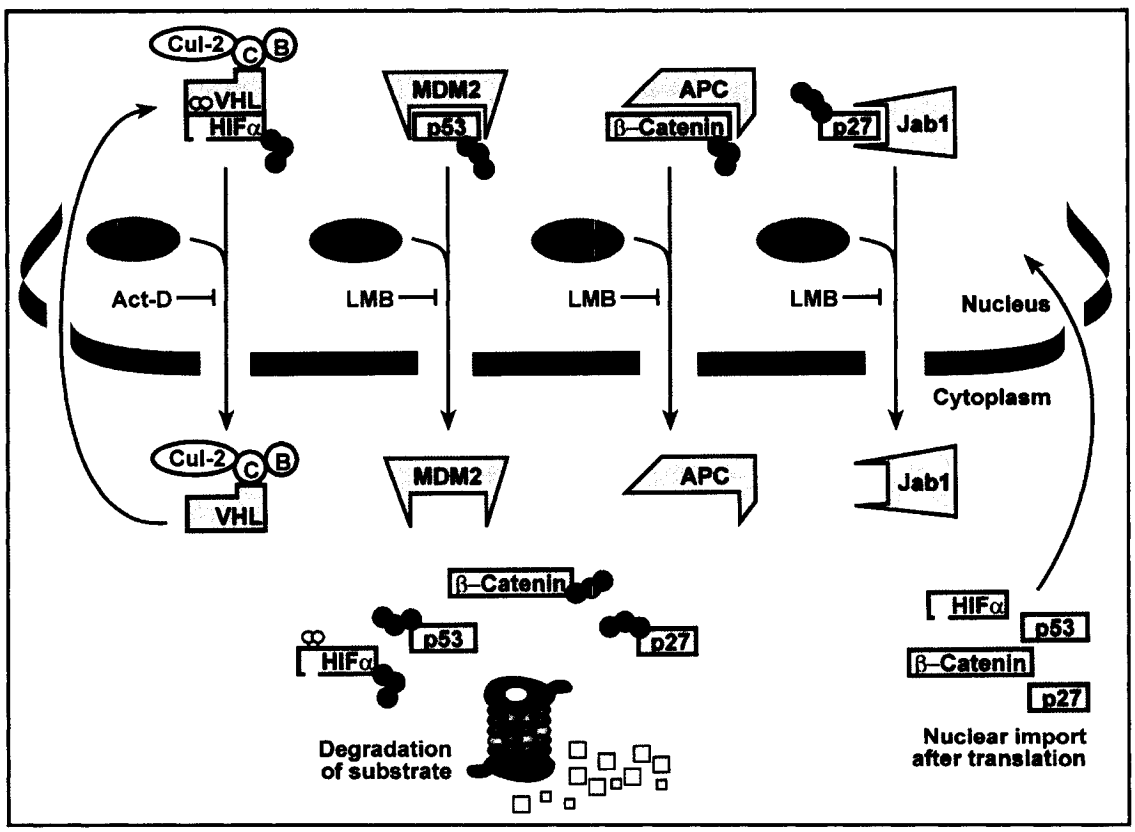
Cul-2
C
B
VHL
HIFα
MDM2
p53
APC
β-Catenin
p27
Jab1
Act-D
LMB
LMB
LMB
Nucleus
Cytoplasm
Cul-2
C
B
VHL
MDM2
APC
Jab1
β-Catenin
p53
HIFα
p27
Degradation
of substrate
HIFα
p53
β-Catenin
p27
Nuclear import
after translation

Figure 1.16

Figure 1.16. Examples of E3 ligases regulating nuclear protein function through nuclear-cytoplasmic shuttling. Similar to the VHL/HIF system, the MDM2 ubiquitin ligase targets p53 for nuclear ubiquitylation followed export for cytoplasmic proteasomal degradation. Similarly, degradation of β-catenin and $p27^{kip1}$ require nuclear export of the E3 ubiquitin ligase APC and Jab1, respectively. While export is required for all these processes, note that exporters can differ. For example, VHL is exported by EF1A whereas MDM2 exits the nucleus via CRM1.

(Fukuchi et al., 2001; Tomoda et al., 1999). While these studies have uncovered a general requirement for nuclear export in the ubiquitin proteasome system and the modulation of tumor suppressors, this raises the question as to how molecules can efficiently find the nuclear pore, other targets or interacting partners in space.

1.5.5. Physical nature of macromolecular dynamics in the cell

Pioneering of technologies utilizing fluorescent proteins from marine organisms, of which the most commonly used is the green fluorescent protein (GFP) from the jellyfish *Aequorea victoria*, or other fluorescent markers have revolutionized the study of macromolecular dynamics (Lippincott-Schwartz et al., 2003; Lippincott-Schwartz et al., 2001). For example, photobleaching technology such as fluorescence recovery after photobleaching (FRAP) and fluorescence loss in photobleaching (FLIP) (Figure 1.17) make it possible to analyze various aspects of the movement of a molecule by measuring speed and assessing affinity to particular cellular components. These techniques have been applied to assess the nature of the movement of proteins within different cellular compartments. Such studies revealed that most proteins follow a stochastic model of energy-independent high diffusional mobility to ensure efficient functional interactions (Dundr et al., 2002; Misteli, 2001; Phair and Misteli, 2000). An advantage of such probabilistic movement is the ability to achieve rapid responses to signaling cues. For example, a slight increase in the quantity of a modified protein results in a relatively high probability of encountering its target. In fact, this dynamic character is not restricted to polypeptides as energy-independent diffusional movement is sufficient to effectively transport mRNA from its site of transcription to the nuclear pore (Politz et al., 1998; Politz et al., 1999).

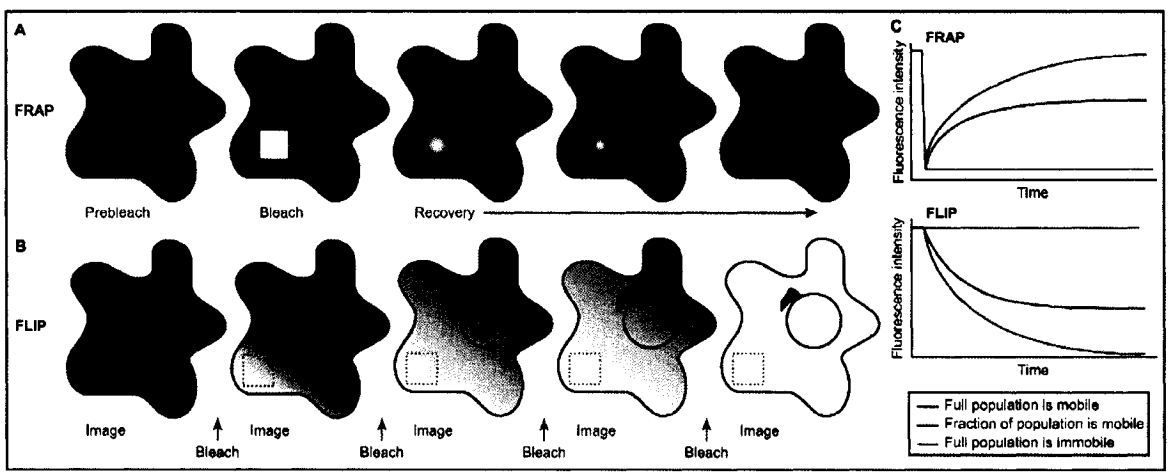
A
FRAP
Prebleach
Bleach
Recovery
B
FLIP
Image
Bleach
Image
Bleach
Image
Bleach
Image
Bleach
Image
C
FRAP
Fluorescence intensity
Time
FLIP
Fluorescence intensity
Time
Full population is mobile
Fraction of population is mobile
Full population is immobile

Figure 1.17

Figure 1.17. Conceptual basis for fluorescence recovery after photobleaching (FRAP) and fluorescence loss in photobleaching (FLIP) technology. FRAP and FLIP can be used to assess the dynamic properties of fluorescently labeled macromolecules in the cell (Lippincott-Schwartz et al., 2003). (**a**) In FRAP, specific cellular regions expressing fluorescent protein chimeras are bleached with the use of a laser pulse that irreversibly quenches the fluorescent signal, and the recovery of signal in the bleached area is recorded by time-lapse confocal microscopy. The kinetics and extent of recovery of fluorescence in a cellular region following bleaching are reflective of the dynamics of the studied fluorescent chimeras. (**b**) In FLIP, a living cell is repeatedly hit with a laser beam in the same region. Loss of fluorescence in an area outside the bleached spot is reflective of protein mobility between that area and the bleached spot.

1.6. VHL's involvement in cancer

1.6.1. VHL-loss abolishes oxygen-sensing capacity

Since PHDs require molecular oxygen, hypoxia prevents hydroxylation of HIFα and its subsequent recognition by VHL (Kaelin, 2002). Stabilized HIF activates its targets to orchestrate the cellular response to low oxygen levels (Semenza, 1998; Semenza, 2003). $VHL^{-/-}$ RCC cells therefore lose their "oxygen sensing" capacity as they constitutively express HIF, which then activates its target genes independent of oxygen tension. This is supported by several studies such as reports showing that VHL-deficiency results in highly vascularized tumors and elevated glycolytic rates (Kaelin, 2002).

1.6.2. HIF-2α, but not the pro-angiogenic HIF-1α, activates the TGF-α/EGFR growth-stimulatory pathway

Thus, HIF activates a myriad of genes that contribute to tumor development by promoting processes such as angiogenesis (VEGF) and glycolysis (Glut-1) (Table 1.1). However, the finding that HIF-2α, but not the pro-angiogenic HIF-1α, activates transforming growth factor-α gene expression to stimulate the epidermal growth factor receptor (EGFR) was the first direct link between HIF activation and the acquisition of autonomous growth capacity in $VHL^{-/-}$ RCC cells (de Paulsen et al., 2001; Franovic et al., 2006; Gunaratnam et al., 2003; Kaelin, 2002; Smith et al., 2005). Several lines of evidence support the hypothesis that HIF-2α-mediated activation of the TGF-α/EGFR autonomous growth program is the major oncogenic pathway in RCC (Figure 1.18). First, RNA interference-mediated silencing of EGFR expression prevented $VHL^{-/-}$ RCC cells from forming tumors in nude mice (Smith et al., 2005). Second, introduction of

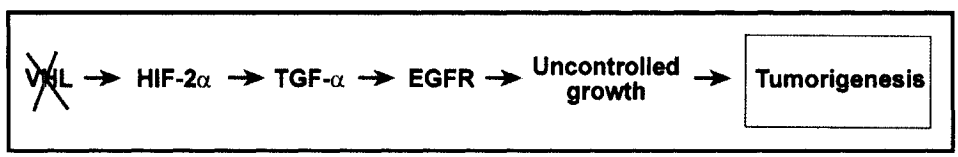

Figure 1.18

Figure 1.18. Oncogenic pathway of RCC. VHL loss uncouples HIF from oxygen-dependent regulation. Constitutively expressed HIF-2α transactivates TGFα, which in turn activates the EGF receptor, conferring autonomous growth capability to affected cells.

HIF-2α variants (but not similar HIF-1α variants), which evade recognition by VHL in the presence of oxygen, into VHL-deficient RCC cells expressing reintroduced VHL abolishes its tumor suppressor function as revealed by tumor formation in nude mice (Kondo et al., 2002; Maranchie et al., 2002). Third, oligonucleotides against TGF-α mRNA or inhibition of ligand cleavage prevent the autonomous growth ability of $VHL^{-/-}$ RCC cells or tumorigenesis (de Paulsen et al., 2001; Franovic et al., 2006). Fourth, HIF-2α dominant negative prevents TGF-α production, blocks EGFR phosphorylation and reduces proliferation of RCC cells in serum-free media (Gunaratnam et al., 2003).

1.6.3. HIF-dependent and -independent functions of VHL

Gene expression analysis indicates that the sets of genes regulated by VHL and HIF are overlapping, but not identical (Wykoff et al., 2000). Consistent with these findings, several apparently HIF-independent functions have been ascribed to VHL. VHL has been proposed to serve as an E3 ligase for the λ subunit of protein kinase C (PKCλ) (Okuda et al., 1999; Okuda et al., 2001; Pal et al., 1998; Pal et al., 1997) and to inhibit the SP1 transcription factor through an unidentified mechanism (Cohen et al., 1999; Mukhopadhyay et al., 1997), but more work should elucidate these proposed functions. However, the role of VHL in extracellular-matrix assembly and epithelial differentiation is clearer (Esteban-Barragan et al., 2002; Lieubeau-Teillet et al., 1998; Ohh et al., 1998). VHL-deficient RCC cells secrete fibronectin but are defective with respect to fibronectin-matrix assembly (Ohh et al., 1998), which is thought to play a role in RCC development. VHL-competent RCC cells are able to deposit an extracellular fibronectin matrix, and this is associated with the differentiated phenotype of these cells (Kurban et al., 2006; Ohh et al., 1998; Stickle et al., 2004). Fibronectin is an extracellular glycoprotein that

signals through integrin cell surface receptors. Loss of fibronectin matrix assembly is another characteristic that has long been recognized as a feature of cellular transformation (Ruoslahti, 1984), as is the ability of tumor cells to avoid cellular differentiation (Hanahan and Weinberg, 2000). In a three-dimensional *in vitro* growth assay that mimics tumor formation *in vivo*, VHL-deficient cells form very dense tumor spheroids comprised of undifferentiated cells packed together with no apparent organization. This contrasts with VHL-competent RCC cells, which form cellular aggregates with tubular and trabecular like structures and proper fibronectin deposition (Lieubeau-Teillet et al., 1998). In fact, Davidowitz *et al.* (2001) found that VHL mediates both the morphological and biochemical differentiation of renal proximal tubule epithelial cells. VHL can induce renal cell differentiation and mediate growth arrest through the integration of cell-cell and cell-extracellular matrix signals. Combined, these findings suggest that the only genetic alteration required for tumor formation and progression in human RCC is loss of VHL function. While defects in fibronectin-matrix assembly are observed in VHL-deficient cells irrespective of HIF expression, it is still unclear whether VHL loss requires HIF activation to regulate the transcription of several genes that are implicated in extracellular-matrix turnover, such as tissue inhibitors of metalloproteinases (TIMPs) and matrix metalloproteinases (MMPs).

Several ubiquitin-like (UBL) proteins have been identified and most of them are believed to have direct effects on ubiquitylation. Interactions of the metazoan ubiquitin-like protein Nedd8 (Neural precursor cell expressed developmentally down-regulated 8), the homologue of yeast Rub1, with the Cul-2 and VHL moieties of VBC/Cul-2 are thought to be required for the normal functioning of VHL in both HIF- and fibronectin-

regulatory systems (Bonicalzi et al., 2001; Liakopoulos et al., 1999; Stickle et al., 2004; Wada et al., 1999a; Wada et al., 1999b).

1.6.4. Correlations between VHL disease types and molecular defects

Comparison of known molecular defects to clinical manifestations has revealed some genotype–phenotype correlations in VHL disease (Table 1.3). Most noticeable is the observation that VHL families with a high risk of phaeochromocytoma (type 2 VHL disease) often harbor a VHL missense mutation. Mutations causing complete loss of the VHL gene product or grossly disrupting VHL protein folding are associated with a noticeably reduced risk of phaeochromocytoma (type 1 VHL disease). Together, these observations have led to the idea that phaeochromocytoma development in VHL disease either reflects a VHL gain of function or requires partial but not complete loss of VHL function. Type 2 VHL families can have a low risk (type 2A) or high risk (type 2B) of kidney cancer. Also noteworthy is the fact that some families have an increased risk of phaeochromocytoma without the other classical stigmata of VHL disease (type 2C VHL disease).

1.7. Physiological/pathological implications for the VHL/HIF system

Understanding HIF is not just important for cancer. Several major diseases of industrialized nations, including myocardial ischemia, stroke and peripheral vascular disease, as well as normal physiological settings such as muscle exercise and embryonic development are characterized by tissue hypoxia (Semenza, 2000a; Semenza, 2000b). HIF plays a principal role in the adaptation to hypoxia and changes induced by it

Type of VHL disease	VHL mutation type	Molecular defect	Clinical manifestation
Type 1	Loss of VHL or a mutation that affects protein folding	Upregulation of HIFα and HIF target genes	Hemangioblastomas Diminished risk of phaeochromocytoma Renal-cell carcinoma
Type 2A	VHL missense mutation	Upregulation of HIFα and HIF target genes	Hemangioblastomas Phaeochromocytoma Low risk of renal-cell carcinoma
Type 2B	VHL missense mutation	Upregulation of HIFα and HIF target genes	Hemangioblastomas Phaeochromocytoma High risk of renal-cell carcinoma
Type 2C	VHL missense mutation	VHL retains ability to degrade HIFα; decreased binding to fibronectin and fibronectin matrix assembly defect	Phaeochromocytoma only

Table 1.3

Table 1.3. Characteristics of different types of VHL disease

Table adapted from (Kaelin, 2002).

include alterations to glucose uptake and metabolism, which sustain energy generation under anaerobic respiration (further discussed in section 1.8), as well as changes in angiogenesis and red-blood-cell production, which increase oxygen delivery to affected tissues. In theory, small molecules that induce the transient stabilization of HIF could improve the cellular and tissue response to hypoxia in settings such as ischemic diseases. This stabilization might be achieved through pharmacological inhibition of PHDs. The feasibility of such an approach was established with drugs that inibit PHDs by antagonizing iron or 2-oxoglutarate in earlier studies of the collagen prolyl hydroxylases (Figure 1.10) (Kaelin, 2002). One of these compounds, FG0041, was shown earlier to preserve myocardial function when given to rats following experimentally-induced myocardial infarction (Nwogu et al., 2001). Although the rationale for these studies contributed these beneficial effects to the potential inhibition of myocardial fibrosis, it has been suggested that it is more likely that these positive effects were related to the stabilization of HIF (Kaelin, 2002). This proposal is strongly supported by the fact that HIF activation correlated with cerebral tissue survival in ischemia-reperfusion experiments performed *in vivo* (Chavez and LaManna, 2002; Sun et al., 2003).

1.8. The role of HIF in basic metabolism

1.8.1. Aerobic energetics

In the presence of oxygen, we extract energy from food through three main stages. First, macromolecules are degraded into monomeric molecules via digestion in extracellular environments. Proteins are broken down into amino acids, polysaccharides into simple sugars, and fats into fatty acids and glycerol. Second, a chain of ten cytosolic reactions,

known as glycolysis, converts each molecule of glucose into two molecules of pyruvate. Sugars other than glucose are similarly converted to pyruvate after their conversion to one of the sugar intermediates of glycolysis. The net energy gain following glycolytic combustion of each glucose molecule is stored into two types of high energy carriers, two molecules of ATP and two molecules of NADH. Third, each pyruvate is then transferred to mitochondria where it is converted into the acetyl coenzyme-A (AcCoA) energy carrier. Fatty acids in the bloodstream are also imported into cells and then moved to mitochondria for the production of additional large amounts of AcCoA. Each AcCoA molecule then enters a series of eight reactions known as the citric acid cycle (CAC; also known as the tricarboxylic acid cycle or the Krebs Cycle) where it is oxidized into oxaloacetate generating two molecules of CO_2 as waste product and several energy carrying molecules: three NADH, one $FADH_2$ (reduced flavin adenine dinucleotide), and one GTP (guanosine triphosphate). The high-energy electrons from NADH and $FADH_2$ are passed along an electron transport chain within the mitochondrial inner membrane, where the energy released by their transfer is used to drive a process that produces ATP and consumes molecular oxygen, which serves as the last electron acceptor yielding water molecules. In addition to its role in energy production, NADH breakdown through the electron transfer chain ensures survival by replenishing glycolysis with NAD^+, a scarce cellular co-enzyme that cannot be used stoichiometrically. In the presence of oxygen, about 10^9 molecules of ATP are in solution in a typical cell at any instant, and in many cells, all this ATP is used and replaced every one to two minutes. Maximal ATP yield per glucose molecule is summarized in Table 1.4.

Processes	Manufactured carriers	Conversion by ETC
Glycolysis	2 ATP, 2 NADH	8 ATP
AcCoA	2 NADH	6 ATP
CAC	6 NADH, 2 $FADH_2$, 2 GTP	22 ATP, 2 GTP
Total	2 ATP, 10 NADH, 2FADH2, 2GTP	36 ATP, 2 GTP

Table 1.4

Table 1.4. Summary of maximal energy yields from the cellular combustion of a glucose molecule.

1.8.2. Mitochondrial evolution and the energy revolution

Mitochondria constitute the double-membrane-bound powerhouse of eukaryotic cells. Concepts of the origin of eukaryotes can be classified into two general classes. Those where a nucleus-bearing amitochondriate eukayortic host cell first emerges then acquires mitochondria, and those that derive the origin of mitochondria in a prokaryotic host that later acquires eukaryotic-specific features. However, additional layers of complexity have recently been introduced to this long debate since it was recently shown that phagotrophy, long viewed as a prerequisite for endosymbiotic relationships, may not be a prerequisite for mitochondrial origins as one prokaryote was found to live inside another non-phagocytic prokaryote (von Dohlen et al., 2001). The single celled eukaryote *Giardia intestinalis* (a pathogen that shuns oxygenated environments and causes diarrhea when it infects the human intestine) is considered to be a living intermediate, a "living fossil" from the time of the prokaryote-to-eukaryote transition, because it possesses a nucleus but was thought to lack mitochondria. However, it was recently discovered that Giardia contains mitosomes, highly reduced mitochondria that do not function in core ATP synthesis but are essential for the assembly of iron-sulphur (Fe-S) clusters. While mitosomes and other reduced versions of mitochondria sustain the debate on the origin of this cellular powerhouse, it is clear that the advent of oxidative phosphorylation facilitated the evolution of energy demanding metabolic pathways otherwise incompatible of anaerobic energy generators, which will now be discussed.

1.8.3. Anaerobic energetics

Cells facing low oxygen tension reorganize their basic metabolic networks, a phenomenon known as anaerobic metabolism, in an effort to maintain energy equilibrium

and viability. Mitochondrial respiration is repressed due to the scarcity of oxygen as an electron acceptor. Hypoxic cells maximize anaerobic energy production by both triggering the Pasteur effect, a HIF-dependent increase in glycolytic rate (Figure 1.19) (Barker et al., 1966; Hardie, 2000; Iyer et al., 1998; Pasteur, 1857; Seagroves et al., 2001), and converting pyruvate to lactate through fermentation, which efficiently replaces mitochondria with regard to the task of replenishing glycolysis with NAD^+ (Figure 1.19) (Gladden, 2001). This causes extracellular acidosis as lactate molecules (La^-) are coupled to hydrogen ions and released in the environment in the form of lactic acid (La^-H^+).

While hypoxic cells attempt to maximize glycolytic energy production through the above described processes, this far from compensates for the loss of mitochondrial respiration and total cellular ATP levels still decrease by over 60-70% relative to normoxic concentrations (Liu et al., 2006). Although dramatic reductions in energy levels are toxic, they might contribute to the Pasteur effect (Hardie, 2000). Similarly, it was suggested that energy starvation could act as a last resort and limit translational energy consumption (Inoki et al., 2003; Liu et al., 2006).

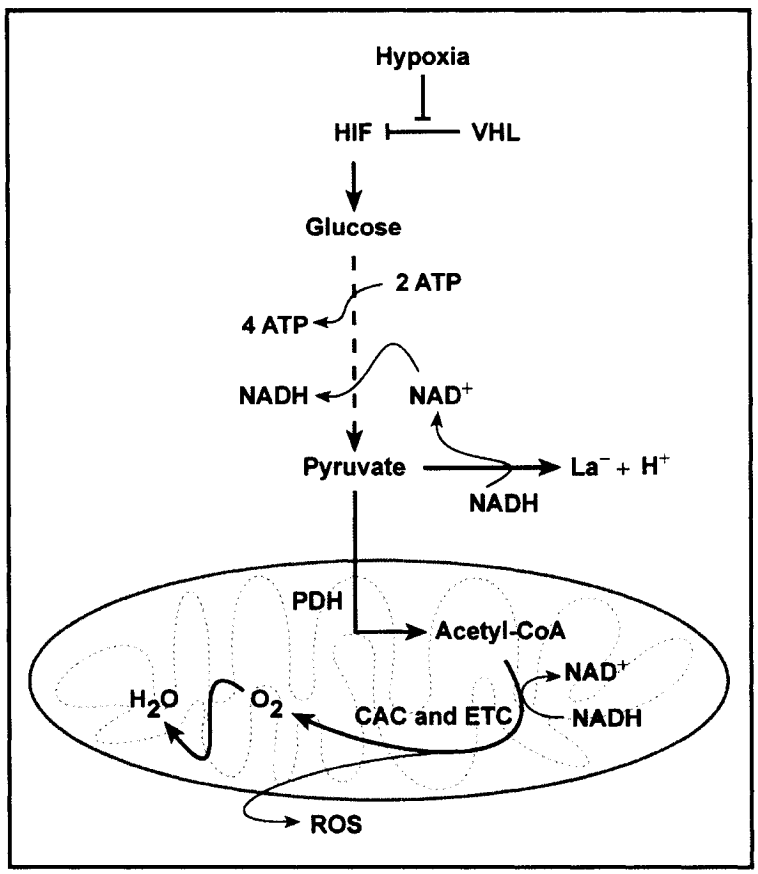
Hypoxia
HIF
VHL
Glucose
2 ATP
4 ATP
NADH
NAD+
Pyruvate
La− + H+
NADH
PDH
Acetyl-CoA
NAD+
H2O
O2
CAC and ETC
NADH
ROS

Figure 1.19

Figure 1.19. Emerging role of HIF in anaerobic metabolism. Stabilization of HIF under low oxygen tension allows it to increase the glycolytic rate (Pasteur effect) and actively block oxidative phosphorylation, resulting in the activation of fermentation, production of lactic acid and acidification of the extracellular milieu. HIF also activates CAIX to help prevent severe fluctuations in intracellular pH.

1.9. Statement of the rationale, hypothesis and objectives

1.9.1. Rationale

RCC affects over 12,000 Canadians each year and is primarily caused by inactivating mutations of the VHL tumor suppressor gene. VHL acts as the particle recognition motif of a multisubunit ubiquitin ligase mediating oxygen-dependent degradation of HIF, which is therefore activated by hypoxia to activate genes that mediate cellular adaptation to low oxygen tension. VHL mutations uncouple HIF ubiquitylation/degradation from oxygen-dependent control resulting in a constitutive hypoxia-like cellular response that drives tumorigenesis. Pharmacologically-induced inhibition of VHL-mediated nuclear export of the E3 ligase complex abrogates HIF degradation in the presence of oxygen, suggesting that modulation of VHL nuclear-cytoplasmic shuttling could be a regulated event under various physiological or pathological settings.

1.9.2. Hypothesis

The VHL tumor suppressor is functionally regulated by physiological conditions or mutations modulating its subcellular trafficking.

1.9.3. Objectives

Objective 1. *Identify physiological conditions altering VHL subcellular trafficking and study their effect on HIF regulation.* We aim to identify signals affecting VHL subcellular trafficking by testing different environmental parameters observed under different physiological and pathological conditions.

Objective 2. *Identify characteristics of the mechanism by which VHL shuttling is altered.* Once a signal is identified, we will investigate how it affects the movement of

VHL between the nucleus and cytoplasm and/or identify VHL sequences involved in sensing such signals.

Objective 3. *Determine if changes to VHL subcellular dynamics allow the tumor suppressor to exert novel biochemical functions.* We envision that changes in the subcellular distribution of VHL could allow it to exert new functions in specific cellular compartments.

Chapter 2. HIF activation by pH-dependent nucleolar sequestration of VHL

Papers and author contribution:

(1) Introduction, Methods, Results, Discusion Part 1:

- Paper:

Mekhail, K., Gunaratnam, L., Bonicalzi, M. E., and Lee, S. (2004) HIF activation by pH-dependent nucleolar sequestration of VHL. Nature Cell Biol. 6:642-647.

- Author Contributions:

K. Mekhail:	Interpretation, text and all figures All experiments
L. Gunaratnam:	Interpretation and contributed to text
M.-E. Bonicalzi:	Former student who first saw VHL in subnuclear foci

(2) Discusion Part 2:

- Paper:

Mekhail, K., Khacho, M., Gunaratnam, L., and Lee, S. (2004) Oxygen sensing by H+: implications for HIF and hypoxic cell memory. Cell Cycle 3:1027-1029.

- Author Contributions:

K. Mekhail:	Interpretation, text and all figures
M. Khacho:	Contributed to text and interpretation
L. Gunaratnam:	Contributed to text and interpretation

HIF activation by pH-dependent nucleolar sequestration of VHL

Karim Mekhail[1], Lakshman Gunaratnam[1], Marie-Eve Bonicalzi[1], and Stephen Lee[1]

[1]Department of Cellular and Molecular Medicine, Faculty of Medicine, University of Ottawa, Ottawa, Ontario, Canada K1H 8M5.

[2]Correspondence should be addressed to S.L. (e-mail: slee@uottawa.ca)

Published Manuscript

Nature Cell Biology 6:642-647 (2004)

Abstract

Hypoxia and acidosis occur in a wide variety of physiological and pathological settings that include muscle stress, tumour development and ischaemic disorders. A central element in the adaptive response to cellular hypoxia is HIF (hypoxia-inducible factor), a transcription factor that activates an array of genes implicated in oxygen homeostasis, tumour vascularization and ischaemic preconditioning (Semenza, 2000a). HIF is activated by hypoxia, but undergoes degradation by the VHL (von Hippel-Lindau) tumour suppressor protein in the presence of oxygen (Jaakkola et al., 2001; Maxwell et al., 1999). Here, we demonstrate that hypoxia induction or normoxic acidosis can neutralize the function of VHL by triggering its nucleolar sequestration, a regulatory mechanism of protein function that is observed rarely (Shou et al., 1999; Tsai and McKay, 2002; Visintin et al., 1999; Weber et al., 1999). VHL is confined to nucleoli until neutral pH conditions are re-instated. Nucleolar sequestration of VHL enables HIF to evade destruction in the presence of oxygen and activate its target genes. Our findings suggest that an increase in hydrogen ions elicits a transient and reversible loss of VHL function by promoting its nucleolar sequestration.

Introduction

HIF is a transcription factor that functions in the cellular response to hypoxic stress, and has been implicated in a wide variety of biological processes that include ischaemia, cardiac arrest, muscle stress and tumour development (Semenza, 2000a; Wagner, 2001). It is primarily regulated by oxygen-dependent proteasomal destruction of its α subunit (HIFα) (Kaelin, 2002; Maxwell et al., 1999). Under normal oxygen tension, HIFα is degraded by a process that requires the VHL tumour suppressor — the recognition motif of an E3 ubiquitin ligase (Kaelin, 2002). Hypoxia suppresses HIF degradation, allowing it to activate its targets, which include vascular endothelial growth factor and glucose transporter-1 (Glut-1) (Harris, 2002). Ischaemic tissues or hypoxic cells normally acidify their extracellular milieu as a physiological consequence of anaerobic glycolysis. This is best exemplified by muscle fatigue, in which myotubes produce lactic acid after exposure to hypoxia. Acidosis has been reported to exert protective effects in rat skeletal muscle, and to improve cellular survival in several physiological and pathological situations (Currin et al., 1991; Giffard et al., 1990; Kaku et al., 1993; Morimoto et al., 1997; Nielsen et al., 2001).

Materials and Methods

Cell lines. C2C12 and PC12 cells from ATCC (Manassas, VA) were differentiated by lowering the serum concentration from 5% to 0.5%, respectively, or by addition of nerve growth factor (NGF, 50 ng ml−1), before infection with adenoviruses. HEK293, 786-0 (VHL-defective), U87MG, HOP62, MCF7 and HeLa cells were also obtained from ATCC (Manassas, VA). VHL-negative 117 cells were a kind gift from J. Gnarra, Louisiana State University. 786 (ref. (Lee et al., 1999)) or 117 cells stably expressing HA–VHL (WT7; a kind gift from W. Kaelin, Harvard University) (Iliopoulos et al., 1995) or VHL–GFP were generated as described (Lee et al., 1999).

Cell culture. Normoxic cells were incubated at 37 °C under a 5% CO2 environment. Hypoxia was achieved by incubation in a hypoxic chamber at 37 °C under a 1% O2, 5% CO2 and N2-balanced atmosphere. For standard (SD) or acidosis-permissive (AP) conditions, buffer-free medium (DMEM; Invitrogen, Carlsbad, CA) was freshly prepared and supplemented with 5% (v/v) foetal bovine serum (FBS) and 1% (v/v) penicillin-streptomycin. aHCO3 was added (44 mM for hypoxic and 10 mM for normoxic experiments) and the pH was adjusted to 7.2 (SD) or 5.8–6.0 (AP) with HCl. ir was bubbled into both media at 22 °C, which stabilizes the pH at 7.2. The AP media slowly reverted to its original pH (initial pH 5.8 or 6.0) under hypoxia or normoxic Warburg effect, whereas the SD medium remained at pH 7.2. Cells treated with conditioned AP (at pH 6.0) or SD (at p 7.2) media (Fig. 2.9) were pre-treated with conditioned AP media at pH 6.9 for 2 h after conditioned AP media at pH 6.7 for one hour to minimize sudden

sharp changes in pH. Adenovirus-infected cells were grown for 24 h under SD conditions before any treatment.

Spheroid culture. Multicellular spheroids (Sutherland, 1988) were prepared by the liquid overlay technique. Briefly, 24-well plates were coated with 250 μl of pre-heated 1% Seaplaque agarose (Cambrex, Rockland, ME) in serum-free medium. 105 cells were plated per 1 ml of SD media per well. To promote cell–cell adhesion, the plates were swirled 30 times at 15 and 30 min after plating. Spheroids were grown for six days in freshly maintained SD media at 37 °C under a 5% CO2 environment. Spheroids were visualized either while living or were frozen, sectioned and Hoechst-stained for DNA.

Plasmids and adenovirus construction. VHL and deletion mutants — referred to as ΔN for N terminal, ΔC for C terminal and Δ for internal truncations — were cloned between an N-terminal Flag-tag and a C-terminal GFP-tag and into pcDNA3.1, as previously described (Bonicalzi et al., 2001; Groulx and Lee, 2002). HeLa cells were transiently transfected with Effectene transfection reagent (Qiagen,Valencia, CA). Adenoviruses were produced using the Cre-lox recombination system (Bonicalzi et al., 2001; Groulx and Lee, 2002; Gunaratnam et al., 2003).

Sub-cellular fractionation. Cells were harvested in transport buffer containing 20 mM Hepes at pH 7.3, 110 mM potassium acetate, 5 mM sodium acetate, 2 mM magnesium acetate, 1 mM EGTA, 2 mM dithiothreitol and a cocktail of protease inhibitors added shortly before use (leupeptin, 2 μg ml−1; aprotinin, 2 μg ml−1; pepstatin A, 1 μg ml−1). Cells were left on ice to equilibrate for 1 min before the addition of Triton X-100 (1% v/v). Permeabilization was monitored by fluorescence microscopy with Hoechst stain 33258 (Sigma, St. Louis, MO), which only stains nuclei of permeabilized cells. Cells

were centrifuged to separate Triton-insoluble from soluble material, and lysed in a final concentration of 5% SDS. Equal final volume was maintained for both fractions. The nuclear extracts were prepared as described17.

Immunoblotting. Cells were either treated as described for sub-cellular fractionation or harvested in 5% SDS in PBS. Samples (20–100 μg of each) were separated on denaturing polyacrylamide gels containing SDS and transferred to methanol-activated polyvinylidene difluoride membrane (NEN, Boston, MA). Membranes were blocked in skimmed milk before incubation with HA, Flag-M2, B23, LDH (Sigma, St. Louis, MO), HIF-1α (BD Transduction Laboratories, Lexington, KY) or VHL monoclonal antibodies18,19 (BD Pharmingen, San Diego, CA). Polyclonal antibodies were used to detect Glut-1 (Alpha Diagnostic International, San Antonio, TX), actin (Sigma) or HIF-2α (Novus, Littleton, CO). After washing with 0.2% Tween-PBS solution, membranes were blotted with secondary antibodies conjugated to horseradish peroxidase (Jackson ImmunoResearch,West Grove, PA) and detected by enhanced chemiluminescence (Pierce, Rockford, IL).

Immunofluorescence microscopy. For Flag, HA, VHL and B23 antibodies, cells were seeded onto coverslips and fixed with pre-chilled (to –20 °C) methanol for 10 min followed by acetone for 1 min. Cells were incubated for 1 h with a primary antibody solution (10% FBS v/v). For anti-HIF-1α antibody, cells were fixed with 1% formaldehyde in PBS for 20 min prior to incubation with a primary antibody solution containing 10% FBS and 1% Triton-X-100 (v/v). All cells were washed several times in PBS before 1 h incubation with a secondary Texas Red-labelled antibody (Jackson ImmunoResearch). See Immunoblotting section for sources of primary antibodies.

Images were captured with an Axiovert S100TV microscope (for living cells), or an Axioskop 2 MOT PLUS (for fixed cells) — both from Zeiss (Thornwood, NY). Total cellular GFP signal was measured by multiplying the area of the cell by the integrated pixel intensity within the cell and subtracting the background value obtained from a cell-free region of the image. Crude nucleolar GFP signal per pixel was obtained by measuring intensity per nucleolar pixel and subtracting mean pixel background. Average pixel intensity associated with nucleoli in neutral conditions was subtracted from the crude nucleolar signal and the value obtained was multiplied by the area of the nucleolar compartment to give the final nucleolar signal. Nucleo-cytoplasmic signal was obtained by subtracting the final nucleolar signal from total cellular signal.

Results

We decided to examine the biochemical properties and sub-cellular localization of VHL in differentiated myotubes, which provide a good model of hypoxia-induced acidosis. We produced an adenovirus that expresses a VHL–GFP (green fluorescent protein) fusion protein, which shares similar biochemical properties with endogenous VHL (Lee et al., 1999). Differentiated myotubes expressing VHL–GFP were incubated in standard media (SD), that was prepared to prevent changes in pH, or in acidosis-permissive media (AP), which enables hypoxic myotubes to acidify their extracellular milieu (see Methods). VHL–GFP was observed in its typical diffuse nuclear-cytoplasmic distribution under neutral pH conditions, regardless of oxygen tension (Fig. 2.1a) (Groulx and Lee, 2002; Lee et al., 1999). A rapid redistribution of VHL–GFP to sub-nuclear foci was observed after a decrease in the extracellular pH of hypoxic myotubes in an AP environment (Fig. 2.1a and 2.2a). VHL–GFP reverted to a diffuse nuclear-cytoplasmic localization under hypoxic conditions after neutralization of the media. Immunofluorescence microscopy with an anti-VHL antibody (Corless et al., 1997; Kibel et al., 1995) revealed the typical nuclear-cytoplasmic distribution of VHL under neutral conditions (Fig. 2.1b and see Fig. 2.3a for additional specificity controls). Hypoxia-induced acidosis resulted in the relocalization of endogenous VHL to sub-nuclear foci (similar to VHL–GFP) without any alteration in its protein levels (Figs. 2.1b and 2.3b). This demonstrated that the observed sub-cellular redistribution of VHL–GFP is not a consequence of the GFP tag or overproduction of the fusion protein. Both forms of VHL — VHL (p30) and VHL19 (p19) — accumulated in sub-nuclear foci of hypoxic-acidotic cells (Figs. 2.1a and 2.2b). The redistribution of VHL–GFP to sub-nuclear foci was also

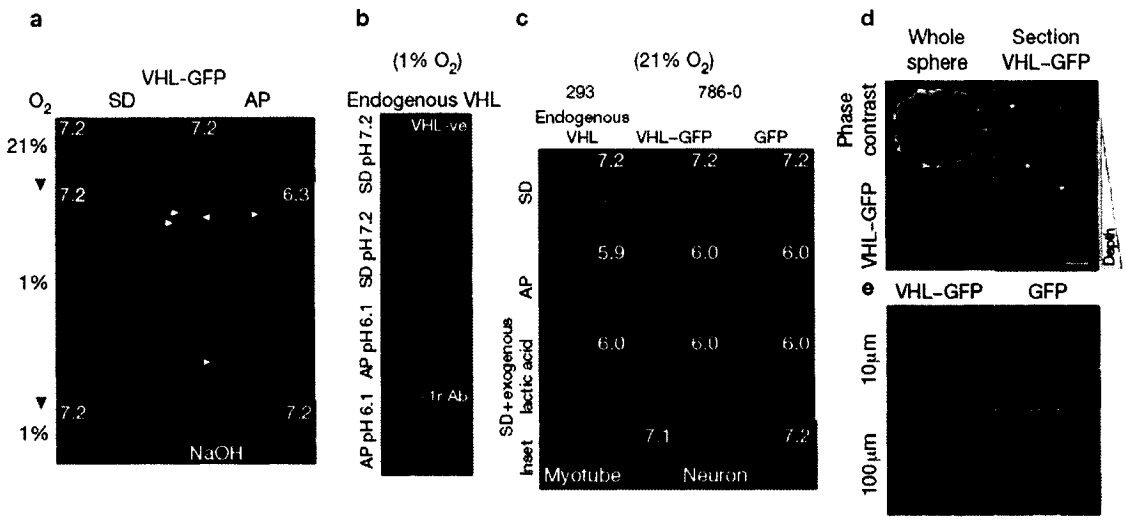
a
VHL-GFP
O_2
SD
AP
21%
1%
1%
7.2
7.2
7.2
6.3
7.2
7.2
NaOH
b
(1% O_2)
Endogenous VHL
VHL -ve
1r Ab
SD pH 7.2
SD pH 7.2
AP pH 6.1
AP pH 6.1
c
(21% O_2)
293
786-0
Endogenous VHL
VHL-GFP
GFP
SD
AP
SD+exogenous lactic acid
Inset
7.2
7.2
7.2
5.9
6.0
6.0
6.0
6.0
6.0
7.1
7.2
Myotube
Neuron
d
Whole sphere
Section VHL-GFP
Phase contrast
VHL-GFP
Depth
e
VHL-GFP
GFP
10μm
100μm

Figure 2.1

Figure 2.1. VHL localizes to sub-nuclear foci under physiological acidosis. (a) Hypoxia-induced acidosis triggers the distribution of VHL–GFP to subnuclear foci (arrowheads) in myotubes. C2C12 differentiated myotubes expressing adenovirus-introduced VHL–GFP were incubated during normoxia (21% O2) in standard (SD) or acidification permissive (AP) media and transferred to hypoxia (1% O2) for 16 h. NaOH was then added to AP media. Extracellular pH is indicated on each panel. Insets show nuclear magnification and Hoechst staining of DNA. (**b**) Endogenous VHL relocalizes to sub-nuclear foci under hypoxia-induced acidosis. 293 cells were transferred to hypoxia in SD or AP media (both at initial pH 7.2). Cells were fixed and stained with a VHL antibody. VHL demonstrated sub-nuclear localization when AP media reached pH 6.1. Controls are VHL-deficient cells (786-0) and primary antibody exclusion (see Fig. 2.3a for additional controls). (**c**) Extracellular acidification by metabolically active cells triggers the redistribution of VHL to sub-nuclear foci in normoxia. 293 cells or VHL-deficient 786-0 cells expressing adenovirus-introduced VHL–GFP or GFP are shown. Cells were incubated in SD (pH stable at 7.2) or AP media (at initial pH 7.2). Alternatively, exogenous lactic acid was added to cells in SD media (pH stable at 6.0). Staining for endogenous VHL or detection of GFP signal identified protein localization. Inset shows C2C12 myotubes and PC12 neurons, which failed to acidify AP media under normoxia and showed no change in the localization of adenovirus-introduced VHL–GFP. (**d**, **e**) VHL–GFP localizes to sub-nuclear foci in the core of spheroids. Spheroids of VHLdeficient 786-0 cells expressing adenovirus-introduced VHL–GFP were grown in SD media (at pH 7.2). Cross-sectioning (5 μm thick) through the centre of spheroids revealed a peripheral nuclear-cytoplasmic distribution (arrows) and a core localized

punctate distribution (dotted circle) of VHL–GFP (**d**). Representative cross-sections from a depth of 10 or 100 μm from the surface of spheroids with Hoechst staining of DNA are shown in **e**. Scale bars represent 300 μm (yellow) or 12 μm (white).

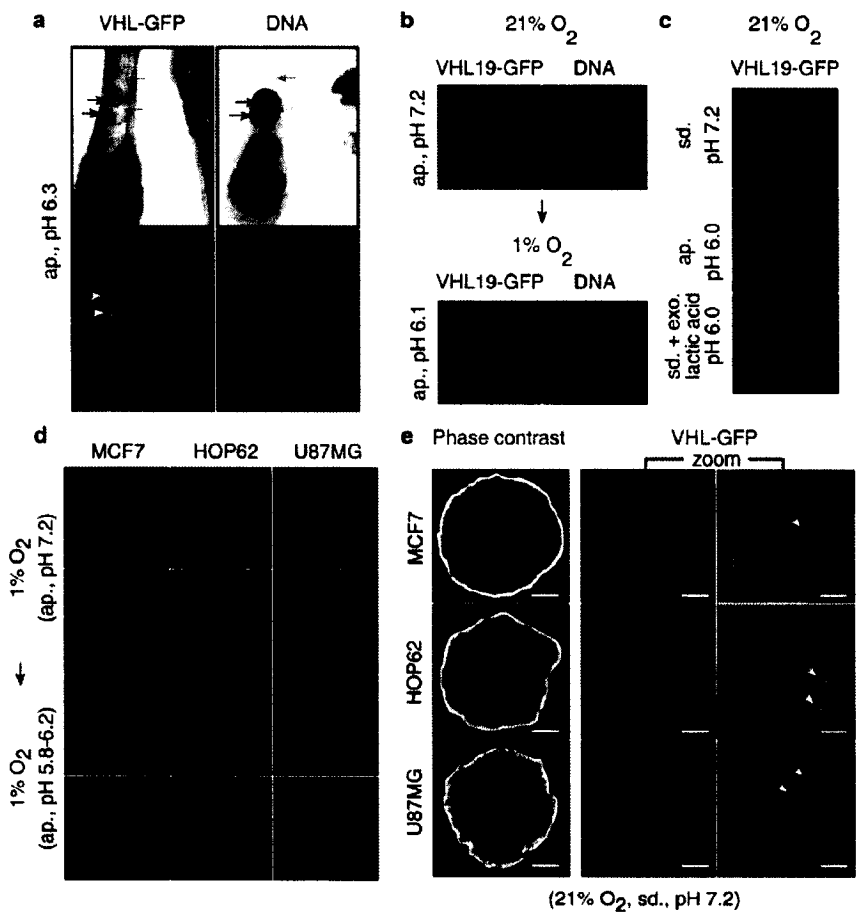
a
VHL-GFP
DNA
ap., pH 6.3
b
21% O2
VHL19-GFP
DNA
ap., pH 7.2
1% O2
VHL19-GFP
DNA
ap., pH 6.1
c
21% O2
VHL19-GFP
sd. pH 7.2
ap. pH 6.0
sd. + exo. lactic acid pH 6.0
d
MCF7
HOP62
U87MG
1% O2 (ap., pH 7.2)
1% O2 (ap., pH 5.8-6.2)
e
Phase contrast
VHL-GFP
zoom
MCF7
HOP62
U87MG
(21% O2, sd., pH 7.2)

Figure 2.2

Figure 2.2. Subnuclear localization of VHL is observed in myotubes and in cancer cell lines with different tissue origin. **(a)** C2C12 differentiated myotubes expressing adenovirus-introduced VHL-GFP were incubated in nomoxia in acidification permissive (AP) media and transferred to hypoxia. VHL-GFP exhibits a prominent subnuclear accumulation (white and black arrows) and a decrease of nucleo-cytoplasmic localization (red arrows) in myotubes following acidification in hypoxia. Dashed lines denote myotubular outline. **(b)** VHL19 exhibits sub-nuclear localization following hypoxia-induced acidosis. VHL-deficient 786-0 cells infected to express VHL19-GFP were transferred to hypoxia under AP conditions. **(c)** Extracellular acidification by metabolically active cells triggered the redistribution of VHL19 to sub-nuclear foci in normoxia. VHL-deficient 786-0 cells expressing adenovirus-introduced VHL19-GFP are shown. Cells were incubated in SD (pH stable at 7.2) or AP media (initial pH 7.2). Alternatively, exogenous lactic acid was added to SD media which was directly added to cells (pH stable at 6.0). See Fig. 2.1c for controls. **(d, e)** Subnuclear localization (denoted by arrows in **(e)**) of VHL is independent of tissue origin. Cells expressing adenovirus-introduced VHL-GFP were cultured in AP media under hypoxia **(d)** or grown as spheroids in SD Media under normoxia **(e)**. Magnification through the core of unadulterated multicellular spheroids is shown. Extracellular pH is indicated for all panels.

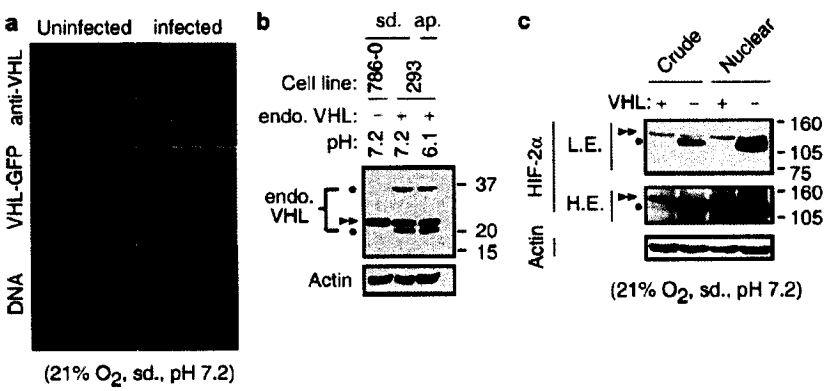
a
Uninfected
infected
anti-VHL
VHL-GFP
DNA
(21% O2, sd., pH 7.2)
b
sd.
ap.
Cell line:
786-0
293
endo. VHL:
pH:
7.2
7.2
6.1
endo. VHL
Actin
37
20
15
c
Crude
Nuclear
VHL: + - + -
HIF-2α
L.E.
H.E.
Actin
160
105
75
160
105
(21% O2, sd., pH 7.2)

Figure 2.3

Figure 2.3. Characterization of VHL and HIF-2α antibodies. **(a)** The monoclonal anti-VHL antibody specifically detects VHL-GFP by immunofluorescence. 786-0 cells that are either VHL-deficient or infected to express VHL-GFP were fixed and immunostained with an anti-VHL antibody. **(b)** 293 cells transferred to hypoxia in SD or AP media (both with initial pH 7.2) exhibit similar levels of endogenous VHL (black dots) under SD and AP conditions. Endpoint pH values are indicated and actin is used as control. Double arrowhead denotes a variable non-specific band. **(c)** The polyclonal anti-HIF-2α antibody readily detects the protein in VHLdeficient cells. Whole-cell or nuclear lysates of 786-0 cells that are either VHL-deficient or stable for HA-VHL expression were blotted for HIF-2α. Dots denote a specific band at 119 kDa whereas arrowheads denote a variable non-specific band. Low (L.E.) and high (H.E.) exposures are shown.

observed in living, differentiated neurons, as well as in cancer cells, from kidney and other tissue origins (Fig. 2.2d and see Further in 2.6a), suggesting that this is a general phenomenon. VHL–GFP was confined to these foci even after re-oxygenation of hypoxic cells (Fig. 2.6a). In contrast, VHL–GFP reverted to a diffuse nuclear-cytoplasmic localization after reinstatement of normal pH conditions in re-oxygenated cells. Similar data were obtained with VHL19–GFP (data not shown). Metabolically active cells, such as dividing cells, are able to engage in aerobic glycolysis (the Warburg effect) followed by secretion of lactic acid (Warburg, 1931; Warburg, 1956). We found that physiological acidification of the extracellular milieu by metabolically active cells, maintained in normoxia, was sufficient to trigger the redistribution of endogenous VHL, VHL–GFP and VHL19–GFP to sub-nuclear foci (Figs. 2.1c and 2.2c). This process was also reversed by neutralization of the media (data not shown). Similar data were obtained after the exogenous addition of lactic acid to oxygenated cells (Figs. 2.1c and 2.2c). VHL–GFP remained localized to the nucleus and cytoplasm in cells such as differentiated neurons and myotubes, which do not acidify AP media in normoxia (Fig. 2.1c, inset). VHL–GFP was also detected in well-defined sub-nuclear foci in the acidic core of spheroids (Figs. 2.1d,e and 2.2e) (Sutherland, 1988). Taken together, these findings suggest that a pH-dependent mechanism regulates the sub-cellular localization of VHL and that it can operate independently of oxygen tension.

Next, we attempted to identify the cellular characteristics of the VHL–GFP-containing foci of acidotic cells. Thus, we created VHL-deficient cells that express VHL–GFP to near physiological levels (Lee et al., 1999). The VHL–GFP signal overlapped with highly dense nuclear regions, as observed by phase-contrast imaging in

normoxic–acidotic cells (Fig. 2.5a). Immunofluorescence microscopy demonstrated that VHL–GFP co-localized with the nucleolar protein B23 in acidosis (Fig. 2.4a). Haemagglutinin (HA) antibodies produced the same foci pattern in cells that stably expressed HA-tagged VHL (HA–VHL; see Fig. 2.5b). Sub-cellular fractionation detected accumulation of VHL exclusively in the nucleolar fraction of cells, confirming that acidosis triggers the complete nucleolar confinement of VHL (Fig. 2.4b). The extracellular pH required for triggering nucleolar confinement of VHL (Fig. 2.4c) or VHL19 (data not shown) displayed oxygen-independent, but cell-type specific, differences within the 5.8–6.6 pH range. Efficient nucleolar accumulation of VHL–GFP was observed once a cell-type-specific pH threshold was achieved through physiological acidosis or after the addition of exogenous lactic acid (Figs. 2.4c and 2.5c, d). This phenomenon is reversible, with a complete redistribution of VHL to a diffuse nuclearcytoplasmic localization within the same pH values, after neutralization of the extracellular milieu (data not shown). Therefore, we reasoned that an increase in the levels of hydrogen ions might trigger nucleolar sequestration of VHL in hypoxia or normoxia to elicit a mechanistically reversible loss of VHL function.

VHL is required for oxygen-dependent degradation of HIF (Jaakkola et al., 2001; Kaelin, 2002; Maxwell et al., 1999). Thus, we examined the functional consequence of hypoxia-induced acidosis on VHL and HIF. VHL remained confined to nucleoli after reoxygenation of hypoxic-acidotic cells (Fig. 2.6a). At neutral pH, normal HIF regulation is reinstated in VHL-deficient cells after the re-introduction of VHL (Fig. 2.6b) (Iliopoulos et al., 1995; Lee et al., 1999). Accumulation of HIF was observed under hypoxia in conditions where there was also a progressive decrease in pH (Fig.2.6b)

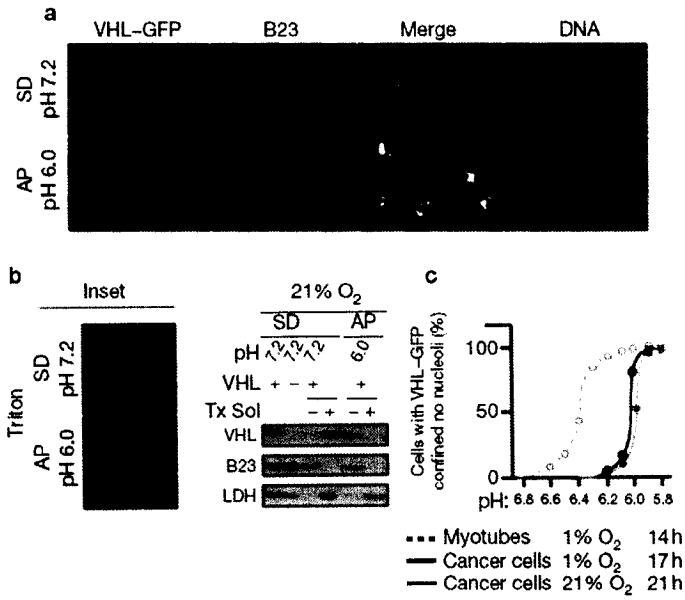
a
VHL-GFP
B23
Merge
DNA
SD pH 7.2
AP pH 6.0
b
Inset
Triton
SD pH 7.2
AP pH 6.0
21% O2
SD
AP
pH 7.2 7.2 7.2 6.0
VHL + − + +
Tx Sol − + − +
VHL
B23
LDH
c
Cells with VHL-GFP confined no nucleoli (%)
100
50
0
pH: 6.8 6.6 6.4 6.2 6.0 5.8
Myotubes 1% O2 14h
Cancer cells 1% O2 17h
Cancer cells 21% O2 21h

Figure 2.4

Figure 2.4. VHL redistributes to the nucleolus during acidosis. (**a**) VHL-deficient 786-0 cells stably expressing VHL–GFP were incubated during normoxia under AP or SD conditions. Fixed cells immunostained for nucleolar B23 reveal co-localization with VHL–GFP under acidosis. (**b**) VHL is exclusively observed in the B23-containing Triton-insoluble fraction of cells after normoxic acidosis. 786-0 cells stably expressing HA–VHL were incubated under SD or AP conditions and fractionated based on Triton solubility (Tx Sol). Lysates were immunoblotted for HA, nucleolar B23 or cytoplasmic LDH. Inset shows 786-0 cells stably expressing VHL–GFP, which were incubated under SD or AP conditions and treated with Triton. (**c**) pH-dependent kinetics of VHL nucleolar localization. C2C12 myotubes or 786-0 cells infected at low titre to express VHL–GFP were incubated in AP media under indicated conditions. Nucleolar versus nucleo–cytoplasmic GFP ratiometric measurements (see methods) were performed at different pH values and the percentage of cells (n = 50) with signal confined to the nucleolus was determined. The time taken for media to reach pH 5.8 is indicated.

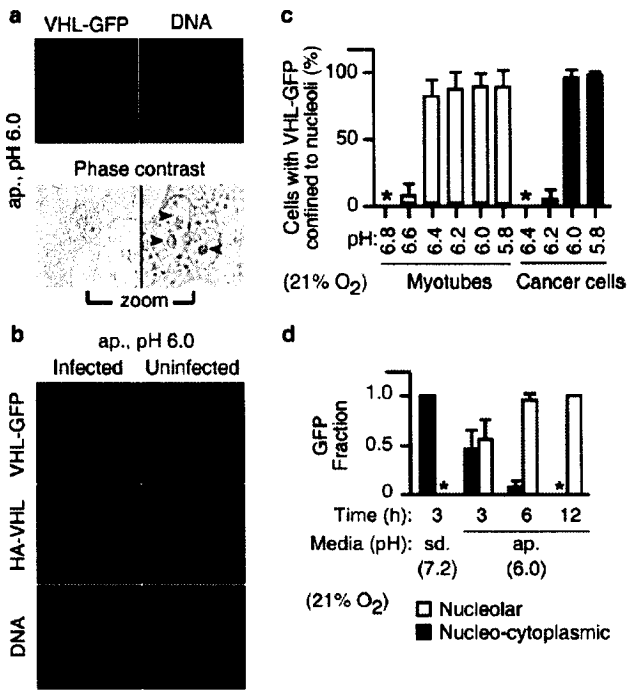
a
VHL-GFP
DNA
ap., pH 6.0
Phase contrast
zoom
b
ap., pH 6.0
Infected
Uninfected
VHL-GFP
HA-VHL
DNA
c
Cells with VHL-GFP confined to nucleoli (%)
100
50
0
pH: 6.8 6.6 6.4 6.2 6.0 5.8 6.4 6.2 6.0 5.8
(21% O2)
Myotubes
Cancer cells
d
GFP Fraction
1.0
0.5
0
Time (h): 3 3 6 12
Media (pH): sd. (7.2) ap. (6.0)
(21% O2)
Nucleolar
Nucleo-cytoplasmic

Figure 2.5

Figure 2.5. VHL redistributes to the nucleolus in a pH-dependent fashion. **(a)** VHL-deficient 786-0 cells stably expressing VHL-GFP were incubated in normoxia under AP conditions. VHL-GFP localized to high density subnuclear foci (arrowheads) as observed by phase contrast microscopy when the pH of AP media reached 6.0. **(b)** 786-0 cells, stably expressing HA-VHL, uninfected or infected to express VHL-GFP, were incubated under AP conditions and submitted to anti-HA immunofluorescence. **(c, d)** pHdependent kinetics of nucleolar localization of VHL. **(c)** C2C12 myotubes or 786-0 cells were infected at low titer to express VHL-GFP. Cells were incubated for 6 h in normoxia in SD media where the pH was stabilized at various values (pH range 6.8-5.8) by addition of exogenous lactic acid. Subcellular ratiometric measurements of GFP signal were performed on cells (n = 49). **(d)** 786-0 cells stably expressing VHL-GFP were incubated in normoxia in SD (pH 7.2) or AP (pH 6.0) media that was previously conditioned for 24 h under hypoxia by the same cell type. Subcellular ratiometric measurements of GFP signal were performed on cells (n = 30). Asterisk indicates absence of signal above background.

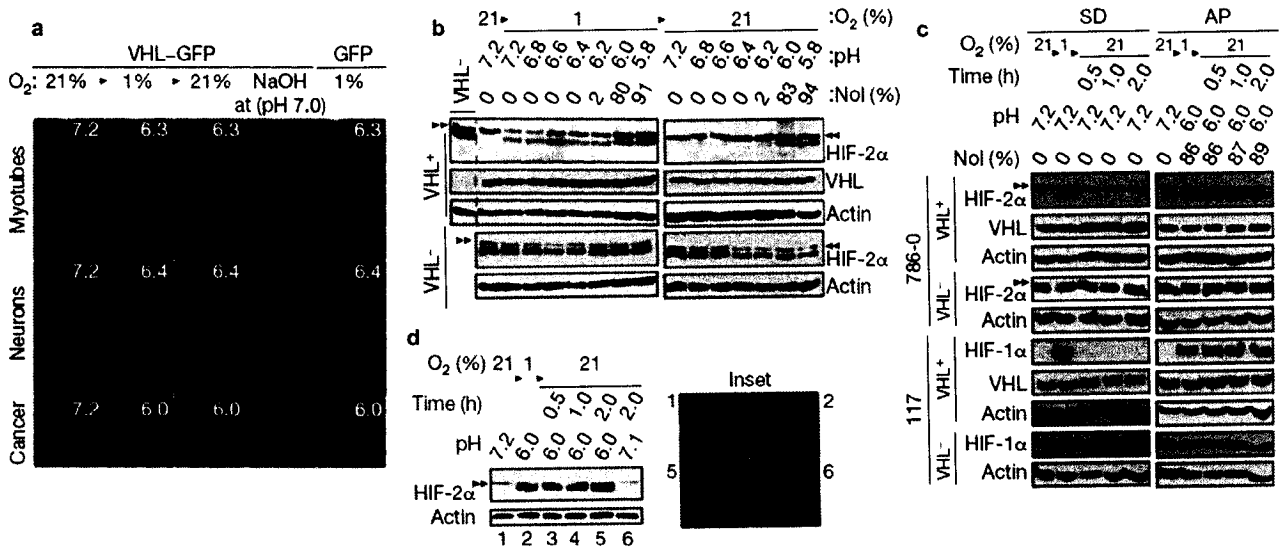
a
VHL-GFP
GFP
O2: 21% ▸ 1% ▸ 21% NaOH at (pH 7.0) 1%
Myotubes
Neurons
Cancer
7.2 6.3 6.3 6.3
7.2 6.4 6.4 6.4
7.2 6.0 6.0 6.0
b
:O2 (%)
:pH
:Nol (%)
VHL-
VHL+
HIF-2α
VHL
Actin
c
SD
AP
O2 (%)
Time (h)
pH
Nol (%)
786-0
117
HIF-2α
HIF-1α
VHL
Actin
d
O2 (%) 21 1 21
Time (h)
pH
HIF-2α
Actin
Inset

Figure 2.6

Figure 2.6. Acidosis prolongs HIF stabilization after re-oxygenation. (**a**) VHL localization to sub-nuclear foci under hypoxia-induced acidosis persisted after oxygenation until neutral pH was reinstated. C2C12 myotubes, PC12 neurons and 786-0 renal cancer cells expressing adenovirus-introduced VHL–GFP were transferred to hypoxia under AP conditions. Cells were transferred back to normoxia under acidic conditions followed by pH neutralization with NaOH. (**b**) Endogenous HIF is not degraded after oxygenation of hypoxic–acidotic cells exhibiting nucleolar VHL. 786-0 cells that are either deficient for VHL expression or stably expressing HA–VHL were incubated in hypoxia for 20 h under AP conditions. At various stages of acidification, cells were harvested in hypoxia or after a 20-min oxygenation period. Lysates were blotted with HIF-2α and HA antibodies. Double arrowhead denotes a variable nonspecific band (see Fig. 2.3c). Controls are VHL-deficient 786-0 cells (21% O2 at pH7.0). VHL localization and the percentage of cells with VHL confined to nucleoli (Nol (%)) were determined by ratiometric measurements of HA immuofluorescence. (**c**) Prolonged stabilization of endogenous HIF is observed after oxygenation of hypoxic-acidotic cells. 117 or 786-0 cells stably expressing VHL–GFP or HA–VHL were transferred to hypoxia (20 h) in SD or AP media, respectively. Cells were harvested before or after different oxygenation periods (0.5, 1 or 2 h). Lysates were blotted with antibodies to HIF-2α, Flag or HA. Percentage of cells with VHL–GFP (117) confined to nucleoli (Nol (%)) was determined by ratiometric measurements. (**d**) Neutralization of acidic extracellular milieu restored nucleo-cytoplasmic distribution of VHL and oxygen-dependent degradation of HIF. 786-0 cells stably expressing HA–VHL were transferred to hypoxia under AP conditions. Cells were incubated in hypoxia in AP media for 20 h.

Cells were harvested before or after different oxygenation periods (0.5, 1 or 2 h; lanes 2–5). Alternatively, cells were oxygenated for 1 h at pH 6.0 and another 1 h after addition of NaOH (pH 7.1, lane 6). Lysates were blotted with antibodies to HIF-2α, Flag or HA. Inset shows corresponding VHL localization.

As previously described, HIF was degraded after re-oxygenation of hypoxic cells (for 20 min) in the pH range 7.2–6.2 (Fig. 2.6b). In contrast, HIF was resistant to degradation after reoxygenation when the extracellular pH reached 6.0–5.8 — conditions in which VHL was observed in nucleoli (Fig. 2.6a, b). HIF evaded oxygen-dependent degradation until neutral pH conditions were achieved and consequent nucleo-cytoplasmic localization of VHL was reinstated (Fig. 2.6c, d). No change in HIF levels were observed in VHL-deficient 786-0 and 117 cells under any of the described conditions (Fig. 2.6b, c). Therefore, HIF remains stable after re-oxygenation of acidotic cells, conditions in which VHL is confined to nucleoli.

These findings led us to design two independent experiments to demonstrate that nucleolar sequestration of VHL is required to prevent HIF degradation after re-oxygenation of hypoxic-acidotic cells. Cells stably expressing VHL were infected with adenovirus expressing VHL. We reasoned that this would perturb the steady state localization of VHL, resulting in its accumulation in the nucleus and cytoplasm of cells exposed to hypoxic acidosis. Dis-equilibrium in the steady-state distribution was achieved by accumulation of VHL–GFP in the nuclear-cytoplasmic compartments of acidotic cells (Fig. 2.7a). This rescued HIF degradation after re-oxygenation of hypoxic-acidotic cells (Fig. 2.7b). Next, we wanted to identify a VHL mutant that fails to degrade HIF but retains the ability to localize to the nucleolus. The ΔC157 deletion mutant of the carboxy-terminal region of VHL retained the ability to target a GFP reporter to nucleoli in acidosis, independently of oxygen tension (Fig. 2.8). This mutant is defective in both E3 ligase complex formation and HIF substrate recognition (Bonicalzi et al., 2001; Cockman et al., 2000; Pause et al., 1997) (see Fig. 2.8a, inset) and failed to restore HIFα

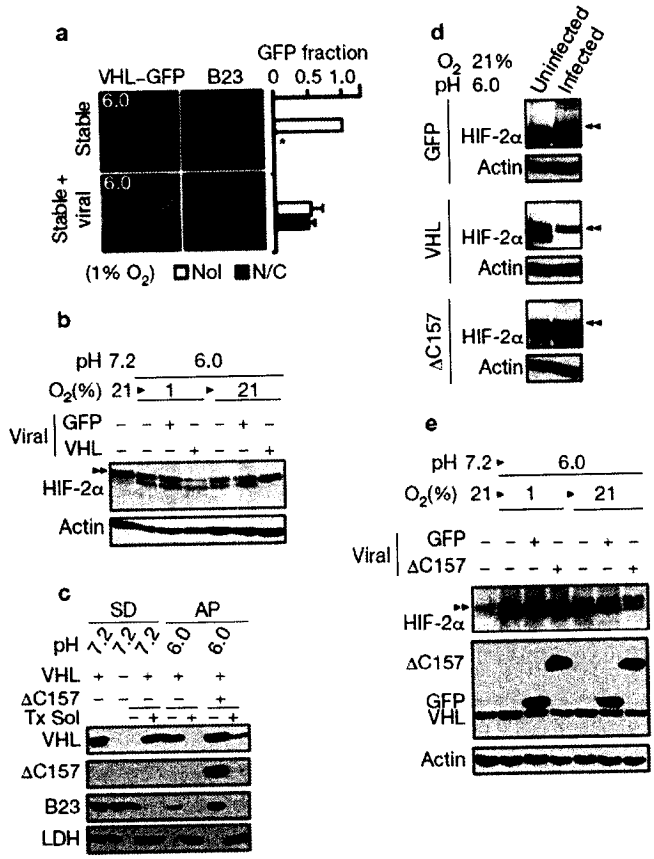
a
VHL-GFP
B23
GFP fraction
0 0.5 1.0
Stable
Stable + viral
6.0
6.0
(1% O2) NoI N/C
b
pH 7.2
6.0
O2(%) 21
1
21
Viral
GFP
VHL
HIF-2α
Actin
c
SD
AP
pH 7.2 7.2 7.2 6.0 6.0
VHL
ΔC157
Tx Sol
VHL
ΔC157
B23
LDH
d
O2 21%
pH 6.0
Uninfected
Infected
GFP
VHL
ΔC157
HIF-2α
Actin
e
pH 7.2
6.0
O2(%) 21
1
21
Viral
GFP
ΔC157
HIF-2α
ΔC157
GFP
VHL
Actin

Figure 2.7

Figure 2.7. Nucleolar sequestration of VHL prevents the degradation of HIF. (**a**) 786-0 cells stably expressing VHL–GFP were either left uninfected or were infected to express additional VHL–GFP. Cells were incubated for 20 h under hypoxia in AP media. Sub-cellular ratiometric measurements of GFP signal were performed on cells (n = 37). (**b**) 786-0 cells stably expressing HA–VHL were either left uninfected or infected to express VHL–GFP or GFP. Cells were incubated under AP conditions for 20 h in hypoxia. Cells were harvested in hypoxia or after a 20 min oxygenation period and analysed by immunoblotting. (**c**) ΔC157 prevents the nucleolar confinement of wild-type VHL in acidosis. 786-0 cells stably expressing HA–VHL were incubated under SD or AP (infected or not with ΔC157–GFP) conditions and fractionated on the basis of Triton solubility. Lysates were immunoblotted for HA, Flag, nucleolar B23 or cytoplasmic LDH. (**d**) ΔC157 is an inactive VHL mutant. VHL-deficient 786-0 cells were uninfected or infected at high titre to express VHL–GFP, ΔC157–GFP or GFP. Cells were incubated under normoxic conditions in AP media where the pH decreased to 6.0. Cells were harvested after 21 h at which point significant amounts of VHL–GFP, ΔC157–GFP and GFP were still detectable in the nucleo-cytoplasmic region of cells. Lysates were blotted with an anti-HIF-2α antibody. (**e**) Introduction of adenoviral ΔC157–GFP, but not GFP, into VHL-competent cells restores endogenous HIF degradation after oxygenation of hypoxic-acidotic cells. 786-0 cells stably expressing HA–VHL were uninfected or infected to express ΔC157–GFP or GFP. Cells were incubated in hypoxia in AP media for 20 h. Cells were harvested in hypoxia or after a 20 min oxygenation. Lysates were blotted with antibodies to HIF-2α, Flag or HA.

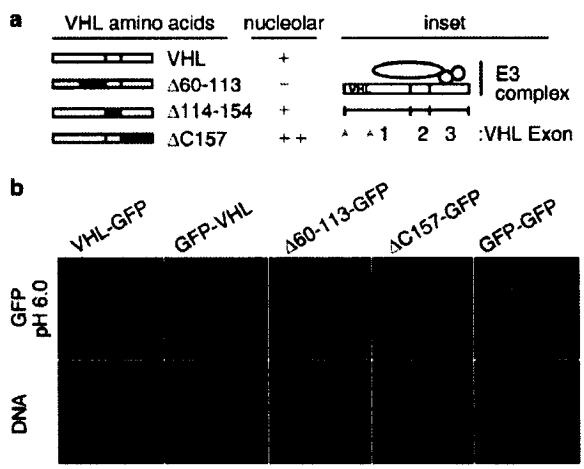
a
VHL amino acids
nucleolar
inset
VHL
+
Δ60-113
−
Δ114-154
+
ΔC157
++
E3
complex
1 2 3 :VHL Exon
b
VHL-GFP
GFP-VHL
Δ60-113-GFP
ΔC157-GFP
GFP-GFP
GFP
pH 6.0
DNA

Figure 2.8

Figure 2.8. VHL mapping analysis. (a) HeLa cells transiently transfected to express the indicated GFP-tagged proteins were incubated in AP Media for 15 h in hypoxia or 24 h in normoxia. Nucleolar sequestration was independent of oxygen tension. Inset shows the requirement of exon-3-encoded residues of VHL for E3 complex formation. Arrowheads denote *VHL* methionine start residues. **(b)** Representative images from normoxic cells in **(a)**.

degradation even when expressed at high levels in normoxic-acidotic (Fig. 2.7d) or normoxicneutral (data not shown and (Bonicalzi et al., 2001)) VHL-deficient cells. Expression of ΔC157 efficiently prevented nucleolar sequestration of wild-type VHL in acidotic cells (Fig. 2.7c) and restored oxygen-dependent regulation of HIF after re-oxygenation of hypoxic-acidotic cells (Fig. 2.7c, e). These results demonstrate that nucleolar confinement of VHL is required for maintenance of HIF stability after returning hypoxic-acidotic cells to normal oxygen tension. More importantly, these data also indicate that the mechanisms involved in oxygen-dependent degradation of HIF remain intact in re-oxygenated acidotic cells, and that HIF stabilization is a direct consequence of VHL nucleolar sequestration.

Next we investigated the effect of normoxic acidosis on HIF activation (Fig. 2.1c). VHL-expressing 786-0 or 117 cells, incubated in normoxia under AP conditions, acidified their extracellular milieu with a concomitant increase in HIF levels as revealed by western blot and immunofluorescence microscopy analyses (Fig. 2.9a, b). Cells displaying partial nucleolar localization of VHL did not exhibit nuclear HIF staining, confirming that nucleolar confinement of VHL is required for HIF activation (Fig. 2.9b). To induce nucleolar sequestration of VHL, we treated cells in normoxia with AP media that had previously been conditioned to acidosis (pH stable at 6.0) by cells in hypoxia. Normoxic incubation of 117 cells stably expressing VHL–GFP in conditioned AP media (at pH 6.0), but not similarly conditioned SD media (at pH 7.2), resulted in the nucleolar sequestration of VHL and an increase in the levels of HIF (Fig. 2.9c). Similar results were obtained when the media was conditioned to acidosis under normoxia (data not shown). To investigate if nucleolar sequestration of VHL enables not only HIF

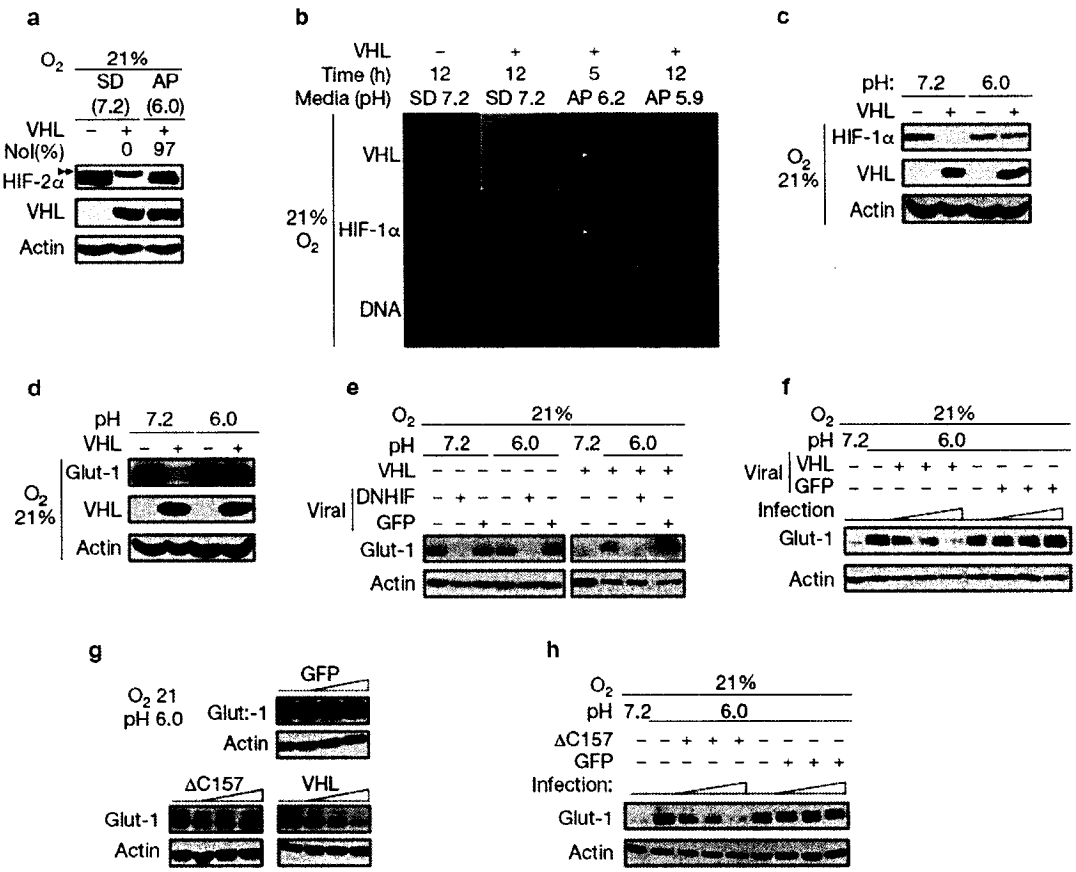
a
O2 21%
SD AP
(7.2) (6.0)
VHL – + +
Nol(%) 0 97
HIF-2α
VHL
Actin
b
VHL – + + +
Time (h) 12 12 5 12
Media (pH) SD 7.2 SD 7.2 AP 6.2 AP 5.9
21% O2
VHL
HIF-1α
DNA
c
pH: 7.2 6.0
VHL – + – +
O2 21%
HIF-1α
VHL
Actin
d
pH 7.2 6.0
VHL – + – +
O2 21%
Glut-1
VHL
Actin
e
O2 21%
pH 7.2 6.0 7.2 6.0
VHL – – – – – – + + + +
Viral DNHIF – + – – + – – – + –
GFP – – + – – + – – – +
Glut-1
Actin
f
O2 21%
pH 7.2 6.0
Viral VHL – – + + + – – – –
GFP – – – – – – + + +
Infection
Glut-1
Actin
g
O2 21
pH 6.0
Glut:-1
Actin
GFP
ΔC157
VHL
Glut-1
Actin
h
O2 21%
pH 7.2 6.0
ΔC157 – – + + + – – – –
GFP – – – – – – + + +
Infection:
Glut-1
Actin

Figure 2.9

Figure 2.9. Normoxic acidosis triggers nucleolar sequestration of VHL to activate HIF. (**a**, **b**) HIF is stabilized after acidification in the presence of oxygen. 786-0 or 117 cells stably expressing VHL–GFP were incubated in SD or AP media for 12 h or for the indicated periods of time. Cells were harvested and blotted with antibodies to HIF-2α or Flag (**a**) or were fixed and immunostained with an antibody to HIF-1α (**b**). Arrowheads indicate HIF-1α in cells exhibiting complete or partial redistribution of VHL–GFP to nucleoli. (**c–h**) For neutral (pH 7.2) or acidotic (pH 6.0) treatments in normoxia, cells were treated for 14 h with SD or AP media previously conditioned by cells in hypoxia for 24 h (see Text). (**c**) 117 cells stably expressing VHL–GFP were incubated in neutral or acidotic conditioned media. Cells were lysed and lysates were blotted with antibodies to HIF-1α or Flag. (**d**) Glut-1 accumulates in acidotic cells. 786-0 cells stably expressing VHL–GFP were incubated in neutral or acidic conditioned media. Lysates were prepared and blotted with a Glut-1 antibody. (**e**) Dominant-negative HIF abolishes endogenous accumulation of Glut-1 in acidotic cells. 786-0 cells stably expressing VHL–GFP and infected to express dominant negative HIF-2α (DNHIF) or GFP were incubated in normoxia with neutral or acidic conditioned media. Cells were harvested for Glut-1 protein immunoblotting. (**f**) Introduction of adenoviral VHL–GFP, but not GFP, into 786-0 cells stably expressing VHL–GFP decreases acidosis-induced Glut-1 levels, as shown by immunoblotting. (**g**) Adenoviral introduction of VHL–GFP, but not ΔC157–GFP or GFP, decreases levels of immunoblotted Glut-1 in acidotic VHL-deficient 786-0 cells. (**h**) Adenovirus-introduced ΔC157, but not GFP, decreased immunoblotted acidosis-induced Glut-1 protein levels in 786-0 cells stably expressing HA–VHL.

accumulation but also its activation,we assessed whether low pH caused accumulation of Glut-1 (the product of a well characterized HIF-regulated gene) under normoxia. Glut-1 levels increased in acidotic, VHL-expressing, cells to levels similar to those observed in VHLdeficient cells (Fig. 2.9d). Dominant-negative HIF (Gunaratnam et al., 2003) abolished Glut-1 accumulation in acidified cells, thereby confirming that pH-dependent accumulation of Glut-1 is a consequence of HIF activation (Fig. 2.9e). Abolishing nucleolar sequestration of stably expressed VHL through the introduction of VHL (Figs. 2.9f and 2.7a) or its inactive mutant ΔC157 (Figs. 2.9g, h; and 2.7c, d) prevented accumulation of Glut-1 during acidosis in a dose-dependent fashion. These results demonstrate that HIF activation under normoxic acidosis requires nucleolar confinement of VHL.

Discussion Part 1

In conclusion, we propose a model in which a new, pH-dependent, VHL regulation mechanism intersects with the previously identified oxygen-dependent control of HIF. According to this model, hypoxia directly elicits HIF activation by abrogating the ability of VHL to degrade HIF (Jaakkola et al., 2001; Maxwell et al., 1999). Acidosis is observed in ischaemic tissues and corresponds to the severity of hypoxic stress. Once achieved, acidosis triggers nucleolar confinement of VHL, abolishing its ability to degrade HIF until neutral pH conditions are restored after re-oxygenation. There are several reports demonstrating that acidosis confers significant protective effects to cells under various stress conditions, including hypoxic stress (Currin et al., 1991; Giffard et al., 1990; Kaku et al., 1993; Morimoto et al., 1997; Nielsen et al., 2001). It is tempting to speculate that cells would benefit from prolonged HIF activation after a hypoxic stress that would be sufficient to induce acidosis. In fact, HIF target genes remain activated after ischaemia-reperfusion, and this is associated with several protective effects (Chavez and LaManna, 2002; Sun et al., 2003). Alternatively, cancer cells can efficiently trigger nucleolar sequestration of VHL in normoxia by acidifying their extracellular milieu, thereby resulting in HIF activation. We suggest that HIF activation, and possibly tumour angiogenesis, can be promoted by low pH as well as by a decrease in oxygen tension. It has been suggested that the nucleolus could function as an organelle by which cellular processes might be regulated through physical confinement of proteins (Bachant and Elledge, 1999). The VHL regulatory process we have described is reminiscent of that observed in another system; here, nucleolar sequestration of MDM2 prevents it from degrading p53 in response to physiological cues (Weber et al., 1999). Finally, our model

describes a gene-regulatory mechanism that relies on cellular sensing of the environmental concentration of hydrogen ions to regulate VHL function.

Acknowledgements

We thank C. Lavigne for technical expertise. This work was supported by a grant from the Canadian Institutes of Health Research (CIHR) to S.L. K.M. is supported by the Natural Science and Engineering Research Council of Canada (NSERC). S.L. is a Harold E. Johns investigator of the National Cancer Institute of Canada (NCIC).

References

Bachant, J.B., and S.J. Elledge. 1999. Mitotic treasures in the nucleolus. *Nature*. 398:757-758.

Bonicalzi, M.E., I. Groulx, N. de Paulsen, and S. Lee. 2001. Role of exon 2-encoded beta -domain of the von Hippel-Lindau tumor suppressor protein. *J. Biol. Chem.* 276:1407.

Chavez, J.C., and J.C. LaManna. 2002. Activation of hypoxia-inducible factor-1 in the rat cerebral cortex after transient global ischemia: potential role of insulin-like growth factor-1. *J. Neurosci.* 22:8922-8931.

Cockman, M.E., N. Masson, D.R. Mole, P. Jaakkola, G.W. Chang, S.C. Clifford, E.R. Maher, C.W. Pugh, P.J. Ratcliffe, and P.H. Maxwell. 2000. Hypoxia inducible factor-alpha binding and ubiquitylation by the von Hippel-Lindau tumor suppressor protein. *J. Biol. Chem.* 275:25733-25741.

Corless, C.L., A.S. Kibel, O. Iliopoulos, and W.G. Kaelin, Jr. 1997. Immunostaining of the von Hippel-Lindau gene product in normal and neoplastic human tissues. *Hum. Pathol.* 28:459-464.

Currin, R.T., G.J. Gores, R.G. Thurman, and J.J. Lemasters. 1991. Protection by acidotic pH against anoxic cell killing in perfused rat liver: evidence for a pH paradox. *FASEB J.* 5:207-210.

Giffard, R.G., H. Monyer, C.W. Christine, and D.W. Choi. 1990. Acidosis reduces NMDA receptor activation, glutamate neurotoxicity, and oxygen-glucose deprivation neuronal injury in cortical cultures. *Brain Res.* 506:339-342.

Groulx, I., and S. Lee. 2002. Oxygen-dependent ubiquitination and degradation of hypoxia-inducible factor requires nuclear-cytoplasmic trafficking of the von Hippel-Lindau tumor suppressor protein. *Mol. Cell. Biol.* 22:5319.

Gunaratnam, L., M. Morley, A. Franovic, N. de Paulsen, K. Mekhail, D.A. Parolin, E. Nakamura, I.A. Lorimer, and S. Lee. 2003. Hypoxia inducible factor activates the transforming growth factor-alpha/epidermal growth factor receptor growth stimulatory pathway in VHL (-/-) renal cell carcinoma cells. *J. Biol. Chem.* 278:44966-44974.

Harris, A.L. 2002. Hypoxia: a key regulatory factor in tumour growth. *Nat. Rev. Cancer.* 2:38-47.

Iliopoulos, O., A. Kibel, S. Gray, and W.G. Kaelin, Jr. 1995. Tumour suppression by the human von Hippel-Lindau gene product. *Nat. Med.* 1:822-826.

Jaakkola, P., D.R. Mole, Y.M. Tian, M.I. Wilson, J. Gielbert, S.J. Gaskell, A. Kriegsheim, H.F. Hebestreit, M. Mukherji, C.J. Schofield, P.H. Maxwell, C.W. Pugh, and P.J. Ratcliffe. 2001. Targeting of HIF-alpha to the von Hippel-Lindau ubiquitylation complex by O2-regulated prolyl hydroxylation. *Science*. 292:468-472.

Kaelin, W.G., Jr. 2002. Molecular basis of the VHL hereditary cancer syndrome. *Nat. Rev. Cancer*. 2:673-682.

Kaku, D.A., R.G. Giffard, and D.W. Choi. 1993. Neuroprotective effects of glutamate antagonists and extracellular acidity. *Science*. 260:1516-1518.

Kibel, A., O. Iliopoulos, J.A. DeCaprio, and W.G. Kaelin, Jr. 1995. Binding of the von Hippel-Lindau tumor suppressor protein to Elongin B and C. *Science*. 269:1444-1446.

Lee, S., M. Neumann, R. Stearman, R. Stauber, A. Pause, G.N. Pavlakis, and R.D. Klausner. 1999. Transcription-dependent nuclear-cytoplasmic trafficking is required for the function of the von Hippel-Lindau tumor suppressor protein. *Mol. Cell. Biol.* 19:1486.

Maxwell, P.H., M.S. Wiesener, G.W. Chang, S.C. Clifford, E.C. Vaux, M.E. Cockman, C.C. Wykoff, C.W. Pugh, E.R. Maher, and P.J. Ratcliffe. 1999. The tumour suppressor protein VHL targets hypoxia-inducible factors for oxygen-dependent proteolysis. *Nature*. 399:271-275.

Morimoto, Y., O. Kemmotsu, and E.S. Alojado. 1997. Extracellular acidosis delays cell death against glucose-oxygen deprivation in neuroblastoma x glioma hybrid cells. *Crit. Care Med.* 25:841.

Nielsen, O.B., F. de Paoli, and K. Overgaard. 2001. Protective effects of lactic acid on force production in rat skeletal muscle. *J. Physiol.* 536:161-166.

Pause, A., S. Lee, R.A. Worrell, D.Y. Chen, W.H. Burgess, W.M. Linehan, and R.D. Klausner. 1997. The von Hippel-Lindau tumor-suppressor gene product forms a stable complex with human CUL-2, a member of the Cdc53 family of proteins. *Proc. Natl. Acad. Sci. USA*. 94:2156-2161.

Semenza, G.L. 2000. HIF-1 and human disease: one highly involved factor. *Genes Dev.* 14:1983-1991.

Shou, W., J.H. Seol, A. Shevchenko, C. Baskerville, D. Moazed, Z.W. Chen, J. Jang, H. Charbonneau, and R.J. Deshaies. 1999. Exit from mitosis is triggered by Tem1-dependent release of the protein phosphatase Cdc14 from nucleolar RENT complex. *Cell.* 97:233-244.

Sun, Y., K. Jin, L. Xie, J. Childs, X.O. Mao, A. Logvinova, and D.A. Greenberg. 2003. VEGF-induced neuroprotection, neurogenesis, and angiogenesis after focal cerebral ischemia. *J. Clin. Invest.* 111:1843-1851.

Sutherland, R.M. 1988. Cell and environment interactions in tumor microregions: the multicell spheroid model. *Science.* 240:177-184.

Tsai, R.Y., and R.D. McKay. 2002. A nucleolar mechanism controlling cell proliferation in stem cells and cancer cells. *Genes Dev.* 16:2991-3003.

Visintin, R., E.S. Hwang, and A. Amon. 1999. Cfi1 prevents premature exit from mitosis by anchoring Cdc14 phosphatase in the nucleolus. *Nature.* 398:818-823.

Wagner, P.D. 2001. Skeletal muscle angiogenesis. A possible role for hypoxia. *Adv. Exp. Med. Biol.* 502:21-38.

Warburg, O. 1931. The metabolism of tumors. R. R. Smith, New York. 129-163 pp.

Warburg, O. 1956. On the origin of cancer cells. *Science.* 123:309-314.

Weber, J.D., L.J. Taylor, M.F. Roussel, C.J. Sherr, and D. Bar-Sagi. 1999. Nucleolar Arf sequesters Mdm2 and activates p53. *Nat. Cell Biol.* 1:20-26.

Discussion Part 2

Oxygen sensing by H+: Implications for HIF and hypoxic cell memory

Karim Mekhail[1], Mireille Khacho[1], Lakshman Gunaratnam[1], and Stephen Lee[1,2]

[1]Department of Cellular and Molecular Medicine, Faculty of Medicine, University of Ottawa, Ottawa, Ontario, Canada K1H 8M5.

[2]Correspondence should be addressed to S.L. (e-mail: slee@uottawa.ca)

Published Manuscript

Cell Cycle 3:1027-1029 (2004)

Discussion – Part 2

Hypoxia and acidosis are common features of several physiological and pathological situations, including cancer and stroke. The HIF (hypoxia-inducible factor) transcription factor plays a seminal role in orchestrating cellular responses to alterations in oxygen availability. HIF is degraded in normal oxygen tension by the VHL (von Hippel-Lindau) tumor suppressor protein but stabilized by hypoxia to activate an array of genes implicated in oxygen homeostasis including vascular endothelial growth factor. Cells respond to a comparatively mild decline in oxygen tension by converting to an anaerobic state of respiration and secreting lactic acid. We recently reported that a decrease in environmental pH triggers sequestration of VHL into the nucleolus neutralizing its ability to degrade HIF. This implies that cells have evolved a parallel mechanism of HIF activation that responds to changes in oxygen levels by sensing extracellular [H^+]. Here we discuss the implications of this new VHL regulatory mechanism on oxygen homeostasis and hypoxic cell memory.

Ischaemia occurs in cardiac arrest, stroke, muscle stress, cancer, and normal development (Compernolle et al., 2002; Kojima et al., 2002; Semenza, 2000a; Wagner, 2001). Within these physiological and pathological settings, the HIF (hypoxia-inducible factor) transcription factor activates genes implicated in cellular response to low oxygen availabilty. Among others, HIF induces genes that modulate angiogenesis, glycolysis, growth and pH regulation (Gunaratnam et al., 2003; Harris, 2002; Semenza, 2003). In the presence of oxygen, the α subunit of HIF (HIFα) is post-translationally modified at key proline residues by enzymes known as prolyl hydroxylases (PHDs) (Fig. 2.10A) (Bruick and McKnight, 2001; Epstein et al., 2001; Ivan et al., 2001; Jaakkola et al., 2001;

Yu et al., 2001). This allows the VHL tumor suppressor, a component of an E3 ubiquitin ligase (Fig. 2.10A), to recognize HIF and target it for degradation (reviewed in (Kaelin, 2002)). PHDs require molecular oxygen and hypoxia prevents hydroxylation of HIF (Bruick and McKnight, 2001; Epstein et al., 2001; Ivan et al., 2001; Jaakkola et al., 2001; Kivirikko and Myllyharju, 1998; Schofield and Zhang, 1999; Yu et al., 2001). This has led to the notion that PHDs act as "oxygen sensors" gauging oxygen tension and determining whether cells should engage in HIF activation.

Cells adapt to a decrease in oxygen tension by engaging in metabolic fermentation following an increase in the glycolytic rate. This results in acidification of the extracellular milieu due to excess production of lactic acid. Acidosis has been reported to be more than an innocent bystander in this process. In fact, low pH values exert protective effects under numerous physiological and pathological settings (Currin et al., 1991; Giffard et al., 1990; Kaku et al., 1993; Morimoto et al., 1997; Nielsen et al., 2001). This led us to investigate the VHL-HIF system in hypoxic cells that are allowed to undertake the natural route to acidosis (Mekhail et al., 2004a). We found that hypoxia-induced acidosis triggered relocalization of VHL from a diffuse nuclear-cytoplasmic pattern to nucleoli (Fig. 2.10B) (Mekhail et al., 2004a). VHL remained confined to nucleoli upon reoxygenation but reverted to its original nuclear-cytoplasmic distribution when neutral pH conditions were reinstated. Nucleolar localization of VHL also occurred in normoxia following extracellular acidification by metabolically active cells (Warburg Effect) (Warburg, 1931; Warburg, 1956). Nucleolar sequestration of VHL stabilized HIF and activated its targets. Therefore, we reasoned that an increase in the levels of hydrogen ions might trigger nucleolar sequestration of VHL in hypoxia or

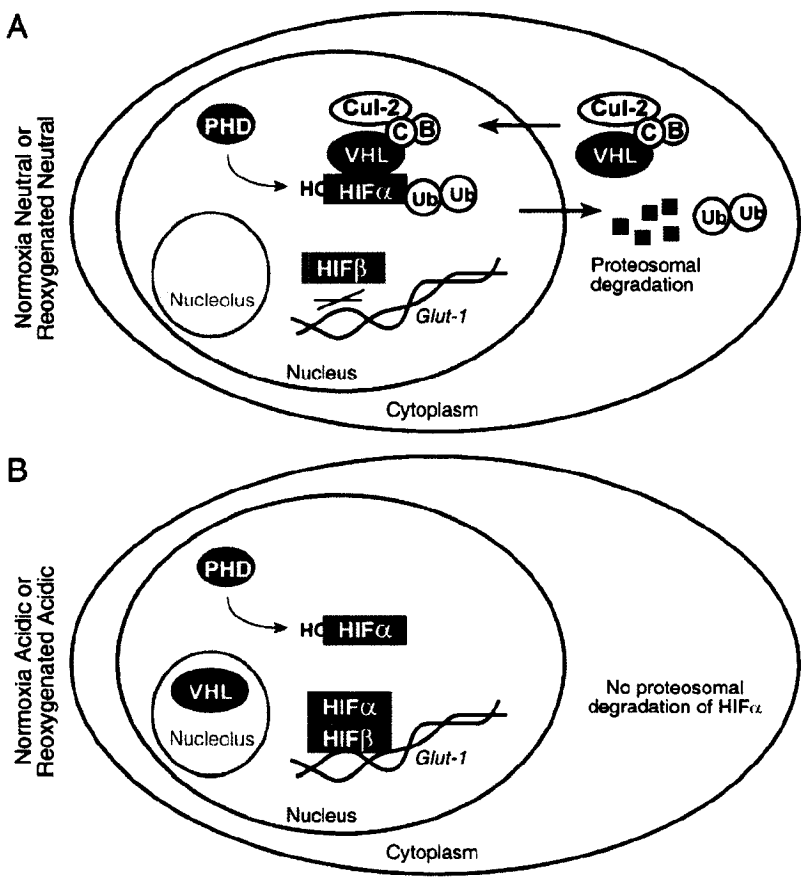
A
Normoxia Neutral or
Reoxygenated Neutral
PHD
Cul-2
C
B
VHL
HO
HIFα
Ub
Ub
Cul-2
C
B
VHL
Ub
Ub
Proteosomal
degradation
Nucleolus
HIFβ
Glut-1
Nucleus
Cytoplasm
B
Normoxia Acidic or
Reoxygenated Acidic
PHD
HO
HIFα
VHL
Nucleolus
HIFα
HIFβ
Glut-1
No proteosomal
degradation of HIFα
Nucleus
Cytoplasm

Figure 2.10

Figure 2.10. HIF regulation by VHL. **(A)** In the presence of oxygen, prolyl hydroxylase (PHD) post-translationally modifies HIFα to increase its affinity towards VHL. The latter acts as a recognition motif of an E3 ubiquitin ligase complex, which includes cullin-2, elongins B and C. VHL targets hydroxylated HIFα for cullin-2-mediated ubiquitination in the nucleus and subsequent cytoplasmic degradation (Fabbro and Henderson, 2003; Groulx and Lee, 2002). Hypoxia inhibits PHD allowing HIFα to heterodimerize with the constitutively expressed HIFβ and activates HIF target genes, including glucose transporter-1 (*Glut-1*). **(B)** Hypoxia-induced acidosis results in a pH-dependent relocalization of VHL to nucleoli and stabilization of HIF. Nucleolar sequestration of VHL prevents it from targeting HIF for degradation in reoxygenated acidotic cells even in the presence of reactivated PHD. VHL remains in the nucleolus until neutral pH conditions are restored. Nucleolar sequestration of VHL following reoxygenation of hypoxic-acidotic cells prolongs HIF stability and hypoxic cell memory. Although formation of the E3 ligase complex is not required for nucleolar localization of VHL, the subcellular distribution of cullin-2, elongins B and C is still unknown under acidosis.

normoxia to elicit a mechanistically reversible loss of VHL function followed by HIF activation.

We propose a model in which pH dependent regulation of VHL intersects with the previously identified oxygen-dependent control of HIF. Acidosis is observed in ischaemic tissues and is a function of the hypoxic stress as defined by the severity and the duration of the decrease in oxygen concentration as well as the microenvironmental buffering capacity. Once achieved, acidosis triggers nucleolar confinement of VHL abolishing its ability to degrade HIF. Nucleolar sequestration-dependent inactivation of VHL is refractory to oxygen levels but not to the reinstatement of neutral extracellular pH. We thus speculate that prolonged HIF stabilization by acidosis-dependent nucleolar sequestration of VHL serves as a mechanism of hypoxic cell memory (Fig. 2.11) that enables cells to discount the effect of reoxygenation. Since acidosis is known to protect cells against several different toxic effects including anoxic cell killing and glucose starvation (Currin et al., 1991; Giffard et al., 1990; Kaku et al., 1993; Morimoto et al., 1997; Nielsen et al., 2001), it is reasonable to suspect that cells would benefit from a hypoxic cell memory. In accordance with this concept, the levels of HIF and the products of its target genes remain elevated following ischaemia-reperfusion, and this is associated with several protective effects (Chavez and LaManna, 2002; Sun et al., 2003).

A closer examination of our model (Fig. 2.11) identifies a central role for pH-dependent regulation of VHL function in oxygen sensing. Cells can engage in anaerobic fermentation and secrete lactic acid once oxygen concentration decreases by 50-70% of normal levels (Gladden, 2001). This argues that cells can sense mild hypoxia and

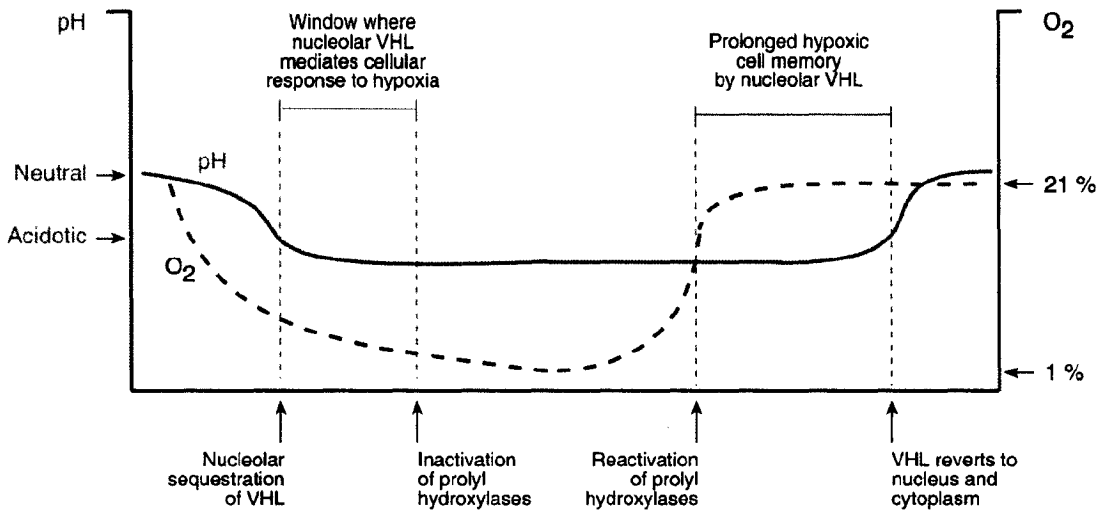
pH
Window where nucleolar VHL mediates cellular response to hypoxia
Prolonged hypoxic cell memory by nucleolar VHL
O_2
Neutral
pH
Acidotic
O_2
21 %
1 %
Nucleolar sequestration of VHL
Inactivation of prolyl hydroxylases
Reactivation of prolyl hydroxylases
VHL reverts to nucleus and cytoplasm

Figure 2.11

Figure 2.11. Oxygen sensing by H^+ and hypoxic cell memory. A moderate decrease in oxygen concentration is accommodated by a shift to metabolic fermentation leading to acidification of the extracellular environment through excess lactic acid production. Extracellular acidosis leads to redistribution of VHL to nucleoli and stabilization of HIFα prior to inactivation of PHDs. Further decrease in oxygen prevents hydroxylation of HIFα. Reoxygenation of acidotic cells reactivates PHDs without affecting nucleolar VHL. This prolongs HIF stability and hypoxic cell memory until neutral conditions are restored.

produce sufficient H^+ to trigger HIF activation before PHD inactivation (Fig. 2.11) (Bruick and McKnight, 2001; Epstein et al., 2001; Gladden, 2001). According to this model, a "respiratory enzyme" would act as the oxygen sensor and regulate HIF activation by directing cells towards the citric acid cycle or fermentation as originally postulated by Otto Heinrich Warburg (Warburg, 1931; Warburg, 1956).

Disruption of the extracellular matrix is thought to facilitate tumor vascularization. In addition to causing unregulated HIF activation, loss of VHL function also disrupts fibronectin deposition (Bonicalzi et al., 2001; Hoffman et al., 2001; Ohh et al., 1998; Stickle et al., 2004). Therefore, inactivation of VHL by nucleolar sequestration may serve the dual role of preventing extracellular matrix assembly and promoting HIF activation in hypoxic-acidotic cells thereby crafting a highly favourable environment to stimulate angiogenesis. This is supported by mathematical models predicting a role for H^+ in tumor development, including disruption of the extracellular matrix (Patel et al., 2001; Webb et al., 1999). Nucleolar sequestration may also abolish uncharacterized VHL functions or even yet allow VHL to assume new duties within the nucleolus. It will be of utmost importance to test whether key VHL functions, in addition to its regulatory role in HIF activation, are affected by the localization of this tumor suppressor to the nucleolus.

Inactivating mutations within the *VHL* gene are associated with von Hippel-Lindau disease — a cancer syndrome predisposing individuals for the development of retinal angioma, central nervous system hemangioblastoma, pheochromocytoma and renal clear cell carcinoma (RCC) (Kaelin, 2002). Loss of HIF regulation by VHL is believed to play a role in cancers retaining wild-type VHL through inactivation of PHDs

in hypoxic tumors (Semenza, 2003). Since acidosis is commonly observed within the core of tumors, it is conceivable that inactivation of VHL may occur by pH-dependent nucleolar sequestration. This would imply that VHL-expressing tumors are not under any selective pressure to acquire inactivating mutations within this gene since its product can be efficiently inactivated by acidosis.

In a 1999 Nature "News and Views", Jeffrey Bachant and Stephen Elledge hypothesized that the nucleolus can serve as an organelle by which cellular processes can be regulated through physical confinement of proteins (Bachant and Elledge, 1999). Our data are consistent with this hypothesis and suggest a common pH-dependent regulatory mechanism of VHL function. This regulatory process is similar to that observed in another system in which the MDM2 E3 ubiquitin ligase is confined to nucleoli to prevent the degradation of p53 in response to physiological cues (Bernardi et al., 2004; Lohrum et al., 2003; Weber et al., 1999). Therefore, the nucleolus is implicated in both the activation and inactivation of tumor suppressor proteins, depending on the stress signal (Bernardi et al., 2004; Lohrum et al., 2003; Mekhail et al., 2004a; Weber et al., 1999).

In conclusion, our recent study identifies nucleolar sequestration as a mechanism of inactivation of HIF destruction by VHL. Due to the abundance of evidence supporting the role of HIF in disease and normal physiology, alterations in pH, or mutations affecting the pH-responsiveness of VHL, may therefore have various important implications. The challenge will be to identify the role of nucleolar VHL within such physiological settings *in vivo*. Furthermore, it is possible that nucleolar sequestration of VHL might occur in response to signals other than acidosis, implying a more complex system of oxygen sensing than previously appreciated. Characterization of the exact

mechanism of nucleolar localization might assist in the identification of such signals and could uncover novel therapeutic targets.

References

Bachant, J.B., and S.J. Elledge. 1999. Mitotic treasures in the nucleolus. *Nature*. 398:757-758.

Bernardi, R., P.P. Scaglioni, S. Bergmann, H.F. Horn, K.H. Vousden, and P.P. Pandolfi. 2004. PML regulates p53 stability by sequestering Mdm2 to the nucleolus. *Nat Cell Biol.* 6:665-672.

Bonicalzi, M.E., I. Groulx, N. de Paulsen, and S. Lee. 2001. Role of exon 2-encoded beta -domain of the von Hippel-Lindau tumor suppressor protein. *J. Biol. Chem.* 276:1407.

Bruick, R.K., and S.L. McKnight. 2001. A conserved family of prolyl-4-hydroxylases that modify HIF. *Science*. 294:1337-1340.

Chavez, J.C., and J.C. LaManna. 2002. Activation of hypoxia-inducible factor-1 in the rat cerebral cortex after transient global ischemia: potential role of insulin-like growth factor-1. *J. Neurosci.* 22:8922-8931.

Compernolle, V., K. Brusselmans, T. Acker, P. Hoet, M. Tjwa, H. Beck, S. Plaisance, Y. Dor, E. Keshet, F. Lupu, B. Nemery, M. Dewerchin, P. Van Veldhoven, K. Plate, L. Moons, D. Collen, and P. Carmeliet. 2002. Loss of HIF-2alpha and inhibition of VEGF impair fetal lung maturation, whereas treatment with VEGF prevents fatal respiratory distress in premature mice. *Nat Med.* 8:702-710.

Currin, R.T., G.J. Gores, R.G. Thurman, and J.J. Lemasters. 1991. Protection by acidotic pH against anoxic cell killing in perfused rat liver: evidence for a pH paradox. *FASEB J.* 5:207-210.

Epstein, A.C., J.M. Gleadle, L.A. McNeill, K.S. Hewitson, J. O'Rourke, D.R. Mole, M. Mukherji, E. Metzen, M.I. Wilson, A. Dhanda, Y.M. Tian, N. Masson, D.L. Hamilton, P. Jaakkola, R. Barstead, J. Hodgkin, P.H. Maxwell, C.W. Pugh, C.J. Schofield, and P.J. Ratcliffe. 2001. C. elegans EGL-9 and mammalian homologs define a family of dioxygenases that regulate HIF by prolyl hydroxylation. *Cell.* 107:43-54.

Fabbro, M., and B.R. Henderson. 2003. Regulation of tumor suppressors by nuclear-cytoplasmic shuttling. *Exp Cell Res.* 282:59-69.

Giffard, R.G., H. Monyer, C.W. Christine, and D.W. Choi. 1990. Acidosis reduces NMDA receptor activation, glutamate neurotoxicity, and oxygen-glucose deprivation neuronal injury in cortical cultures. *Brain Res.* 506:339-342.

Gladden, L.B. 2001. Lactic acid: New roles in a new millennium. *Proc. Natl. Acad. Sci. USA.* 98:395-397.

Groulx, I., and S. Lee. 2002. Oxygen-dependent ubiquitination and degradation of hypoxia-inducible factor requires nuclear-cytoplasmic trafficking of the von Hippel-Lindau tumor suppressor protein. *Mol. Cell. Biol.* 22:5319.

Gunaratnam, L., M. Morley, A. Franovic, N. de Paulsen, K. Mekhail, D.A. Parolin, E. Nakamura, I.A. Lorimer, and S. Lee. 2003. Hypoxia inducible factor activates the transforming growth factor-alpha/epidermal growth factor receptor growth stimulatory pathway in VHL (-/-) renal cell carcinoma cells. *J. Biol. Chem.* 278:44966-44974.

Harris, A.L. 2002. Hypoxia: a key regulatory factor in tumour growth. *Nat. Rev. Cancer.* 2:38-47.

Hoffman, M.A., M. Ohh, H. Yang, J.M. Klco, M. Ivan, and W.G. Kaelin, Jr. 2001. von Hippel-Lindau protein mutants linked to type 2C VHL disease preserve the ability to downregulate HIF. *Hum. Mol. Genet.* 10:1019-1027.

Ivan, M., K. Kondo, H. Yang, W. Kim, J. Valiando, M. Ohh, A. Salic, J.M. Asara, W.S. Lane, and W.G. Kaelin, Jr. 2001. HIFalpha targeted for VHL-mediated destruction by proline hydroxylation: implications for O2 sensing. *Science*. 292:464-468.

Jaakkola, P., D.R. Mole, Y.M. Tian, M.I. Wilson, J. Gielbert, S.J. Gaskell, A. Kriegsheim, H.F. Hebestreit, M. Mukherji, C.J. Schofield, P.H. Maxwell, C.W. Pugh, and P.J. Ratcliffe. 2001. Targeting of HIF-alpha to the von Hippel-Lindau ubiquitylation complex by O2-regulated prolyl hydroxylation. *Science*. 292:468-472.

Kaelin, W.G., Jr. 2002. Molecular basis of the VHL hereditary cancer syndrome. *Nat. Rev. Cancer*. 2:673-682.

Kaku, D.A., R.G. Giffard, and D.W. Choi. 1993. Neuroprotective effects of glutamate antagonists and extracellular acidity. *Science*. 260:1516-1518.

Kivirikko, K.I., and J. Myllyharju. 1998. Prolyl 4-hydroxylases and their protein disulfide isomerase subunit. *Matrix Biol.* 16:357-368.

Kojima, H., H. Gu, S. Nomura, C.C. Caldwell, T. Kobata, P. Carmeliet, G.L. Semenza, and M.V. Sitkovsky. 2002. Abnormal B lymphocyte development and autoimmunity in hypoxia-inducible factor 1alpha -deficient chimeric mice. *Proc Natl Acad Sci USA*. 99:2170-2174.

Lohrum, M.A., R.L. Ludwig, M.H. Kubbutat, M. Hanlon, and K.H. Vousden. 2003. Regulation of HDM2 activity by the ribosomal protein L11. *Cancer Cell.* 3:577-587.

Mekhail, K., L. Gunaratnam, M.E. Bonicalzi, and S. Lee. 2004. HIF activation by pH-dependent nucleolar sequestration of VHL. *Nat. Cell Biol.* 6:642-647.

Morimoto, Y., O. Kemmotsu, and E.S. Alojado. 1997. Extracellular acidosis delays cell death against glucose-oxygen deprivation in neuroblastoma x glioma hybrid cells. *Crit. Care Med.* 25:841.

Nielsen, O.B., F. de Paoli, and K. Overgaard. 2001. Protective effects of lactic acid on force production in rat skeletal muscle. *J. Physiol.* 536:161-166.

Ohh, M., R.L. Yauch, K.M. Lonergan, J.M. Whaley, A.O. Stemmer-Rachamimov, D.N. Louis, B.J. Gavin, N. Kley, W.G. Kaelin, Jr., and O. Iliopoulos. 1998. The von Hippel-Lindau tumor suppressor protein is required for proper assembly of an extracellular fibronectin matrix. *Mol. Cell.* 1:959-968.

Patel, A.A., E.T. Gawlinski, S.K. Lemieux, and R.A. Gatenby. 2001. A cellular automaton model of early tumor growth and invasion. *J Theor Biol.* 213:315-331.

Schofield, C.J., and Z. Zhang. 1999. Structural and mechanistic studies on 2-oxoglutarate-dependent oxygenases and related enzymes. *Curr. Opin. Struct. Biol.* 9:722-731.

Semenza, G.L. 2000. HIF-1 and human disease: one highly involved factor. *Genes Dev.* 14:1983-1991.

Semenza, G.L. 2003. Targeting HIF-1 for cancer therapy. *Nature Rev. Cancer.* 3:721-732.

Stickle, N.H., J. Chung, J.M. Klco, R.P. Hill, W.G. Kaelin, Jr., and M. Ohh. 2004. pVHL modification by NEDD8 is required for fibronectin matrix assembly and suppression of tumor development. *Mol Cell Biol.* 24:3251-3261.

Sun, Y., K. Jin, L. Xie, J. Childs, X.O. Mao, A. Logvinova, and D.A. Greenberg. 2003. VEGF-induced neuroprotection, neurogenesis, and angiogenesis after focal cerebral ischemia. *J. Clin. Invest.* 111:1843-1851.

Wagner, P.D. 2001. Skeletal muscle angiogenesis. A possible role for hypoxia. *Adv. Exp. Med. Biol.* 502:21-38.

Warburg, O. 1931. The metabolism of tumors. R. R. Smith, New York. 129-163 pp.

Warburg, O. 1956. On the origin of cancer cells. *Science*. 123:309-314.

Webb, S.D., J.A. Sherratt, and R.G. Fish. 1999. Alterations in proteolytic activity at low pH and its association with invasion: a theoretical model. *Clin Exp Metastasis*. 17:397-407.

Weber, J.D., L.J. Taylor, M.F. Roussel, C.J. Sherr, and D. Bar-Sagi. 1999. Nucleolar Arf sequesters Mdm2 and activates p53. *Nat. Cell Biol.* 1:20-26.

Yu, F., S.B. White, Q. Zhao, and F.S. Lee. 2001. HIF-1alpha binding to VHL is regulated by stimulus-sensitive proline hydroxylation. *Proc. Natl. Acad. Sci. USA*. 98:9630-9635.

Inter-chapter Transition

The nucleolus has traditionally been viewed as a factory for the production of ribosomes (Lam et al., 2005). More recently, this nuclear compartment has been linked to numerous cellular activities including cell cycle control (Azzam et al., 2004; Shou et al., 2001; Shou et al., 1999; Visintin et al., 1999), DNA damage repair (van den Boom et al., 2004), and tRNA processing (Paushkin et al., 2004). Although the nucleolus has a distinct set of "resident" proteins, it is now clear that these proteins are in continuous flux between the nucleolus and other cellular compartments (Andersen et al., 2005; Carmo-Fonseca, 2002; Chen and Huang, 2001; Dundr et al., 2002; Dundr et al., 2000; Misteli, 2001; Phair and Misteli, 2000; Tsai and McKay, 2005). In the next chapter, we explore how the highly dynamic nucleolus inactivates the function of E3 enzymes, such as VHL and MDM2, as these macromolecules would be predicted to retain their dynamic nature and maintain functional molecular interactions even after a change in steady-state subcellular distribution.

Chapter 3. Regulation of ubiquitin ligase dynamics by the nucleolus

Papers and author contribution:

- Paper:

Mekhail, K., Khacho, M., Carrigan, A., Hache, R. J., Gunaratnam, L., and Lee, S. (2005) Regulation of ubiquitin ligase dynamics by the nucleolus. J. Cell Biol. 170:733-744.

- Author Contributions:

K. Mekhail	Interpretation, text and all figures Performed all but one experiment
M. Khacho	Performed an immunoprecipitation.
A. Carrigan	Assisted in initial photobleaching experiments
R. J. Hache	Assisted in photobleaching, provided confocal microscope, and reviewed manuscript before submision
L. Gunaratnam	Contributed to interpretation

Regulation of ubiquitin ligase dynamics by the nucleolus

Karim Mekhail[1], Mireille Khacho[1], Amanda Carrigan[2], Robert R.J. Hache[2], Lakshman Gunaratnam[1], and Stephen Lee[1,3]

[1]Department of Cellular and Molecular Medicine, Faculty of Medicine, University of Ottawa, Ottawa, Ontario, Canada K1H 8M5. [2]Ottawa Health Research Institute, University of Ottawa, Ottawa, Ontario, Canada, K1Y 4E9.

[3]Correspondence should be addressed to S.L. (e-mail: slee@uottawa.ca)

Published Manuscript

The Journal of Cell Biology 170:733-744 (2005)

Abstract

Cellular pathways relay information through dynamic protein interactions. We have assessed the kinetic properties of the MDM2 and VHL ubiquitin ligases in living cells under physiological conditions that alter the stability of their respective p53 and HIF substrates. Photobleaching experiments reveal that MDM2 and VHL are highly mobile proteins in settings where their substrates are efficiently degraded. The nucleolar architecture converts MDM2 and VHL to a static state in response to regulatory cues that are associated with substrate stability. Following signal termination, the nucleolus is able to rapidly release these proteins from static detention, thereby restoring their high mobility profiles. A protein surface region of VHL's β-sheet domain was identified as a discrete [H^+]-responsive nucleolar detention signal ($NoDS^{H+}$) that targets the VHL/Cullin-2 ubiquitin ligase complex to nucleoli in response to physiological fluctuations in environmental pH. Data shown here provide the first evidence that cells have evolved a mechanism to regulate molecular networks by reversibly switching proteins between a mobile and static state.

Introduction

Conjugation of ubiquitin (ubiquitylation) to proteins destines them for very different fates in the cell (Ciechanover, 2005; Muratani and Tansey, 2003; Weissman, 2001). Although targeting proteins for degradation via the 26S proteasome is the best-studied role of ubiquitylation, this modification is integral to several biochemical pathways including receptor internalization (Terrell et al., 1998), chromatin maintenance (Muratani and Tansey, 2003) and DNA repair (Gillette et al., 2001; Russell et al., 1999). The ubiquitin system is sustained by the interaction of multiple dynamic molecular networks that begin with the loading of ubiquitin onto an ubiquitin-activating enzyme (E1). The ubiquitin moiety is then transferred to an ubiquitin-conjugating enzyme (E2); and finally, an ubiquitin protein ligase (E3) catalyses the transfer of ubiquitin from E2 to the lysine residue of a specific substrate, thereby altering its cellular fate.

There are many more E3s in the cell than there are E1s and E2s combined and it is thought that E3s determine the specificity of substrate recognition within the ubiquitin system. The function of an ubiquitin ligase can be regulated by controlling the ligase or its substrate at various levels such as post-translational modifications, interactions with regulatory factors or subcellular localization (Petroski and Deshaies, 2005).

The complexity of E3 regulatory mechanisms is well demonstrated by the mechanisms controlling the degradation of the p53 tumor suppressor protein (Michael and Oren, 2003). The MDM2 ubiquitin ligase targets p53 for ubiquitylation in the nucleus followed by nuclear export and degradation by cytoplasmic 26S proteasome (Freedman and Levine, 1998; Momand et al., 1992; Oliner et al., 1993; Roth et al., 1998). Various signals can alter the function of MDM2 within this setting. DNA damage

rapidly activates the ATM (ataxia telangiectasia mutated) protein, which phosphorylates MDM2 to prevent the ubiquitylation of p53 (Appella and Anderson, 2001). Replicative senescence induces the tumor suppressor ARF to bind MDM2 and inactivate it by both immediately reducing its ability to recognize p53 in the nucleoplasm (Llanos et al., 2001) as well as translocating MDM2 to the nucleolus (Tao and Levine, 1999; Weber et al., 1999), a major nuclear compartment (Carmo-Fonseca et al., 2000). Similarly, perturbations to ribosomal biogenesis induce the ribosomal protein L11 to bind MDM2 and inhibit its function by relocating it to the nucleolus (Lohrum et al., 2003).

Functional regulation of E3s by the nucleolus has also been observed in the von Hippel-Lindau tumor suppressor (VHL)/Hypoxia-inducible factor (HIF) system (reviewed in (Kaelin, 2002; Mekhail et al., 2004a). HIF activates an array of genes that mediate cellular response to low oxygen availability (Semenza, 2000a). In the presence of oxygen, the α subunit of HIF (HIFα) is post-translationally modified by enzymes known as prolyl hydroxylases (PHDs). This allows the VHL tumor suppressor, the particle recognition motif of an elongin C/Cullin-2 ubiquitin ligase, to recognize HIFα and target it for nuclear ubiquitylation. VHL-mediated shuttling of HIFα to the cytoplasm then results in its destruction by the 26S proteasome (Groulx and Lee, 2002; Lee et al., 1999) in a manner reminiscent of the MDM2/p53 system. Several physiological cues can modulate the function of VHL within this setting. PHDs require molecular oxygen and hypoxia prevents hydroxylation of HIF, allowing it to evade recognition by VHL and degradation. In addition, we previously reported that a decrease in environmental pH triggers the relocation of VHL to the nucleolus, neutralizing its

ability to degrade nuclear HIF even in the presence of oxygen (Mekhail et al., 2004a; Mekhail et al., 2004b).

The nucleolus has traditionally been viewed as a factory for the production of ribosomes (Lam et al., 2005). More recently, this nuclear compartment has been linked to numerous cellular activities including cell cycle control (Azzam et al., 2004; Shou et al., 2001; Shou et al., 1999; Visintin et al., 1999), DNA damage repair (van den Boom et al., 2004), and tRNA processing (Paushkin et al., 2004). Although the nucleolus has a distinct set of "resident" proteins, it is now clear that these proteins are in continuous flux between the nucleolus and other cellular compartments (Andersen et al., 2005; Carmo-Fonseca, 2002; Chen and Huang, 2001; Dundr et al., 2002; Dundr et al., 2000; Misteli, 2001; Phair and Misteli, 2000; Tsai and McKay, 2005). This dynamic nature is facilitated by a fundamental characteristic of nuclear compartments; that is the lack of a delineating membrane. For example, thousands of molecules of the rRNA processing protein fibrillarin (FIB), which displays steady state nucleolar localization, exit the nucleolus each second (Phair and Misteli, 2000). The highly dynamic properties of proteins in the nucleus follow a stochastic model of high molecular mobility to ensure efficient functional interactions (Misteli, 2001). An advantage of such probabilistic movement is the ability to achieve rapid responses to signaling cues. For example, a slight increase in the quantity of a modified protein results in a relatively high probability of encountering its target. As mentioned above, resident nucleolar proteins are dynamic molecules that can functionally engage in subcellular trafficking between the nucleolus and other cellular compartments. It remains therefore unclear how the highly dynamic

nucleolus inactivates the function of E3 enzymes as these macromolecules would be predicted to retain their dynamic nature and maintain functional molecular interactions.

Here we report the unexpected observation that the nucleolar architecture is able to reversibly capture and alter the dynamic properties of ubiquitin ligases. We show that VHL and MDM2 are highly mobile proteins that can be statically detained by the nucleolus to prevent functionally required molecular interactions in response to physiological cues. Based on these data, we suggest that cells have evolved a mechanism to regulate the function of proteins by reversibly switching them between mobile and static states.

Materials and Methods

Cells and materials. C2C12 and PC12 cells from ATCC (Manassas, VA) were differentiated by lowering the serum concentration from 5% to 0.5% or by addition of nerve growth factor (50 ng ml^{-1}), respectively, before infection with adenoviruses. 786-0 (VHL-defective), U87MG, HOP62, MCF7, MDA-MB-231, SF295, and H9C2 cells were also obtained from ATCC (Manassas, VA). VHL-negative 117 cells were a kind gift from James Gnarra, Louisiana State University. 786-0 (Lee et al., 1999), 117 (Mekhail et al., 2004a), or MCF7 cells stably expressing VHL–GFP were generated as described (Lee et al., 1999). Where indicated, fluorescein diacetate (FDA, 5 μM) and propidium iodide (PI, 2 μM) (Sigma, St. Louis, MO) were added to cells 20 min from endpoint.

Cell culture. Normoxic cells were incubated at 37°C under 5% CO_2 environment. Hypoxia was achieved by incubation in a hypoxic chamber at 37°C under a 1% O_2, 5% CO_2 and N_2-balanced atmosphere. Acidosis (VHL) (Mekhail et al., 2004a) and ribosomal perturbation (MDM2) (Lohrum et al., 2003) experiments were conducted as previously described. For standard (SD) or acidosis-permissive (AP) conditions, buffer-free medium (DMEM; Invitrogen, Carlsbad, CA) was freshly prepared and supplemented with 5% (v/v) foetal bovine serum (FBS) and 1% (v/v) penicillin-streptomycin. $NaHCO_3$ (44mM) was added and the pH was adjusted to 7.2 (SD) or 5.4–7.2 (AP) with HCl. Air was bubbled into both media at 22°C, which stabilizes the pH at 7.2. AP media slowly reverted to its original pH (5.4-7.2) under hypoxia, whereas the SD medium remained at pH 7.2. MDM2 ribosomal stress (RS) conditions were induced in SD media by addition of 15 nM ActD (Calbiochem) for the last two hours of a 6 h treatment with 20 μM

MG132 (Calbiochem) (Lohrum et al., 2003). Transfected or adenovirus-infected cells were grown for 24 h under standard conditions before any treatment.

Plasmids and adenoviruses. VHL, its variants and mutants were cloned between an N-terminal Flag-tag and a C-terminal GFP-tag and into pcDNA3.1, as previously described (Bonicalzi et al., 2001; Groulx and Lee, 2002). Adenoviruses were produced using the Cre-lox recombination system. Cullin-2 construct is previously described (Groulx et al., 2000). We sincerely thank Tom Misteli (NCI, NIH, Bethesda, MD) for providing UBF1-GFP and FIB-GFP constructs, Mark Olson (University of Mississippi Medical Center, Jackson Mississippi) for B23-GFP construct, Gang Pei (Shangai Institute of Biological Sciences, Shangai, China) for MDM2-GFP, Uri Alon (Weizmann Institute of Science, Rehovot, Israel) and Galit Lahav (Harvard Medical School, Boston, MA) for MDM2-YFP. Transient transfections were conducted with Effectene transfection reagent (Qiagen, Valencia, CA).

Immunoprecipitation. Cells lysis and immunoprecipitations were conducted as previously described (Groulx and Lee, 2002). Briefly, M2 beads were added to total cell lysates containing 1 mg of protein. After 1 h tumbling at 4°C, beads were washed several times, eluted with flag peptides. Eluates were boiled before undergoing western blotting. Gels were silver stained according to manufacturer's protocol (Bio-Rad, Hercules, CA).

Immunoblotting. Samples were separated on denaturing polyacrylamide gels containing SDS and transferred to methanol-activated polyvinylidene difluoride membrane (NEN, Boston, MA). Membranes were blocked in skimmed milk before incubation with antibodies to VHL (BD Pharmingen, SanDiego, CA) (Corless et al., 1997; Kibel et al.,

1995; Mekhail et al., 2004a) or HIF-2α (Novus, Littleton, CO) (Mekhail et al., 2004a). After washing with 0.2% Tween-PBS solution, membranes were blotted with a secondary antibody conjugated to horseradish peroxidase (Jackson ImmunoResearch, West Grove, PA) and detected by Western Lightning Chemiluminescence Reagent Plus (Perkin Elmer, Boston, MA).

Immunofluorescence microscopy. Cells were seeded onto coverslips and fixed with pre-chilled (to -20 °C) methanol for 10 min followed by acetone for 1min. An anti-B23 monoclonal antibody (Sigma, St. Louis, MO) was used. Cells were incubated for 1h with a primary antibody solution containing 10% FBS and 1% Triton-X-100 (v/v). Cells were washed several times in PBS before 1 h incubation with a secondary Texas Red-labeled antibody (Jackson ImmunoResearch). Images of fixed cells were captured with an Axioskop 2 MOT PLUS microscope (Zeiss, Thornwood, NY) using a digital charged-coupled device camera (Qimaging, Burnaby, BC). Compartmental fluorescence was measured as described (Lee et al., 1999; Mekhail et al., 2004a).

Photobleaching and microscopy. Cells cultured on 40 mm-diameter glass coverslips were visualized on an MRC 1024 confocal microscope (Bio-Rad) in a FCS2 environmental chamber (Bioptechs) maintained at 37°C or, where indicated, directly into 35-mm dishes with coverslip bottoms. A 60X plan Apo oil immersion lens with a 1.4 NA was used for bleaching and imaging. Indicated areas were exposed to 5 rapid pulses of a 488-nm argon laser at 100% power and image acquisition was conducted at 1% of full laser power. For FRAP experiments, images were collected at 1 s or 5 s intervals. Recovery of the fluorescent signal within a bleached region was calculated as described

by Phair and Misteli (2000) following $I_{rel}=(I_{(t)}/I_{(0)})*(T_{(0)}/T_{(t)})$, where $T_{(t)}$ the total cellular intensity at time t, $T_{(0)}$ total cellular intensity before bleach, $I_{(0)}$ the intensity in the bleached area before bleach, and $I_{(t)}$ the intensity in the previously bleached area at time t. For inverse FRAP (iFRAP) nuclear export experiments the whole cytoplasm was bleached and cells were monitored in 30 s intervals. Relative loss of total fluorescence in the unbleached nucleus was calculated as $I_{rel}=(I_{(t)}/I_{(0)})*(N_{(0)}/N_{(t)})$, where $I_{(t)}$ is the average intensity of the unbleached nucleus at time point t, $I_{(0)}$ is the average pre-bleach intensity of the nucleus of interest and $N_{(0)}$ and $N_{(t)}$ are the average total cellular fluorescence intensities of a neighboring cell in the same field of vision at pre-bleach or at timepoint t, respectively. For FLIP experiments, cells were repeatedly bleached and imaged at 5 s intervals and fluorescence loss in unbleached areas was calculated similar to iFRAP calculations to account for any losses in fluorescence by normalizing the fluorescence in the cell of interest to that of a neighboring cell. Where indicated, cycloheximide (20 μg ml^{-1}) was added 1 h from endpoint. For all bleaching experiments, at least 10 data sets were analyzed for each result. Average pixel intensities were normalized for background fluorescence. Images of living cells from experiments that do not implicate bleaching were captured with an Axiovert S100TV microscope (Zeiss, Thornwood, NY) equipped with a 40X/1.2 C-Apochromat water immersion objective using a digital charged-coupled device camera (Empix). Pseudoclouring for bleaching and fusion experiments was achieved by applying the gradient map function of Photoshop (Adobe) to a montage of picture frames prepared with Image J (NIH) software. Other software packages used to capture images, analyze the data, and generate graphs include Northern Eclipse (Empix), Excel (Microsoft) and FreeHand (Macromedia).

Polykaryon assay. For VHL-GFP relocation to the nucleolus in homokaryon fusion assays, cells were transfected according to manufacturer's protocol to express fluorescent labeled proteins and incubated under in standard conditions for 24 h (Lee et al., 1999). Usually between 40% and 60% of cells presented strong fluorescence. Cells were washed twice with warm PBS and fused for 2 min by addition of a warm 50% solution of polyethylene glycol (PEG) in PBS (Sigma, St. Louis, MO). PEG was removed thoroughly by four washes with warm PBS and cells were incubated for 30 min under standard conditions. Cells were then replenished with AP media (see Cell culture) and transferred to hypoxia. Following acidification, cells were monitored for the distribution of VHL-GFP in polykaryonic cells. For VHL-GFP and B23-GFP dynamic trafficking assays (Fig. 3.8, B and C), cells were transfected to express GFP-tagged proteins or left unaltered. The cells were then mixed at a 1:10 ratio, plated in 35-mm-diameter culture dish with a girded coverslip as its base, and exposed to hypoxia in AP media. Following acidification and redistribution of VHL-GFP to nucleoli, cells were fused by PEG treatment as described above. This process yielded a significant number of polykaryonic cells where the fluorescence observed in the cell is only associated with nucleoli of only one or two nuclei, while other nuclei within the same polykaryonic cell displayed no fluorescence. Hypoxic cells were then rapidly washed twice with non-buffered acidic media (pH 6.0-6.5), replenished with their original acidified AP media, and cells were monitored by fluorescence microscopy.

Results

[H+]-regulated kinetics of VHL subcellular trafficking

Ischaemic tissues or hypoxic cells normally acidify their extracellular milieu as a physiological consequence of anaerobic glycolysis. This is best exemplified by muscle fatigue, in which myotubes produce lactic acid following exposure to hypoxia. Study of the ubiquitin ligase component VHL within this setting revealed its functional regulation by changes in environmental H^+ concentrations (Mekhail et al., 2004a). VHL engages in nuclear/cytoplasmic trafficking in neutral conditions but accumulates in the nucleolus upon a decrease in extracellular pH, a process that results in stabilization of its substrate HIF. Differentiated myotubes can be incubated in standard media (SD), which prevents fluctuations in pH, or in acidosis-permissive media (AP), which is prepared to enable hypoxic cells to acidify their extracellular milieu to varying degrees (see Materials and Methods) (Mekhail et al., 2004a). VHL-GFP is observed in its typical diffuse nuclear cytoplasmic distribution under neutral pH conditions, independent of oxygen tension (Fig. 3.1A, left panel, and (Mekhail et al., 2004a)). A rapid redistribution of VHL-GFP to nucleoli was observed only when hypoxic myotubes were incubated in AP media that allow the myotubes to acidify their environment to pH 6.40 or lower (Fig. 3.1, A and D; and see Fig. 3.2, A and B, for cell viability controls), indicating the existence of a pH threshold required for triggering nucleolar localization of VHL. The threshold displayed cell-type specific differences within the 6.60-5.80 pH range (Fig. 3.1C and Fig. 3.3). VHL efficiently reverted to a diffuse nuclear-cytoplasmic localization under hypoxic conditions only when cells were replenished with media at values higher than the pH threshold required to trigger nucleolar localization (Fig. 3.1, B to D). Closer examination

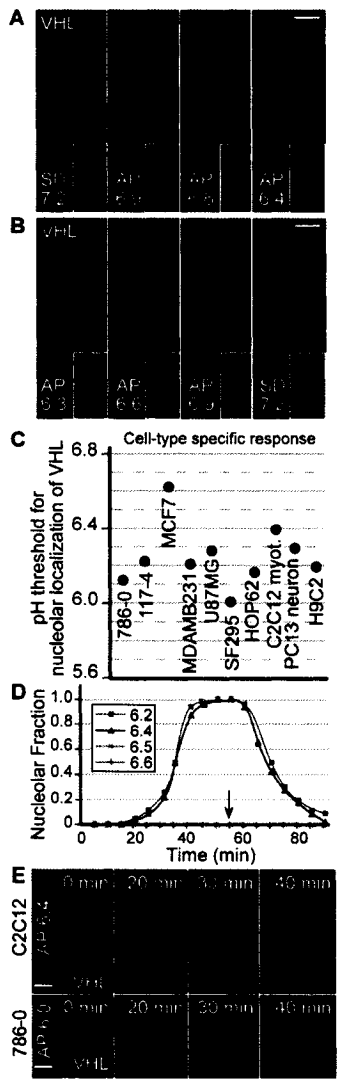
A
VHL
B
VHL
C
Cell-type specific response
pH threshold for nucleolar localization of VHL
6.8
6.4
6.0
5.6
786-0
117-4
MCF7
MDAMB231
U87MG
SF295
HOP62
C2C12 myot.
PC13 neuron
H9C2
D
Nucleolar Fraction
1.0
0.8
0.6
0.4
0.2
0
6.2
6.4
6.5
6.6
0
20
40
60
80
Time (min)
E
C2C12
786-0
VHL
VHL

Figure 3.1

Figure 3.1. pH-dependent kinetics of VHL subcellular trafficking. (**A**) C2C12 differentiated myotubes were cultured in standard media (SD) and infected to express adenovirus-introduced VHL-GFP. Cells were replenished with either fresh SD media (pH 7.2) or different acidification permissive media (AP, initial pH 7.2) that allow maximal extracellular acidification to pH 6.9, 6.6, 6.4, 6.2 or 6.0 (see Materials and Methods). Cells were transferred to hypoxia (1% O_2) for 18 h. VHL redistributed to nucleoli only in conditions of pH 6.4 or lower (images of pH 6.2 and 6.0 are not shown). Extracellular pH is indicated on each panel. Insets show Hoechst staining of DNA. Scale bars represent 10 μm. (**B**) Following localization of VHL-GFP to the nucleolus, myotubes were replenished with AP media previously maximally acidified to indicated pH levels, or with fresh SD media. VHL reverted to nucleo-cytoplasmic distribution only when the pH of the media was higher than 6.4. (**C**) Different cell-types were treated as in (**A**) and (**B**) to identify the pH thresholds required for nucleolar targeting of VHL (n = 40 for each tested pH value). (**D**) Kinetics of VHL nucleolar localization in acidosis and release following neutralization in differentiated myotubes. Cells were exposed to different AP media as in (**A**) to induce VHL nucleolar redistribution and all media were neutralized to pH 7.2 by addition of NaOH (arrow). Time zero indicates time at which the pH of AP media reached 6.4. For the 6.5 and 6.7 sets, time zero is matched to that of the pH 6.4 set. (**E**) Cells were incubated in AP media (initial pH 7.2) that blocks acidification beyond pH 6.0. After reaching the acidification level matching the pH threshold required to trigger nucleolar targeting of any given cell-type (time zero), the localization of VHL-GFP was monitored over time. Upon reaching the pH threshold,

VHL shifts from mainly cytoplasmic to mainly nucleoplasmic before triggering nucleolar localization.

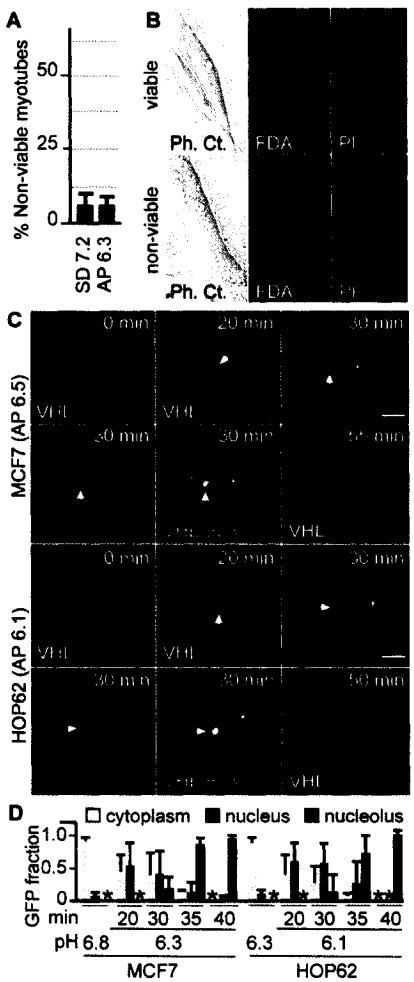
A
% Non-viable myotubes
50
25
0
SD 7.2
AP 6.3
B
viable
Ph. Ct.
FDA
PI
non-viable
Ph. Ct.
FDA
PI
C
MCF7 (AP 6.5)
0 min
20 min
30 min
VHL
HOP62 (AP 6.1)
D
cytoplasm
nucleus
nucleolus
GFP fraction
1.0
0.5
0
min
20 30 35 40
20 30 35 40
pH 6.8
6.3
6.3
6.1
MCF7
HOP62

Figure 3.2

Figure 3.2. Characteristics of cells and VHL subcellular trafficking in hypoxia-acidosis. (**A** and **B**) Differentiated myotubes are viable in hypoxia-acidosis. (**A**) C2C12 differentiated myotubes were cultured in SD or AP media under hypoxia for 20 h. Fluorescein diacetate (FDA, 5 μM) and propidium iodide (PI, 2 μM) were added 30 min from endpoint. Non-viable myotubes were scored as FDA-negative and PI-positive. Representative myotubes are shown in (**B**). (**C** and **D**) After reaching the pH threshold, VHL shifts from mainly cytoplasmic to mainly nucleoplasmic before triggering nucleolar localization. Cells were incubated in AP media (initial pH 7.2) that blocks acidification beyond pH 6.0. After reaching the acidification level matching the pH threshold required to trigger nucleolar targeting of any given cell-type (time zero), the localization of VHL-GFP was monitored over time. (**C**) At 30 min, cells were fixed and submitted to anti-B23 immunofluorescence to identify the nucleolus. (**D**) Subcellular ratiometric measurements of fluorescence. Shown is the average VHL-GFP fluorescence associated with different compartments of a single cell (red line, n = 15) at different time points after reaching pH thresholds for the indicated cell lines. Total cellular fluorescence is set to 1.0 in each case. Asterisk indicates absence of signal above background.

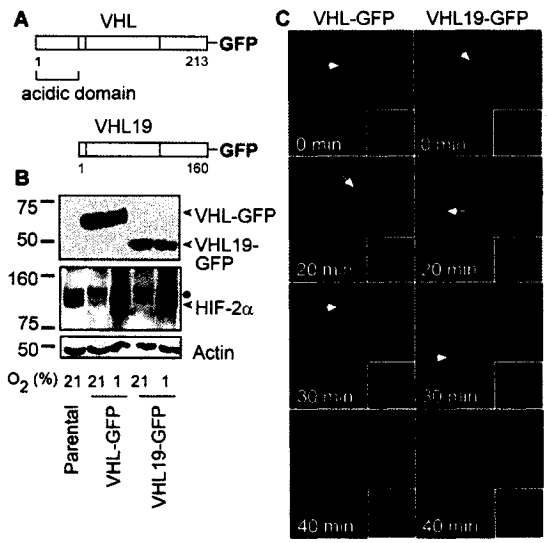
A
VHL
GFP
1
213
acidic domain
VHL19
GFP
1
160
B
75
50
160
75
50
VHL-GFP
VHL19-GFP
HIF-2α
Actin
O2 (%) 21 21 1 21 1
Parental
VHL-GFP
VHL19-GFP
C
VHL-GFP
VHL19-GFP
0 min
20 min
30 min
40 min

Figure 3.3

Figure 3.3. Both forms of VHL relocate to the nucleolus in response to the same pH threshold in cells stably expressing the GFP-tagged proteins. (A) Schematic representation of both forms of VHL – VHL (p30) and VHL19 (p19). (B) 786-0 cells were transfected to stably express GFP-tagged VHL or VHL19. Cells were incubated under standard conditions in normoxia or hypoxia for 8 h. Cells were harvested and lysates were immunoblotted with antibodies to GFP and HIF-2α. Actin blotting served as control. (C) 786-0 cells stably expressing VHL-GFP or VHL19-GFP were transferred to hypoxia in AP media (initial pH 7.2). Following maximal acidification to pH 6.0, both VHL forms displayed a similar rate and pattern of localization to the nucleolus.

of this system reveals that the relocation of VHL to the nucleolus is a two step process, where the protein displays an initial shift from mainly cytoplasmic to mainly nucleoplasmic localization prior to initiating any detectable targeting to the nucleolus, in all tested cell lines (Fig. 3.1 E; and Fig 3.2, C and D). These data suggest that the subcellular trafficking dynamics of VHL are regulated by a multilayered cellular mechanism that gauges environmental hydrogen ion concentrations.

Different kinetics of nucleolar VHL and resident nucleolar proteins following transcriptional inhibition

Due to the role of the nucleolus in ribosomal biogenesis, perturbations to transcription, such as by treatment with low levels of actinomycin D (ActD), alter the trafficking properties of steady state nucleolar proteins between the nucleolus and the nucleoplasm (Andersen et al., 2005; Chen and Huang, 2001). For example, the human immunodeficiency virus (HIV) mRNA exporter REV is a dynamic nucleolar protein that redistributes to the nucleoplasm and cytoplasm following transcriptional inhibition under both neutral (data not shown, and (Daelemans et al., 2005; Stauber et al., 1995)) and acidic (Fig. 3.4, A and top row of B) conditions. In contrast, the nucleolar localization of VHL in acidosis persisted in the absence of transcription (Fig. 3.4 B, bottom row). Similar results were obtained in experiments using VHL-BFP and REV-GFP (data not shown). The ability of REV to rapidly alter its steady state distribution under these conditions is greatly enhanced by its strong nuclear export sequence (NES). We therefore tested whether fusion of this NES to VHL would enable it to release from nucleoli of acidotic cells following transcriptional inhibition. VHL-GFP-NES fusion localized almost exclusively to the cytoplasm under neutral conditions but was restricted

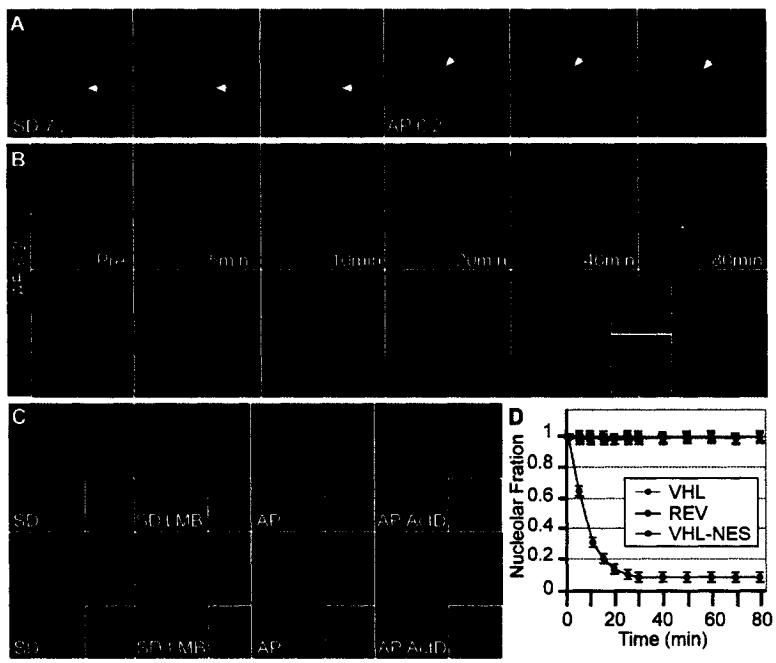
A
B
C
D
Pre
5min
15min
30min
40min
60min
SD
SD LMB
AP
AP AsiD
Nucleolar Fration
1
0.8
0.6
0.4
0.2
0
0
20
40
60
80
Time (min)
VHL
REV
VHL-NES

Figure 3.4

Figure 3.4. Kinetics of nucleolar VHL and REV. (**A** and **B**) MCF7 cells co-transfected to express VHL-GFP and REV-BFP were incubated in hypoxia in SD or AP conditions. Following localization of VHL-GFP to the nucleolus, cells were either fixed and immunostained for nucleolar B23 (**A**) or treated with actinomycin D (ActD, 10 μg/mL) and monitored over time (**B**). (**C** and **D**) VHL-GFP-NES fusion protein is not released from nucleoli following ActD treatment. MCF7 cells were transfected to express VHL-GFP, VHL-GFP-NES or GFP-NES alone and transferred to hypoxia in SD or AP media. Shown are images 50 min after AP media reached the pH 6.5 threshold. Where indicated, leptomycin B (LMB) was added when AP media reached pH 6.65 (usually 30-40 min) prior to pH 6.5 timepoint. (**D**) Ratiometric fluorescence measurements of hypoxic-acidotic cells initially displaying nucleolar REV-BFP, VHL-GFP and VHL-GFP-NES following ActD treatment.

to nucleoli at steady state under acidosis (Fig. 3.4 C). ActD treatment failed to release the VHL-GFP-NES fusion protein from nucleoli (Fig. 3.4, C and D) suggesting that the subcellular trafficking dynamics of VHL in the nucleolus significantly differ from the dynamics of resident nucleolar proteins.

Physiological regulation of VHL ubiquitin ligase dynamics by the nucleolus

We therefore used fluorescence recovery after photobleaching (FRAP) to assess how the nucleolus affects the dynamic properties of GFP-tagged VHL in living cells (Lippincott-Schwartz et al., 2003). Specific cellular regions expressing fusion proteins were bleached with the use of a laser pulse that irreversibly quenches the GFP signal, and the recovery of signal in the bleached area was recorded by time-lapse confocal microscopy. The kinetics and extent of recovery of fluorescence in a cellular region following bleaching are reflective of the dynamics of the studied fluorescent chimeras.

Cells cultured under standard neutral conditions displayed an essentially complete recovery of VHL-GFP fluorescence within seconds of bleaching nucleoplasmic (Fig. 3.5, A and G) or cytoplasmic (shown further in Fig. 3.11 D) regions. We first assessed the capacity of the nucleolus to sustain dynamic shuttling under acidosis by monitoring resident nucleolar proteins, such as the rRNA processing factors fibrillarin (FIB) and nucleophosmin (NPM or B23) as well as the RNA polymerase I preinitation factor upstream binding factor 1 (UBF1). Acidosis did not alter the steady state distribution of any of the studied resident nucleolar proteins (Fig. 3.5, D and E) compared to neutral conditions. In addition, these proteins displayed a rapid pH-independent recovery of fluorescence following bleaching of a single nucleolus within cells with multiple nucleoli (Fig. 3.5, C and F), indicating dynamic protein shuttling between nucleoli of acidotic

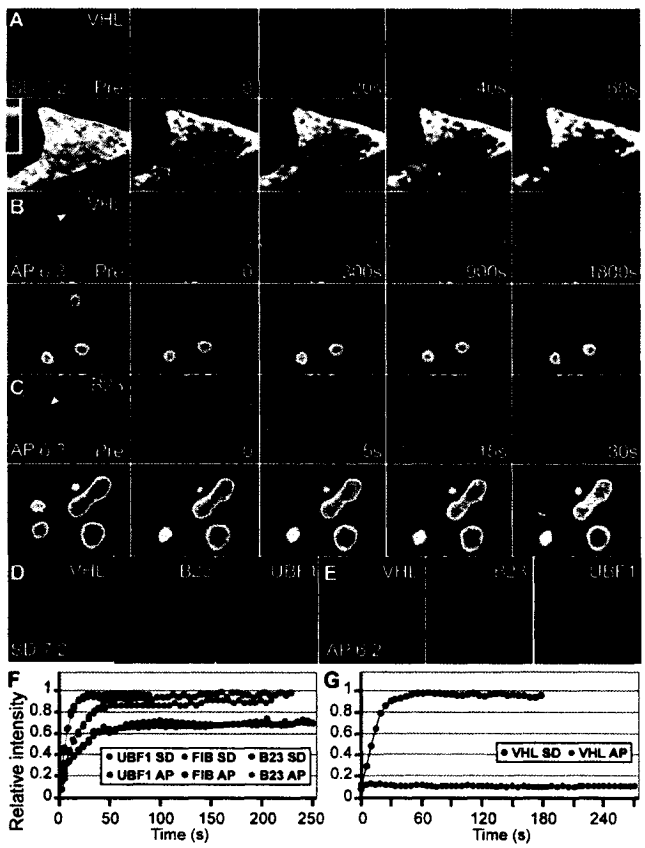
A
VHL
B
VHL
C
D
VHL
E
VHL
F
Relative intensity
1
0.8
0.6
0.4
0.2
0
0
50
100
150
200
250
Time (s)
UBF1 SD
FIB SD
B23 SD
UBF1 AP
FIB AP
B23 AP
G
1
0.8
0.6
0.4
0.2
0
0
60
120
180
240
Time (s)
VHL SD
VHL AP

Figure 3.5

Figure 3.5. FRAP analysis reveals that VHL does not shuttle between nucleoli in acidosis. MCF7 cells transiently transfected to express low levels of VHL-GFP, B23-GFP, FIB-GFP or UBF1-GFP were incubated in hypoxia under SD or AP conditions. (**A** to **C**) Cells were imaged before and after bleaching of indicated nucleoplasmic regions (dashed square) or specific nucleoli (arrows). Post-bleach time is indicated in seconds. Areas of interest are shown as pseudocolored panels to better illustrate minimal changes in fluorescence. (**D** and **E**) Steady state localization of GFP-tagged proteins following incubation in SD or AP media under hypoxia. (**F** and **G**) Quantitation of recovery kinetics. Fluorescence intensity in the bleached region was measured and expressed as relative recovery (see Materials and Methods). For quantitation, at least 10 cells were analyzed for each result.

cells. In contrast, nucleolar VHL failed to display recovery of fluorescence under the same culture and bleaching parameters (Fig. 3.5, B and G), suggesting that acidosis alters the mobility profile of VHL. Similar to previous reports, reduction of the temperature from 37°C to 22°C did not have any significant effect on the kinetics or extent of recovery of any of the tested proteins in the nucleus or cytoplasm (data not shown and see (Phair and Misteli, 2000)). These data suggest that the redistribution of VHL to the nucleolus in response to increases in extracellular hydrogen ion concentrations may alter its general dynamic characteristics in the cell.

The dynamics of VHL were next analyzed by fluorescence loss in photobleaching (FLIP) experiments (Lippincott-Schwartz et al., 2003). In FLIP, a living cell is repeatedly hit with a laser beam in the same region. Loss of fluorescence in an area outside the bleached spot is reflective of protein mobility between that area and the bleached spot. A rapid loss of VHL-GFP fluorescence was observed in essentially the whole nucleus following repetitive bleaching of a small nucleoplasmic region in cells incubated under neutral conditions (Fig. 3.6 A). Studies presented further in this report (Fig. 3.7) will study the nuclear-cytoplasmic trafficking properties of VHL. These observations indicate that VHL participates in dynamic molecular networks.

Next, cells were transfected to express low levels of VHL-GFP to allow for a complete redistribution of the protein chimera to the nucleolus following acidification in hypoxia (Fig. 3.6 B, first panel and see (Mekhail et al., 2004a)). Under these conditions, VHL-GFP fluorescence in the nucleolus was unaffected by repetitive bleaching of a nucleoplasmic (Fig. 3.6, B and F) or cytoplasmic (data not shown) region. In stark contrast, resident nucleolar proteins rapidly dissociate from the nucleolus in hypoxic-

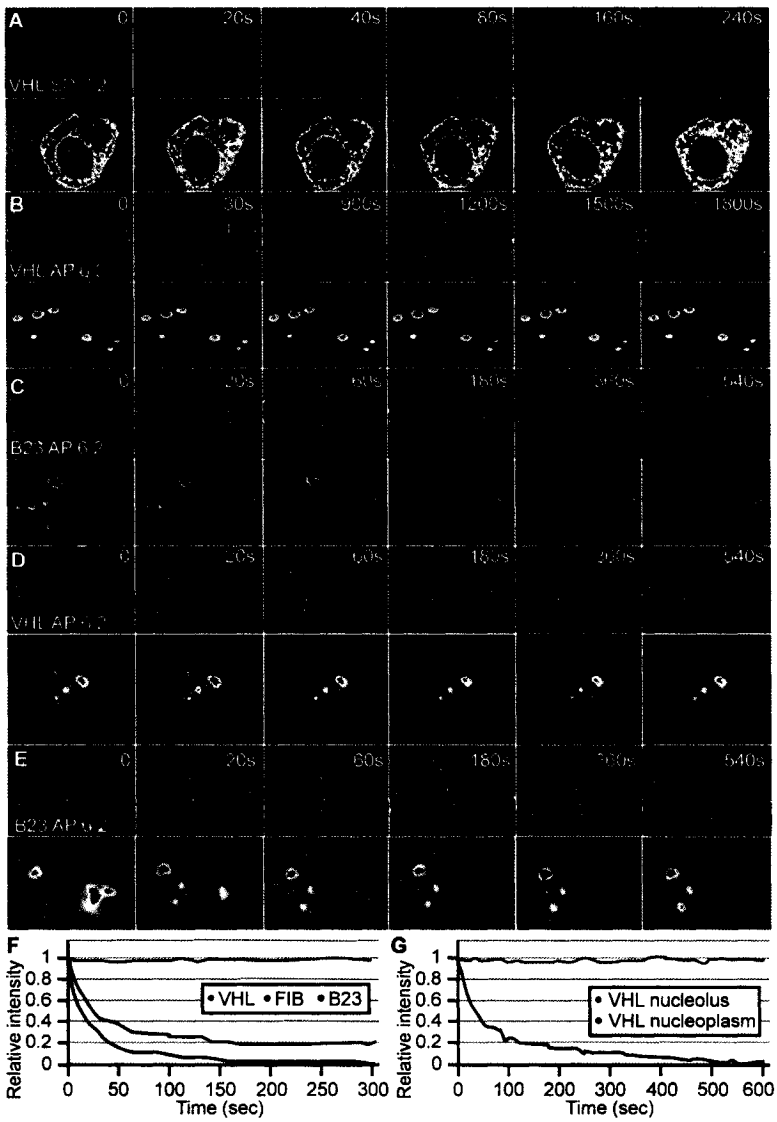
A
0
20s
40s
80s
160s
240s
B
0
30s
90s
1200s
1500s
1800s
C
0
20s
80s
160s
240s
340s
D
0
20s
80s
160s
240s
340s
E
0
20s
80s
160s
240s
340s
F
Relative intensity
1
0.8
0.6
0.4
0.2
0
0
50
100
150
200
250
300
Time (sec)
• VHL • FIB • B23
G
Relative intensity
1
0.8
0.6
0.4
0.2
0
0
100
200
300
400
500
600
Time (sec)
• VHL nucleolus
• VHL nucleoplasm

Figure 3.6

Figure 3.6. FLIP analysis reveals that nucleolar VHL does not traffic between the nucleolus and nucleoplasm in acidosis. MCF7 cells transiently transfected to express low (**A** to **C**, and **F**) or high (**D**, **E**, and **G**) levels of VHL-GFP or B23-GFP were incubated in hypoxia under SD or AP conditions. At timepoints matching the relocation of VHL-GFP (low levels set) to nucleoli, all cells were submitted to a FLIP analysis where nucleoplasmic regions (white squares) were repeatedly bleached. Cells were imaged between pulses. (**F** and **G**) Corresponding kinetics of loss of fluorescence.

acidotic cells (Fig. 3.6, C and F). We next examined whether interaction with the nucleolar architecture is required for acidosis-mediated modification of VHL dynamics. Cells were thus transfected to express higher levels of VHL-GFP, saturating nucleolar binding sites and preventing the full redistribution of the fluorescent protein chimera to the nucleolus following acidification in hypoxia (Fig. 3.6 D, first panel). This establishes two different protein pools in the cell, nucleoplasmic and nucleolar. While repetitive bleaching of a nuclear region in these cells resulted in complete loss of nucleoplasmic fluorescence, nucleolar VHL-GFP signal remained constant over the course of the experiment (Fig. 3.6, D, E and G). No significant bleaching was observed in neighboring nuclei in all of the experiments. Similar to nuclear VHL-GFP under neutral conditions, the nucleoplasmic pool of VHL-GFP in acidosis was able to engage in nuclear export as revealed by inverse FRAP (iFRAP) analysis of living cells (Lippincott-Schwartz et al., 2003), thereby indicating that this nucleoplasmic pool retains functional interactions with the nucleopore architecture in acidosis (Fig. 3.7). These data indicate that the interaction of VHL with the nucleolar architecture is required for acidosis-mediated modification of VHL protein dynamics.

We next studied VHL dynamics using polykaryon fusion assays, which provide an alternative approach to photobleaching in assessing changes in subcellular trafficking of proteins (Walther et al., 2003). Cells expressing VHL-GFP were fused in a standard polyethylene glycol (PEG) fusion assay. VHL remains nuclear-cytoplasmic in polykaryonic cells (Fig. 3.8 A, a and b) (Lee et al., 1999). Transfer to hypoxia resulted in acidification of the media and VHL-GFP displayed its typical two-step localization process to the nucleolus (Fig. 3.8 A, c-g). It is important to note that nucleolar VHL

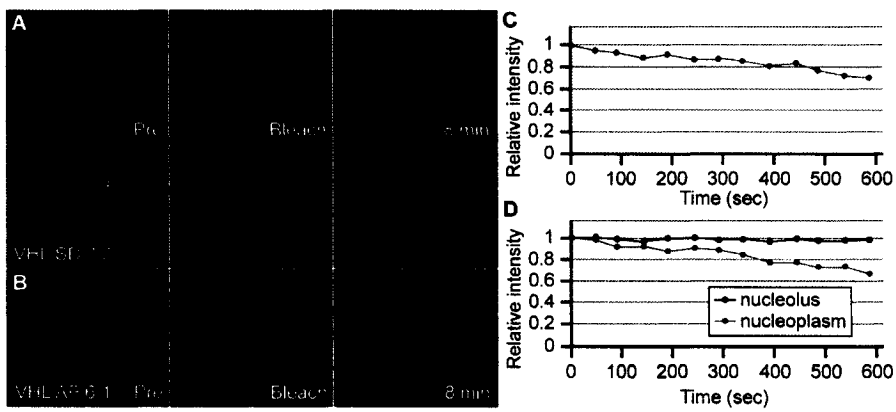
A
B
C
Relative intensity
1
0.8
0.6
0.4
0.2
0
0 100 200 300 400 500 600
Time (sec)
D
Relative intensity
nucleolus
nucleoplasm
0 100 200 300 400 500 600
Time (sec)

Figure 3.7

Figure 3.7. Comparison of nuclear export of VHL under neutral and acidic conditions using inverse FRAP (iFRAP). (**A** and **B**) MCF7 cells transfected to express high levels of VHL-GFP were incubated in hypoxia for 20 h under SD or AP conditions. Cells were imaged before and after bleaching of total cytoplasmic fluorescence as achieved by bleaching large regions indicated by dashed squares. Loss of nuclear fluorescence, indicative of nuclear export potential, was monitored by time-lapse microscopy. (**C** and **D**) Quantitation of nuclear export kinetics is represented in red. No change was observed in nucleolar VHL-GFP signal.

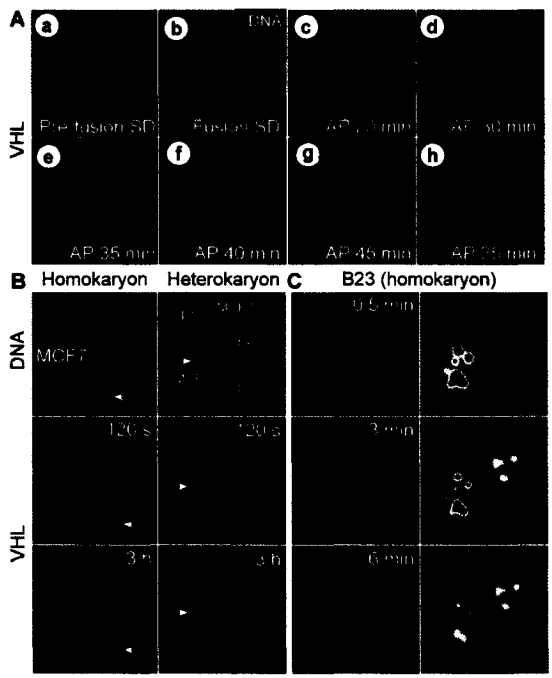
A
VHL
DNA
Pre fusion SD
Fusion SD
AP 35 min
AP 40 min
AP 45 min
B
Homokaryon
Heterokaryon
C
B23 (homokaryon)
DNA
VHL
MCF7
120 s
3 h
0.5 min
3 min
6 min

Figure 3.8

Figure 3.8. Long-term detention of VHL within the nucleolar space revealed by the inability of VHL to release from nucleoli in a polykaryon fusion assay. (A) MCF7 cells transiently expressing VHL-GFP were fused in a standard polyethylene glycol (PEG) fusion assay and incubated in SD media for 30 min (b). Cells were replenished with AP media and transferred to hypoxia. VHL-GFP localization was monitored following reaching the pH 6.5 threshold (c to g). Nuclei within a polykaryonic cell were always synchronized in the rates of nucleolar appearance of VHL-GFP. This is not necessarily the case for monokaryonic cells in close proximity under AP conditions (h). (B) Unaltered MCF7 cells were co-cultured under standard conditions with either MCF7 (homokaryon assay) or NIH 3T3 (heterokaryon assay) cells transfected to transiently express VHL-GFP. Cells were then transferred to hypoxia in AP media. Following nucleolar localization of VHL-GFP, cells were fused and monitored by timelapse microscopy. Hoechst staining of DNA was used to identify donor and acceptor cells. (C) Unaltered MCF7 cells were co-cultured under standard conditions with MCF7 cells transfected to transiently express B23-GFP. Cells were cultured in AP media, fused and monitored as in (B).

signal was equally distributed between the nuclei of a polykaryonic cell (Fig. 3.8 A), indicating that VHL-GFP displays no preference for the nucleoli of one nucleus over another. Next, we co-cultured VHL-GFP-expressing and non-expressing cells under standard conditions, then transferred them to hypoxia in AP media. Following the redistribution of VHL-GFP to nucleoli, cells were rapidly fused and replenished with their own acidified AP media. This process yielded a significant number of polykaryonic cells where the fluorescence observed in the cell is only associated with nucleoli of only one or two nuclei, while other nuclei displayed no fluorescence (Fig. 3.8 B). VHL-GFP failed to exhibit any change in localization up to three hours post-fusion. In contrast, under the same conditions, B23-GFP (Fig. 3.8 C) and REV-GFP (data not shown) redistributed from the nucleoli of a single cell to the nucleo-cytoplasm and nucleoli of the acceptor (non-transfected) cells of polykaryons. In addition to bleaching experiments, results from the fusion assays reveal a role for the nucleolus in regulating the subcellular dynamic profile of the VHL tumor suppressor.

Static detention of MDM2 and VHL ubiquitin ligase by the nucleolus

MDM2 displays a diffuse nuclear localization under standard culture conditions. FRAP and FLIP experiments revealed that MDM2 is a highly dynamic protein within this setting (Fig. 3.9 A and 3.10 A). MDM2 localizes to the nucleolus in response to perturbations in ribosomal biogenesis following treatment with low levels of ActD that inhibit RNA polymerase I (Fig. 3.9 B and 3.10 B) (Lohrum et al., 2003). MDM2 is unable to target p53 for degradation under these conditions. We therefore assessed the dynamics of MDM2 following relocation to the nucleolus. When nucleolar, the dynamic profile of MDM2 significantly changed as GFP fluorescence did not exhibit any

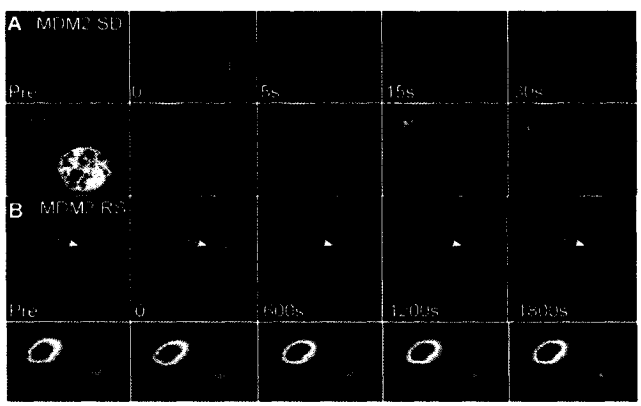

Figure 3.9

Figure 3.9. FRAP analysis reveals that the redistribution of MDM2 from nucleoplasm to nucleoli in response to perturbations in ribosomal biogenesis alters general MDM2 dynamic state. MCF7 cells transfected to express low levels of MDM2-GFP were cultured either under standard conditions (**A**), or ribosomal stress (RS) (**B**) induced by ActD treatment (see (Lohrum et al., 2003) and Materials and Methods). Cells were submitted to FRAP analysis as described for VHL in figure 3 by bleaching the indicated nucleoplasmic regions (white squares) or specific nucleoli (arrows). Pseudocolored zoom of area indicated by dashed rectangle is shown in (**B**).

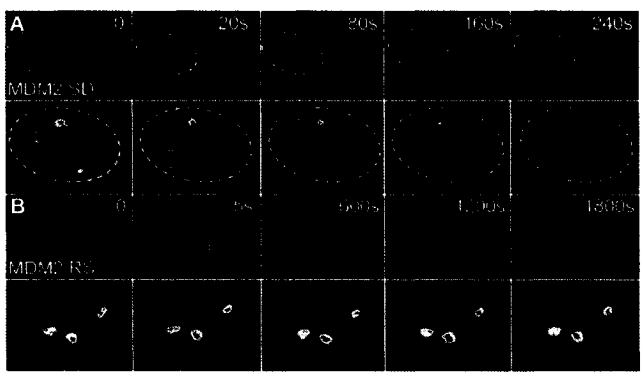

Figure 3.10

Figure 3.10. FLIP analysis indicate that the redistribution of MDM2 from nucleoplasm to nucleoli alters general MDM2 dynamic state. MCF7 cells transfected to express low levels of MDM2-GFP were cultured either under standard conditions (**A**), or ribosomal stress (RS) (**B**) induced by ActD treatment (see (Lohrum et al., 2003) and Materials and Methods). Cells were submitted to FLIP analysis as described for VHL in figure 4 by bleaching the indicated nucleoplasmic regions (white squares).

recovery/redistribution in FRAP experiments following bleaching of the nucleolus (Fig. 3.9 B) or loss in FLIP experiments following repetitive bleaching of a nucleoplasmic (Fig. 3.10 B) or cytoplasmic (data not shown) region. Similar to VHL (Fig. 3.6, D and G), the interaction of MDM2 with the nucleolar architecture is required for modification of its trafficking dynamics as evidenced by the quick recovery of MDM2 in the nucleoplasm of transcriptionally inhibited cells expressing high levels of the protein in FRAP (Fig. 3.11A). We next evaluated the dynamics of VHL and MDM2 ligases within the nucleolar space. VHL and MDM2 did not exhibit any fluorescence recovery following bleaching of an area within the nucleolus (Fig. 3.11, A and C). In contrast, B23 remained localized to nucleoli at steady state within our experimental settings (SD, AP, and RS) retaining its highly mobile properties though prolonged incubation with ActD resulted in B23 accumulating in the nucleoplasm (Fig. 3.11 B, and data not shown). Upon photobleaching, a border is created between the bleached area and the gradient of concentration established by the remaining fluorescent molecules (Fig. 3.11 C). For moving proteins, this border changes its shape as well as its position within the field of vision over time. Statically detained cellular components do not exhibit significant changes in these variables. We therefore compared the characteristics of borders of concentration gradients established by bleaching fluorescently labeled proteins when localized to different regions of the cell. While analysis of concentration gradient borders in the nucleoplasm and cytoplasm revealed a highly dynamic profile of protein mobility, borders established within the nucleolar space neither changed in shape nor moved within the field of vision for up to 2 h following bleaching (Fig. 3.11 C to F, and data not shown). A similar static protein profile was observed for MDM2 in the nucleolus (data

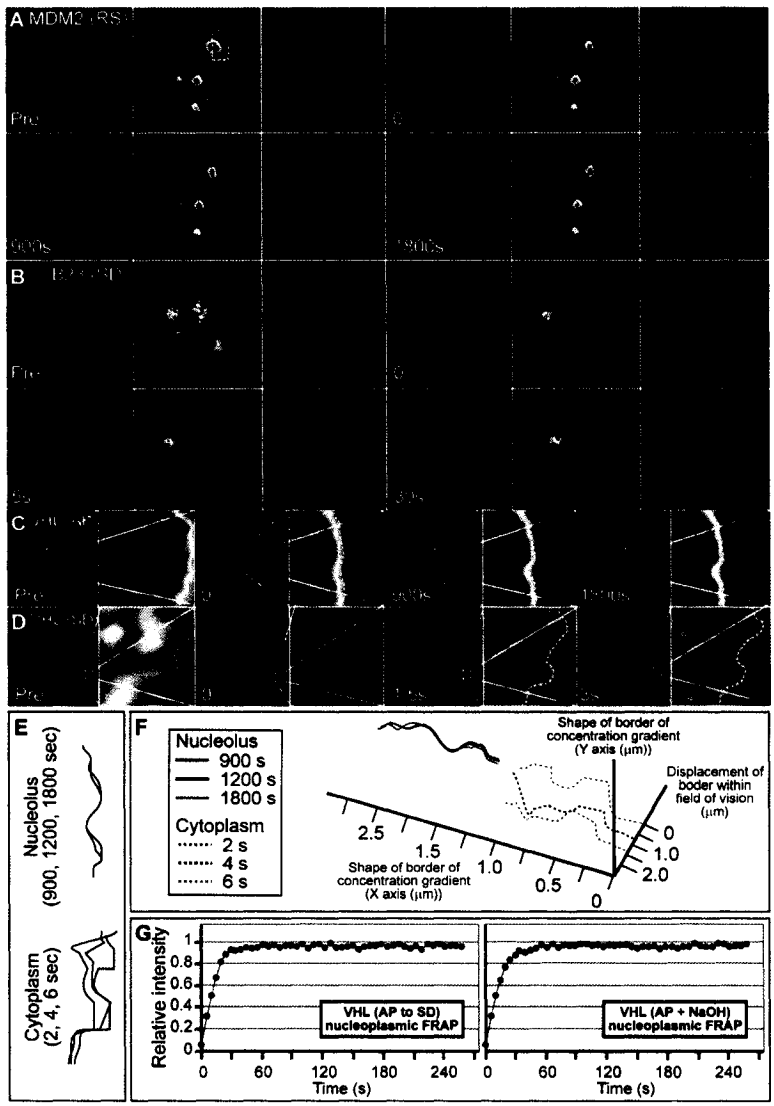
A
Pre
900s
B
Pre
C
Pre
D
Pre
E
Nucleolus
(900, 1200, 1800 sec)
Cytoplasm
(2, 4, 6 sec)
F
Nucleolus
900 s
1200 s
1800 s
Cytoplasm
2 s
4 s
6 s
Shape of border of concentration gradient (Y axis (μm))
Displacement of boder within field of vision (μm)
Shape of border of concentration gradient (X axis (μm))
2.5
1.5
1.0
0.5
0
0
1.0
2.0
G
Relative intensity
VHL (AP to SD) nucleoplasmic FRAP
VHL (AP + NaOH) nucleoplasmic FRAP
Time (s)
Time (s)

Figure 3.11

Figure 3.11. Reversible static detention of VHL and MDM2 by the nucleolar architecture. MCF7 cells were transfected to express GFP-tagged MDM2 (**A**), B23 (**B**), or VHL (**C-G**) and incubated under SD, AP or RS conditions as indicated. A region representing about half of the nucleolar space (white squares) of a single nucleolus was bleached and cells were monitored by timelapse fluorescence microscopy. Note the absence of any changes in fluorescence for nucleolar VHL and MDM2. Zoom of a single nucleolus is shown in (**C**). Changes in the shape of the border (dashed white outline set by bleaching) of the protein concentration gradient from different timepoints as in (**C**) and (**D**) are overlayed in (**E**). (**F**) Borders with changing (cytoplasm) or unaltered (nucleolus) shapes (plotted on X and Y axes) were monitored for their displacement away from their original position within the field of vision. Only borders set within the nucleolar space did not exhibit any movement. (**G**) Following hypoxia-induced acidification of AP media and confinement of VHL-GFP to the nucleolus, NaOH was added to neutralize AP media (to pH 7.2) or cells were replenished with fresh SD media (pH 7.2) to induce the reversion of VHL-GFP to the nucleo-cytoplasm (also see Figure 3.1). FRAP analyses in which small nucleoplasmic regions were bleached reveal that VHL-GFP resumes its high mobility profile following a return to neutral pH conditions.

not shown). These findings suggest that VHL and MDM2 are targeted for static detention in the nucleolus in response to physiological cues.

Detention of ubiquitin ligases by the nucleolar architecture is a reversible process

Data presented so far suggest that the nucleolus captures the highly mobile VHL for static detention upon the establishment of cell-type specific extracellular pH threshold. We asked whether this process is reversible and if VHL can be released from nucleoli to recover its highly mobile state. VHL rapidly reverts to a diffuse nuclear cytoplasmic localization only following the reinstatement of neutral pH conditions under hypoxia or normoxia conditions (Fig. 3.1) (Mekhail et al., 2004a). Following reversion, fluorescence rapidly recovered after bleaching small nucleoplasmic regions (Fig. 3.11 G). These data indicate that the regulated inactivation of ligases following targeting to the nucleolus relies on their transient conversion to static participants of particular molecular networks.

Identification of a novel, discrete, pH-responsive nucleolar detention signal ($NoDS^{H+}$)

Targeting of proteins to nucleoli is achieved by nucleolar localization (NoLS) or retention (NoRS) sequences. These sequences are relatively large and differ considerably from nuclear import or export sequences, which are comprised of only a few amino acid residues. We, therefore, decided to identify the domain of the VBC/Cul-2 complex that mediates [H+]-regulated nucleolar sequestration of VHL. VHL is a component of the multi-protein ubiquitin ligase complex that targets the transcription factor HIF for proteasomal destruction. The complex is composed of at least VHL, elongin B, elongin C, Cullin-2 and Rbx1 (VBC/Cul-2) (Fig. 3.12 A) (Kaelin, 2002). The ΔC157 deletion

mutant of VHL, which is defective in E3 ligase complex formation (Fig. 3.12 A), retains the ability to target a GFP reporter to nucleoli in acidosis (Fig. 3.12 B, first four panels) (Bonicalzi et al., 2001; Cockman et al., 2000; Mekhail et al., 2004a; Pause et al., 1997). In contrast, Cullin-2 failed to target a GFP reporter to nucleoli of VHL-deficient cells under the same conditions (Fig. 3.12 B). Although these data suggest that complex formation is not required for nucleolar targeting of VHL, immunoprecipitation analysis of acidotic cells suggested that VHL can still assemble within the VBC/Cul-2 complex under acidic conditions (Fig. 3.12 C). Furthermore, when co-transfected with at least an equimolar amount of VHL, Cullin-2 co-localized with VHL in the nucleoli of acidotic cells (Fig. 3.12, D to F). Cullin-2 is also immobile in the nucleolus of acidic cells suggesting that VHL responds to changes in extracellular pH and dictates the dynamic status of the assembled VBC/Cul-2 E3 ligase complex (data not shown). Taken together, these data identify a novel role for the VHL tumor suppressor in regulating the subcellular trafficking dynamics of the VBC/Cul-2 ubiquitin ligase complex by targeting it to the nucleolus in response to an increase in environmental H^+ concentrations.

Mapping analyses of MDM2 and its associated proteins have previously identified small aminopeptide sequences that can target a GFP reporter protein to the nucleolus in response to various physiological signals (Lohrum et al., 2003; Weber et al., 2000). Deletion mutant analysis of VHL was therefore conducted to identify minimal nucleolar detention sequences. While several regions within the β-domain of VHL displayed relatively weak nucleolar localization activity in response to acidosis, a domain encoding residues 100-130 recapitulated the nucleolar targeting capability of wild type VHL (Fig. 3.12, G to I). VHL(100-130) efficiently mediated the nucleolar detention of a GFP

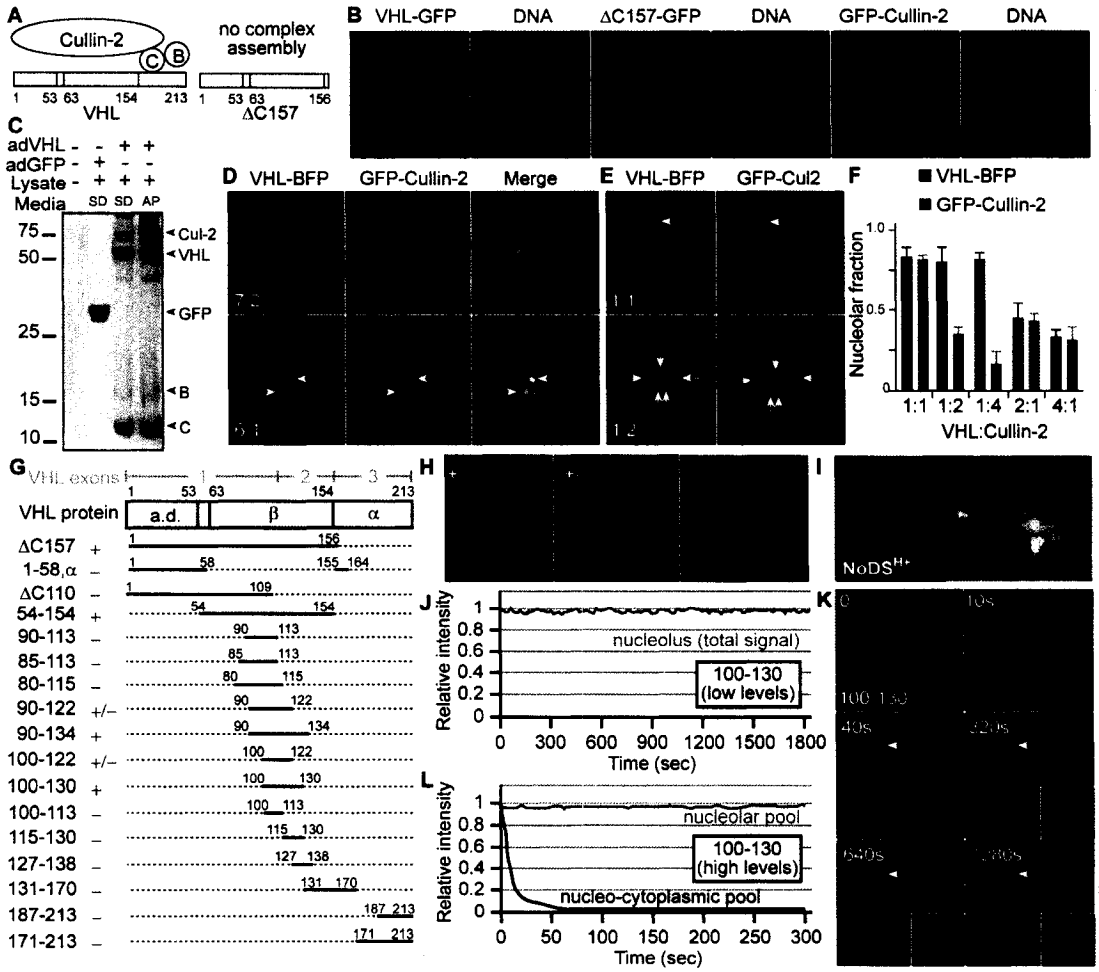
A
Cullin-2
C
B
no complex assembly
1 53 63 154 213
VHL
1 53 63 156
ΔC157
B VHL-GFP DNA ΔC157-GFP DNA GFP-Cullin-2 DNA
C
adVHL - - + +
adGFP - + - -
Lysate - + + +
Media SD SD AP
75
50
25
15
10
Cul-2
VHL
GFP
B
C
D VHL-BFP GFP-Cullin-2 Merge
E VHL-BFP GFP-Cul2
F
VHL-BFP
GFP-Cullin-2
Nucleolar fraction
1.0
0.5
0
1:1 1:2 1:4 2:1 4:1
VHL:Cullin-2
G
VHL exons 1 2 3
1 53 63 154 213
VHL protein
a.d.
β
α
ΔC157 +
1-58,α –
ΔC110 –
54-154 +
90-113 –
85-113 –
80-115 –
90-122 +/–
90-134 +
100-122 +/–
100-130 +
100-113 –
115-130 –
127-138 –
131-170 –
187-213 –
171-213 –
H
I
NoDS^H+
J
Relative intensity
nucleolus (total signal)
100-130
(low levels)
Time (sec)
K
0 10s
100 130
40s 220s
640s 760s
L
Relative intensity
nucleolar pool
100-130
(high levels)
nucleo-cytoplasmic pool
Time (sec)

Figure 3.12

Figure 3.12. pH-responsive nucleolar detention signal (NoDSH$^+$) allows VHL to target the VBC/Cul-2 ubiquitin ligase complex for static detention in the nucleolus. (**A**) Schematic representation of the VBC/Cul-2 complex. ΔC157 is a mutant of VHL that fails to assemble the complex. Positions of different amino acids of VHL are indicated. (**B**) Complex formation is not required for nucleolar localization. VHL-deficient 786-0 cells were infected to express GFP-tagged VHL, ΔC157 or Cullin-2 and transferred to hypoxia in AP media. Acidosis triggered the nucleolar relocation of VHL-GFP and ΔC157-GFP, but not of GFP-Cullin-2. (**C** to **F**) VHL targets components of its ubiquitin ligase complex to the nucleolus. (**C**) VHL-deficient 786-0 cells were left uninfected or infected to express flag-tagged VHL-GFP or GFP alone and incubated in hypoxia in SD or AP media. When about 60% of the cells in AP conditions displayed about 30% nucleolar accumulation of VHL-GFP, cells were lysed and submitted to anti-flag immunoprecipitation and silver staining. Acidosis did not cause any sudden disruption of the VBC/Cul-2 complex. (**D**) VHL-deficient 786-0 cells co-transfected to transiently express VHL-BFP and GFP-Cullin-2 (1:1 ratio) were transferred to hypoxia in SD or AP conditions. Cullin-2 co-localized with VHL to the nucleolus in acidosis. (**E** and **F**) VHL-deficient 786-0 cells were co-transfected to transiently express VHL-BFP and GFP-Cullin-2 to varying ratios (indicated on panels and graph). VHL is the limiting factor in the nucleolar co-localization of VHL and Cullin-2. (**G**) VHL mapping analysis. MCF7 cells transfected to transiently express indicated GFP-tagged proteins were incubated in AP media for 20 h in hypoxia. Schematic of *VHL* exons and derived amino-acid domains are shown. Nucleolar localization was scored according to representative images in (**H**). Amino acid residues 100-130 of the VHL protein were identified as the

minimal domain to recapitulate the nucleolar localization potential of the wild type VHL tumor suppressor protein in acidosis. a.d. denotes acidic domain. (**I**) VHL(100-130) represents a surface pocket on the VHL protein as revealed by molecular modeling (PyMOL). Each amino acid within that sequence is represented in a different colour for better visualization. MCF7 cells were transfected to transiently express VHL(100-130)-GFP at low (**J**) or high (**K** and **L**) levels and transferred to hypoxia under AP conditions. Upon reaching a plateau for nucleolar targeting, cells were submitted to FLIP analysis in which a nucleoplasmic region (white square in **K**) was repeatedly bleached. Insets in (**K**) show a pseudocolored zoom of a nucleolus (arrow).

reporter in acidosis as revealed by FLIP experiments (Fig. 3.12 J). Neutralization of the media released VHL(100-130) into the nucleoplasm where it resumed its dynamic mobility profile (data not shown). In addition, similar to the wild-type protein (Fig. 3.6, D and G), increasing the expression level of VHL(100-130) created a static nucleolar and a dynamic nucleo-cytoplasmic pool (Fig. 3.12, K and L). Unlike VHL(100-130), previously identified NLS and NES sequences fail to respond to increases in extracellular hydrogen ion concentrations (Fig. 3.13), highlighting the functional specificity of the herein identified domain. These findings identify a novel and discrete protein domain as a new type of protein localization sequence that we now refer to as Nucleolar Detention Sequence regulated by H^+ ($NoDS^{H+}$).

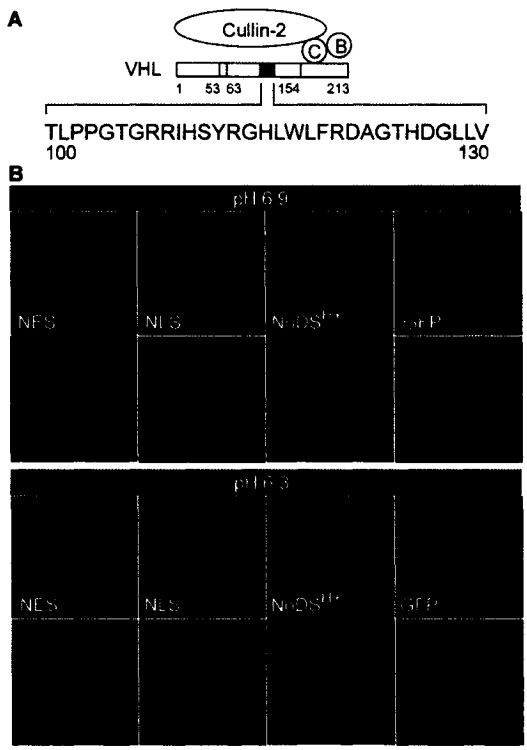
A
Cullin-2
C
B
VHL
1 53 63 154 213
TLPPGTGRRIHSYRGHLWLFRDAGTHDGLLV
100 130
B
pH 6.9
NES
NLS
pH 6.3
NES
NLS

Figure 3.13

Figure 3.13. Characteristics of the NoDSH^{+} sequence. (**A**) Shown is a schematic representation of the VBC/Cul-2 complex. The NoDS^{H+} of VHL is highlighted in red and its constituent amino acids (residues 100-130 of VHL, inclusively) are indicated. (**B**) MCF7 cells were transiently transfected to express GFP-tagged NES, NLS, NoDS^{H+} or GFP alone. Cells were incubated in hypoxia under AP conditions with maximal acidifications of pH 6.9 or 6.3.

Discussion

We provide evidence that the nucleolar architecture serves as a scaffold to convert highly mobile ubiquitin ligases to static participants of their molecular networks in response to physiological cues. This has various implications for our understanding of the role of nuclear compartments in regulating the output of dynamic molecular networks. Unlike certain core histones, which ensure chromatin stability by adopting a constitutive profile of relative immobility (Abney et al., 1997; Kimura and Cook, 2001), most proteins, including heterochromatin protein-1 (HP1) (Cheutin et al., 2003; Festenstein et al., 2003; Maison and Almouzni, 2004), follow a stochastic model of high molecular mobility to ensure efficient functional interactions. We propose a model by which dynamic molecular networks, such as the ubiquitylation system, are built on complex interactions between mobile and relatively static participants. According to this model, modulation of these interactions through regulation of the dynamic state of the participants alters the output of the network. It is known that the interaction of the VBC/Cul-2 and MDM2 ubiquitin ligases with the functional nuclear pore architecture is required for nuclear export and subsequent degradation of their substrates (Fig. 3.14 A) (Freedman and Levine, 1998; Groulx and Lee, 2002; Lee et al., 1999; Momand et al., 1992; Oliner et al., 1993; Roth et al., 1998). While constituents of the nuclear pore can move between subcellular compartments, functional pore architecture is confined to the nuclear envelope and persist for long periods of time within well-defined spatial regions (Rabut et al., 2004). Therefore, eliminating the physical interaction between an immobile and a mobile participant only requires the immobilization of the dynamic participant at a different spatial coordinate. In the herein described system, key interactions are

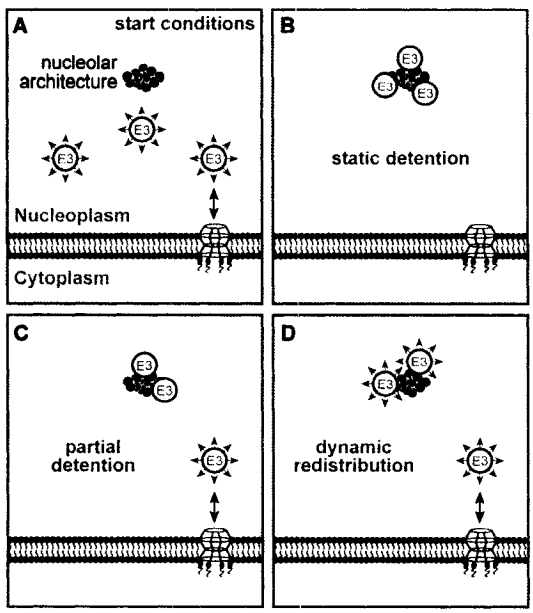
A
start conditions
nucleolar architecture
E3
Nucleoplasm
Cytoplasm
B
static detention
C
partial detention
D
dynamic redistribution

Figure 3.14

Figure 3.14. Regulation of ubiquitylation networks by the nucleolus. (**A**) Ubiquitin ligases follow a stochastic model of molecular mobility to ensure functional interactions such as those with the functional nuclear pore architecture at the nuclear envelope. (**B**) Complete static detention of ligases within the nucleolar space abolishes these required molecular interactions. (**C**) Detention of a fraction of the protein population results in a static nucleolar pool while a second pool sustains dynamic functions in the nucleoplasm or cytoplasm. (**D**) Dynamic change in the steady state distribution of a protein from mainly nucleo-cytoplasmic to mainly nucleolar allows the protein to assume dynamic functions in the nucleolus and other cellular compartments.

abolished following static detention of the ubiquitin ligases within the nucleolar space, a phenomenon that alters network output (i.e. degradation of substrates) (Fig. 3.14 B) as previously shown by work from our and other groups (Lohrum et al., 2003; Mekhail et al., 2004a; Tao and Levine, 1999; Weber et al., 1999). These data suggest that static nucleolar detention selectively abolishes ubiquitin ligase functions requiring interactions with immobile constituents of the ubiquitylation networks. Whether VHL or MDM2 retain other functions when sequestered in nucleoli, or assume new roles, remains unknown.

The redistribution of dynamic nucleo-cytoplasmic proteins to the nucleolus can be classified in three main categories. First, complete nucleolar detention results in the conversion of a mobile protein to a static participant of its molecular network (Fig. 3.14 B). Second, detention of a fraction of the protein population results in a static nucleolar pool while a second pool sustains dynamic functions in the nucleoplasm or cytoplasm (Fig. 3.14 C). Third, dynamic change in the steady state distribution of a protein from mainly nucleo-cytoplasmic to mainly nucleolar allows the protein to assume dynamic functions in the nucleolus and other cellular compartments (Fig. 3.14 D). It is possible that a single protein can be targeted to the nucleolus through different mechanisms (Fig. 3.14, B to D) to custom-tailor specific dynamic profiles in response to different signals. Alternatively, ubiquitin ligases can be regulated through non-nucleolar mechanisms, such as inactivating post-translational modifications, to control ubiquitylation without altering general dynamic properties of the ligase in the cell.

Specific amino peptide sequences, such as NLS, NES, and NoLS, target proteins to various cellular regions. Mapping analysis of the VHL tumor suppressor protein

identified a new type of protein localization sequence, $NoDS^{H+}$, which is activated following a decrease in extracellular pH to target proteins for static detention in the nucleolus. $NoDS^{H+}$ is inactivated following a return to neutral pH conditions, causing rapid release of detained proteins into the nucleoplasm. The $NoDS^{H+}$ is one of the first discrete domains that have been identified to target proteins to the nucleolus and differs considerably from other NoLS and NoRS signals in its size and mode of regulation. The $NoDS^{H+}$ is characterized by the presence of several arginine residues (Fig. 3.13A), which are known to be involved in targeting proteins to the nucleolus. It is possible that these residues are involved in pH-regulated targeting of VHL to nucleoli while other residues play a role in static detention. Further investigation will be required to decipher the mechanisms by which extracellular hydrogen ions activate the $NoDS^{H+}$ of VHL. It will also be important to screen proteins for similar sequences as they could play vital roles in altering general protein dynamics and metabolism in response to changes in extracellular hydrogen ion concentration. Consistent with the hypothesis that nucleolar sequestration may be a general phenomenon is the recent report that the nucleolus can capture and release several proteins in response to different cellular cues (Andersen et al., 2005).

In conclusion, our findings highlight the role of the nucleolus in regulating protein dynamics, localization, and function. We propose a model by which, via reversible interactions with the nucleolar architecture, ubiquitin ligases alternate between dynamic and static states to alter the output of their complex molecular networks. There is ample evidence that proteins are highly mobile molecules that function through stochastic interactions with binding partners. This report provides evidence that cells have evolved

a mechanism to regulate molecular networks by switching proteins between mobile and immobile states and highlight the role of the nucleolus in sequestering molecules.

Acknowledgements

This work is supported by a grant from the Canadian Institutes of Health Research (CIHR) to S.L. S.L. is the recipient of the National Cancer Institute of Canada Harold E. Johns Award. K. M. is supported by a Canada Graduate Scholarship (CGS-D) from the Natural Science and Engineering Research Council of Canada (NSERC). We thank Mark Olson (University of Mississippi Medical Center, Jackson, Mississippi), Tom Misteli (National Cancer Institute, National Institutes of Health, Bethesda, MD), Gang Pei (Shangai Institute of Biological Sciences, Shangai, China), Uri Alon (Weizmann Institute of Science, Rehovot, Israel), and Galit Lahav (Harvard Medical School, Boston, MA) for kindly providing plasmids. We thank Josianne Payette and Andrew Ridsdale for valuable technical support.

References

Abney, J.R., B. Cutler, M.L. Fillbach, D. Axelrod, and B.A. Scalettar. 1997. Chromatin dynamics in interphase nuclei and its implications for nuclear structure. *J. Cell Biol.* 137:1459-1468.

Andersen, J.S., Y.W. Lam, A.K. Leung, S.E. Ong, C.E. Lyon, A.I. Lamond, and M. Mann. 2005. Nucleolar proteome dynamics. *Nature*. 433:77-83.

Appella, E., and C.W. Anderson. 2001. Post-translational modifications and activation of p53 by genotoxic stresses. *Eur. J. Biochem.* 268:2764-2772.

Azzam, R., S.L. Chen, W. Shou, A.S. Mah, G. Alexandru, K. Nasmyth, R.S. Annan, S.A. Carr, and R.J. Deshaies. 2004. Phosphorylation by cyclin B-Cdk underlies release of mitotic exit activator Cdc14 from the nucleolus. *Science*. 305:516-519.

Bonicalzi, M.E., I. Groulx, N. de Paulsen, and S. Lee. 2001. Role of exon 2-encoded beta -domain of the von Hippel-Lindau tumor suppressor protein. *J. Biol. Chem.* 276:1407.

Carmo-Fonseca, M. 2002. The contribution of nuclear compartmentalization to gene regulation. *Cell*. 108:513-521.

Carmo-Fonseca, M., L. Mendes-Soares, and I. Campos. 2000. To be or not to be in the nucleolus. *Nature Cell Biol.* 2:E107-112.

Chen, D., and S. Huang. 2001. Nucleolar components involved in ribosome biogenesis cycle between the nucleolus and nucleoplasm in interphase cells. *J. Cell Biol.* 153:169-176.

Cheutin, T., A.J. McNairn, T. Jenuwein, D.M. Gilbert, P.B. Singh, and T. Misteli. 2003. Maintenance of stable heterochromatin domains by dynamic HP1 binding. *Science*. 299:721-725.

Ciechanover, A. 2005. Proteolysis: from the lysosome to ubiquitin and the proteasome. *Nat. Rev. Mol. Cell. Biol.* 6:79-87.

Cockman, M.E., N. Masson, D.R. Mole, P. Jaakkola, G.W. Chang, S.C. Clifford, E.R. Maher, C.W. Pugh, P.J. Ratcliffe, and P.H. Maxwell. 2000. Hypoxia inducible factor-alpha binding and ubiquitylation by the von Hippel-Lindau tumor suppressor protein. *J. Biol. Chem.* 275:25733-25741.

Corless, C.L., A.S. Kibel, O. Iliopoulos, and W.G. Kaelin, Jr. 1997. Immunostaining of the von Hippel-Lindau gene product in normal and neoplastic human tissues. *Hum. Pathol.* 28:459-464.

Daelemans, D., S.V. Costes, S. Lockett, and G.N. Pavlakis. 2005. Kinetic and molecular analysis of nuclear export factor CRM1 association with its cargo in vivo. *Mol. Cell. Biol.* 25:728-739.

Dundr, M., U. Hoffmann-Rohrer, Q. Hu, I. Grummt, L.I. Rothblum, R.D. Phair, and T. Misteli. 2002. A kinetic framework for a mammalian RNA polymerase in vivo. *Science*. 298:1623-1626.

Dundr, M., T. Misteli, and M.O. Olson. 2000. The dynamics of postmitotic reassembly of the nucleolus. *J. Cell Biol.* 150:433-446.

Festenstein, R., S.N. Pagakis, K. Hiragami, D. Lyon, A. Verreault, B. Sekkali, and D. Kioussis. 2003. Modulation of heterochromatin protein 1 dynamics in primary Mammalian cells. *Science*. 299:719-721.

Freedman, D.A., and A.J. Levine. 1998. Nuclear export is required for degradation of endogenous p53 by MDM2 and human papillomavirus E6. *Mol. Cell. Biol.* 18:7288-7293.

Gillette, T.G., W. Huang, S.J. Russell, S.H. Reed, S.A. Johnston, and E.C. Friedberg. 2001. The 19S complex of the proteasome regulates nucleotide excision repair in yeast. *Genes Dev.* 15:1528-1539.

Groulx, I., M.E. Bonicalzi, and S. Lee. 2000. Ran-mediated nuclear export of the von Hippel-Lindau tumor suppressor protein occurs independently of its assembly with cullin-2. *J. Biol. Chem.* 275:8991-9000.

Groulx, I., and S. Lee. 2002. Oxygen-dependent ubiquitination and degradation of hypoxia-inducible factor requires nuclear-cytoplasmic trafficking of the von Hippel-Lindau tumor suppressor protein. *Mol. Cell. Biol.* 22:5319.

Kaelin, W.G., Jr. 2002. Molecular basis of the VHL hereditary cancer syndrome. *Nat. Rev. Cancer*. 2:673-682.

Kibel, A., O. Iliopoulos, J.A. DeCaprio, and W.G. Kaelin, Jr. 1995. Binding of the von Hippel-Lindau tumor suppressor protein to Elongin B and C. *Science*. 269:1444-1446.

Kimura, H., and P.R. Cook. 2001. Kinetics of core histones in living human cells: little exchange of H3 and H4 and some rapid exchange of H2B. *J. Cell Biol.* 153:1341-1353.

Lam, Y.W., L. Trinkle-Mulcahy, and A.I. Lamond. 2005. The nucleolus. *J. Cell Sci.* 118:1335-1337.

Lee, S., M. Neumann, R. Stearman, R. Stauber, A. Pause, G.N. Pavlakis, and R.D. Klausner. 1999. Transcription-dependent nuclear-cytoplasmic trafficking is required for the function of the von Hippel-Lindau tumor suppressor protein. *Mol. Cell. Biol.* 19:1486.

Lippincott-Schwartz, J., N. Altan-Bonnet, and G.H. Patterson. 2003. Photobleaching and photoactivation: following protein dynamics in living cells. *Nat. Cell Biol.* Suppl:S7-14.

Llanos, S., P.A. Clark, J. Rowe, and G. Peters. 2001. Stabilization of p53 by p14ARF without relocation of MDM2 to the nucleolus. *Nat. Cell Biol.* 3:445-452.

Lohrum, M.A., R.L. Ludwig, M.H. Kubbutat, M. Hanlon, and K.H. Vousden. 2003. Regulation of HDM2 activity by the ribosomal protein L11. *Cancer Cell.* 3:577-587.

Maison, C., and G. Almouzni. 2004. HP1 and the dynamics of heterochromatin maintenance. *Nat. Rev. Mol. Cell. Biol.* 5:296-304.

Mekhail, K., L. Gunaratnam, M.E. Bonicalzi, and S. Lee. 2004a. HIF activation by pH-dependent nucleolar sequestration of VHL. *Nat. Cell Biol.* 6:642-647.

Mekhail, K., M. Khacho, L. Gunaratnam, and S. Lee. 2004b. Oxygen sensing by H+: implications for HIF and hypoxic cell memory. *Cell Cycle.* 3:1027-1029.

Michael, D., and M. Oren. 2003. The p53-Mdm2 module and the ubiquitin system. *Semin. Cancer Biol.* 13:49-58.

Misteli, T. 2001. Protein dynamics: implications for nuclear architecture and gene expression. *Science.* 291:843.

Momand, J., G.P. Zambetti, D.C. Olson, D. George, and A.J. Levine. 1992. The mdm-2 oncogene product forms a complex with the p53 protein and inhibits p53-mediated transactivation. *Cell.* 69:1237-1245.

Muratani, M., and W.P. Tansey. 2003. How the ubiquitin-proteasome system controls transcription. *Nat. Rev. Mol. Cell. Biol.* 4:192-201.

Oliner, J.D., J.A. Pietenpol, S. Thiagalingam, J. Gyuris, K.W. Kinzler, and B. Vogelstein. 1993. Oncoprotein MDM2 conceals the activation domain of tumour suppressor p53. *Nature*. 362:857-860.

Pause, A., S. Lee, R.A. Worrell, D.Y. Chen, W.H. Burgess, W.M. Linehan, and R.D. Klausner. 1997. The von Hippel-Lindau tumor-suppressor gene product forms a stable complex with human CUL-2, a member of the Cdc53 family of proteins. *Proc. Natl. Acad. Sci. USA*. 94:2156-2161.

Paushkin, S.V., M. Patel, B.S. Furia, S.W. Peltz, and C.R. Trotta. 2004. Identification of a human endonuclease complex reveals a link between tRNA splicing and pre-mRNA 3' end formation. *Cell.* 117:311-321.

Petroski, M.D., and R.J. Deshaies. 2005. Function and regulation of cullin-RING ubiquitin ligases. *Nat. Rev. Mol. Cell. Biol.* 6:9-20.

Phair, R.D., and T. Misteli. 2000. High mobility of proteins in the mammalian cell nucleus. *Nature*. 404:604.

Rabut, G., V. Doye, and J. Ellenberg. 2004. Mapping the dynamic organization of the nuclear pore complex inside single living cells. *Nat. Cell Biol.* 6:1114-1121.

Roth, J., M. Dobbelstein, D.A. Freedman, T. Shenk, and A.J. Levine. 1998. Nucleo-cytoplasmic shuttling of the hdm2 oncoprotein regulates the levels of the p53

protein via a pathway used by the human immunodeficiency virus rev protein. *EMBO J.* 17:554-564.

Russell, S.J., S.H. Reed, W. Huang, E.C. Friedberg, and S.A. Johnston. 1999. The 19S regulatory complex of the proteasome functions independently of proteolysis in nucleotide excision repair. *Mol. Cell.* 3:687-695.

Semenza, G.L. 2000. HIF-1 and human disease: one highly involved factor. *Genes Dev.* 14:1983-1991.

Shou, W., K.M. Sakamoto, J. Keener, K.W. Morimoto, E.E. Traverso, R. Azzam, G.J. Hoppe, R.M. Feldman, J. DeModena, D. Moazed, H. Charbonneau, M. Nomura, and R.J. Deshaies. 2001. Net1 stimulates RNA polymerase I transcription and regulates nucleolar structure independently of controlling mitotic exit. *Mol. Cell.* 8:45-55.

Shou, W., J.H. Seol, A. Shevchenko, C. Baskerville, D. Moazed, Z.W. Chen, J. Jang, H. Charbonneau, and R.J. Deshaies. 1999. Exit from mitosis is triggered by Tem1-dependent release of the protein phosphatase Cdc14 from nucleolar RENT complex. *Cell.* 97:233-244.

Stauber, R., G.A. Gaitanaris, and G.N. Pavlakis. 1995. Analysis of trafficking of Rev and transdominant Rev proteins in living cells using green fluorescent protein fusions: transdominant Rev blocks the export of Rev from the nucleus to the cytoplasm. *Virology.* 213:439-449.

Tao, W., and A.J. Levine. 1999. P19(ARF) stabilizes p53 by blocking nucleo-cytoplasmic shuttling of Mdm2. *Proc. Natl. Acad. Sci. USA.* 96:6937-6941.

Terrell, J., S. Shih, R. Dunn, and L. Hicke. 1998. A function for monoubiquitination in the internalization of a G protein-coupled receptor. *Mol. Cell.* 1:193-202.

Tsai, R.Y., and R.D. McKay. 2005. A multistep, GTP-driven mechanism controlling the dynamic cycling of nucleostemin. *J. Cell Biol.* 168:179-184.

van den Boom, V., E. Citterio, D. Hoogstraten, A. Zotter, J.M. Egly, W.A. van Cappellen, J.H. Hoeijmakers, A.B. Houtsmuller, and W. Vermeulen. 2004. DNA damage stabilizes interaction of CSB with the transcription elongation machinery. *J. Cell Biol.* 166:27-36.

Visintin, R., E.S. Hwang, and A. Amon. 1999. Cfi1 prevents premature exit from mitosis by anchoring Cdc14 phosphatase in the nucleolus. *Nature*. 398:818-823.

Walther, R.F., C. Lamprecht, A. Ridsdale, I. Groulx, S. Lee, Y.A. Lefebvre, and R.J. Hache. 2003. Nuclear export of the glucocorticoid receptor is accelerated by cell fusion-dependent release of calreticulin. *J Biol Chem*. 278:37858-37864.

Weber, J.D., M.L. Kuo, B. Bothner, E.L. DiGiammarino, R.W. Kriwacki, M.F. Roussel, and C.J. Sherr. 2000. Cooperative signals governing ARF-mdm2 interaction and nucleolar localization of the complex. *Mol. Cell. Biol.* 20:2517-2528.

Weber, J.D., L.J. Taylor, M.F. Roussel, C.J. Sherr, and D. Bar-Sagi. 1999. Nucleolar Arf sequesters Mdm2 and activates p53. *Nat. Cell Biol.* 1:20-26.

Weissman, A.M. 2001. Themes and variations on ubiquitylation. *Nat. Rev. Mol. Cell. Biol.* 2:169-178.

Inter-chapter Transition

Cells must balance energy supply and demand to remain a sustainable biological system. It has been suggested that prolonged hypoxia induces energy starvation and triggers cell death (Liu et al., 2006). However, Physicians and physiologists have long recognized that acidosis protects cells facing limited oxygen tensions in various physiological and pathological settings, including muscle exercise, tumor development, and ischemic disorders (Allen and Westerblad, 2004; Bing et al., 1973; Currin et al., 1991; Giffard et al., 1990; Kaku et al., 1993; Morimoto et al., 1997; Nielsen et al., 2001; Penttila and Trump, 1974). In light of the defensive effects of acidosis in ischemic physiology and the impact of cellular H^+ production on molecular networks controling HIF and hypoxic gene expression (Mekhail et al., 2004a; Mekhail et al., 2005; Mekhail et al., 2004b), we hypothesized that cells have evolved a mechanism utilizing acidosis to maintain energy equilibrium and viability under hypoxia.

Chapter 4. Restriction of rRNA synthesis by VHL maintains energy equilibrium under hypoxia

Papers and author contribution:

- Paper:

Mekhail, K., Rivero-Lopez, L., Khacho, M., and Lee, S. (2006) Restriction of rRNA synthesis by VHL maintains energy equilibrium under hypoxia. Cell Cycle 5:2401-2413.

- Author Contributions:

K. Mekhail	Interpretation, text and all figures Performed all experiments
L. Rivero-Lopez	ChIP and viability experiments were performed by both K. Mekhail and L. Rivero-Lopez
M. Khacho	Performed data not shown experiments indicating that nucleolar sequestration of VHL does not require RNA.

Restriction of ribosomal biogenesis by pH-dependent interactions between VHL and the nucleolus: A possible mechanism for the protective effect of acidosis under hypoxia

Karim Mekhail[1], Luis Rivero-Lopez[1], Mireille Khacho[1], and Stephen Lee[1,2]

[1]Department of Cellular and Molecular Medicine, Faculty of Medicine, University of Ottawa, Ottawa, Ontario, Canada K1H 8M5.

[2]Correspondence should be addressed to S.L. (e-mail: slee@uottawa.ca)

Published Manuscript

Cell Cycle 5:2401-2413 (2006)

Abstract

Biological evolution abides by an unbending rule obligating organisms to maintain energy equilibrium. It has been suggested that prolonged hypoxia induces energy starvation and triggers cell death. We report that cells have evolved pH-sensitive mechanisms that lower energy demands to avoid these deleterious effects under low oxygen tension. We found that fermentation-induced acidosis allows hypoxic cells to maintain energy equilibrium and viability under hypoxia by restricting ribosomal biogenesis, the most energy-demanding cellular process. Acidosis triggers nucleolar condensation, decreases precursor ribosomal RNA (pre-rRNA) synthesis, and reduces the dynamic profile of the ribosomal DNA (rDNA)-associated protein UBF1 and its interaction with ribosomal RNA (rRNA) genes. These changes require the pH-dependent interaction of the von Hippel-Lindau (VHL) tumor suppressor with intergenic rDNA. Abrogating this program by silencing VHL expression, competing rDNA-VHL interaction or preventing extracellular acidification triggers energy starvation and cell death under hypoxia. While the hypoxia-inducible factor (HIF) and other factors may promote extracellular acidification, acidosis does not require hypoxia or HIF activation to restrict nucleolar rDNA. Physiologically, our data suggest that cells are able to maintain constant ATP levels following a shift to hypoxia by modulating and gauging the environmental concentration of hydrogen ions. These findings also provide an explanation for the protective effect of acidosis in ischemic settings such as development, stroke, and cancer.

Introduction

Introduction of molecular oxygen into an anaerobic biosphere over 2.2 billion years ago triggered a drastic reorganization and expansion of complex molecular networks (Falkowski, 2006). Under normal oxygen tension (normoxia), contemporary eukaryotic cells use this diatom to maximize the amount of energy extracted from glucose catabolism. Glycolytic conversion of each glucose into two pyruvate molecules generates only two ATPs. However, each pyruvate is then transferred to mitochondria to be converted into acetyl coenzyme-A (AcCoA) via pyruvate dehydrogenase (PDH). Further mitochondrial catabolism of AcCoA through the citric acid cycle (CAC) and the passage of high-energy electrons along a transfer chain where molecular oxygen is the last acceptor generate a large amount of ATP and replenish glycolysis with nicotinamide adenine dinucleotides (NAD^+), a scarce cellular co-enzyme that cannot be used stoichiometrically.

Cells facing low oxygen tension (hypoxia) shift to, or rely more, on anaerobic metabolism, which is defined here as the sum of processes generating ATP without utilizing oxygen, in an effort to maintain energy equilibrium and viability (Gladden, 2001; Gladden, 2004; Kuznetsov et al., 2004). Mitochondrial respiration is repressed both passively by the scarcity of oxygen as an electron acceptor and possibly actively by the hypoxia-inducible factor (HIF), a heterodimeric transcription factor involved in the maintenance of oxygen homeostasis (Giaccia et al., 2004; Harris, 2002; Kaelin, 2002; Semenza, 1998). In the presence of oxygen, enzymes known as prolyl hydroxylases (PHDs) hydroxylate key proline residues within the α subunit of HIF (HIFα) (Bruick and McKnight, 2001; Epstein et al., 2001; Ivan et al., 2001; Jaakkola et al., 2001; Yu et al.,

2001). These post-translational modifications allow the von Hippel-Lindau tumor suppressor (VHL) to mediate the ubiquitylation of HIFα in the nucleus (Bonicalzi et al., 2001; Groulx et al., 2000; Groulx and Lee, 2002; Iwai et al., 1999; Kamura et al., 2000; Kibel et al., 1995; Lee et al., 1999; Lisztwan et al., 1999; Lonergan et al., 1998; Maxwell et al., 1999; Ohh et al., 2000; Pause et al., 1997; Pause et al., 1999; Tanimoto et al., 2000). VHL-mediated nuclear export then targets HIFα for degradation via the 26S in the cytoplasm. PHDs require molecular oxygen and hypoxia prevents hydroxylation of HIFα, allowing it to evade recognition by VHL. Stabilized HIFα dimerizes with the constitutively expressed β subunit of HIF (HIFβ). HIF can then activate its target genes, which include glucose transporter-1 (Glut-1), vascular endothelium growth factor (VEGF), and carbonic anhydrase IX (CAIX).

Following a shift to hypoxia, initial production of reactive oxygen species (ROS) by an electron transfer chain (ETC) destabilized by decreasing oxygen levels seems to contribute to the induction of HIF (Brunelle et al., 2005; Guzy et al., 2005; Kaelin, 2005; Mansfield et al., 2005; Page et al., 2002; Richard et al., 2000), which in turn activates the PDH inhibitor pyruvate dehydrogenase kinase-1 (PDK-1) (Kim et al., 2006; Papandreou et al., 2006; Simon, 2006). The latter actively represses mitochondrial respiration to prevent toxic accumulations of ROS and ensures that no pyruvate is wasted in the form of AcCoA. Instead, hypoxic cells maximize anaerobic energy production by both triggering the Pasteur effect, a HIF-dependent increase in glycolytic rate (Harris, 2002; Iyer et al., 1998; Obach et al., 2004; Pasteur, 1857; Seagroves et al., 2001; Semenza et al., 1994), and converting pyruvate to lactate through fermentation, which efficiently replaces mitochondria with regard to the task of replenishing glycolysis with NAD^+ (Gladden,

2001). This causes extracellular acidosis as lactate molecules (La^-) are coupled to hydrogen ions and released in the environment in the form of lactic acid (La^-H^+). Although the production of lactic acid is often viewed as a terminal event of anaerobic metabolism, physicians and physiologists have long recognized that acidosis protects cells facing limited oxygen tensions in various physiological and pathological settings, including muscle exercise, tumor development, and ischemic disorders (Allen and Westerblad, 2004; Bing et al., 1973; Currin et al., 1991; Giffard et al., 1990; Kaku et al., 1993; Morimoto et al., 1997; Nielsen et al., 2001; Penttila and Trump, 1974). We previously found that hypoxia-induced acidosis triggers nucleolar sequestration of VHL. This allows HIF to evade destruction and activate its target genes, including those involved in different aspects of energy supply, suggesting the existence of a hypoxic cell memory (Mekhail et al., 2004a; Mekhail et al., 2004b).

While hypoxic cells increase glycolytic ATP production, this process does not compensate for the loss of mitochondrial respiration resulting in energy starvation and cell death under prolonged hypoxia (Liu et al., 2006). We reasoned that either hypoxia drives energy shortage or that anaerobic metabolism encompasses an additional program that guards energy balance and viability. In light of the defensive effects of acidosis in ischemic physiology, we hypothesized that cells have evolved a mechanism utilizing fermentation protons to maintain energy equilibrium by increasing the production or decreasing the consumption of energy.

Here, we report the unexpected finding that cells regulate energy demand by sensing the environmental concentration of hydrogen ions. H^+ produced under hypoxia promotes interactions between VHL and the intergenic spacers (IGS) of rRNA genes (rDNA) to

reduce rRNA synthesis. This silencing program restricts ribosomal biogenesis, the most energy-demanding cellular process, to preserve energy equilibrium and viability. Our data suggest that cells maintain constant ATP levels regardless of oxygen tension by controlling and gauging the environmental concentration of hydrogen ions. In addition, these findings also provide a potential explanation for the protective effect of acidosis in ischemic settings such as development, stroke, and cancer.

Materials and Methods

Cells and materials. C2C12 cells from ATCC (Manassas, VA) were differentiated by lowering the serum concentration from 5% to 0.5%. MCF7, 786-0 (VHL-defective), U87MG, and NIH3T3 cells were also obtained from ATCC (Manassas, VA). The generation of 786-0 cells stably expressing HA-VHL is previously described (Iliopoulos et al., 1995). Viability was assessed with a 20 min and 5 min pretreatment with fluorescein diacetate (FDA, 5 μM) and propidium iodide (PI, 2 μM) (Sigma, St. Louis, MO), respectively. FDA and PI are unaffected by pH as neutralization of an acidic set or acidification of a neutral set immediately prior to addition of the dyes yielded essentially the same results. 6-deoxyglucose (6-DOG, 6 mM), sodium azide (NaN_3, 0.02 %, v/v), and actinomycin-D (Act-D, 10 $\mu g.ml^{-1}$, Calbiochem) was used where indicated. 6-DOG is insensitive to pH as glucose uptake and lactate release equally decreased following treatment of hypoxic cells with the drug under both neutral and acidic conditions.

Cell culture. Normoxic cells were incubated at 37°C under 5% CO_2 environment. Hypoxia was achieved by incubation in a hypoxic chamber at 37°C under a 1% O_2, 5% CO_2 and N_2-balanced atmosphere. Acidosis experiments were conducted as previously described (Mekhail et al., 2004a; Mekhail et al., 2005). For standard (SD) or acidosis-permissive (AP) conditions, buffer-free medium (DMEM; Invitrogen, Carlsbad, CA) was freshly prepared and supplemented with 5% (v/v) fetal bovine serum (FBS) and 1% (v/v) penicillin-streptomycin. Unless otherwise indicated, $NaHCO_3$ was added at a 44mM concentration and the pH was adjusted to 7.0 (SD) or 6.0–7.0 (AP) with HCl. Air was bubbled into both media at 22°C, which stabilizes the pH at 7.0. AP media slowly

reverted to its original pH (6.0-7.0) under hypoxia, whereas the SD medium remained at pH 7.0. Transfected or adenovirus-infected cells were grown for 24 h under standard conditions before any treatment.

Plasmids and adenoviruses. VHL, its variants and mutants were cloned between an N-terminal Flag-tag and a C-terminal GFP-tag and into pcDNA3.1, as previously described (Groulx and Lee, 2002; Mekhail et al., 2004a). Adenoviruses were produced using the Cre-lox recombination system. We sincerely thank Tom Misteli (NCI, NIH, Bethesda, MD) for providing the UBF1-GFP construct, and Mark Olson (University of Mississippi Medical Center, Jackson Mississippi) for providing the B23-GFP construct. Transient transfections were conducted with Effectene transfection reagent (Qiagen, Valencia, CA).

Reverse transcriptase PCR. Analysis was conducted using previously described primers and procedures (Grandori et al., 2005; Gunaratnam et al., 2003; Kim et al., 2001; Li et al., 2005; Winter et al., 2000; Yamamoto et al., 2004). Briefly, cycling parameters for messengers were as follows. Pre-rRNA 5'-ETS: 95 °C for 3 min, followed by 25 cycles of [95 °C for 1 min, 65 °C for 1 min, 72 °C for 1 min] and then 72 °C for 5 min; ARPP P0: 95°C for 2 min, followed by 23 cycles of [95°C for 1 min, 58°C for 30 s, 72°C for 1 min], and then 72°C for 3 min; 5S rRNA: 94°C for 3 min, followed by 23 cycles of [95°C for 30 s, 58°C for 30 s, 72°C for 1 min], and then 72°C for 5 min; VHL: 95°C for 3 min, followed by 25 cycles of [94°C for 1 min, 55°C for 1 min, 72°C for 1 min], and then 72°C for 5 min; β-actin: 94 °C for 2 min, followed by 25 cycles of [94°C for 20 s, 60°C for 20 s, 72 °C for 40 s], and then 72 °C for 10 min.

BrUTP-labeling and detection of nascent rRNA. BrUTP experiments were performed as described (Thiry et al., 2000). RNAPII transcription was inhibited with a 2 h α-

amanitin (10 μg.ml^{-1}) pretreatment. Cells, BrUTP-pulsed only, or pulsed and chased for 10 min, were formaldehyde-fixed and methanol-permeabilized. Nascent rRNA was detected by immunofluorescence analysis using a monoclonal anti-BrdU antibody (Roche Diagnostics, Penzberg, Germany) and an anti-mouse fluorescein-labeled secondary antibody (Roche Diagnostics, Penzberg, Germany). As previously reported (Thiry et al., 2000), 15-20% of cells were labeled and images of cells were captured with an Axioskop 2 MOT PLUS microscope (Zeiss, Thornwood, NY) using a digital charged-coupled device camera (Qimaging, Burnaby, BC).

Chromatin crosslinking and immunoprecipitation. Experiments were performed using the EZ ChIP™ Chromatin Immunoprecipitation Kit (Upstate Biotechnologies, Lake Placid, NY). Crosslinked cells were lysed and DNA was sonicated to 100-500 bp use of a Sonifier-450 sonicator (Branson; output 3.0, duty cycle 30%). Antibodies detect Flag-M2 (1 μg) (Sigma, St. Louis, MO), RNA pol-II (1 μg), acetylated H3 (10 μg), acetylated H4 (10 μl) (Upstate Biotechnologies). PCR conditions were 94°C for 3 min, followed by 45 cycles of [94°C for 20 s, 59°C for 30 s, 72°C for 30 s], and then 72°C for 2 min (Grandori et al., 2005). Primers P1 (952 to 1030) , P4 (3990 to 4092), P8 (8204 to 8300), P13 (12855 to 12970), P18 (18155 to 18280), P27 (27366 to 27477), P32 (32734 to 32859), P42 (41982 to 42075), and P42.9 (42943 to 43033), were from reference (Grandori et al., 2005) and nucleotide positions from start site are based on the Genbank rDNA sequence with accession number U13369.

Photobleaching and microscopy. As described (Mekhail et al., 2005), cells were cultured on glass coverslips with a 40 mm diameter in an FCS2 environmental chamber (Bioptechs) maintained at 37°C or directly into 35 mm dishes with coverslip bottoms and

visualized with a confocal microscope (MRC 1024; Bio-Rad Laboratories). A 60X plan Apo oil immersion lens with a 1.4 NA was used for bleaching and imaging. Indicated areas were exposed to five rapid pulses of a 488 nm argon laser at 100% power and image acquisition was conducted at 1% of full laser power. For FRAP experiments, images were collected at 10s intervals. Recovery of the fluorescent signal within a bleached region was calculated as described (Mekhail et al., 2005) following $I_{rel} = (I_{(t)}/I_{(0)}) * (T_{(0)}/T_{(t)})$, where $T_{(t)}$ is the total cellular intensity at time t, $T_{(0)}$ is total cellular intensity before bleach, $I_{(0)}$ is the intensity in the bleached area before bleach, and $I_{(t)}$ is the intensity in the previously bleached area at time t. For FLIP experiments, cells were repeatedly bleached and imaged at 5s intervals and fluorescence loss in unbleached areas was calculated to account for any losses in fluorescence by normalizing the fluorescence in the cell of interest to that of a neighboring cell according to $I_{rel} = (I_{(t)}/I_{(0)}) * (N_{(0)}/N_{(t)})$, where $I_{(t)}$ is the average intensity of the unbleached nucleus at time point t, $I_{(0)}$ is the average prebleach intensity of the nucleus of interest, and $N_{(0)}$ and $N_{(t)}$ are the average total cellular fluorescence intensities of a neighboring cell in the same field of vision at prebleach or at time point t, respectively. For all bleaching experiments, at least 3 datasets were analyzed for each result. No differences in protein dynamics were observed when cycloheximide (20 $\mu g.ml^{-1}$) was added 1 h from endpoint. Average pixel intensities were normalized for background fluorescence. Images of living cells from experiments that do not implicate bleaching or of immunofluorescence experiments were captured with a microscope (Axiovert S100TV; Carl Zeiss MicroImaging, Inc.) equipped with a 40X C-Apochromat water immersion objective with a 1.2 NA using a digital charged-coupled device camera (Empix). Pseudocoloring and software packages used to

capture images, analyze data, and generate graphs are previously described (Mekhail et al., 2005).

siRNA. Cells were transiently transfected with double-stranded 21-nucleotide-long small interfering RNA (siRNA) to VHL (siVHL) or with a scramble control (siControl) (Ambion, Austin, TX). See Fig. 4.5G for characterization and controls.

ATP, glucose, and lactate measurements. For ATP, concentrations were measured with the CellTiter-Glo Luminescent Assay (Promega, WI) using a LUMIstar Galaxy luminometer (BMG Labtechnologies, Durham, North Carolina) according to manufacturer's protocol. 15000 Cells plated in 100 μl of media per well of a 96-well plate (Dynex Technologies, Chantilly, VA) were used. Glucose uptake and lactate release were measured by analysis of media using the Glucose Hexokinase Assay (Sigma, Saint Louis, MO) and the Lactate Reagent and Lactate Standard Set (Trinity Biotech, Saint Louis, MO), respectively, according to manufacturer's protocol.

Western blot analysis. Samples were prepared and western blots were performed as described (Mekhail et al., 2004a). Primary monoclonal antibodies recognize HA, Flag-M2 (Sigma, St. Louis, MO), VHL (BD Pharmingen, San Diego, CA), or Caspase-3 (Cell Signaling, Beverly, MA). A primary polyclonal antibody detecting β-actin (Sigma, St. Louis, MO) was also used. A secondary antibody conjugated to horseradish peroxidase (Jackson ImmunoResearch, West Grove, PA) was used and detected by Western Lightning Chemiluminescence Reagent Plus (Perkin Elmer, Boston, MA).

Immunofluorescence. Cells were seeded onto coverslips and fixed with pre-chilled (to -20 °C) methanol for 10 min followed by acetone for 1min. An anti-VHL monoclonal

antibody (BD Pharmingen, San Diego, CA) was used. Cells were incubated for 1h with a primary antibody solution containing 10% FBS and 1% Triton-X-100 (v/v). Cells were washed several times in PBS before 1 h incubation with a secondary Texas Red-labeled antibody (Jackson ImmunoResearch).

Nude mouse xenograft assays. Nude mouse xenograft assays were done as described elsewhere (Iliopoulos et al., 1995). In brief, 5 x 10^6 viable U87MG glioblastoma cells (trypan blue dye exclusion method) were subcutaneously injected in the flanks of female nude mice (Charles River, Wilmington, MA). Tumors were excised two weeks post-injection according to the animal facility protocol (University of Ottawa).

Immunohistochemistry. Experiments were done blinded. 8 μm sections mounted on sialinized slides (DakoCytomation, Carpinteria, CA) were dewaxed in xylene and rehydrated using graded ethanol washes. For antigen retrieval, sections were immersed in preheated Dako target retrieval solution (DakoCytomation, Carpinteria, CA) and heat treated in a water bath. Primary antibodies were anti-human monoclonal VHL (BD Pharmingen, San Diego, CA), anti-human monoclonal LDH (Sigma, St. Louis, MO) and anti-human monoclonal B23 (Sigma, St. Louis, MO), all used at 1/1000. Negative controls were performed for all experiments and included irrelevant primary immunoglobulins of the same isotype or species. Antigen/antibody complexes were revealed by the Envision system (DakoCytomation, Carpinteria, CA) according to the manufacturer's protocol. Sections were counterstained with hematoxylin for 10 s, dehydrated in graded ethanol washes, and mounted with coverslips.

Results

H^+ limits energy expenditure in hypoxia

To study how cellular energy levels are altered under anaerobic metabolism (see introduction for definition), we incubated cells from various tissue origins in standard (SD) media, that prevents fluctuations in pH, or in acidification-permissive (AP) media, which is prepared to enable cells to naturally acidify their extracellular milieu to varying degrees under hypoxia (see Materials and Methods) (Mekhail et al., 2004a; Mekhail et al., 2005). Similar to previous reports, hypoxia induced significant reductions in total ATP levels when cells were incubated under standard conditions (Fig. 4.1A, and data discussed further in Fig. 4.7) (Liu et al., 2006). Unexpectedly, ATP concentrations were preserved when hypoxic cells acidified their environment to cell-type-specific pH thresholds (Fig. 4.1A). The establishment of acidosis was associated with increased cellular viability as revealed by fluorescein-diacetate (FDA) staining and propidium iodide (PI) exclusion in co-staining experiments (Fig. 4.1, B and C). We next set out to determine if H^+-dependent maintenance of energy levels is the consequence of increased production or decreased consumption of ATP. Increases in glucose uptake and lactate release, which are triggered by hypoxia, were insensitive to fluctuations in pH (Fig. 4.1, D and E), suggesting that acidosis does not increase ATP levels by modulating glycolysis, the Pasteur effect, or possible residual mitochondrial respiration. To study the effect of pH on energy consumption, hypoxic cells were treated with 6-deoxyglucose (6-DOG) to inhibit glycolytic energy production and ATP levels were monitored. Energy expenditure was lower in acidotic cells as demonstrated by a slower rate of ATP depletion (Fig. 4.1F). In addition, ATP levels under hypoxia-neutral conditions declined

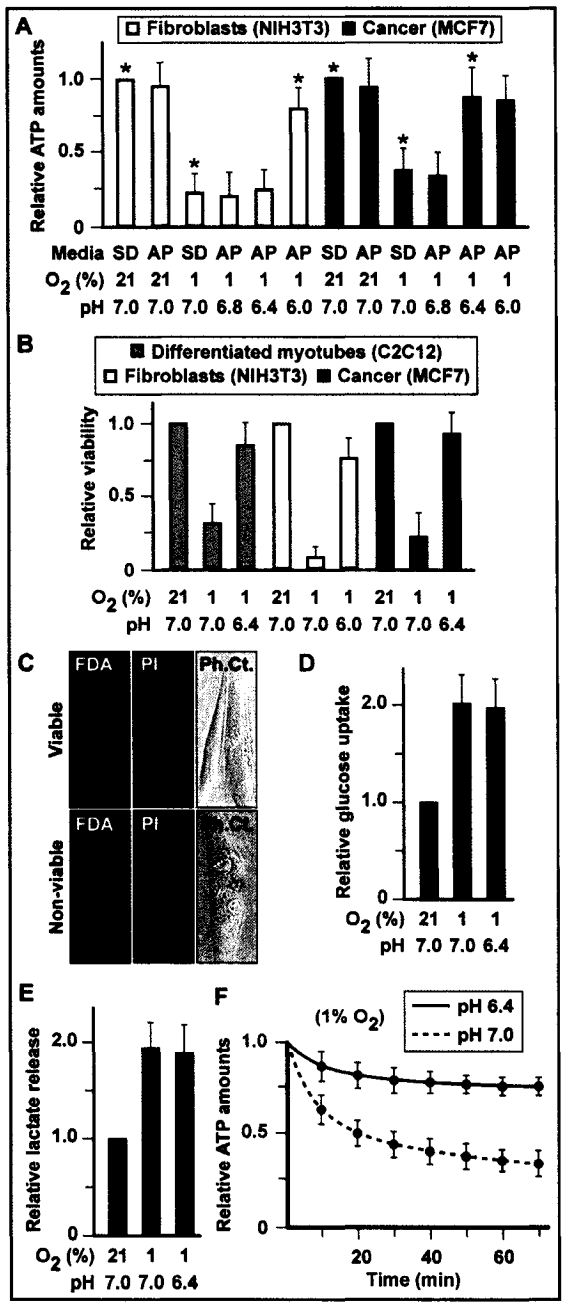
A
Fibroblasts (NIH3T3)
Cancer (MCF7)
Relative ATP amounts
1.0
0.5
0
Media SD AP SD AP AP AP SD AP SD AP AP AP
O2 (%) 21 21 1 1 1 1 21 21 1 1 1 1
pH 7.0 7.0 7.0 6.8 6.4 6.0 7.0 7.0 7.0 6.8 6.4 6.0
B
Differentiated myotubes (C2C12)
Fibroblasts (NIH3T3)
Cancer (MCF7)
Relative viability
1.0
0.5
0
O2 (%) 21 1 1 21 1 1 21 1 1
pH 7.0 7.0 6.4 7.0 7.0 6.0 7.0 7.0 6.4
C
FDA
PI
Ph.Ct.
Viable
Non-viable
D
Relative glucose uptake
2.0
1.0
0
O2 (%) 21 1 1
pH 7.0 7.0 6.4
E
Relative lactate release
2.0
1.0
0
O2 (%) 21 1 1
pH 7.0 7.0 6.4
F
(1% O2)
pH 6.4
pH 7.0
Relative ATP amounts
1.0
0.5
0
20
40
60
Time (min)

Figure 4.1

Figure 4.1. Acidosis reduces cellular energy demand. (A) Acidosis preserves cellular energy levels under hypoxia. Fibroblasts or breast carcinoma cells were cultured either in standard media (SD, initial pH 7.0) or different acidification permissive media (AP, initial pH 7.0) that allow maximal hypoxia-induced extracellular acidification to pH 6.8, 6.4, or 6.0. Cells were then cultured under normoxia (21% O_2) or hypoxia (1% O_2) for 22 h, endpoint pH was measured, and cellular ATP levels were measured and normalized to cell number. Single asterisk denotes conditions of interest which will be tested hereon after. N is 9 for three independent experiments performed in triplicates, values are means, and bars represent standard error. Shown normoxic AP media had maximal acidification potential of pH 6.0 but media remained at pH 7.0 at endpoint. (B and C) H^+ preserves viability. Breast carcinoma cells, fibroblasts, or differentiated myotubes were cultured as in (A). FDA and PI were added 3.5 h later for 30 min. Viability scores are ratios of the number of FDA-positive cells relative to the total number of FDA-positive and PI-positive cells (B). Scores were obtained from three independent experiments (B) and representative myotubes are shown in (C). Bars represent standard error. (D and E) H^+ production under hypoxia does not affect glycolysis or the Pasteur effect. MCF7 cells were cultured as in (A) then glucose uptake and lactate release were measured and normalized to cell number. (F) H^+ reduces energy demand under hypoxia. MCF7 cells were cultured as in (A). Following a 20 min 6-deoxyglucose treatment, ATP levels were measured and normalized to cell number and to the difference of initial ATP concentrations before addition of drug.

before any apparent cell death (Fig. 4.1, A and B), suggesting that mechanisms triggering the reduction in energy levels are upstream of the processes affecting viability. Taken together, this suggests that cells rely on fermentation protons and the ensuing acidosis to preserve cellular energy levels and viability by restricting energy demand to levels matching limited supply.

pH-dependent nucleolar condensation and restriction of rDNA transcription

While examining several cellular energy-parameters, we noticed that nucleoli of cells engaged in anaerobic acidosis exhibit changes that are characteristic of the transcriptional silencing of rDNA. Light microscopy revealed that nucleoli undergo a decrease in size (Fig. 4.2A). This was confirmed by assessment of the localization of the green fluorescent protein (GFP)-tagged B23 protein (Fig. 4.2, A and B). While short exposure (3 h) of cells to RNA polymerase-I (RNAPI) inhibitors such as treatment with low concentrations of actinomycin-D (Act-D) only decrease nucleolar size, prolonged exposure (8 h) to these drugs results in the toxic fragmentation of nucleoli (Fig. 4.2A, and asterisks and inset in 2B) (Olson and Dundr, 2005). Unlike such toxic pharmacological treatments, prolonged incubation under physiological acidosis (up to 30 h) did not induce any nucleolar fragmentation (Fig. 4.2, A and B), suggesting that acidosis might inhibit RNAPI and restrict ribosomal biogenesis in a fashion that does not disrupt nucleolar integrity. Next, immunohistochemistry analysis was performed on sections from glioblastoma tumors grown in the flanks of nude mice. Staining for endogenous B23 protein revealed that nucleoli of cells positioned closer to the core of tumors, which is thought to be more acidic (Engin et al., 1995; Engin et al., 1994; Wike-Hooley et al., 1984), exhibit a noticeably more condensed phenotype compared to nucleoli at the

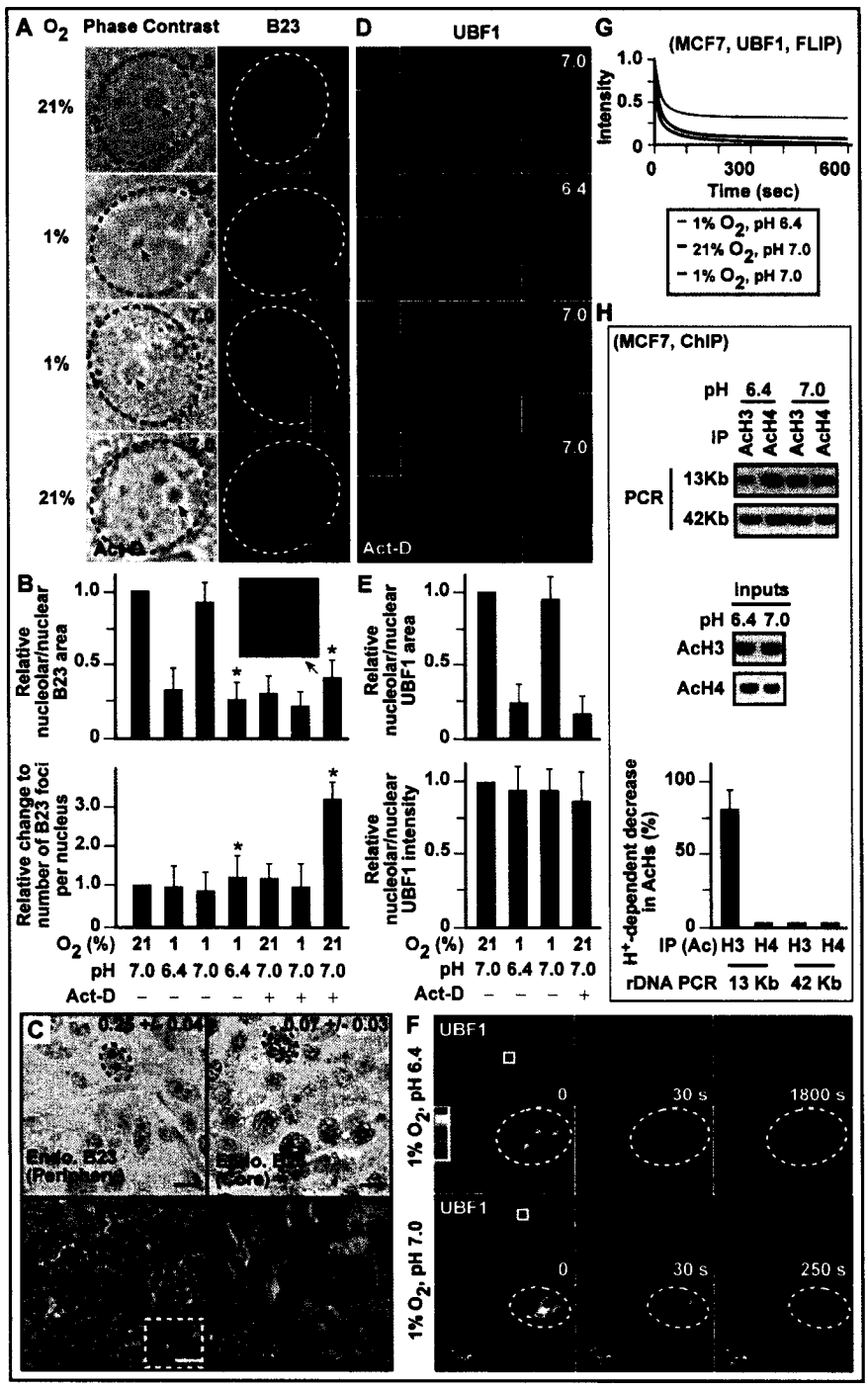
A
O_2
Phase Contrast
B23
21%
1%
1%
21%
Actin
D
UBF1
7.0
6.4
7.0
7.0
Act-D
G
(MCF7, UBF1, FLIP)
Intensity
1.0
0.5
0
0
300
600
Time (sec)
- 1% O_2, pH 6.4
- 21% O_2, pH 7.0
- 1% O_2, pH 7.0
H
(MCF7, ChIP)
pH 6.4 7.0
IP AcH3 AcH4 AcH3 AcH4
PCR
13Kb
42Kb
Inputs
pH 6.4 7.0
AcH3
AcH4
B
Relative nucleolar/nuclear B23 area
E
Relative nucleolar/nuclear UBF1 area
Relative change to number of B23 foci per nucleus
Relative nucleolar/nuclear UBF1 intensity
H^+-dependent decrease in AcHs (%)
O_2 (%) 21 1 1 1 21 1 21
pH 7.0 6.4 7.0 6.4 7.0 7.0 7.0
Act-D - - - - + + +
O_2 (%) 21 1 1 21
pH 7.0 6.4 7.0 7.0
Act-D - - - +
IP (Ac) H3 H4 H3 H4
rDNA PCR 13 Kb 42 Kb
C
Endo. B23 (Periphery)
Endo. B23 (Core)
F
UBF1
1% O_2, pH 6.4
0
30 s
1800 s
UBF1
1% O_2, pH 7.0
0
30 s
250 s

Figure 4.2

Figure 4.2. H^+ triggers nucleolar condensation. (A and B) Acidosis-dependent nucleolar condensation under hypoxia. MCF7 cells expressing B23-GFP were cultured under indicated conditions for 22 h and nucleoli were assessed by phase contrast imaging or GFP fluorescence. Representative pictures are shown in (A) and measurements of the ratio of nucleolar GFP area (all nucleoli within a nucleus) relative to nuclear area (outlined by dashed circles revealed by Hoechst staining of DNA in insets) are shown in (B) (N is 30 cells analyzed from three independent experiments and bars represent standard error). Extracellular pH is indicated on each panel. Act-D was added 3 h from endpoint, where indicated, and single asterisks (B) denote longer treatments (30 h acidosis, 8 h Act-D). (C) Nucleolar condensation observed in the acidic core of glioblastoma tumors grown in the flanks of nude mice. Sections (8 μm) were either submitted to H&E staining or to immunohistochemistry analysis to detect endogenous B23 protein. Ratios of nucleolar B23 to nuclear area were 0.25 and 0.07 near the tumor periphery and the core, respectively. Scale bars represent 5 μm (black) or 20 μm (yellow). (D to G) pH-dependent alteration of both steady-state and dynamic profiles of rDNA-interacting proteins under hypoxia. UBF1-GFP expressed in MCF7 cells cultured as in (A) was assessed for changes in steady-state distribution (D and E) (N is 30 cells analyzed from three independent experiments and bars represent standard error) or in dynamic profile by FLIP analysis (F and G). Insets in (D) show Hoechst staining of DNA or zoom of specific nucleoli (dashed squares). For FLIP, nucleoplasmic regions (white squares) were repeatedly bleached while cells are imaged between pulses, and pseudocolored images with nuclear outlines (dashed circles) highlighting changes in GFP fluorescence (F) and corresponding kinetics of loss of fluorescence (G) are shown. (H)

ChIP analysis performed on MCF7 cells cultured for 22 h under indicated conditions reveals an H^+-dependent reduction in the levels of acetylated histone H3 bound to rDNA near the rDNA transcriptional unit termination site 13 Kb from the start site. Representative gels and graph of quantitation of the changes in histone acetylation are shown. Results are normalized to cell number and inputs, and minimal IgG-associated background was subtracted in the quantitation process where results are means from three independent ChIP experiments and bars represent standard error.

periphery (Fig. 4.2C). Fibrillar centers constitute the nucleolar subcompartment where rDNA resides. Silencing of RNAPI is usually accompanied by the coalescence of fibrillar centers (FCs) into a few well-defined foci, a phenomenon associated with the segregation of nucleolar subcompartments (Olson and Dundr, 2005). Coalescence of FCs under acidosis was revealed by assessment of the localization of the GFP-tagged FC protein rDNA upstream binding factor-1 (UBF1) (Fig. 4.2, D and E). DNA-associated proteins exhibit increased residence time on DNA under transcriptional silencing conditions (Meshorer et al., 2006). The dynamic properties of GFP-tagged UBF1 were thus analyzed by fluorescence loss in photobleaching (FLIP) experiments (Lippincott-Schwartz et al., 2003). In FLIP, a living cell is repeatedly hit with a laser beam in the same region. Loss of fluorescence in an area outside the bleached spot is reflective of protein mobility between that area and the bleached spot. A rapid loss of UBF1-GFP fluorescence was observed in essentially the whole nucleus following repetitive bleaching of a small nucleoplasmic region in cells incubated under neutral conditions (Fig. 4.2, F and G), highlighting the dynamic character of the protein chimera. UBF1-GFP displayed an H^+-dependent increase in its residence time on rDNA with 34% of the protein pool still detectable after a 30 min FLIP experiment within coalesced FCs (Fig. 4.2, F and G). As previously reported, UBF1-GFP was highly mobile at earlier time points (Mekhail et al., 2005). None of these changes occurred when cells were prevented from acidifying their extracellular milieu under anaerobic conditions (Fig. 4.2). Thus, we reasoned that by temporarily restricting ribosomal anabolism, the most energy-consuming cellular process (50-80% of total consumption) (Holzel et al., 2005; Schmidt, 1999; Thomas, 2000), fermentative protons would match anaerobic energy demands with limited supply.

Consistent with this notion, chromatin crosslinking and immunoprecipitation (ChIP) revealed a decrease of about 75% in the level of acetylated histone H3 (AcH3) associated with the transcriptional termination site of rDNA (Fig. 4.2H, and see Fig. 4.5E for schematic of an rDNA gene unit), a region often hyperacetylated by RNAPI-inducing signals such as Myc expression (Grandori et al., 2005; Grummt and Pikaard, 2003). The 5'-external transcribed spacer (5'-ETS) region of precursor rRNA (pre-rRNA) is rapidly processed following rDNA transcription and measurement of its levels by reverse transcriptase PCR (RT-PCR) directly reflects the rate of RNAPI activity (Fig. 4.5E) (Grandori et al., 2005). RT-PCR analysis employing primers specific to 5'-ETS revealed an H^+-dependent decrease in pre-rRNA synthesis (Fig. 4.3A), which occurred before reductions in the levels of rRNA products were observed (Fig. 4.3B). A regulatory role for H^+ in rDNA transcription was supported by an acidosis-dependent reduction in the level of BrUTP incorporation into nascent rRNA in BrUTP pulse-chase experiments (Fig. 4.3C, notice that asterisk-marked green panels have triple the exposure time relative to other panels for the purpose of presentation) and by an H^+-dependent decrease in the levels of UBF1 proteins bound to the rDNA promoter in ChIP experiments (Fig. 4.3, D and E). rRNA processing was essentially unaltered by oxygen or pH levels since direct ethidium bromide staining revealed equimolar reductions of all three rRNA products (Fig. 4.3A) and since the vectorial path of BrUTP-labeled rRNA emanating from the nucleolus was preserved (Fig. 4.3C). No difference was observed in the ability of RNA polymerases II and III to synthesize ARPP-P0/Actin and 5S rRNA, respectively (Fig. 4.3A). Thus, acidosis restricts rDNA transcription under hypoxia.

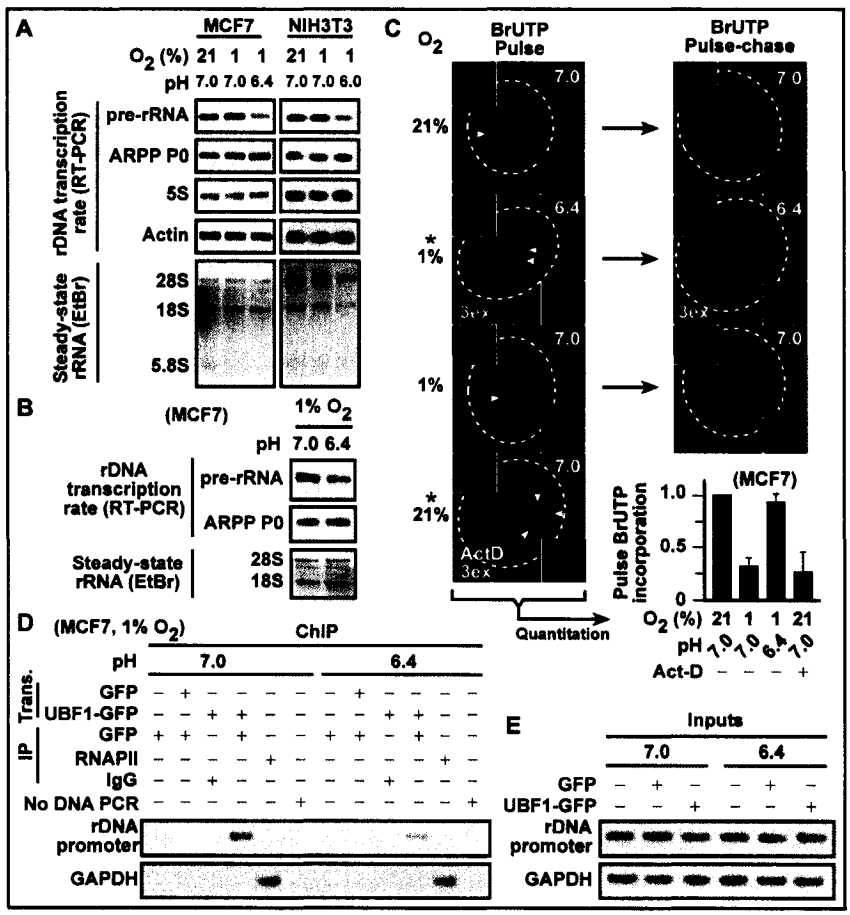
A
MCF7
NIH3T3
O2 (%) 21 1 1 21 1 1
pH 7.0 7.0 6.4 7.0 7.0 6.0
rDNA transcription rate (RT-PCR)
pre-rRNA
ARPP P0
5S
Actin
Steady-state rRNA (EtBr)
28S
18S
5.8S
B
(MCF7)
1% O2
pH 7.0 6.4
rDNA transcription rate (RT-PCR)
pre-rRNA
ARPP P0
Steady-state rRNA (EtBr)
28S
18S
C
O2
BrUTP Pulse
BrUTP Pulse-chase
21%
1%
1%
21%
7.0
6.4
7.0
7.0
3ex
ActD 3ex
Quantitation
(MCF7)
Pulse BrUTP incorporation
1.0
0.5
0
O2 (%) 21 1 1 21
pH 7.0 7.0 6.4 7.0
Act-D – – – +
D
(MCF7, 1% O2)
ChIP
pH
7.0
6.4
Trans.
GFP
UBF1-GFP
IP
GFP
RNAPII
IgG
No DNA PCR
rDNA promoter
GAPDH
E
Inputs
7.0
6.4
GFP
UBF1-GFP
rDNA promoter
GAPDH

Figure 4.3

Figure 4.3. Fermentation protons restrict rDNA transcription. (A) H^+ reduces the levels of pre-rRNA under hypoxia. RT-PCR analysis was performed on mRNA normalized by cell number from cells cultured for 22 h under indicated conditions. Steady-state levels of 28S, 18S, and 5.8S rRNAs were revealed by direct ethidium bromide (EtBr) staining. Results are representative of three independent experiments. (B) pH-dependent reductions in pre-rRNA levels are observed prior to any detectable changes in the steady state levels of 28S and 18S rRNA as revealed by RT-PCR and EtBr staining of samples from MCF7 cells incubated for 18 h in hypoxia. (C) H^+ lowers BrUTP incorporation in nascent rRNA but does not affect the vectorial path characteristic of rRNA processing emanating from the nucleolus. Nascent rRNA was pulsed with BrUTP and visualized by immunofluorescence before or after a 10 min chase. Asterisk-marked green panels were captured at triple the exposure time (3ex) relative to other conditions to better illustrate BrUTP incorporation patterns but all quantitation analysis were based on images obtained at a 1ex exposure time (N is 30 cells and bars represent standard error). Insets are zooms of arrow-marked regions. (D) ChIP analysis reveals that acidosis lowers the levels of UBF1 protein bound to the rDNA promoter. MCF7 cells were transfected to express UBF1-GFP, GFP alone or left unaltered. Cells were incubated under indicated conditions for 22 h. Extracts from equal number of cells were submitted to immunoprecipitations using indicated specific antibodies followed by PCR using primers specific to the rDNA promoter. Binding of RNAPII to the GAPDH gene served as positive control and input controls are shown.

Nucleolar rDNA is remodeled by H^+ and not directly by HIF or oxygen

HIF is a transcription factor implicated in the cellular oxygen homeostatic response under hypoxia, including induction of the Pasteur effect through activation of various genes encoding glycolytic enzymes or co-factors (Harris, 2002; Iyer et al., 1998; Obach et al., 2004; Pasteur, 1857; Seagroves et al., 2001; Semenza et al., 1994). Substitution of key proline residues within HIF-1α or HIF-2α to alanine generates HIFα variants (vHIF-1α and vHIF-2α) that evade proteasomal degradation and activate HIF target genes such as glucose transporter-1 (Glut-1) in the presence of oxygen (Fig. 4.4A) (Kondo et al., 2002; Smith et al., 2005). Both vHIF-1α and vHIF-2α failed to affect pre-rRNA levels (Fig. 4.4A) or induce any nucleolar condensation in normoxia (Fig. 4.4B, data not shown, and see Fig. 4.2A). This suggests that HIF activation is not sufficient to remodel nucleoli in the presence of oxygen.

Introduction of dominant negative HIF (dnHIF) into MCF7 cells reduced the rate at which they acidified their extracellular milieu, as expected (Fig. 4.4C) (Gunaratnam et al., 2003; Maemura et al., 1999). However, nucleolar condensation was still observed in these cells upon reaching pH 6.4 (Fig. 4.4, C and D). We next tested the direct involvement of HIF activation in the observed pH-dependent control of rDNA under low oxygen tension by incubating MCF7 cells expressing dnHIF (see (Gunaratnam et al., 2003) for full characterization of this molecule) in SD media under hypoxia for 16 h (pH stable at 7.0), which stabilized both HIF-1α and HIF-2α but abrogated their ability to activate Glut-1 (Fig. 4.4E, lanes 1 to 6). Cells were then replenished for 4 h with AP media conditioned to acidosis by direct addition of HCl (pH stable at 6.4) (Fig. 4.4E) or by another batch of cells (data not shown). Although HIF activity remained abrogated

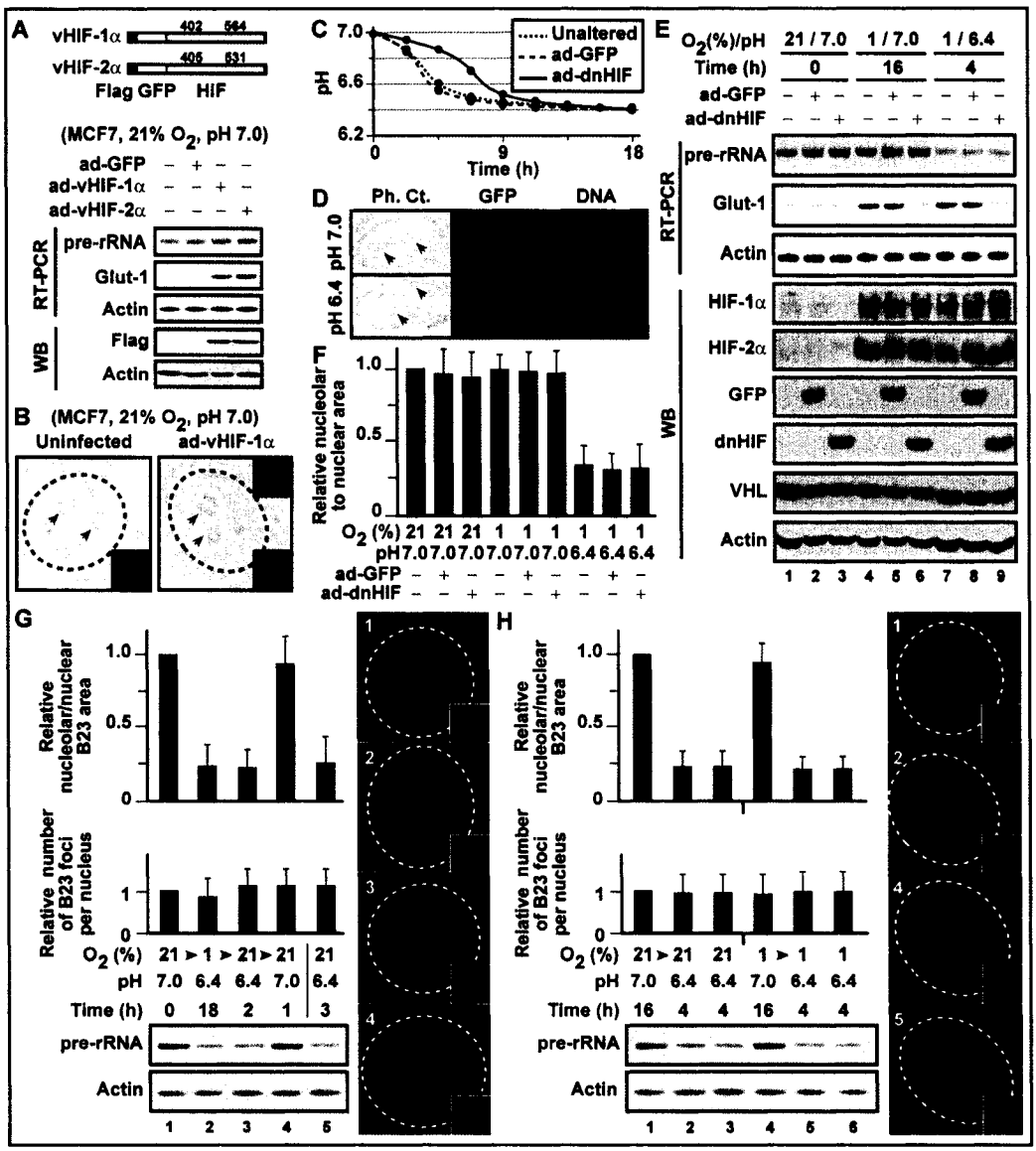
A
vHIF-1α
vHIF-2α
Flag GFP HIF
(MCF7, 21% O2, pH 7.0)
ad-GFP
ad-vHIF-1α
ad-vHIF-2α
RT-PCR
pre-rRNA
Glut-1
Actin
WB
Flag
Actin
B
(MCF7, 21% O2, pH 7.0)
Uninfected
ad-vHIF-1α
C
Unaltered
ad-GFP
ad-dnHIF
pH
Time (h)
D
Ph. Ct.
GFP
DNA
pH 7.0
pH 6.4
E
O2(%)/pH
Time (h)
ad-GFP
ad-dnHIF
pre-rRNA
Glut-1
Actin
HIF-1α
HIF-2α
GFP
dnHIF
VHL
Actin
RT-PCR
WB
F
Relative nucleolar to nuclear area
O2 (%)
pH
ad-GFP
ad-dnHIF
G
Relative nucleolar/nuclear B23 area
Relative number of B23 foci per nucleus
O2 (%)
pH
Time (h)
pre-rRNA
Actin
H
Relative nucleolar/nuclear B23 area
Relative number of B23 foci per nucleus
O2 (%)
pH
Time (h)
pre-rRNA
Actin

Figure 4.4

Figure 4.4. Acidosis does not require hypoxia or HIF activation to remodel nucleolar rDNA. (A and B) Expression of HIF variants that evade degradation in the presence of oxygen fail to induce nucleolar condensation. MCF7 cells expressing adenovirus-introduced HIFα variants harboring mutations of key proline residues to alanine, which allow these variants to evade degradation in the presence of oxygen, were submitted to Western blot and RT-PCR analysis (A) and assessed for changes in nucleolar morphology by phase contrast microscopy as shown by representative images in (B) where insets are Hoechst staining of DNA and GFP fluorescence. (C and D) Adenovirus-mediated introduction of GFP-tagged dnHIF, but not GFP alone, lowers the rate of acidification of the extracellular milieu by MCF7 cells under hypoxia (C) but does not prevent nucleolar condensation which is observed in representative MCF7 cells expressing GFP-tagged dnHIF (22 h hypoxia). Arrow heads highlight differences in nucleolar size. (E and F) Acidosis-dependent modulation of rDNA under hypoxia does not require HIF activity. MCF7 cells that are unaltered or expressing adenovirus-introduced GFP-tagged dnHIF or GFP alone were incubated in SD media under hypoxia for 16 h (pH stable at 7.0) then replenished for 4 h with AP media that had been conditioned to acidosis (pH stable at 6.4) by direct addition of the exogenous acid HCl. Cells were submitted to RT-PCR and western blotting (WB) at different time points (E) and quantitation of nucleolar condensation was performed on phase contrast images of cells from a parallel set (N is 30 cells, values are means, and bars represent standard error). (G) Nucleolar condensation and reductions in pre-rRNA levels triggered by hypoxia-induced acidosis persist after oxygenation until neutral pH is reinstated. MCF7 sets transfected to express B23-GFP (graph) or left unaltered (gels) were grown under

standard conditions in normoxia (lane 1) then replenished with AP media and transferred to hypoxia for 22 h resulting in extracellular acidification (lane 2). Cells were then reoxygenated for 2 h (lane 3) before neutralization of the media with NaOH for another hour (lane 4). Control cells that were reoxygenated for 3 h without neutralization are also shown (lane 5). Cells were monitored for changes in B23 distribution (N is 30 cells, values are means, and bars represent standard error) and mRNA was isolated for RT-PCR analysis. Representative images corresponding to numbered lanes of gels are shown. (H) Acidosis can trigger nucleolar condensation and reductions in pre-rRNA levels in the presence of oxygen. MCF7 sets transfected to express B23-GFP (graph) or left unaltered (gels) were cultured in normoxia (lane 1) or hypoxia (lane 4) in SD media for 16 h then replenished with AP media that was previously conditioned to pH 6.4 by another batch of hypoxic MCF7 cells (lanes 2 and 5) or by direct addition of HCl (lanes 3 and 6). Cells were monitored for changes in B23 distribution (N is 30 cells, values are means, and bars represent standard error) and mRNA was isolated for RT-PCR analysis. Representative images corresponding to numbered lanes of gels are shown. Gels are representative of three independent experiments.

after acidification of dnHIF-expressing cells as revealed by Glut-1 mRNA levels (Fig. 4.4E, lanes 7 to 9) (Mekhail et al., 2004a; Mekhail et al., 2005), nucleolar condensation still occurred under hypoxia-acidosis (Fig. 4.4F). Variations in the levels of reactive oxygen species, which reflect mitochondrial status, have been proposed to modulate HIF activity under hypoxia (Brunelle et al., 2005; Guzy et al., 2005; Kaelin, 2005; Mansfield et al., 2005; Page et al., 2002; Richard et al., 2000). Since HIF activity was not affected by pH under hypoxia (Fig. 4.4E, lanes 7 and 8, compared to lanes 4 and 5), it is reasonable to suspect that ROS production is similar under both neutral and acidic conditions within our experimental settings. This suggests that the observed effects of H^+ on nucleoli are not due to gross pH-dependent differences in ROS production or mitochondrial status. These findings eliminate the direct involvement of HIF in pH-dependent rDNA control, except for its well documented and herein observed role in the induction of the Pasteur effect and subsequent extracellular acidification.

Although the goal of this study is to assess how acidosis affects cellular energetics under hypoxia, we studied how the intersection of pH and oxygen affects nucleoli to gain insight into the nature of this homeostatic program. We found that cells submitted to hypoxia-induced acidosis triggered nucleolar condensation and reductions in the levels of pre-rRNA, both of which persisted following reoxygenation (Fig. 4.4G). Treatment of cells with AP media that had previously been conditioned to acidosis by another batch of cells in hypoxia (Fig. 4.4H, lanes 2 and 5, compared to lanes 1 and 4) or by direct addition of acid (Fig. 4.4H, lanes 3 and 6, compared to lanes 1 and 4) (pH stable at 6.4) triggered nucleolar condensation and reduced pre-rRNA levels both in the presence or absence of oxygen. SD media that was similarly conditioned by cells under hypoxia

failed to induce any change in nucleolar morphology (data not shown). Taken together, while HIF and other factors may promote extracellular acidification through processes such as the Pasteur effect, acidosis does not require hypoxia or HIF activation to restrict rDNA.

Acidosis-dependent restriction of rDNA requires nucleolar VHL

Next, we set out to identify biochemical characteristics of the pH-dependent process modulating nucleolar condensation. Morphological changes to the nucleolus and pre-rRNA synthesis were observed only after reaching cell-type-specific hydrogen ion concentrations correlating with pH thresholds required to target the VHL tumor suppressor for static nucleolar detention (Fig. 4.1, 4.2, and 4.5A) (Mekhail et al., 2004a; Mekhail et al., 2005). Immunohistochemistry analysis performed on sections of glioblastoma tumors revealed that the localization of endogenous VHL shifts from mainly cytoplasmic in cells near the tumor surface to mainly nucleolar deeper in the core of tumors (Fig. 4.5B). Confocal microscopy of GFP-tagged VHL revealed that the tumor suppressor first appears in the nucleolus within well-defined foci (Fig. 4.5C, left panel) similar to condensed rDNA regions (Fig. 4.2D). We used fluorescence recovery after photobleaching (FRAP) to assess the kinetic properties of VHL-GFP within these foci and determine the potential involvement of this tumor suppressor in H^+-dependent rDNA silencing (Lippincott-Schwartz et al., 2003; Meshorer et al., 2006). Specific cellular regions expressing fusion proteins were bleached with the use of a laser pulse that irreversibly quenches the GFP signal, and the recovery of signal in the bleached area was recorded by time-lapse confocal microscopy. The kinetics and extent of recovery of fluorescence in a cellular region following bleaching are reflective of the dynamics of the

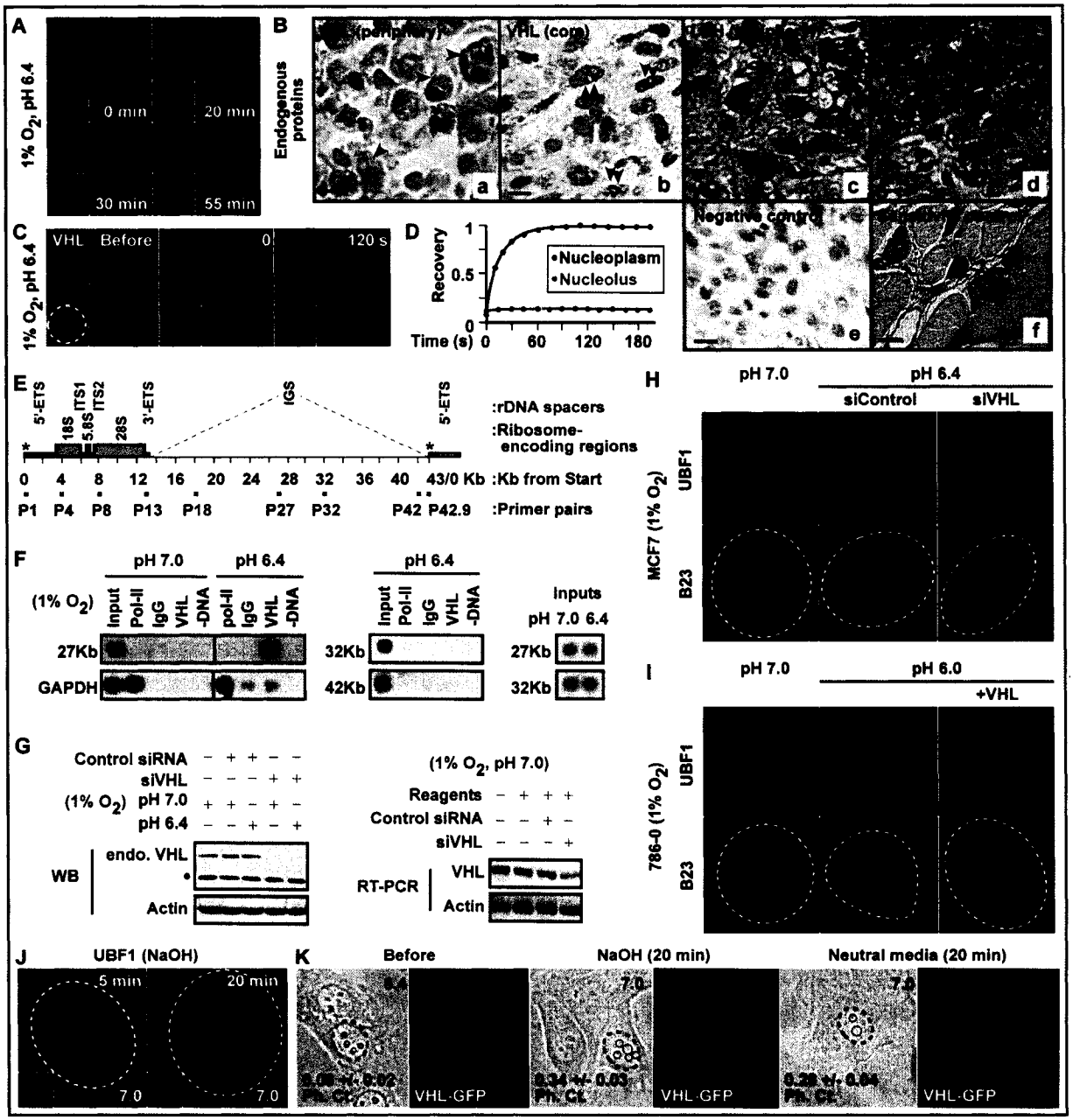
A
1% O2, pH 6.4
0 min
20 min
30 min
55 min
B
Endogenous proteins
VHL (cyto)
a
b
c
d
e
f
C
1% O2, pH 6.4
VHL Before
0
120 s
D
Recovery
Nucleoplasm
Nucleolus
Time (s) 0 60 120 180
E
5'-ETS
18S
ITS1
5.8S
ITS2
28S
3'-ETS
IGS
5'-ETS
:rDNA spacers
:Ribosome-encoding regions
0 4 8 12 16 20 24 28 32 36 40 43/0 Kb :Kb from Start
P1 P4 P8 P13 P18 P27 P32 P42 P42.9 :Primer pairs
F
pH 7.0
pH 6.4
(1% O2)
Input
Pol-II
IgG
VHL
-DNA
27Kb
GAPDH
32Kb
42Kb
Inputs
pH 7.0 6.4
G
Control siRNA
siVHL
(1% O2) pH 7.0
pH 6.4
WB
endo. VHL
Actin
(1% O2, pH 7.0)
Reagents
Control siRNA
siVHL
RT-PCR
VHL
Actin
H
pH 7.0
pH 6.4
siControl
siVHL
MCF7 (1% O2)
UBF1
B23
I
pH 7.0
pH 6.0
+VHL
786-0 (1% O2)
UBF1
B23
J
UBF1 (NaOH)
5 min
20 min
7.0
7.0
K
Before
NaOH (20 min)
Neutral media (20 min)
7.4
7.0
7.0
VHL-GFP
VHL-GFP
VHL-GFP

Figure 4.5

Figure 4.5. Nucleolar condensation implicates VHL-rDNA interactions. (A) pH-dependent targeting of VHL to the nucleolus. MCF7 cells stably expressing GFP-tagged VHL were incubated under hypoxia for 17 h (t_0) and VHL was monitored for changes in steady state distribution. Insets show Hoechst staining of DNA. (B) Endogenous VHL localizes to nucleoli in the acidic core of tumors. Glioblastoma (U87MG) sections (8 μm) (a-e) or sections of surrounding muscle tissue (f) were submitted to immunohistochemistry analysis using antibodies recognizing endogenous VHL or LDH. Note that while VHL localization changes from mainly cytoplasmic near the tumor periphery to an exclusively nucleolar distribution near the core of the tumor, LDH is cytoplasmic independent of distance from tumor surface. Scale bars represent 5 μm. (C and D) FRAP analysis reveals H^+-dependent static detention of VHL in subnucleolar foci reminiscent of condensed fibrillar centers. Nucleoplasmic fluorescence was first reduced by five laser pulses (yellow square) before performing FRAP. Inset is a zoom of area marked by white square showing a specific nucleolus (dashed circle). Cells were imaged before and after bleaching arrow-marked focus (C) and kinetics of fluorescence recovery was revealed by time-lapse microscopy and plotted against the kinetics of VHL in the nucleoplasm of another cell incubated under the same conditions (D). (E) Human rRNA gene unit. Primer pairs (■) for ChIP and their positions in Kb relative to the transcription start site (*) are shown. E/I-TS, external/internal transcribed spacer; IGS, intergenic spacer. (F) ChIP analysis reveals VHL/rDNA interactions. MCF7 cells expressing adenovirus-introduced VHL-GFP were incubated under hypoxia for 22 h then ChIP was performed. VHL interacts with the IGS of rDNA around the 27 Kb region. Controls are the pH-independent interaction of RNAPII with the GAPDH gene, the absence of any

detectable interaction of VHL with other regions of rDNA (only two of these regions are shown as others yielded similar results), and inputs. (G) Characterization of siVHL. Western blotting (WB) and RT-PCR analysis reveal that transiently expressed siVHL silences endogenous VHL expression in hypoxic MCF7 cells independent of pH. Results from cells expressing a random siRNA control (siControl) are also shown. (H to K) VHL is required for H^+-dependent nucleolar condensation. MCF7 cells expressing siVHL (H) or VHL-deficient 786-0 cells (I) do not exhibit H^+-dependent nucleolar condensation after a 22 h hypoxic incubation but reintroduction of HA-tagged VHL into VHL-deficient 786-0 cells by stable expression sensitizes these cells to the effect of H^+ on rDNA (I). MCF7 cells were transfected to transiently express UBF1-GFP (J) or infected to express VHL-GFP (K) then transferred to hypoxia to induce acidosis and nucleolar condensation. Acidotic media was then neutralized by addition of sodium hydroxide (NaOH) or cells were replenished with fresh SD media for 20 min (J and K). Ratios of nucleolar to nuclear area with SEM are shown for each panel in (K). Certain nuclei (dashed circles), nucleoli (red circles) and subnucleolar foci (arrows) are outlined to highlight nucleolar condensation states. Extracellular pH is indicated on each panel.

studied fluorescent chimeras. While nucleoplasmic VHL was highly mobile in hypoxic cells under neutral conditions, the protein was statically detained within these early subnucleolar foci (Fig. 4.5, C and D), suggesting a role for VHL in the acidosis-dependent regulation of rDNA (Meshorer et al., 2006).

ChIP analysis revealed that nucleolar VHL was physically linked, directly or indirectly, with the intergenic spacer of rDNA around 27 Kb from the transcriptional start site (Fig. 4.5, E and F) (Thiry and Lafontaine, 2005). Silencing of endogenous VHL expression in MCF7 cells by use of small-interfering RNA (siVHL), which was equally functional under neutral and acidic conditions (Fig. 4.5G), abolished H^+-dependent nucleolar condensation (Fig. 4.5H). VHL-deficient cells (Kaelin, 2002) failed to condense nucleoli, a phenomenon that was rescued by the reintroduction of hemaglutinin-tagged VHL (HA-VHL) (Fig. 4.5I). Neutralization of the extracellular milieu by addition of NaOH or replenishing the cells with fresh neutral SD media abolished nucleolar condensation only after essentially all of the VHL protein pool was released from nucleoli (Fig. 4.5, J and K), suggesting that condensation does not require complete sequestration of the VHL protein pool.

pre-rRNA levels were insensitive to pH in VHL-deficient cells (Fig. 4.6A) but stable expression of HA-VHL in these cells restored H^+-dependent reductions in the levels of the precursor (Fig. 4.6A). Silencing endogenous VHL expression in MCF7 cells abolished acidosis-dependent restriction of ribosomal biogenesis in the presence or absence of oxygen (Fig. 4.6B). ΔC157 is a deletion mutant of VHL that localizes to the nucleolus and can compete with the wild-type tumor suppressor protein for nucleolar localization (Mekhail et al., 2004a). ΔC157 failed to induce nucleolar condensation when

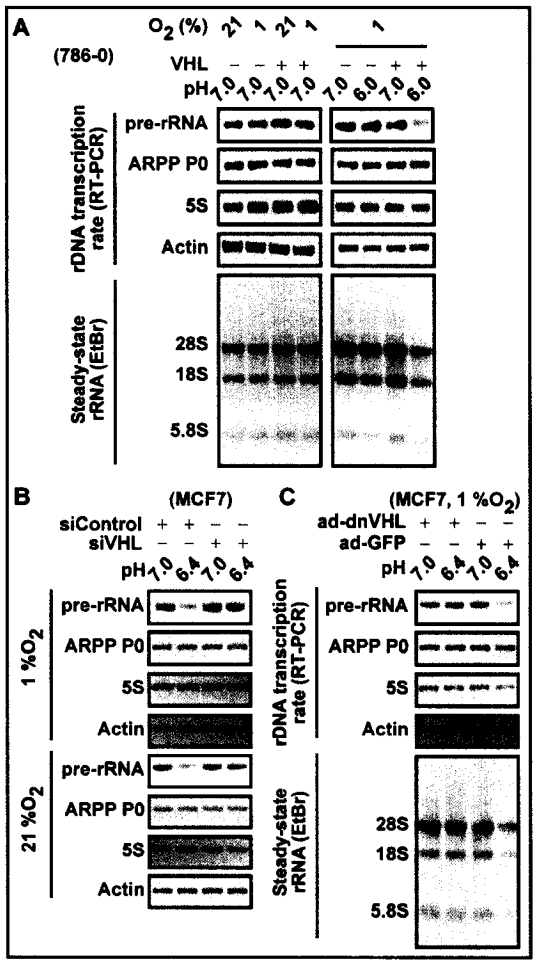
A
(786-0)
O2 (%) 21 1 21 1 1
VHL – – + + – – + +
pH 7.0 7.0 7.0 7.0 7.0 6.0 7.0 6.0
rDNA transcription rate (RT-PCR)
pre-rRNA
ARPP P0
5S
Actin
Steady-state rRNA (EtBr)
28S
18S
5.8S
B
(MCF7)
siControl + + – –
siVHL – – + +
pH 7.0 6.4 7.0 6.4
1 %O2
21 %O2
pre-rRNA
ARPP P0
5S
Actin
C
(MCF7, 1 %O2)
ad-dnVHL + + – –
ad-GFP – – + +
pH 7.0 6.4 7.0 6.4
rDNA transcription rate (RT-PCR)
Steady-state rRNA (EtBr)
28S
18S
5.8S

Figure 4.6

Figure 4.6. Nucleolar VHL is required for the acidosis-dependent decrease in rDNA transcription. (A) VHL-deficient 786-0 cells do not exhibit H^+-dependent rDNA silencing characteristics after a 22 h incubation under indicated conditions. Reintroduction of HA-tagged VHL into VHL-deficient 786-0 cells by stable expression sensitizes these cells to the effect of H^+ on rDNA. (B and C) Silencing VHL expression with transiently transfected siVHL (B) or competing nucleolus-VHL interactions with adenovirus-introduced dnVHL (C) desensitizes MCF7 cells to the effects of acidosis on nucleolar rDNA. Concentration of $NaHCO_3$ buffer in the media was 44 mM for hypoxia and 18 mM for normoxia experiments.

expressed in VHL-deficient cells incubated under hypoxia-acidosis, indicating that this mutant can be used as a dominant negative molecule (dnVHL) (data not shown). Expression of dnVHL into MCF7 cells abolished the constriction imposed by H^+ on ribosomal anabolism (Fig. 4.6C). These findings suggest that acidosis-mediated restriction of nucleolar rDNA requires the H^+-dependent relocation of VHL to the nucleolus.

Abrogating H^+-dependent rDNA restriction by silencing VHL expression or competing VHL-rDNA interactions prevents acidosis from sustaining energy equilibrium and viability under hypoxia

We next tested if abrogating rDNA silencing would prevent acidosis from preserving cellular energy equilibrium and viability. A small fraction of the MCF7 cellular population (less than 2%), which failed to target VHL to the nucleolus under acidosis (Mekhail et al., 2004a), incorporated tryptan blue under hypoxia-acidosis (Fig. 4.7A). Silencing endogenous VHL expression in MCF7 cells prevented acidosis-dependent preservation of ATP levels and viability under hypoxia (Fig. 4.7B). VHL-deficient 786-0 cells failed to maintain ATP concentrations or exhibit protection by acidosis under hypoxia but were resensitized to both of these effects of acidosis following the re-establishment of HA-VHL expression (Fig. 4.7, B and C). These experiments were performed at time points where endogenous VHL was confined to nucleoli (Fig. 4.7D), where the tumor suppressor is known to be statically detained (Fig. 4.5D and see (Mekhail et al., 2005)), eliminating the potential implication of non-nucleolar functions of VHL in the herein observed energy homeostatic program. Although dnVHL introduced into VHL-deficient cells is statically detained by the nucleolar architecture

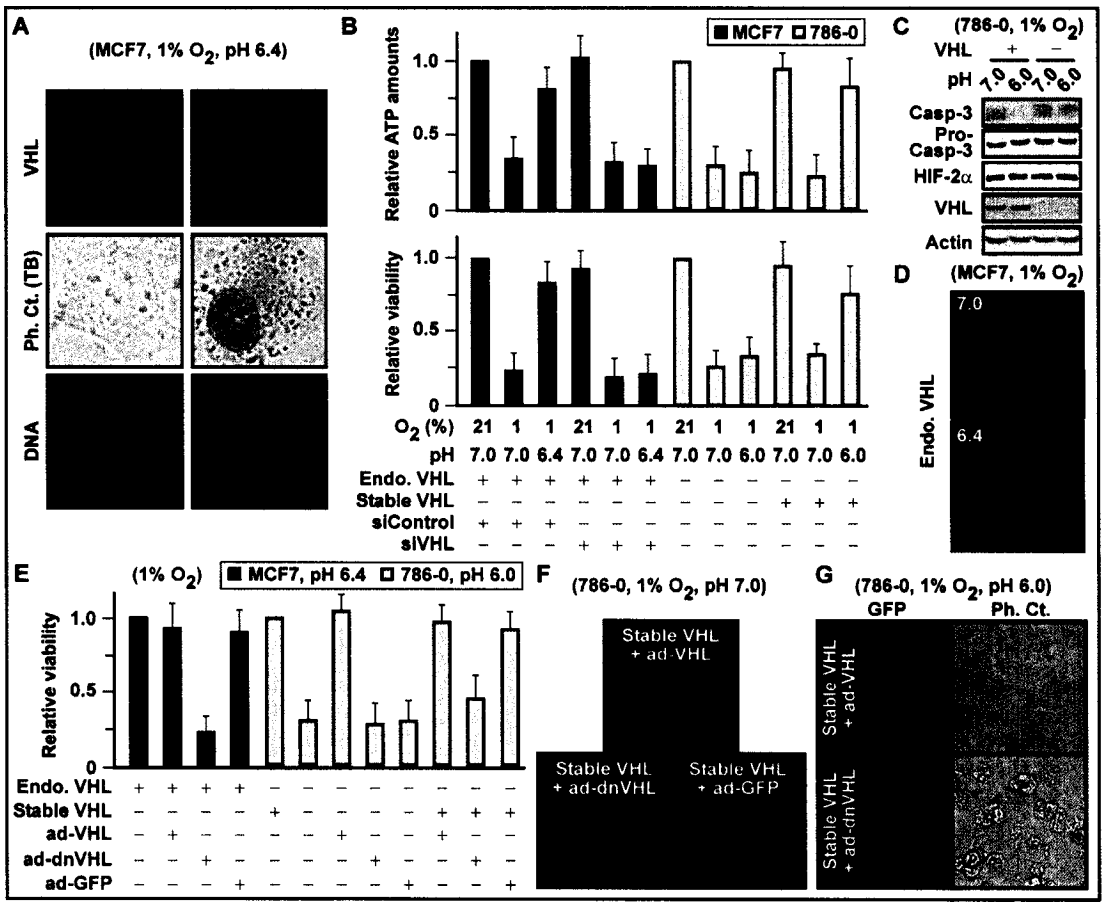
A
(MCF7, 1% O2, pH 6.4)
VHL
Ph. Ct. (TB)
DNA
B
MCF7 786-0
Relative ATP amounts
Relative viability
O2 (%) 21 1 1 21 1 1 21 1 1 21 1 1
pH 7.0 7.0 6.4 7.0 7.0 6.4 7.0 7.0 6.0 7.0 7.0 6.0
Endo. VHL
Stable VHL
siControl
siVHL
C
(786-0, 1% O2)
VHL
pH
Casp-3
Pro-Casp-3
HIF-2α
VHL
Actin
D
(MCF7, 1% O2)
Endo. VHL
7.0
6.4
E
(1% O2)
MCF7, pH 6.4 786-0, pH 6.0
Relative viability
Endo. VHL
Stable VHL
ad-VHL
ad-dnVHL
ad-GFP
F
(786-0, 1% O2, pH 7.0)
Stable VHL + ad-VHL
Stable VHL + ad-dnVHL
Stable VHL + ad-GFP
G
(786-0, 1% O2, pH 6.0)
GFP
Ph. Ct.
Stable VHL + ad-VHL
Stable VHL + ad-dnVHL

Figure 4.7

Figure 4.7. Abrogating H^+-dependent rDNA restriction by silencing VHL expression or competing VHL-rDNA interactions prevents acidosis from sustaining energy equilibrium and viability under hypoxia. (A) Correlation between nucleolar localization of VHL and survival under hypoxia-acidosis. MCF7 cells incubated for 22 h under hypoxia in AP media were submitted to trypan blue staining. Shown on the right is a representative cell of the small number of cells (less than 2%) that did not exhibit nucleolar VHL localization and stained positive for trypan blue under acidosis. (B) Abrogation of H^+-dependent restriction of ribosomal biogenesis by induced or naturally occurring loss of VHL expression abolishes acidosis-dependent maintenance of energy equilibrium and viability under hypoxia. Transfection of MCF7 cells with siVHL, but not siControl, desensitizes the cells to the protective effects of acidosis. VHL-deficient 786-0 cells were sensitized to acidosis by stable transfection-mediated reintroduction of HA-tagged VHL. Cells were analyzed for ATP levels at 22 h (9 wells from three independent experiments performed in triplicates were assessed, values are means and bars represent standard error) and for viability by the FDA/PI cotreatment method 4 h later (viability scores from three independent experiments are shown). (C) 786-0 cells that are either deficient for VHL expression or stably expressing reintroduced HA-tagged VHL were cultured for 26 h in hypoxia under indicated conditions and assessed for viability by caspase-3 immunoblotting where actin and other proteins were also detected as controls. (D) Immunofluorescence analysis with an antibody specific to endogenous VHL reveals its nucleolar distribution in MCF7 cells incubated for 22 h in hypoxia under AP conditions. (E) MCF7 cells or 786-0 cells (with or without stably expressed HA-VHL) were infected with an adenovirus expressing VHL-GFP, dnVHL-GFP, GFP alone,

or left unaltered. Cells were then incubated for 26 h under indicated conditions and viability was assessed as in (B). (F and G) Representative GFP fluorescence or phase contrast imaging of cells in (E) at time zero (F) and at endpoint (G).

(Mekhail et al., 2005), this dominant negative molecule did not sensitize these cells to the protective effect of acidosis nor did it increase toxicity under hypoxia (Fig. 4.7E). In stark contrast, introduction of dnVHL at levels sufficient to compete with a significant fraction of the wild-type protein pool into both 786-0 cells stably expressing re-introduced HA-VHL as well as MCF7 cells abolished the protective effect of acidosis under hypoxia (Fig. 4.7, E to G) (Mekhail et al., 2004a). These results demonstrate that cells produce H^+ to remain a sustainable and viable energy system.

Discussion

We report the unexpected finding that cells regulate energy demand by sensing environmental H^+ concentration. Cells maintain their total energy levels and remain viable regardless of oxygen tension only when allowed to undertake the natural route to acidosis, a process explained by H^+-dependent reduction in cellular ATP expenditure. We demonstrate that acidosis restricts ribosomal biogenesis, the most energy-demanding cellular process, at the level of pre-rRNA transcription. Determination of the cell-type-specific pH thresholds required for RNAPI transcriptional silencing led us to investigate the potential implication of the H^+-dependent nucleolar targeting of VHL in this process. Nucleolar VHL interacts with the IGS of rDNA and was required for H^+-dependent nucleolar condensation and reduction of rRNA synthesis. Abrogating this process by disrupting expression or nucleolar accumulation of VHL abolishes the ability of acidosis to lower cellular energy demand, triggers energy starvation and decreases viability. While HIF and other factors may promote extracellular acidification through processes such as the Pasteur effect, acidosis does not require hypoxia or HIF activation to restrict ribosomal biogenesis. These findings suggest that H^+ plays a crucial role in basic metabolism and provide a potential explanation for the protective effect of acidosis under ischemic physiology and pathology.

We would like to amend the model of basic cellular metabolism by adding a central role for H^+ in modulating the demand side of the cellular energy equation. We propose a model where fermentation, in addition to sustaining ATP production by replenishing glycolysis with NAD^+ under hypoxia, also generates H^+ to restrict ribosomal biogenesis, thereby limiting energy expenditure (Fig. 4.8). We envision two different

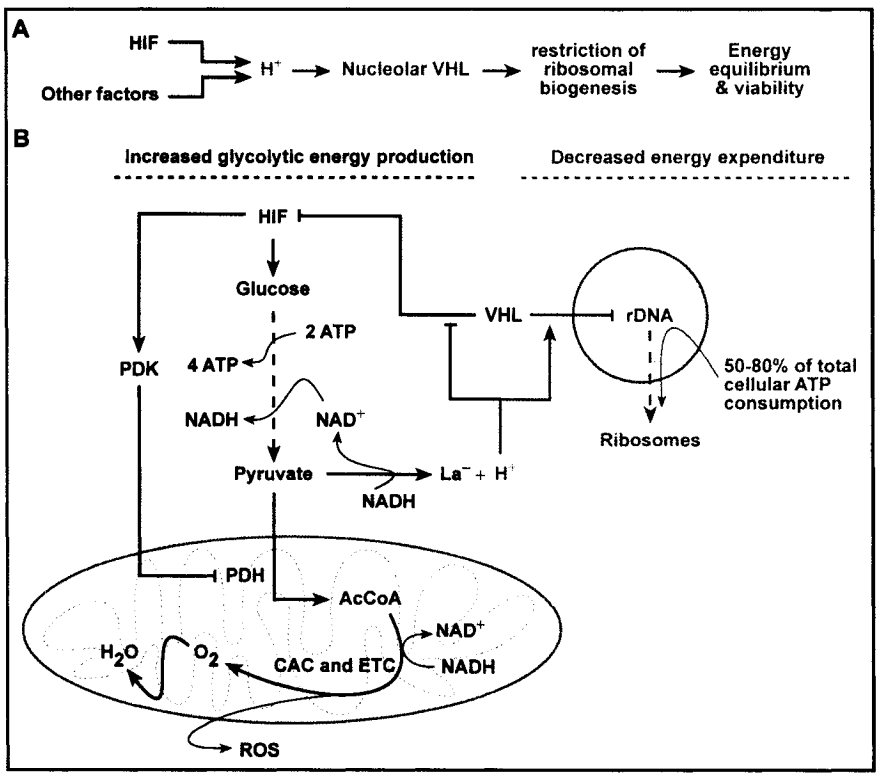
A
HIF
Other factors
H+
Nucleolar VHL
restriction of ribosomal biogenesis
Energy equilibrium & viability
B
Increased glycolytic energy production
Decreased energy expenditure
HIF
Glucose
2 ATP
4 ATP
PDK
NADH
NAD+
Pyruvate
La− + H+
NADH
VHL
rDNA
Ribosomes
50-80% of total cellular ATP consumption
PDH
AcCoA
NAD+
NADH
H2O
O2
CAC and ETC
ROS

Figure 4.8

Figure 4.8. Model for the modulation of cellular energy demand by H^+. (A) Several factors, including HIF activation under hypoxia, promote H^+ production and acidosis. Cells sensing increases in the environmental hydrogen ion concentration target VHL to the nucleolus to participate in the restriction of the energy-demanding process of ribosomal biogenesis preserving energy equilibrium and viability under low energy supply. (B) The role of H^+ in anaerobic metabolism. Fermentation, in addition to sustaining ATP production by replenishing anaerobic glycolysis with NAD^+, also generates H^+ to restrict ribosomal biogenesis and limit energy consumption. Two different paths could lead to the induction of this energy-saving process. First, increased lactic acid production at 25-75% of VO_2max, levels not low enough to directly induce HIF, targets VHL to the nucleolus where it silences rDNA to restrict ATP consumption. Nucleolar sequestration of VHL also induces HIF to actively block mitochondrial respiration and promote energy production by anaerobic glycolysis. Alternatively, sharper reductions in oxygen first stabilize HIF, which then induces anaerobic glycolysis allowing fermentation to generate the hydrogen ions needed to lower cellular energy demands.

paths that could lead to the induction of this energy-saving process. In the first scenario, increased lactic acid production at 25-75% of maximal cellular oxygen uptake (VO_2max) (Gladden, 2001), levels likely not low enough to directly stabilize HIF (Chan et al., 2005), would target VHL to the nucleolus resulting in rDNA silencing and HIF activation to both restrict ATP consumption and promote energy production by glycolysis, respectively (Fig. 4.8). Alternatively, sharper reductions in oxygen could first stabilize HIF, which then induces anaerobic glycolysis allowing fermentation to generate the hydrogen ions needed to lower cellular energy demands. Therefore, we propose that cells maintain constant ATP levels regardless of their relative engagement in aerobic or anaerobic metabolism, contrasting the previously suggested notion that hypoxia leads to energy starvation.

We share a view of the nucleolus where it acts as a hub that ensures cellular adaptation to alterations in environmental parameters (Andersen et al., 2005; Olson, 2004; Weber et al., 1999). In addition to excluding VHL from certain molecular networks to promote the transcription of hypoxia-inducible genes (Mekhail et al., 2005), static nucleolar detention introduces VHL into a network that silences rDNA. Several molecules, including the replication factor PCNA as well as the transcription and repair factor TFIIH, respond to various signals and seem to alternate between dynamic and static states through interactions with different DNA domains (Hoogstraten et al., 2002; Meshorer et al., 2006; Sporbert et al., 2002). It is tempting to speculate that at least some of these molecules are implicated in molecular interactions reflective of "symbiotic relationships", similar to that of VHL with rDNA, where chromatin is modulated by

statically detained proteins, which in turn abandon dynamic functions in other molecular networks.

The history of nucleolar evolution indicates that the IGS of rDNA underwent a disproportionate expansion in size relative to rRNA transcriptional units (Thiry and Lafontaine, 2005). IGS is known to play key roles in the regulation of rDNA (Reeder, 1984). For example, non-protein-coding IGS transcripts are required for the establishment and maintenance of specific heterochromatic configurations at the promoter of a subset of rDNA arrays (Mayer et al., 2006). Interestingly, we found that VHL interacts with IGS at regions containing repeats proposed to act as enhancers for RNAPI transcription (Mais et al., 2005). A possible role for nucleolar VHL in rDNA silencing could consist of inactivating such sequences by direct chemical modification, by preventing their interactions with regulatory molecules, or by recruiting silencing proteins. Whether evolutionary expansion in IGS size contributed to the evolution of the pH-dependent rDNA silencing program described here and whether ethanol fermentation activates similar mechanisms in different species or phyla is of considerable interest but remains to be determined.

Only a certain subpopulation of rRNA genes is active at any given time in the cell (Grummt and Pikaard, 2003). pH levels could be modulating rDNA transcription through two different approaches that are not necessarily mutually exclusive. Cells can control the number of transcripts that are made from each gene. Alternatively, as there are hundreds of rRNA genes, another strategy would be to turn subsets of the rRNA gene pool either "on" or "off". Since both mechanisms could be rapid and efficient, future work should aid in identifying the exact approach that is employed by acidosis (Grummt

and Pikaard, 2003). Unlike acidosis, several previously identified regulated rDNA silencing signals result in nucleolar disintegration, a phenomenon that is believed to be caused by the complete loss of RNAPI activity and is associated with decreased viability (Sinclair and Guarente, 1997; Sinclair et al., 1997). Acidosis might preserve nucleolar integrity by the fact that it only decreases, rather than completely abolish, rDNA transcription or by actively stabilizing the nucleolar architecture through another pathway. Identification of these processes should help identify precise and targeted approaches to test if restriction of rDNA under hypoxia-neutral conditions, without affecting the expression or nucleolar localization of VHL, would mimic acidosis and prevent energy starvation. We noticed that the occupancy of a fraction of VHL's nucleolar binding sites by dnVHL was sufficient to completely abrogate H^+-dependent rDNA silencing. A possible explanation of these findings is that the stepwise spreading of VHL, and possibly other proteins, along the rDNA lattice restricts pre-rRNA synthesis but this remains to be tested. Such a model would be similar to that proposed for another system; here the stepwise spreading of the yeast Sir2 protein and its associated proteins along the DNA lattice is required for transcriptional silencing (Grewal and Moazed, 2003; Moazed et al., 2004; Straight et al., 1999).

Sustainable biological systems balance the production and expenditure of energy. Introduction of oxygen into an anaerobic biosphere over 2.2 billion years ago triggered a drastic reorganization and expansion of complex molecular networks (Falkowski, 2006). The advent of mitochondrial respiration and the steady rise in atmospheric oxygen facilitated the evolution of energy-demanding metabolic pathways otherwise incompatible with anaerobic energy production. Contemporary organisms that

provisionally retreat to the less sophisticated energy generators under low oxygen tensions must therefore decrease cellular energy consumption to preserve equilibrium and avoid the deleterious effects of energy starvation. Our work reveals that cells rely on H^+ to accurately harmonize cellular energy demands with shifting supply and provides an explanation for the protective effect of acidosis in ischemic and hypoxic settings.

Acknowledgements

We sincerely thank Josianne Payette and Sayed Aziz for excellent technical expertise. This work is supported by a grant from the Canadian Institutes of Health Research (CIHR) to S. Lee, a Doctoral Canada Graduate Scholarship (CGS-D) of the Natural Science and Engineering Research Council of Canada (NSERC) to K. Mekhail, and an Ontario Graduate Scholarship (OGS) to L. Rivero-Lopez. S. Lee is the recipient of the National Cancer Institute of Canada (NCIC) Harold E. Johns Award.

References

Allen, D., and H. Westerblad. 2004. Lactic acid: The latest performance-enhancing drug. *Science*. 305:1112-1113.

Andersen, J.S., Y.W. Lam, A.K. Leung, S.E. Ong, C.E. Lyon, A.I. Lamond, and M. Mann. 2005. Nucleolar proteome dynamics. *Nature*. 433:77-83.

Bing, O.H., W.W. Brooks, and J.V. Messer. 1973. Heart muscle viability following hypoxia: protective effect of acidosis. *Science*. 180:1297-1298.

Bonicalzi, M.E., I. Groulx, N. de Paulsen, and S. Lee. 2001. Role of exon 2-encoded beta -domain of the von Hippel-Lindau tumor suppressor protein. *J. Biol. Chem.* 276:1407.

Bruick, R.K., and S.L. McKnight. 2001. A conserved family of prolyl-4-hydroxylases that modify HIF. *Science*. 294:1337-1340.

Brunelle, J.K., E.L. Bell, N.M. Quesada, K. Vercauteren, V. Tiranti, M. Zeviani, R.C. Scarpulla, and N.S. Chandel. 2005. Oxygen sensing requires mitochondrial ROS but not oxidative phosphorylation. *Cell Metab.* 1:409-414.

Chan, D.A., P.D. Sutphin, S.E. Yen, and A.J. Giaccia. 2005. Coordinate regulation of the oxygen-dependent degradation domains of hypoxia-inducible factor 1 alpha. *Mol. Cell. Biol.* 25:6415-6426.

Currin, R.T., G.J. Gores, R.G. Thurman, and J.J. Lemasters. 1991. Protection by acidotic pH against anoxic cell killing in perfused rat liver: evidence for a pH paradox. *FASEB J.* 5:207-210.

Engin, K., D.B. Leeper, J.R. Cater, A.J. Thistlethwaite, L. Tupchong, and J.D. McFarlane. 1995. Extracellular pH distribution in human tumours. *Int. J. Hyperthermia.* 11:211-216.

Engin, K., D.B. Leeper, A.J. Thistlethwaite, L. Tupchong, and J.D. McFarlane. 1994. Tumor extracellular pH as a prognostic factor in thermoradiotherapy. *Int. J. Radiat. Oncol. Biol. Phys.* 29:125-132.

Epstein, A.C., J.M. Gleadle, L.A. McNeill, K.S. Hewitson, J. O'Rourke, D.R. Mole, M. Mukherji, E. Metzen, M.I. Wilson, A. Dhanda, Y.M. Tian, N. Masson, D.L. Hamilton, P. Jaakkola, R. Barstead, J. Hodgkin, P.H. Maxwell, C.W. Pugh, C.J. Schofield, and P.J. Ratcliffe. 2001. C. elegans EGL-9 and mammalian homologs define a family of dioxygenases that regulate HIF by prolyl hydroxylation. *Cell.* 107:43-54.

Falkowski, P.G. 2006. Evolution. Tracing oxygen's imprint on earth's metabolic evolution. *Science.* 311:1724-1725.

Giaccia, A.J., M.C. Simon, and R. Johnson. 2004. The biology of hypoxia: the role of oxygen sensing in development, normal function, and disease. *Genes Dev.* 18:2183-2194.

Giffard, R.G., H. Monyer, C.W. Christine, and D.W. Choi. 1990. Acidosis reduces NMDA receptor activation, glutamate neurotoxicity, and oxygen-glucose deprivation neuronal injury in cortical cultures. *Brain Res.* 506:339-342.

Gladden, L.B. 2001. Lactic acid: New roles in a new millennium. *Proc. Natl. Acad. Sci. USA.* 98:395-397.

Gladden, L.B. 2004. Lactate metabolism: a new paradigm for the third millennium. *J. Physiol.* 558:5.

Grandori, C., N. Gomez-Roman, Z.A. Felton-Edkins, C. Ngouenet, D.A. Galloway, R.N. Eisenman, and R.J. White. 2005. c-Myc binds to human ribosomal DNA and stimulates transcription of rRNA genes by RNA polymerase I. *Nat. Cell Biol.* 7:311-318.

Grewal, S.I., and D. Moazed. 2003. Heterochromatin and epigenetic control of gene expression. *Science*. 301:798-802.

Groulx, I., M.E. Bonicalzi, and S. Lee. 2000. Ran-mediated nuclear export of the von Hippel-Lindau tumor suppressor protein occurs independently of its assembly with cullin-2. *J. Biol. Chem.* 275:8991-9000.

Groulx, I., and S. Lee. 2002. Oxygen-dependent ubiquitination and degradation of hypoxia-inducible factor requires nuclear-cytoplasmic trafficking of the von Hippel-Lindau tumor suppressor protein. *Mol. Cell. Biol.* 22:5319.

Grummt, I., and C.S. Pikaard. 2003. Epigenetic silencing of RNA polymerase I transcription. *Nat. Rev. Mol. Cell Biol.* 4:641-649.

Gunaratnam, L., M. Morley, A. Franovic, N. de Paulsen, K. Mekhail, D.A. Parolin, E. Nakamura, I.A. Lorimer, and S. Lee. 2003. Hypoxia inducible factor activates the transforming growth factor-alpha/epidermal growth factor receptor growth stimulatory pathway in VHL (-/-) renal cell carcinoma cells. *J. Biol. Chem.* 278:44966-44974.

Guzy, R.D., B. Hoyos, E. Robin, H. Chen, L. Liu, K.D. Mansfield, M.C. Simon, U. Hammerling, and P.T. Schumacker. 2005. Mitochondrial complex III is required for hypoxia-induced ROS production and cellular oxygen sensing. *Cell Metab.* 1:401-408.

Harris, A.L. 2002. Hypoxia: a key regulatory factor in tumour growth. *Nat. Rev. Cancer.* 2:38-47.

Holzel, M., M. Rohrmoser, M. Schlee, T. Grimm, T. Harasim, A. Malamoussi, A. Gruber-Eber, E. Kremmer, W. Hiddemann, G.W. Bornkamm, and D. Eick. 2005. Mammalian WDR12 is a novel member of the Pes1-Bop1 complex and is required for ribosome biogenesis and cell proliferation. *J. Cell Biol.* 170:367-378.

Hoogstraten, D., A.L. Nigg, H. Heath, L.H. Mullenders, R. van Driel, J.H. Hoeijmakers, W. Vermeulen, and A.B. Houtsmuller. 2002. Rapid switching of TFIIH between RNA polymerase I and II transcription and DNA repair in vivo. *Mol. Cell.* 10:1163-1174.

Iliopoulos, O., A. Kibel, S. Gray, and W.G. Kaelin, Jr. 1995. Tumour suppression by the human von Hippel-Lindau gene product. *Nat. Med.* 1:822-826.

Ivan, M., K. Kondo, H. Yang, W. Kim, J. Valiando, M. Ohh, A. Salic, J.M. Asara, W.S. Lane, and W.G. Kaelin, Jr. 2001. HIFalpha targeted for VHL-mediated destruction by proline hydroxylation: implications for O2 sensing. *Science.* 292:464-468.

Iwai, K., K. Yamanaka, T. Kamura, N. Minato, R.C. Conaway, J.W. Conaway, R.D. Klausner, and A. Pause. 1999. Identification of the von Hippel-lindau tumor-

suppressor protein as part of an active E3 ubiquitin ligase complex. *Proc. Natl. Acad. Sci. USA*. 96:12436-12441.

Iyer, N.V., L.E. Kotch, F. Agani, S.W. Leung, E. Laughner, R.H. Wenger, M. Gassmann, J.D. Gearhart, A.M. Lawler, A.Y. Yu, and G.L. Semenza. 1998. Cellular and developmental control of O2 homeostasis by hypoxia-inducible factor 1 alpha. *Genes Dev.* 12:149-162.

Jaakkola, P., D.R. Mole, Y.M. Tian, M.I. Wilson, J. Gielbert, S.J. Gaskell, A. Kriegsheim, H.F. Hebestreit, M. Mukherji, C.J. Schofield, P.H. Maxwell, C.W. Pugh, and P.J. Ratcliffe. 2001. Targeting of HIF-alpha to the von Hippel-Lindau ubiquitylation complex by O2-regulated prolyl hydroxylation. *Science*. 292:468-472.

Kaelin, W.G., Jr. 2002. Molecular basis of the VHL hereditary cancer syndrome. *Nat. Rev. Cancer*. 2:673-682.

Kaelin, W.G., Jr. 2005. ROS: really involved in oxygen sensing. *Cell Metab.* 1:357-358.

Kaku, D.A., R.G. Giffard, and D.W. Choi. 1993. Neuroprotective effects of glutamate antagonists and extracellular acidity. *Science*. 260:1516-1518.

Kamura, T., S. Sato, K. Iwai, M. Czyzyk-Krzeska, R.C. Conaway, and J.W. Conaway. 2000. Activation of HIF1alpha ubiquitination by a reconstituted von Hippel-Lindau (VHL) tumor suppressor complex. *Proc. Natl. Acad. Sci. USA*. 97:10430-10435.

Kibel, A., O. Iliopoulos, J.A. DeCaprio, and W.G. Kaelin, Jr. 1995. Binding of the von Hippel-Lindau tumor suppressor protein to Elongin B and C. *Science*. 269:1444-1446.

Kim, J.W., I. Tchernyshyov, G.L. Semenza, and C.V. Dang. 2006. HIF-1-mediated expression of pyruvate dehydrogenase kinase: a metabolic switch required for cellular adaptation to hypoxia. *Cell Metab.* 3:177-185.

Kim, M.S., H.J. Kwon, Y.M. Lee, J.H. Baek, J.E. Jang, S.W. Lee, E.J. Moon, H.S. Kim, S.K. Lee, H.Y. Chung, C.W. Kim, and K.W. Kim. 2001. Histone deacetylases induce angiogenesis by negative regulation of tumor suppressor genes. *Nat. Med.* 7:437-443.

Kondo, K., J. Klco, E. Nakamura, M. Lechpammer, and W.G. Kaelin, Jr. 2002. Inhibition of HIF is necessary for tumor suppression by the von Hippel-Lindau protein. *Cancer Cell*. 1:237-246.

Kuznetsov, A.V., M. Janakiraman, R. Margreiter, and J. Troppmair. 2004. Regulating cell survival by controlling cellular energy production: novel functions for ancient signaling pathways? *FEBS Lett.* 577:1-4.

Lee, S., M. Neumann, R. Stearman, R. Stauber, A. Pause, G.N. Pavlakis, and R.D. Klausner. 1999. Transcription-dependent nuclear-cytoplasmic trafficking is required for the function of the von Hippel-Lindau tumor suppressor protein. *Mol. Cell. Biol.* 19:1486.

Li, J., R. Santoro, K. Koberna, and I. Grummt. 2005. The chromatin remodeling complex NoRC controls replication timing of rRNA genes. *EMBO J.* 24:120-127.

Lippincott-Schwartz, J., N. Altan-Bonnet, and G.H. Patterson. 2003. Photobleaching and photoactivation: following protein dynamics in living cells. *Nat. Cell Biol.* Suppl:S7-14.

Lisztwan, J., G. Imbert, C. Wirbelauer, M. Gstaiger, and W. Krek. 1999. The von Hippel-Lindau tumor suppressor protein is a component of an E3 ubiquitin-protein ligase activity. *Genes Dev.* 13:1822-1833.

Liu, L., T.P. Cash, R.G. Jones, B. Keith, C.B. Thompson, and M.C. Simon. 2006. Hypoxia-induced energy stress regulates mRNA translation and cell growth. *Mol. Cell.* 21:521-531.

Lonergan, K.M., O. Iliopoulos, M. Ohh, T. Kamura, R.C. Conaway, J.W. Conaway, and W.G. Kaelin, Jr. 1998. Regulation of hypoxia-inducible mRNAs by the von Hippel-Lindau tumor suppressor protein requires binding to complexes containing elongins B/C and Cul2. *Mol. Cell. Biol.* 18:732-741.

Maemura, K., C.M. Hsieh, M.K. Jain, S. Fukumoto, M.D. Layne, Y. Liu, S. Kourembanas, S.F. Yet, M.A. Perrella, and M.E. Lee. 1999. Generation of a dominant-negative mutant of endothelial PAS domain protein 1 by deletion of a potent C-terminal transactivation domain. *J. Biol. Chem.* 274:31565-31570.

Mais, C., J.E. Wright, J.L. Prieto, S.L. Raggett, and B. McStay. 2005. UBF-binding site arrays form pseudo-NORs and sequester the RNA polymerase I transcription machinery. *Genes Dev.* 19:50.

Mansfield, K.D., R.D. Guzy, Y. Pan, R.M. Young, T.P. Cash, P.T. Schumacker, and M.C. Simon. 2005. Mitochondrial dysfunction resulting from loss of cytochrome

c impairs cellular oxygen sensing and hypoxic HIF-alpha activation. *Cell Metab.* 1:393-399.

Maxwell, P.H., M.S. Wiesener, G.W. Chang, S.C. Clifford, E.C. Vaux, M.E. Cockman, C.C. Wykoff, C.W. Pugh, E.R. Maher, and P.J. Ratcliffe. 1999. The tumour suppressor protein VHL targets hypoxia-inducible factors for oxygen-dependent proteolysis. *Nature*. 399:271-275.

Mayer, C., K.M. Schmitz, J. Li, I. Grummt, and R. Santoro. 2006. Intergenic transcripts regulate the epigenetic state of rRNA genes. *Mol. Cell*. 22:351-361.

Mekhail, K., L. Gunaratnam, M.E. Bonicalzi, and S. Lee. 2004a. HIF activation by pH-dependent nucleolar sequestration of VHL. *Nat. Cell Biol.* 6:642-647.

Mekhail, K., M. Khacho, A. Carrigan, R.R. Hache, L. Gunaratnam, and S. Lee. 2005. Regulation of ubiquitin ligase dynamics by the nucleolus. *J. Cell Biol.* 170:733-744.

Mekhail, K., M. Khacho, L. Gunaratnam, and S. Lee. 2004b. Oxygen sensing by H+: implications for HIF and hypoxic cell memory. *Cell Cycle*. 3:1027-1029.

Meshorer, E., D. Yellajoshula, E. George, P.J. Scambler, D.T. Brown, and T. Misteli. 2006. Hyperdynamic plasticity of chromatin proteins in pluripotent embryonic stem cells. *Dev. Cell*. 10:105-116.

Moazed, D., A.D. Rudner, J. Huang, G.J. Hoppe, and J.C. Tanny. 2004. A model for step-wise assembly of heterochromatin in yeast. *Novartis Found Symp*. 259:48-56; discussion 56-62, 163-169.

Morimoto, Y., O. Kemmotsu, and E.S. Alojado. 1997. Extracellular acidosis delays cell death against glucose-oxygen deprivation in neuroblastoma x glioma hybrid cells. *Crit. Care Med.* 25:841.

Nielsen, O.B., F. de Paoli, and K. Overgaard. 2001. Protective effects of lactic acid on force production in rat skeletal muscle. *J. Physiol.* 536:161-166.

Obach, M., A. Navarro-Sabate, J. Caro, X. Kong, J. Duran, M. Gomez, J.C. Perales, F. Ventura, J.L. Rosa, and R. Bartrons. 2004. 6-Phosphofructo-2-kinase (pfkfb3) gene promoter contains hypoxia-inducible factor-1 binding sites necessary for transactivation in response to hypoxia. *J. Biol. Chem.* 279:53562-53570.

Ohh, M., C.W. Park, M. Ivan, M.A. Hoffman, T.Y. Kim, L.E. Huang, N. Pavletich, V. Chau, and W.G. Kaelin. 2000. Ubiquitination of hypoxia-inducible factor requires direct binding to the beta-domain of the von Hippel-Lindau protein. *Nat. Cell Biol.* 2:423-427.

Olson, M.O. 2004. Sensing cellular stress: another new function for the nucleolus? *Sci. S.T.K.E.* 2004:pe10.

Olson, M.O., and M. Dundr. 2005. The moving parts of the nucleolus. *Histochem. Cell Biol.* 123:203-216.

Page, E.L., G.A. Robitaille, J. Pouyssegur, and D.E. Richard. 2002. Induction of hypoxia-inducible factor-1alpha by transcriptional and translational mechanisms. *J. Biol. Chem.* 277:48403-48409.

Papandreou, I., R.A. Cairns, L. Fontana, A.L. Lim, and N.C. Denko. 2006. HIF-1 mediates adaptation to hypoxia by actively downregulating mitochondrial oxygen consumption. *Cell Metab.* 3:187-197.

Pasteur, L. 1857. Mémoire sur la fermentation appellée lactique. *Comptes rendus de l'Académie des Sciences à Paris*. 45:913.

Pause, A., S. Lee, R.A. Worrell, D.Y. Chen, W.H. Burgess, W.M. Linehan, and R.D. Klausner. 1997. The von Hippel-Lindau tumor-suppressor gene product forms a stable complex with human CUL-2, a member of the Cdc53 family of proteins. *Proc. Natl. Acad. Sci. USA*. 94:2156-2161.

Pause, A., B. Peterson, G. Schaffar, R. Stearman, and R.D. Klausner. 1999. Studying interactions of four proteins in the yeast two-hybrid system: structural resemblance of the pVHL/elongin BC/hCUL-2 complex with the ubiquitin ligase complex SKP1/cullin/F-box protein. *Proc. Natl. Acad. Sci. USA*. 96:9533-9538.

Penttila, A., and B.F. Trump. 1974. Extracellular acidosis protects Ehrlich ascites tumor cells and rat renal cortex against anoxic injury. *Science*. 185:277-278.

Reeder, R.H. 1984. Enhancers and ribosomal gene spacers. *Cell*. 38:349.

Richard, D.E., E. Berra, and J. Pouyssegur. 2000. Nonhypoxic pathway mediates the induction of hypoxia-inducible factor 1alpha in vascular smooth muscle cells. *J. Biol. Chem.* 275:26765-26771.

Schmidt, E.V. 1999. The role of c-myc in cellular growth control. *Oncogene*. 18:2988-2996.

Seagroves, T.N., H.E. Ryan, H. Lu, B.G. Wouters, M. Knapp, P. Thibault, K. Laderoute, and R.S. Johnson. 2001. Transcription factor HIF-1 is a necessary mediator of the pasteur effect in mammalian cells. *Mol. Cell. Biol.* 21:3436-3444.

Semenza, G.L. 1998. Hypoxia-inducible factor 1: master regulator of O2 homeostasis. *Curr. Opin. Genet. Dev.* 8:588-594.

Semenza, G.L., P.H. Roth, H.M. Fang, and G.L. Wang. 1994. Transcriptional regulation of genes encoding glycolytic enzymes by hypoxia-inducible factor 1. *J. Biol. Chem.* 269:23757-23763.

Simon, M.C. 2006. Coming up for air: HIF-1 and mitochondrial oxygen consumption. *Cell Metab.* 3:150-151.

Sinclair, D.A., and L. Guarente. 1997. Extrachromosomal rDNA circles: a cause of aging in yeast. *Cell.* 91:1033-1042.

Sinclair, D.A., K. Mills, and L. Guarente. 1997. Accelerated aging and nucleolar fragmentation in yeast sgs1 mutants. *Science.* 277:1313-1316.

Smith, K., L. Gunaratnam, M. Morley, A. Franovic, K. Mekhail, and S. Lee. 2005. Silencing of epidermal growth factor receptor suppresses hypoxia-inducible factor-2-driven VHL-/- renal cancer. *Cancer Res.* 65:5221-5230.

Sporbert, A., A. Gahl, R. Ankerhold, H. Leonhardt, and M.C. Cardoso. 2002. DNA polymerase clamp shows little turnover at established replication sites but sequential de novo assembly at adjacent origin clusters. *Mol. Cell.* 10:1355-1365.

Straight, A.F., W. Shou, G.J. Dowd, C.W. Turck, R.J. Deshaies, A.D. Johnson, and D. Moazed. 1999. Net1, a Sir2-associated nucleolar protein required for rDNA silencing and nucleolar integrity. *Cell.* 97:245-256.

Tanimoto, K., Y. Makino, T. Pereira, and L. Poellinger. 2000. Mechanism of regulation of the hypoxia-inducible factor-1 alpha by the von Hippel-Lindau tumor suppressor protein. *EMBO J.* 19:4298-4309.

Thiry, M., T. Cheutin, M.F. O'Donohue, H. Kaplan, and D. Ploton. 2000. Dynamics and three-dimensional localization of ribosomal RNA within the nucleolus. *RNA.* 6:1750-1761.

Thiry, M., and D.L. Lafontaine. 2005. Birth of a nucleolus: the evolution of nucleolar compartments. *Trends Cell Biol.* 15:194-199.

Thomas, G. 2000. An encore for ribosome biogenesis in the control of cell proliferation. *Nat. Cell Biol.* 2:E71-72.

Weber, J.D., L.J. Taylor, M.F. Roussel, C.J. Sherr, and D. Bar-Sagi. 1999. Nucleolar Arf sequesters Mdm2 and activates p53. *Nat. Cell Biol.* 1:20-26.

Wike-Hooley, J.L., J. Haveman, and H.S. Reinhold. 1984. The relevance of tumour pH to the treatment of malignant disease. *Radiother. Oncol.* 2:343-366.

Winter, A.G., G. Sourvinos, S.J. Allison, K. Tosh, P.H. Scott, D.A. Spandidos, and R.J. White. 2000. RNA polymerase III transcription factor TFIIIC2 is overexpressed in ovarian tumors. *Proc. Natl. Acad. Sci. USA.* 97:12619-12624.

Yamamoto, K., M. Yamamoto, K. Hanada, Y. Nogi, T. Matsuyama, and M. Muramatsu. 2004. Multiple protein-protein interactions by RNA polymerase I-associated

factor PAF49 and role of PAF49 in rRNA transcription. *Mol. Cell. Biol.* 24:6338-6349.

Yu, F., S.B. White, Q. Zhao, and F.S. Lee. 2001. HIF-1alpha binding to VHL is regulated by stimulus-sensitive proline hydroxylation. *Proc. Natl. Acad. Sci. USA*. 98:9630-9635.

Chapter 5. General Discussion

Chapter 5. General Discussion

5.1. Role of nucleolar targeting of VHL in basic metabolism

Hypoxia and acidosis occur under various physiological and pathological settings. We initially found that acidosis-dependent nucleolar sequestration of VHL activates HIF to remodel gene expression independent of oxygen levels (Mekhail et al., 2004a; Mekhail et al., 2004b). This led us to uncover that the nucleolar architecture reversibly converts ubiquitin ligases such as VHL and MDM2 to a static state in response to regulatory cues that are associated with their respective substrates HIF and p53 (Mekhail et al., 2005). Surprisingly, H^+-dependent nucleolar localization of VHL silences rDNA to restrict ribosomal biogenesis, the most energy-demanding cellular process, thereby preserving cellular energy equilibrium and viability under hypoxia. Taken together, our findings suggest that hydrogen ions play a central role in modulating basic metabolism and gene expression in the cell by utilizing the subnuclear architecture to shuffle proteins between different molecular networks.

5.2. Nuclear compartmentalization sharpens signaling

Genes implicated in similar processes, even if spread out across linear genomes, are often united in nuclear space. Up to hundreds and thousands of rRNA genes undergo such packaging in mammalian and plant nuclei through a process requiring RNAPI activity, respectively. Yeast tRNA genes, though dispersed in the linear genome, colocalize with the small nucleolar RNA (snoRNA) U14 at the nucleolus (Thompson et al., 2003). Furthermore, inactivation of the promoter at a single tRNA locus abolishes its nucleolar

association (Thompson et al., 2003). It is believed that three-dimensional clustering of similar genes increases the efficiency and accuracy of transcriptional regulation. For example, this allows cells to concentrate regulatory macromolecules such as transcription and processing factors close to the three-dimensional coordinates of these genes ensuring efficient responses to signaling cues. Thus, the repetitive nature and clustering of rRNA genes likely contributes to the efficient translation of increases in the environmental concentration of H^+ into HIF activation and ribosomal restriction.

5.3. Static detention as a general signaling mechanism for the functional regulation of macromolecules

We share a view of the nucleolus as a hub that ensures cellular adaptation to alterations in environmental parameters (Andersen et al., 2005; Olson, 2004). In addition to excluding VHL from certain molecular networks targeting HIF for degradation (Mekhail et al., 2005), static nucleolar detention introduces VHL into a network that silences rDNA. We propose that various signals can reorganize molecular networks by reversibly switching their participants between dynamic and static states. Such processes may involve several nuclear compartments and chromatin-based domains, other than the nucleolus. It was indeed observed that several molecules were trapped in condensed, uncharacterized chromatin regions outside the nucleolus after pharmacologically-induced energy starvation (Shav-Tal et al., 2004a; Shav-Tal et al., 2004b). Other studies revealed that the replication factor PCNA moves rapidly through the nucleus but resides for several minutes in replication foci during S phase (Sporbert et al., 2002) and that the transcription and repair factor TFIIH undergoes diffusional motion when not engaged, but becomes

temporarily immobilized at RNA polymerase I and II transcription sites upon induction of DNA damage (Hoogstraten et al., 2002). It is tempting to speculate that at least some of these settings implicate molecular interactions representing "symbiotic relationships", similar to that of VHL with rDNA, where chromatin is modulated by statically detained proteins, which in turn abandon dynamic functions in other molecular networks. Thus, signaling cues rely on different chromatin domains to efficiently shuffle macromolecules between various molecular networks.

5.4. Possible functions for VHL in the nucleolus

While large dextran molecules have easier access to "open" DNA (Gorisch et al., 2005), large macromolecular complexes of several hundred kilo Daltons still have access to even highly condensed chromatin regions (Verschure et al., 2003). A VHL mutant that fails to assemble the VBC/Cul-2 complex but retains nucleolar targeting capacity fails to silence rDNA and preserve energy equilibrium suggesting that targeting of the VBC/Cul-2 ubiquitin ligase complex for static nucleolar detention might contribute to VHL's role in the transcriptional regulation of rRNA genes (Mekhail et al., 2005). The CUL4-DDB-ROC1 ligase complex ubiquitylates histones H3 and H4 weakening their interaction with DNA to facilitate the recruitment of repair proteins to damaged regions of the genetic code (Wang et al., 2006). Several scenarios for the role of the VBC/Cul-2 complex in the nucleolus can be formulated. For example, it is possible that VBC/Cul-2 employs a dominant negative strategy with complexes such as CUL4-DDB-ROC1 or that VBC/Cul-2 ubiquitylates and inactivates euchromatin-sustaining factors to promote rDNA heterochromatinization. It is also possible that sequestration of VBC/Cul-2 prevents it from ubiquitylating an unidentified substrate or inhibits the function of various members

of the complex outside the nucleolus. For example, Cul-2 is required for normal progression through the cell cycle (Feng et al., 1999) and it is possible that its transient nucleolar sequestration could temporarily halt progression through the cell cycle until energy and ribosome levels are restored.

5.5. Nucleolar evolution and regulation of rDNA transcription

In evolution, it is clear that the size of IGS underwent a disproportionate expansion relative to that of rRNA transcriptional units (Thiry and Lafontaine, 2005). While the role of IGS in the regulation of RNAPI-mediated transcription was first recognized around the 1970s and 1980s (Reeder, 1984; Reeder et al., 1983), details of its mode of action are only starting to emerge. For example, interactions between the RNAPI transcriptional machinery and key DNA repeats dispersed across the entire IGS are crucial for optimal transcription of rRNA loci (Mais et al., 2005). In addition, recently identified non-protein-coding IGS transcripts are required for the establishment and maintenance of specific heterochromatic configurations at the promoter of a subset of rDNA arrays (Mayer et al., 2006). Whether evolutionary expansion in IGS size contributed to the evolution of the pH-dependent rDNA silencing program described here and whether ethanol fermentation activates similar mechanisms in different species or phyla is of considerable interest but remains to be determined. Interestingly, we found that VHL interacts with IGS at regions containing repeats believed to act as enhancers for RNAPI-dependent transcription (Mais et al., 2005). A possible role for nucleolar VHL in rDNA silencing could consist of inactivating such sequences by chemical modification or, more likely, by preventing their interactions with regulatory molecules. Unlike acidosis, several previously identified rDNA silencing signals result in nucleolar

disintegration, a phenomenon that is believed to be caused by the complete loss of RNAPI activity and is associated with decreased viability (Sinclair and Guarente, 1997; Sinclair et al., 1997). Acidosis might preserve nucleolar integrity by only decreasing rather than abolishing rDNA transcription or by actively stabilizing the nucleolar architecture. In fact, temperature-dependent targeting of heat shock proteins (HSPs) such as HSP40 and HSP70 to the nucleolus has been proposed to preserve the integrity of this major nuclear subcompartment under stress (Hattori et al., 1993).

Only a subpopulation of rRNA genes is active at any given time in the cell (Grummt and Pikaard, 2003). pH levels could be modulating rDNA transcription through two different approaches that are not necessarily mutually exclusive. Cells can control the number of transcripts that are made from each gene. Alternatively, as there are hundreds of rRNA genes, another strategy would be to turn subsets of the rRNA gene pool either "on" or "off". Since both mechanisms could be rapid and efficient, we still cannot favor one over the other (Grummt and Pikaard, 2003). Identification of the strategy employed by acidosis could also shed light on the mechanisms by which VHL proteins find their binding sites in the nucleolus.

5.6. Nucleolar localization and detention of VHL

Unpublished data generated in our lab through saturated mutagenesis analysis revealed that the cooperation of several three-residue hydrophobic amino-acid repeats with two arginine-rich domains targets VHL for static nucleolar detention. Removal of some of these hydrophobic repeats decreased the fraction of the VHL protein pool that is statically detained by the nucleolar architecture. This could be reflective of a varied abundance of nucleolar binding sites for different sets of hydrophobic repeats. For example, there

could be three times as much nucleolar sites recognizing leucine-leucine-valine (LLV) repeats than those binding leucine-tryptophan-leucine (LWL). In a less likely scenario, this could suggest that all these hydrophobic repeats recognize the same type of binding site, which exhibits slight differences across the rDNA lattice. Different scenarios could be envisioned for the nature of biochemical interactions mediating static nucleolar detention. Since all hydrophobic repeats cluster on the surface of the VHL protein, this could create a "hydrophobic trap" that might be sustained by interactions with other macromolecules to cause condensation of the chromatin structure, thereby keeping VHL captive in a highly condensed nucleolar mesh. Another way could simply include the enzymatic formation of biochemical bonds between VHL and the rDNA lattice. It is also intriguing to speculate about the possible approach utilized by VHL to physically locate its binding sites on the nucleolar chromatin lattice. Homing of DNA interacting proteins can be classified in three categories: stochastic, hopping, and sliding. A recent study investigating the dynamics of restriction enzymes demonstrated that sliding mechanisms are implicated only if the different binding sites are separated by distances of 30 nucleotides or less (Gowers et al., 2005). Considering the large distances between intergenic spacers on the rDNA lattice, it is reasonable to suggest that random or hopping mechanisms are implicated in the processes allowing VHL to mediate pH-dependent rDNA silencing. Sliding might still occur within a given spacer. In addition, considering the rapid nature of nucleolar targeting of VHL, it is possible that the tumor suppressor is subject to a nucleation effect where having a single VHL protein bound to rDNA facilitates the recruitment of other VHL molecules. VHL relies on the basic elongation factor EF1A to exit the nucleus (Khacho et al., 2006). Ribosomal/growth stress induces

the interaction of zinc finger protein 1 (ZPR1) with EF1A and the targeting of the dimer to the nucleolus (Galcheva-Gargova et al., 1998; Gangwani et al., 1998). It is possible that ZPR1, EF1A or other nucleolar proteins are implicated in pH-dependent nucleolar localization of VHL, but this remains to be determined.

5.7. H^+-driven molecular network remodeling by the nucleolus

We propose a model where dynamic and overlapping molecular networks are built on complex interactions between mobile and relatively static participants. According to this model, modulation of these interactions through regulation of the dynamic state of the participants alters the output of the networks. Interaction between VHL and the functional nuclear pore architecture is required for nuclear export and subsequent degradation of its substrate HIFα (Figure 5.1A) (Groulx and Lee, 2002; Lee et al., 1999). While constituents of the nuclear pore can move between subcellular compartments, functional pore architecture is confined to the nuclear envelope and persists for long periods of time within well-defined spatial regions (Rabut et al., 2004). Therefore, H^+ eliminates the physical interaction between an immobile (nuclear pore) and a mobile (VHL) participant by immobilizing the latter at a different spatial coordinate (nucleolus) (Figure 5.1B). This inactivates the HIF-regulatory E3 network and triggers a specific gene expression signature. However, the cell is a large and intricate agglomerate of intersecting molecular networks. While H^+ promotes the removal of VHL from the HIF-regulatory network, our data also suggest that static detention of VHL allows it to assume a new role in molecular networks mediating rDNA silencing (Figure 5.1, A to C). It is interesting to note that since HIF promotes extracellular acidification, inactivation of the

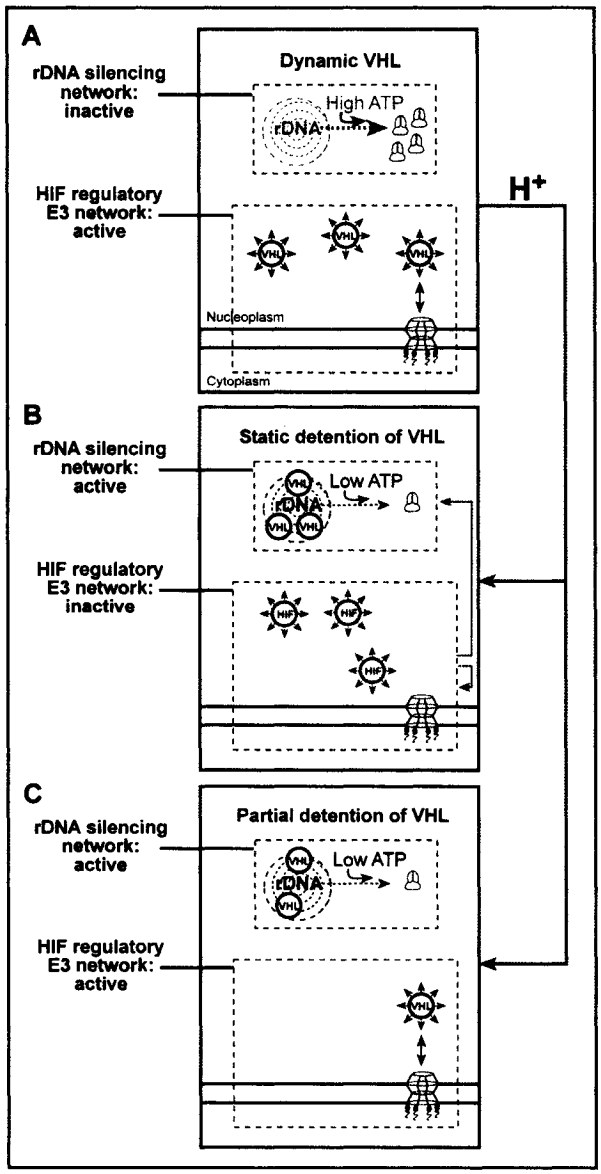
A
rDNA silencing network: inactive
Dynamic VHL
High ATP
rDNA
HIF regulatory E3 network: active
VHL
H+
Nucleoplasm
Cytoplasm
B
rDNA silencing network: active
Static detention of VHL
Low ATP
rDNA
HIF regulatory E3 network: inactive
HIF
C
rDNA silencing network: active
Partial detention of VHL
Low ATP
rDNA
HIF regulatory E3 network: active
VHL

Figure 5.1

Figure 5.1. H^+-driven remodeling of molecular networks by the nucleolar architecture. Interactions such as those between VHL and the relatively immobile nuclear pore architecture at the nuclear envelope ensure the activation of HIF-regulatory networks targeting the transcription factor for degradation (A). H^+ triggers static detention of VHL by the nucleolar architecture (blue arrows). While partial detention of VHL is sufficient to allow it to participate in a molecular network that restricts ribosomal biogenesis at the level of rDNA transcription, complete static detention of the protein within the nucleolar space is required for inactivation of the HIF-regulatory E3 network (B and C). It is still unclear if VHL mediates rDNA silencing by acting as an ubiquitin ligase or by assuming a new molecular role (see discussion for possible functions). Note that since HIF promotes extracellular acidification, inactivation of the HIF-regulatory E3 network through acidosis, hypoxia or other routes, further promotes both HIF activation and rDNA silencing (5B, green arrows).

HIF-regulatory E3 network through acidosis, hypoxia or other routes, further promotes both HIF activation and rDNA silencing (Figure 5B, green arrows).

5.8. Future Directions

Short term. Database searches allowed us to identify over a hundred proteins each harboring a number of key three-residue hydrophobic repeats (mostly LΨV, where Ψ symbolizes a various hydrophobic repeats) and at least one arginine-rich domain. This list includes a number of heat shock proteins that display steady-state cytoplasmic distribution under standard growth conditions (Bukau and Horwich, 1998). While the ATP-dependent chaperones HSP40, HSP60 and HSP70 were on the list as they contained several hydrophobic repeats, the ATP-independent chaperone HSP110 was not as it did not contain any characteristic hydrophobic repeats (Easton et al., 2000). Unpublished work conducted by Luis Rivero-Lopez in our lab demonstrated that HSP40, HSP60 and HSP70 are targeted for static detention by the nucleolar architecture under acidosis but that the steady state distribution of HSP110 is insensitive to fluctuations in pH. The working hypothesis is that anaerobic metabolism utilizes H^+ to remodel the heat shock molecular network by inactivating the high-energy-consuming chaperones HSP40, HSP60 and HSP70 and relying on the most energy-efficient chaperone HSP110. Although this awaits further characterization, saturation of HSP60 nucleolar binding sites decreases cellular viability. However, these data provide strong support for the hypothesis set forth by our group (Mekhail et al., 2005) and stating that cells have evolved a mechanism to regulate molecular networks by reversibly switching proteins

between a mobile and static state. More importantly, this suggests that nucleolar sequestration of macromolecules is a general process of functional protein regulation.

GFP-tagged and endogenous VHL localized in nucleoli of cells located closer to the core of *in vitro* tumors grown by the spheroid method and glioblastoma tumors grown in the flanks of nude mice, respectively (Mekhail et al., 2004a; Mekhail et al., 2006). Current and future experiments are investigating the effect of silencing VHL expression, or competing with VHL for nucleolar sequestration using a dominant negative approach, on tumor development.

Long term. We plan to (1) investigate the nature of interactions between rDNA sequences and VHL and signals that trigger them, (2) identify molecules that target VHL to the nucleolus and/or assist it in mediating transcriptional silencing, and (3) identify, if any, potential pH-dependent post-translational modifications of VHL. It will also be important to study how cells sense changes in environmental hydrogen ion concentrations and the contribution of VHL to the protective effect of acidosis within *in vivo* models of ischemic attacks such as strokes induced in mice following middle cerebral artery occlusion.

5.9. Conclusions and "pHarewell"

Here, we demonstrate that cells have evolved homeostatic mechanisms that regulate complex molecular networks by reversibly switching proteins between dynamics and static states. More specifically, this work reveals a central role for H^+ in changing the pool of genes expressed in cells experiencing environmental changes. This role of H^+ allows cells to adapt to alterations in external parameters. Our work also provides a

potential explanation for why the prognostic effects of H^+ are positive in clinical settings such as strokes and heart attacks but are negative in cancer progression.

Appendix A – References (Complete List)

Abney, J.R., B. Cutler, M.L. Fillbach, D. Axelrod, and B.A. Scalettar. 1997. Chromatin dynamics in interphase nuclei and its implications for nuclear structure. *J. Cell Biol.* 137:1459-1468.

Allen, D., and H. Westerblad. 2004. Lactic acid: The latest performance-enhancing drug. *Science*. 305:1112-1113.

Andersen, J.S., Y.W. Lam, A.K. Leung, S.E. Ong, C.E. Lyon, A.I. Lamond, and M. Mann. 2005. Nucleolar proteome dynamics. *Nature*. 433:77-83.

Appella, E., and C.W. Anderson. 2001. Post-translational modifications and activation of p53 by genotoxic stresses. *Eur. J. Biochem.* 268:2764-2772.

Arany, Z., L.E. Huang, R. Eckner, S. Bhattacharya, C. Jiang, M.A. Goldberg, H.F. Bunn, and D.M. Livingston. 1996. An essential role for p300/CBP in the cellular response to hypoxia. *Proc Natl Acad Sci U S A*. 93:12969-12973.

Azzam, R., S.L. Chen, W. Shou, A.S. Mah, G. Alexandru, K. Nasmyth, R.S. Annan, S.A. Carr, and R.J. Deshaies. 2004. Phosphorylation by cyclin B-Cdk underlies release of mitotic exit activator Cdc14 from the nucleolus. *Science*. 305:516-519.

Bachant, J.B., and S.J. Elledge. 1999. Mitotic treasures in the nucleolus. *Nature*. 398:757-758.

Bachmair, A., and A. Varshavsky. 1989. The degradation signal in a short-lived protein. *Cell*. 56:1019-1032.

Barker, J., M.A. Khan, and T. Solomos. 1966. Mechanism of the Pasteur effect. *Nature*. 211:547-548.

Beck, I., S. Ramirez, R. Weinmann, and J. Caro. 1991. Enhancer element at the 3'-flanking region controls transcriptional response to hypoxia in the human erythropoietin gene. *J Biol Chem.* 266:15563-15566.

Bernardi, R., P.P. Scaglioni, S. Bergmann, H.F. Horn, K.H. Vousden, and P.P. Pandolfi. 2004. PML regulates p53 stability by sequestering Mdm2 to the nucleolus. *Nat Cell Biol.* 6:665-672.

Bing, O.H., W.W. Brooks, and J.V. Messer. 1973. Heart muscle viability following hypoxia: protective effect of acidosis. *Science.* 180:1297-1298.

Blanchard, K.L., A.M. Acquaviva, D.L. Galson, and H.F. Bunn. 1992. Hypoxic induction of the human erythropoietin gene: cooperation between the promoter and enhancer, each of which contains steroid receptor response elements. *Mol Cell Biol.* 12:5373-5385.

Blankenship, C., J.G. Naglich, J.M. Whaley, B. Seizinger, and N. Kley. 1999. Alternate choice of initiation codon produces a biologically active product of the von Hippel Lindau gene with tumor suppressor activity. *Oncogene.* 18:1529-1535.

Bonicalzi, M.E., I. Groulx, N. de Paulsen, and S. Lee. 2001. Role of exon 2-encoded beta -domain of the von Hippel-Lindau tumor suppressor protein. *J. Biol. Chem.* 276:1407.

Bracken, C.P., M.L. Whitelaw, and D.J. Peet. 2005. Activity of hypoxia-inducible factor 2alpha is regulated by association with the NF-kappaB essential modulator. *J Biol Chem.* 280:14240-14251.

Bruick, R.K., and S.L. McKnight. 2001. A conserved family of prolyl-4-hydroxylases that modify HIF. *Science.* 294:1337-1340.

Brunelle, J.K., E.L. Bell, N.M. Quesada, K. Vercauteren, V. Tiranti, M. Zeviani, R.C. Scarpulla, and N.S. Chandel. 2005. Oxygen sensing requires mitochondrial ROS but not oxidative phosphorylation. *Cell Metab.* 1:409-414.

Bukau, B., and A.L. Horwich. 1998. The Hsp70 and Hsp60 chaperone machines. *Cell.* 92:351-366.

Bukowski, R.M., and A.C. Novick. 2000. Renal cell carcinoma:Molecular biology, immunology, and clinical management. Humana Press Inc., New Jersey. 434 pp.

Carmo-Fonseca, M. 2002. The contribution of nuclear compartmentalization to gene regulation. *Cell.* 108:513-521.

Carmo-Fonseca, M., L. Mendes-Soares, and I. Campos. 2000. To be or not to be in the nucleolus. *Nature Cell Biol.* 2:E107-112.

Carrero, P., K. Okamoto, P. Coumailleau, S. O'Brien, H. Tanaka, and L. Poellinger. 2000. Redox-regulated recruitment of the transcriptional coactivators CREB-binding protein and SRC-1 to hypoxia-inducible factor 1alpha. *Mol Cell Biol.* 20:402-415.

Chan, D.A., P.D. Sutphin, S.E. Yen, and A.J. Giaccia. 2005. Coordinate regulation of the oxygen-dependent degradation domains of hypoxia-inducible factor 1 alpha. *Mol. Cell. Biol.* 25:6415-6426.

Chavez, J.C., and J.C. LaManna. 2002. Activation of hypoxia-inducible factor-1 in the rat cerebral cortex after transient global ischemia: potential role of insulin-like growth factor-1. *J. Neurosci.* 22:8922-8931.

Chen, D., and S. Huang. 2001. Nucleolar components involved in ribosome biogenesis cycle between the nucleolus and nucleoplasm in interphase cells. *J. Cell Biol.* 153:169-176.

Chen, J., W.O. Lui, M.D. Vos, G.J. Clark, M. Takahashi, J. Schoumans, S.K. Khoo, D. Petillo, T. Lavery, J. Sugimura, D. Astuti, C. Zhang, S. Kagawa, E.R. Maher, C. Larsson, A.S. Alberts, H.O. Kanayama, and B.T. Teh. 2003. The t(1;3) breakpoint-spanning genes LSAMP and NORE1 are involved in clear cell renal cell carcinomas. *Cancer Cell.* 4:405-413.

Cheutin, T., A.J. McNairn, T. Jenuwein, D.M. Gilbert, P.B. Singh, and T. Misteli. 2003. Maintenance of stable heterochromatin domains by dynamic HP1 binding. *Science.* 299:721-725.

Ciechanover, A. 2005. Proteolysis: from the lysosome to ubiquitin and the proteasome. *Nat. Rev. Mol. Cell. Biol.* 6:79-87.

Cockman, M.E., N. Masson, D.R. Mole, P. Jaakkola, G.W. Chang, S.C. Clifford, E.R. Maher, C.W. Pugh, P.J. Ratcliffe, and P.H. Maxwell. 2000. Hypoxia inducible factor-alpha binding and ubiquitylation by the von Hippel-Lindau tumor suppressor protein. *J. Biol. Chem.* 275:25733-25741.

Cohen, H.T., M. Zhou, A.M. Welsh, S. Zarghamee, H. Scholz, D. Mukhopadhyay, T. Kishida, B. Zbar, B. Knebelmann, and V.P. Sukhatme. 1999. An important von Hippel-Lindau tumor suppressor domain mediates Sp1-binding and self-association. *Biochem Biophys Res Commun.* 266:43-50.

Collins, E.T. 1894. Intra-ocular growth (two cases, brother and sister, with peculiar vascular new growth, probably retinal, affecting both eyes). *Trans. Ophthalmol. Soc. UK.* 14:141-149.

Compernolle, V., K. Brusselmans, T. Acker, P. Hoet, M. Tjwa, H. Beck, S. Plaisance, Y. Dor, E. Keshet, F. Lupu, B. Nemery, M. Dewerchin, P. Van Veldhoven, K. Plate,

L. Moons, D. Collen, and P. Carmeliet. 2002. Loss of HIF-2alpha and inhibition of VEGF impair fetal lung maturation, whereas treatment with VEGF prevents fatal respiratory distress in premature mice. *Nat Med.* 8:702-710.

Corless, C.L., A.S. Kibel, O. Iliopoulos, and W.G. Kaelin, Jr. 1997. Immunostaining of the von Hippel-Lindau gene product in normal and neoplastic human tissues. *Hum. Pathol.* 28:459-464.

Currin, R.T., G.J. Gores, R.G. Thurman, and J.J. Lemasters. 1991. Protection by acidotic pH against anoxic cell killing in perfused rat liver: evidence for a pH paradox. *FASEB J.* 5:207-210.

Daelemans, D., S.V. Costes, S. Lockett, and G.N. Pavlakis. 2005. Kinetic and molecular analysis of nuclear export factor CRM1 association with its cargo in vivo. *Mol. Cell. Biol.* 25:728-739.

Davidowitz, E.J., A.R. Schoenfeld, and R.D. Burk. 2001. VHL induces renal cell differentiation and growth arrest through integration of cell-cell and cell-extracellular matrix signaling. *Mol Cell Biol.* 21:865-874.

de Paulsen, N., A. Brychzy, M.C. Fournier, R.D. Klausner, J.R. Gnarra, A. Pause, and S. Lee. 2001. Role of transforming growth factor-alpha in von Hippel--Lindau (VHL)(-/-) clear cell renal carcinoma cell proliferation: a possible mechanism coupling VHL tumor suppressor inactivation and tumorigenesis. *Proc. Natl. Acad. Sci. U.S.A.* 98:1387-1392.

Duan, D.R., J.S. Humphrey, D.Y. Chen, Y. Weng, J. Sukegawa, S. Lee, J.R. Gnarra, W.M. Linehan, and R.D. Klausner. 1995a. Characterization of the VHL tumor

suppressor gene product: localization, complex formation, and the effect of natural inactivating mutations. *Proc. Natl. Acad. Sci. U.S.A.* 92:6459-6463.

Duan, D.R., A. Pause, W.H. Burgess, T. Aso, D.Y. Chen, K.P. Garrett, R.C. Conaway, J.W. Conaway, W.M. Linehan, and R.D. Klausner. 1995b. Inhibition of transcription elongation by the VHL tumor suppressor protein. *Science*. 269:1402-1406.

Dundr, M., U. Hoffmann-Rohrer, Q. Hu, I. Grummt, L.I. Rothblum, R.D. Phair, and T. Misteli. 2002. A kinetic framework for a mammalian RNA polymerase in vivo. *Science*. 298:1623-1626.

Dundr, M., T. Misteli, and M.O. Olson. 2000. The dynamics of postmitotic reassembly of the nucleolus. *J. Cell Biol.* 150:433-446.

Easton, D.P., Y. Kaneko, and J.R. Subjeck. 2000. The hsp110 and Grp1 70 stress proteins: newly recognized relatives of the Hsp70s. *Cell Stress Chaperones*. 5:276-290.

Ema, M., S. Taya, N. Yokotani, K. Sogawa, Y. Matsuda, and Y. Fujii-Kuriyama. 1997. A novel bHLH-PAS factor with close sequence similarity to hypoxia-inducible factor 1alpha regulates the VEGF expression and is potentially involved in lung and vascular development. *Proc Natl Acad Sci U S A*. 94:4273-4278.

Engin, K., D.B. Leeper, J.R. Cater, A.J. Thistlethwaite, L. Tupchong, and J.D. McFarlane. 1995. Extracellular pH distribution in human tumours. *Int. J. Hyperthermia*. 11:211-216.

Engin, K., D.B. Leeper, A.J. Thistlethwaite, L. Tupchong, and J.D. McFarlane. 1994. Tumor extracellular pH as a prognostic factor in thermoradiotherapy. *Int. J. Radiat. Oncol. Biol. Phys.* 29:125-132.

Epstein, A.C., J.M. Gleadle, L.A. McNeill, K.S. Hewitson, J. O'Rourke, D.R. Mole, M. Mukherji, E. Metzen, M.I. Wilson, A. Dhanda, Y.M. Tian, N. Masson, D.L. Hamilton, P. Jaakkola, R. Barstead, J. Hodgkin, P.H. Maxwell, C.W. Pugh, C.J. Schofield, and P.J. Ratcliffe. 2001. C. elegans EGL-9 and mammalian homologs define a family of dioxygenases that regulate HIF by prolyl hydroxylation. *Cell.* 107:43-54.

Esteban-Barragan, M.A., P. Avila, M. Alvarez-Tejado, M.D. Gutierrez, A. Garcia-Pardo, F. Sanchez-Madrid, and M.O. Landazuri. 2002. Role of the von Hippel-Lindau tumor suppressor gene in the formation of beta1-integrin fibrillar adhesions. *Cancer Res.* 62:2929-2936.

Eytan, E., D. Ganoth, T. Armon, and A. Hershko. 1989. ATP-dependent incorporation of 20S protease into the 26S complex that degrades proteins conjugated to ubiquitin. *Proc Natl Acad Sci U S A.* 86:7751-7755.

Fabbro, M., and B.R. Henderson. 2003. Regulation of tumor suppressors by nuclear-cytoplasmic shuttling. *Exp Cell Res.* 282:59-69.

Fahrenkrog, B., and U. Aebi. 2003. The nuclear pore complex: nucleocytoplasmic transport and beyond. *Nat Rev Mol Cell Biol.* 4:757-766.

Falkowski, P.G. 2006. Evolution. Tracing oxygen's imprint on earth's metabolic evolution. *Science.* 311:1724-1725.

Feng, H., W. Zhong, G. Punkosdy, S. Gu, L. Zhou, E.K. Seabolt, and E.T. Kipreos. 1999. CUL-2 is required for the G1-to-S-phase transition and mitotic chromosome condensation in Caenorhabditis elegans. *Nat Cell Biol.* 1:486-492.

Festenstein, R., S.N. Pagakis, K. Hiragami, D. Lyon, A. Verreault, B. Sekkali, and D. Kioussis. 2003. Modulation of heterochromatin protein 1 dynamics in primary Mammalian cells. *Science.* 299:719-721.

Fischer, U., J. Huber, W.C. Boelens, I.W. Mattaj, and R. Luhrmann. 1995. The HIV-1 Rev activation domain is a nuclear export signal that accesses an export pathway used by specific cellular RNAs. *Cell.* 82:475-483.

Fornerod, M., M. Ohno, M. Yoshida, and I.W. Mattaj. 1997. CRM1 is an export receptor for leucine-rich nuclear export signals. *Cell.* 90:1051-1060.

Forsythe, J.A., B.H. Jiang, N.V. Iyer, F. Agani, S.W. Leung, R.D. Koos, and G.L. Semenza. 1996. Activation of vascular endothelial growth factor gene transcription by hypoxia-inducible factor 1. *Mol Cell Biol.* 16:4604-4613.

Franovic, A., I. Robert, K. Smith, G. Kurban, A. Pause, L. Gunaratnam, and S. Lee. 2006. Multiple Acquired Renal Carcinoma Tumor Capabilities Abolished upon Silencing of ADAM17. *Cancer Res.* 66:8083-8090.

Freedman, D.A., and A.J. Levine. 1998. Nuclear export is required for degradation of endogenous p53 by MDM2 and human papillomavirus E6. *Mol. Cell. Biol.* 18:7288-7293.

Fukuchi, M., T. Imamura, T. Chiba, T. Ebisawa, M. Kawabata, K. Tanaka, and K. Miyazono. 2001. Ligand-dependent degradation of Smad3 by a ubiquitin ligase complex of ROC1 and associated proteins. *Mol Biol Cell.* 12:1431-1443.

Galcheva-Gargova, Z., L. Gangwani, K.N. Konstantinov, M. Mikrut, S.J. Theroux, T. Enoch, and R.J. Davis. 1998. The cytoplasmic zinc finger protein ZPR1 accumulates in the nucleolus of proliferating cells. *Mol Biol Cell.* 9:2963-2971.

Gangwani, L., M. Mikrut, Z. Galcheva-Gargova, and R.J. Davis. 1998. Interaction of ZPR1 with translation elongation factor-1alpha in proliferating cells. *J Cell Biol.* 143:1471-1484.

Giaccia, A.J., M.C. Simon, and R. Johnson. 2004. The biology of hypoxia: the role of oxygen sensing in development, normal function, and disease. *Genes Dev.* 18:2183-2194.

Giffard, R.G., H. Monyer, C.W. Christine, and D.W. Choi. 1990. Acidosis reduces NMDA receptor activation, glutamate neurotoxicity, and oxygen-glucose deprivation neuronal injury in cortical cultures. *Brain Res.* 506:339-342.

Gillette, T.G., W. Huang, S.J. Russell, S.H. Reed, S.A. Johnston, and E.C. Friedberg. 2001. The 19S complex of the proteasome regulates nucleotide excision repair in yeast. *Genes Dev.* 15:1528-1539.

Gladden, L.B. 2001. Lactic acid: New roles in a new millennium. *Proc. Natl. Acad. Sci. USA.* 98:395-397.

Gladden, L.B. 2004. Lactate metabolism: a new paradigm for the third millennium. *J. Physiol.* 558:5.

Glickman, M.H., D.M. Rubin, O. Coux, I. Wefes, G. Pfeifer, Z. Cjeka, W. Baumeister, V.A. Fried, and D. Finley. 1998. A subcomplex of the proteasome regulatory particle required for ubiquitin-conjugate degradation and related to the COP9-signalosome and eIF3. *Cell.* 94:615-623.

Gnarra, J.R., D.R. Duan, Y. Weng, J.S. Humphrey, D.Y. Chen, S. Lee, A. Pause, C.F. Dudley, F. Latif, I. Kuzmin, L. Schmidt, F.M. Duh, T. Stackhouse, F. Chen, T. Kishida, M.H. Wei, M.I. Lerman, B. Zbar, R.D. Klausner, and W.M. Linehan. 1996a. Molecular cloning of the von Hippel-Lindau tumor suppressor gene and its role in renal carcinoma. *Biochim Biophys Acta.* 1242:201-210.

Gnarra, J.R., K. Tory, Y. Weng, L. Schmidt, M.H. Wei, H. Li, F. Latif, S. Liu, F. Chen, F.M. Duh, and et al. 1994. Mutations of the VHL tumour suppressor gene in renal carcinoma. *Nat Genet.* 7:85-90.

Gnarra, J.R., S. Zhou, M.J. Merrill, J.R. Wagner, A. Krumm, E. Papavassiliou, E.H. Oldfield, R.D. Klausner, and W.M. Linehan. 1996b. Post-transcriptional regulation of vascular endothelial growth factor mRNA by the product of the VHL tumor suppressor gene. *Proc Natl Acad Sci U S A.* 93:10589-10594.

Golde, D.W., W.G. Hocking, H.P. Koeffler, and J.W. Adamson. 1981. Polycythemia: mechanisms and management. *Ann Intern Med.* 95:71-87.

Gorisch, S.M., M. Wachsmuth, K.F. Toth, P. Lichter, and K. Rippe. 2005. Histone acetylation increases chromatin accessibility. *J Cell Sci.* 118:5825-5834.

Gorospe, M., J.M. Egan, B. Zbar, M. Lerman, L. Geil, I. Kuzmin, and N.J. Holbrook. 1999. Protective function of von Hippel-Lindau protein against impaired protein processing in renal carcinoma cells. *Mol Cell Biol.* 19:1289-1300.

Gowers, D.M., G.G. Wilson, and S.E. Halford. 2005. Measurement of the contributions of 1D and 3D pathways to the translocation of a protein along DNA. *Proc Natl Acad Sci U S A.* 102:15883-15888.

Grandori, C., N. Gomez-Roman, Z.A. Felton-Edkins, C. Ngouenet, D.A. Galloway, R.N. Eisenman, and R.J. White. 2005. c-Myc binds to human ribosomal DNA and stimulates transcription of rRNA genes by RNA polymerase I. *Nat. Cell Biol.* 7:311-318.

Grewal, S.I., and D. Moazed. 2003. Heterochromatin and epigenetic control of gene expression. *Science*. 301:798-802.

Groulx, I., M.E. Bonicalzi, and S. Lee. 2000. Ran-mediated nuclear export of the von Hippel-Lindau tumor suppressor protein occurs independently of its assembly with cullin-2. *J. Biol. Chem.* 275:8991-9000.

Groulx, I., and S. Lee. 2002. Oxygen-dependent ubiquitination and degradation of hypoxia-inducible factor requires nuclear-cytoplasmic trafficking of the von Hippel-Lindau tumor suppressor protein. *Mol. Cell. Biol.* 22:5319.

Grummt, I., and C.S. Pikaard. 2003. Epigenetic silencing of RNA polymerase I transcription. *Nat. Rev. Mol. Cell Biol.* 4:641-649.

Gu, J., J. Milligan, and L.E. Huang. 2001. Molecular mechanism of hypoxia-inducible factor 1alpha -p300 interaction. A leucine-rich interface regulated by a single cysteine. *J Biol Chem.* 276:3550-3554.

Gunaratnam, L., M. Morley, A. Franovic, N. de Paulsen, K. Mekhail, D.A. Parolin, E. Nakamura, I.A. Lorimer, and S. Lee. 2003. Hypoxia inducible factor activates the transforming growth factor-alpha/epidermal growth factor receptor growth stimulatory pathway in VHL (-/-) renal cell carcinoma cells. *J. Biol. Chem.* 278:44966-44974.

Guzy, R.D., B. Hoyos, E. Robin, H. Chen, L. Liu, K.D. Mansfield, M.C. Simon, U. Hammerling, and P.T. Schumacker. 2005. Mitochondrial complex III is required for hypoxia-induced ROS production and cellular oxygen sensing. *Cell Metab.* 1:401-408.

Hanahan, D., and R.A. Weinberg. 2000. The hallmarks of cancer. *Cell.* 100:57-70.

Hardie, D.G. 2000. Metabolic control: a new solution to an old problem. *Curr. Biol.* 10:R757-759.

Harris, A.L. 2002. Hypoxia: a key regulatory factor in tumour growth. *Nat. Rev. Cancer.* 2:38-47.

Hattori, H., T. Kaneda, B. Lokeshwar, A. Laszlo, and K. Ohtsuka. 1993. A stress-inducible 40 kDa protein (hsp40): purification by modified two-dimensional gel electrophoresis and co-localization with hsc70(p73) in heat-shocked HeLa cells. *J Cell Sci.* 104 (Pt 3):629-638.

Herlyn, M., R. Kath, N. Williams, I. Valyi-Nagy, and U. Rodeck. 1990. Growth-regulatory factors for normal, premalignant, and malignant human cells in vitro. *Adv Cancer Res.* 54:213-234.

Herman, J., F. Latif, Y. Weng, M. Lerman, B. Zbar, S. Liu, D. Samid, D. Duan, J. Gnarra, W. Linehan, and S. Baylin. 1994. Silencing of the VHL Tumor-Suppressor Gene by DNA Methylation in Renal Carcinoma. *PNAS.* 91:9700-9704.

Hershko, A., E. Leshinsky, D. Ganoth, and H. Heller. 1984. ATP-dependent degradation of ubiquitin-protein conjugates. *Proc Natl Acad Sci U S A.* 81:1619-1623.

Hoffman, L., G. Pratt, and M. Rechsteiner. 1992. Multiple forms of the 20 S multicatalytic and the 26 S ubiquitin/ATP-dependent proteases from rabbit reticulocyte lysate. *J Biol Chem.* 267:22362-22368.

Hoffman, M.A., M. Ohh, H. Yang, J.M. Klco, M. Ivan, and W.G. Kaelin, Jr. 2001. von Hippel-Lindau protein mutants linked to type 2C VHL disease preserve the ability to downregulate HIF. *Hum. Mol. Genet.* 10:1019-1027.

Holzel, M., M. Rohrmoser, M. Schlee, T. Grimm, T. Harasim, A. Malamoussi, A. Gruber-Eber, E. Kremmer, W. Hiddemann, G.W. Bornkamm, and D. Eick. 2005. Mammalian WDR12 is a novel member of the Pes1-Bop1 complex and is required for ribosome biogenesis and cell proliferation. *J. Cell Biol.* 170:367-378.

Hon, W.C., M.I. Wilson, K. Harlos, T.D. Claridge, C.J. Schofield, C.W. Pugh, P.H. Maxwell, P.J. Ratcliffe, D.I. Stuart, and E.Y. Jones. 2002. Structural basis for the recognition of hydroxyproline in HIF-1 alpha by pVHL. *Nature*. 417:975-978.

Hoogstraten, D., A.L. Nigg, H. Heath, L.H. Mullenders, R. van Driel, J.H. Hoeijmakers, W. Vermeulen, and A.B. Houtsmuller. 2002. Rapid switching of TFIIH between RNA polymerase I and II transcription and DNA repair in vivo. *Mol. Cell.* 10:1163-1174.

Hough, R., G. Pratt, and M. Rechsteiner. 1986. Ubiquitin-lysozyme conjugates. Identification and characterization of an ATP-dependent protease from rabbit reticulocyte lysates. *J Biol Chem.* 261:2400-2408.

Hough, R., G. Pratt, and M. Rechsteiner. 1987. Purification of two high molecular weight proteases from rabbit reticulocyte lysate. *J Biol Chem.* 262:8303-8313.

Huang, L.E., Z. Arany, D.M. Livingston, and H.F. Bunn. 1996. Activation of hypoxia-inducible transcription factor depends primarily upon redox-sensitive stabilization of its alpha subunit. *J Biol Chem.* 271:32253-32259.

Huibregtse, J.M., M. Scheffner, S. Beaudenon, and P.M. Howley. 1995. A family of proteins structurally and functionally related to the E6-AP ubiquitin-protein ligase. *Proc Natl Acad Sci U S A.* 92:5249.

Iliopoulos, O., A. Kibel, S. Gray, and W.G. Kaelin, Jr. 1995. Tumour suppression by the human von Hippel-Lindau gene product. *Nat. Med.* 1:822-826.

Iliopoulos, O., A.P. Levy, C. Jiang, W.G. Kaelin, Jr., and M.A. Goldberg. 1996. Negative regulation of hypoxia-inducible genes by the von Hippel-Lindau protein. *Proc. Natl. Acad. Sci. U.S.A.* 93:10595-10599.

Iliopoulos, O., M. Ohh, and W.G. Kaelin, Jr. 1998. pVHL19 is a biologically active product of the von Hippel-Lindau gene arising from internal translation initiation. *Proc. Natl. Acad. Sci. U.S.A.* 95:11661-11666.

Inoki, K., T. Zhu, and K.L. Guan. 2003. TSC2 mediates cellular energy response to control cell growth and survival. *Cell.* 115:577-590.

Ivan, M., K. Kondo, H. Yang, W. Kim, J. Valiando, M. Ohh, A. Salic, J.M. Asara, W.S. Lane, and W.G. Kaelin, Jr. 2001. HIFalpha targeted for VHL-mediated destruction by proline hydroxylation: implications for O2 sensing. *Science.* 292:464-468.

Iwai, K., K. Yamanaka, T. Kamura, N. Minato, R.C. Conaway, J.W. Conaway, R.D. Klausner, and A. Pause. 1999. Identification of the von Hippel-lindau tumor-

suppressor protein as part of an active E3 ubiquitin ligase complex. *Proc. Natl. Acad. Sci. USA*. 96:12436-12441.

Iyer, N.V., L.E. Kotch, F. Agani, S.W. Leung, E. Laughner, R.H. Wenger, M. Gassmann, J.D. Gearhart, A.M. Lawler, A.Y. Yu, and G.L. Semenza. 1998. Cellular and developmental control of O2 homeostasis by hypoxia-inducible factor 1 alpha. *Genes Dev.* 12:149-162.

Jaakkola, P., D.R. Mole, Y.M. Tian, M.I. Wilson, J. Gielbert, S.J. Gaskell, A. Kriegsheim, H.F. Hebestreit, M. Mukherji, C.J. Schofield, P.H. Maxwell, C.W. Pugh, and P.J. Ratcliffe. 2001. Targeting of HIF-alpha to the von Hippel-Lindau ubiquitylation complex by O2-regulated prolyl hydroxylation. *Science*. 292:468-472.

Joazeiro, C.A., and A.M. Weissman. 2000. RING finger proteins: mediators of ubiquitin ligase activity. *Cell*. 102:549-552.

Kaelin, W.G., Jr. 2002. Molecular basis of the VHL hereditary cancer syndrome. *Nat. Rev. Cancer*. 2:673-682.

Kaelin, W.G., Jr. 2005. ROS: really involved in oxygen sensing. *Cell Metab.* 1:357-358.

Kaelin, W.G., and E.R. Maher. 1998. The VHL tumour-suppressor gene paradigm. *Trends in Genetics*. 14:423-426.

Kaku, D.A., R.G. Giffard, and D.W. Choi. 1993. Neuroprotective effects of glutamate antagonists and extracellular acidity. *Science*. 260:1516-1518.

Kallio, P.J., W.J. Wilson, S. O'Brien, Y. Makino, and L. Poellinger. 1999. Regulation of the hypoxia-inducible transcription factor 1alpha by the ubiquitin-proteasome pathway. *J Biol Chem*. 274:6519-6525.

Kamura, T., D.M. Koepp, M.N. Conrad, D. Skowyra, R.J. Moreland, O. Iliopoulos, W.S. Lane, W.G. Kaelin, Jr., S.J. Elledge, R.C. Conaway, J.W. Harper, and J.W. Conaway. 1999. Rbx1, a component of the VHL tumor suppressor complex and SCF ubiquitin ligase. *Science*. 284:657-661.

Kamura, T., S. Sato, K. Iwai, M. Czyzyk-Krzeska, R.C. Conaway, and J.W. Conaway. 2000. Activation of HIF1alpha ubiquitination by a reconstituted von Hippel-Lindau (VHL) tumor suppressor complex. *Proc. Natl. Acad. Sci. USA*. 97:10430-10435.

Khacho, M., K. Mekhail, J. Cote, A. Pause, and S. Lee. 2006. EDNA exploits the translational machinery to export proteins from the nucleus. *J. Biol. Chem. (in preparation)*.

Kibel, A., O. Iliopoulos, J.A. DeCaprio, and W.G. Kaelin, Jr. 1995. Binding of the von Hippel-Lindau tumor suppressor protein to Elongin B and C. *Science*. 269:1444-1446.

Kim, J.W., I. Tchernyshyov, G.L. Semenza, and C.V. Dang. 2006. HIF-1-mediated expression of pyruvate dehydrogenase kinase: a metabolic switch required for cellular adaptation to hypoxia. *Cell Metab.* 3:177-185.

Kim, M.S., H.J. Kwon, Y.M. Lee, J.H. Baek, J.E. Jang, S.W. Lee, E.J. Moon, H.S. Kim, S.K. Lee, H.Y. Chung, C.W. Kim, and K.W. Kim. 2001. Histone deacetylases induce angiogenesis by negative regulation of tumor suppressor genes. *Nat. Med.* 7:437-443.

Kimura, H., and P.R. Cook. 2001. Kinetics of core histones in living human cells: little exchange of H3 and H4 and some rapid exchange of H2B. *J. Cell Biol.* 153:1341-1353.

Kinzler, K.W., and B. Vogelstein. 1997. Cancer-susceptibility genes: Gatekeepers and caretakers. *Nature*. 386:761, 763.

Kivirikko, K.I., and J. Myllyharju. 1998. Prolyl 4-hydroxylases and their protein disulfide isomerase subunit. *Matrix Biol.* 16:357-368.

Knudson, A.G., Jr. 1971. Mutation and cancer: statistical study of retinoblastoma. *Proc Natl Acad Sci U S A*. 68:820-823.

Knudson, A.G., Jr. 1985. Hereditary cancer, oncogenes, and antioncogenes. *Cancer Res.* 45:1437-1443.

Koegl, M., T. Hoppe, S. Schlenker, H.D. Ulrich, T.U. Mayer, and S. Jentsch. 1999. A novel ubiquitination factor, E4, is involved in multiubiquitin chain assembly. *Cell.* 96:635-644.

Kojima, H., H. Gu, S. Nomura, C.C. Caldwell, T. Kobata, P. Carmeliet, G.L. Semenza, and M.V. Sitkovsky. 2002. Abnormal B lymphocyte development and autoimmunity in hypoxia-inducible factor 1alpha -deficient chimeric mice. *Proc Natl Acad Sci USA*. 99:2170-2174.

Kondo, K., J. Klco, E. Nakamura, M. Lechpammer, and W.G. Kaelin, Jr. 2002. Inhibition of HIF is necessary for tumor suppression by the von Hippel-Lindau protein. *Cancer Cell*. 1:237-246.

Kotch, L.E., N.V. Iyer, E. Laughner, and G.L. Semenza. 1999. Defective vascularization of HIF-1alpha-null embryos is not associated with VEGF deficiency but with mesenchymal cell death. *Dev Biol.* 209:254-267.

Krieg, M., R. Haas, H. Brauch, T. Acker, I. Flamme, and K.H. Plate. 2000. Up-regulation of hypoxia-inducible factors HIF-1alpha and HIF-2alpha under normoxic conditions in renal carcinoma cells by von Hippel-Lindau tumor suppressor gene loss of function. *Oncogene.* 19:5435-5443.

Kung, A.L., S. Wang, J.M. Klco, W.G. Kaelin, and D.M. Livingston. 2000. Suppression of tumor growth through disruption of hypoxia-inducible transcription. *Nat Med.* 6:1335-1340.

Kurban, G., V. Hudon, E. Duplan, M. Ohh, and A. Pause. 2006. Characterization of a von Hippel Lindau pathway involved in extracellular matrix remodeling, cell invasion, and angiogenesis. *Cancer Res.* 66:1313-1319.

Kuznetsov, A.V., M. Janakiraman, R. Margreiter, and J. Troppmair. 2004. Regulating cell survival by controlling cellular energy production: novel functions for ancient signaling pathways? *FEBS Lett.* 577:1-4.

Kvietikova, I., R.H. Wenger, H.H. Marti, and M. Gassmann. 1995. The transcription factors ATF-1 and CREB-1 bind constitutively to the hypoxia-inducible factor-1 (HIF-1) DNA recognition site. *Nucleic Acids Res.* 23:4542-4550.

Lam, Y.W., L. Trinkle-Mulcahy, and A.I. Lamond. 2005. The nucleolus. *J. Cell Sci.* 118:1335-1337.

Lando, D., D.J. Peet, J.J. Gorman, D.A. Whelan, M.L. Whitelaw, and R.K. Bruick. 2002a. FIH-1 is an asparaginyl hydroxylase enzyme that regulates the transcriptional activity of hypoxia-inducible factor. *Genes Dev.* 16:1466-1471.

Lando, D., D.J. Peet, D.A. Whelan, J.J. Gorman, and M.L. Whitelaw. 2002b. Asparagine hydroxylation of the HIF transactivation domain a hypoxic switch. *Science.* 295:858-861.

Latif, F., K. Tory, J. Gnarra, M. Yao, F.M. Duh, M.L. Orcutt, T. Stackhouse, I. Kuzmin, W. Modi, L. Geil, and et al. 1993. Identification of the von Hippel-Lindau disease tumor suppressor gene. *Science.* 260:1317-1320.

Lee, S., D.Y. Chen, J.S. Humphrey, J.R. Gnarra, W.M. Linehan, and R.D. Klausner. 1996. Nuclear/cytoplasmic localization of the von Hippel-Lindau tumor suppressor gene product is determined by cell density. *Proc. Natl. Acad. Sci. U.S.A.* 93:1770-1775.

Lee, S., M. Neumann, R. Stearman, R. Stauber, A. Pause, G.N. Pavlakis, and R.D. Klausner. 1999. Transcription-dependent nuclear-cytoplasmic trafficking is required for the function of the von Hippel-Lindau tumor suppressor protein. *Mol. Cell. Biol.* 19:1486.

Levitt, N.C., and I.D. Hickson. 2002. Caretaker tumour suppressor genes that defend genome integrity. *Trends Mol Med.* 8:179-186.

Li, J., R. Santoro, K. Koberna, and I. Grummt. 2005. The chromatin remodeling complex NoRC controls replication timing of rRNA genes. *EMBO J.* 24:120-127.

Liakopoulos, D., T. Busgen, A. Brychzy, S. Jentsch, and A. Pause. 1999. Conjugation of the ubiquitin-like protein NEDD8 to cullin-2 is linked to von Hippel-Lindau tumor suppressor function. *Proc Natl Acad Sci U S A.* 96:5510-5515.

Lieubeau-Teillet, B., J. Rak, S. Jothy, O. Iliopoulos, W. Kaelin, and R.S. Kerbel. 1998. von Hippel-Lindau gene-mediated growth suppression and induction of differentiation in renal cell carcinoma cells grown as multicellular tumor spheroids. *Cancer Res.* 58:4957-4962.

Lindau, A. 1927. Zur Frage der Angiomatosis Retinae und Ihrer Hirncomplikation. *Acta Ophthalmol.* 4:193-226.

Linehan, W.M., M.M. Walther, and B. Zbar. 2003. The genetic basis of cancer of the kidney. *J Urol.* 170:2163-2172.

Lippincott-Schwartz, J., N. Altan-Bonnet, and G.H. Patterson. 2003. Photobleaching and photoactivation: following protein dynamics in living cells. *Nat. Cell Biol.* Suppl:S7-14.

Lippincott-Schwartz, J., E. Snapp, and A. Kenworthy. 2001. Studying protein dynamics in living cells. *Nat Rev Mol Cell Biol.* 2:444-456.

Lisztwan, J., G. Imbert, C. Wirbelauer, M. Gstaiger, and W. Krek. 1999. The von Hippel-Lindau tumor suppressor protein is a component of an E3 ubiquitin-protein ligase activity. *Genes Dev.* 13:1822-1833.

Liu, L., T.P. Cash, R.G. Jones, B. Keith, C.B. Thompson, and M.C. Simon. 2006. Hypoxia-induced energy stress regulates mRNA translation and cell growth. *Mol. Cell.* 21:521-531.

Llanos, S., P.A. Clark, J. Rowe, and G. Peters. 2001. Stabilization of p53 by p14ARF without relocation of MDM2 to the nucleolus. *Nat. Cell Biol.* 3:445-452.

Lohrum, M.A., R.L. Ludwig, M.H. Kubbutat, M. Hanlon, and K.H. Vousden. 2003. Regulation of HDM2 activity by the ribosomal protein L11. *Cancer Cell.* 3:577-587.

Lonergan, K.M., O. Iliopoulos, M. Ohh, T. Kamura, R.C. Conaway, J.W. Conaway, and W.G. Kaelin, Jr. 1998. Regulation of hypoxia-inducible mRNAs by the von Hippel-Lindau tumor suppressor protein requires binding to complexes containing elongins B/C and Cul2. *Mol. Cell. Biol.* 18:732-741.

Maemura, K., C.M. Hsieh, M.K. Jain, S. Fukumoto, M.D. Layne, Y. Liu, S. Kourembanas, S.F. Yet, M.A. Perrella, and M.E. Lee. 1999. Generation of a dominant-negative mutant of endothelial PAS domain protein 1 by deletion of a potent C-terminal transactivation domain. *J. Biol. Chem.* 274:31565-31570.

Maher, E.R., L. Iselius, J.R. Yates, M. Littler, C. Benjamin, R. Harris, J. Sampson, A. Williams, M.A. Ferguson-Smith, and N. Morton. 1991. Von Hippel-Lindau disease: a genetic study. *J Med Genet.* 28:443-447.

Maher, E.R., and W.G. Kaelin, Jr. 1997. von Hippel-Lindau disease. *Medicine (Baltimore).* 76:381-391.

Mais, C., J.E. Wright, J.L. Prieto, S.L. Raggett, and B. McStay. 2005. UBF-binding site arrays form pseudo-NORs and sequester the RNA polymerase I transcription machinery. *Genes Dev.* 19:50.

Maison, C., and G. Almouzni. 2004. HP1 and the dynamics of heterochromatin maintenance. *Nat. Rev. Mol. Cell. Biol.* 5:296-304.

Mansfield, K.D., R.D. Guzy, Y. Pan, R.M. Young, T.P. Cash, P.T. Schumacker, and M.C. Simon. 2005. Mitochondrial dysfunction resulting from loss of cytochrome c impairs cellular oxygen sensing and hypoxic HIF-alpha activation. *Cell Metab.* 1:393-399.

Maranchie, J.K., J.R. Vasselli, J. Riss, J.S. Bonifacino, W.M. Linehan, and R.D. Klausner. 2002. The contribution of VHL substrate binding and HIF1-alpha to the phenotype of VHL loss in renal cell carcinoma. *Cancer Cell.* 1:247-255.

Maxwell, P.H., M.S. Wiesener, G.W. Chang, S.C. Clifford, E.C. Vaux, M.E. Cockman, C.C. Wykoff, C.W. Pugh, E.R. Maher, and P.J. Ratcliffe. 1999. The tumour suppressor protein VHL targets hypoxia-inducible factors for oxygen-dependent proteolysis. *Nature.* 399:271-275.

Mayer, C., K.M. Schmitz, J. Li, I. Grummt, and R. Santoro. 2006. Intergenic transcripts regulate the epigenetic state of rRNA genes. *Mol. Cell.* 22:351-361.

Maynard, M.A., A.J. Evans, T. Hosomi, S. Hara, M.A. Jewett, and M. Ohh. 2005. Human HIF-3alpha4 is a dominant-negative regulator of HIF-1 and is down-regulated in renal cell carcinoma. *Faseb J.* 19:1396-1406.

Maynard, M.A., H. Qi, J. Chung, E.H. Lee, Y. Kondo, S. Hara, R.C. Conaway, J.W. Conaway, and M. Ohh. 2003. Multiple splice variants of the human HIF-3 alpha locus are targets of the von Hippel-Lindau E3 ubiquitin ligase complex. *J Biol Chem.* 278:11032-11040.

Mekhail, K., L. Gunaratnam, M.E. Bonicalzi, and S. Lee. 2004a. HIF activation by pH-dependent nucleolar sequestration of VHL. *Nat. Cell Biol.* 6:642-647.

Mekhail, K., M. Khacho, A. Carrigan, R.R. Hache, L. Gunaratnam, and S. Lee. 2005. Regulation of ubiquitin ligase dynamics by the nucleolus. *J. Cell Biol.* 170:733-744.

Mekhail, K., M. Khacho, L. Gunaratnam, and S. Lee. 2004b. Oxygen sensing by H+: implications for HIF and hypoxic cell memory. *Cell Cycle*. 3:1027-1029.

Mekhail, K., L. Rivero-Lopez, M. Khacho, and S. Lee. 2006. Restriction of rRNA synthesis by VHL maintains energy equilibrium under hypoxia. *Cell Cycle*. 5:2401-2413.

Meshorer, E., D. Yellajoshula, E. George, P.J. Scambler, D.T. Brown, and T. Misteli. 2006. Hyperdynamic plasticity of chromatin proteins in pluripotent embryonic stem cells. *Dev. Cell*. 10:105-116.

Michael, D., and M. Oren. 2003. The p53-Mdm2 module and the ubiquitin system. *Semin. Cancer Biol.* 13:49-58.

Min, J.H., H. Yang, M. Ivan, F. Gertler, W.G. Kaelin, Jr., and N.P. Pavletich. 2002. Structure of an HIF-1alpha -pVHL complex: hydroxyproline recognition in signaling. *Science*. 296:1886-1889.

Misteli, T. 2001. Protein dynamics: implications for nuclear architecture and gene expression. *Science*. 291:843.

Moazed, D., A.D. Rudner, J. Huang, G.J. Hoppe, and J.C. Tanny. 2004. A model for step-wise assembly of heterochromatin in yeast. *Novartis Found Symp*. 259:48-56; discussion 56-62, 163-169.

Momand, J., G.P. Zambetti, D.C. Olson, D. George, and A.J. Levine. 1992. The mdm-2 oncogene product forms a complex with the p53 protein and inhibits p53-mediated transactivation. *Cell.* 69:1237-1245.

Morimoto, Y., O. Kemmotsu, and E.S. Alojado. 1997. Extracellular acidosis delays cell death against glucose-oxygen deprivation in neuroblastoma x glioma hybrid cells. *Crit. Care Med.* 25:841.

Motzer, R.J., N.H. Bander, and D.M. Nanus. 1996. Renal-cell carcinoma. *N Engl J Med.* 335:865-875.

Mukhopadhyay, D., B. Knebelmann, H.T. Cohen, S. Ananth, and V.P. Sukhatme. 1997. The von Hippel-Lindau tumor suppressor gene product interacts with Sp1 to repress vascular endothelial growth factor promoter activity. *Mol Cell Biol.* 17:5629-5639.

Muratani, M., and W.P. Tansey. 2003. How the ubiquitin-proteasome system controls transcription. *Nat. Rev. Mol. Cell. Biol.* 4:192-201.

Myllyharju, J. 2003. Prolyl 4-hydroxylases, the key enzymes of collagen biosynthesis. *Matrix Biol.* 22:15-24.

Nielsen, O.B., F. de Paoli, and K. Overgaard. 2001. Protective effects of lactic acid on force production in rat skeletal muscle. *J. Physiol.* 536:161-166.

Nwogu, J.I., D. Geenen, M. Bean, M.C. Brenner, X. Huang, and P.M. Buttrick. 2001. Inhibition of collagen synthesis with prolyl 4-hydroxylase inhibitor improves left ventricular function and alters the pattern of left ventricular dilatation after myocardial infarction. *Circulation.* 104:2216-2221.

Obach, M., A. Navarro-Sabate, J. Caro, X. Kong, J. Duran, M. Gomez, J.C. Perales, F. Ventura, J.L. Rosa, and R. Bartrons. 2004. 6-Phosphofructo-2-kinase (pfkfb3) gene promoter contains hypoxia-inducible factor-1 binding sites necessary for transactivation in response to hypoxia. *J. Biol. Chem.* 279:53562-53570.

Ohh, M., C.W. Park, M. Ivan, M.A. Hoffman, T.Y. Kim, L.E. Huang, N. Pavletich, V. Chau, and W.G. Kaelin. 2000. Ubiquitination of hypoxia-inducible factor requires direct binding to the beta-domain of the von Hippel-Lindau protein. *Nat. Cell Biol.* 2:423-427.

Ohh, M., R.L. Yauch, K.M. Lonergan, J.M. Whaley, A.O. Stemmer-Rachamimov, D.N. Louis, B.J. Gavin, N. Kley, W.G. Kaelin, Jr., and O. Iliopoulos. 1998. The von Hippel-Lindau tumor suppressor protein is required for proper assembly of an extracellular fibronectin matrix. *Mol. Cell.* 1:959-968.

Okuda, H., S. Hirai, Y. Takaki, M. Kamada, M. Baba, N. Sakai, T. Kishida, S. Kaneko, M. Yao, S. Ohno, and T. Shuin. 1999. Direct interaction of the beta-domain of VHL tumor suppressor protein with the regulatory domain of atypical PKC isotypes. *Biochem Biophys Res Commun.* 263:491-497.

Okuda, H., K. Saitoh, S. Hirai, K. Iwai, Y. Takaki, M. Baba, N. Minato, S. Ohno, and T. Shuin. 2001. The von Hippel-Lindau tumor suppressor protein mediates ubiquitination of activated atypical protein kinase C. *J Biol Chem.* 276:43611-43617.

Oliner, J.D., J.A. Pietenpol, S. Thiagalingam, J. Gyuris, K.W. Kinzler, and B. Vogelstein. 1993. Oncoprotein MDM2 conceals the activation domain of tumour suppressor p53. *Nature*. 362:857-860.

Olson, M.O. 2004. Sensing cellular stress: another new function for the nucleolus? *Sci. S.T.K.E.* 2004:pe10.

Olson, M.O., and M. Dundr. 2005. The moving parts of the nucleolus. *Histochem. Cell Biol.* 123:203-216.

Ossareh-Nazari, B., F. Bachelerie, and C. Dargemont. 1997. Evidence for a role of CRM1 in signal-mediated nuclear protein export. *Science*. 278:141-144.

Page, E.L., G.A. Robitaille, J. Pouyssegur, and D.E. Richard. 2002. Induction of hypoxia-inducible factor-1alpha by transcriptional and translational mechanisms. *J. Biol. Chem.* 277:48403-48409.

Pal, S., K.P. Claffey, H.T. Cohen, and D. Mukhopadhyay. 1998. Activation of Sp1-mediated vascular permeability factor/vascular endothelial growth factor transcription requires specific interaction with protein kinase C zeta. *J Biol Chem.* 273:26277-26280.

Pal, S., K.P. Claffey, H.F. Dvorak, and D. Mukhopadhyay. 1997. The von Hippel-Lindau gene product inhibits vascular permeability factor/vascular endothelial growth factor expression in renal cell carcinoma by blocking protein kinase C pathways. *J Biol Chem.* 272:27509-27512.

Papandreou, I., R.A. Cairns, L. Fontana, A.L. Lim, and N.C. Denko. 2006. HIF-1 mediates adaptation to hypoxia by actively downregulating mitochondrial oxygen consumption. *Cell Metab.* 3:187-197.

Pasteur, L. 1857. Mémoire sur la fermentation appellée lactique. *Comptes rendus de l'Académie des Sciences à Paris*. 45:913.

Patel, A.A., E.T. Gawlinski, S.K. Lemieux, and R.A. Gatenby. 2001. A cellular automaton model of early tumor growth and invasion. *J Theor Biol.* 213:315-331.

Pause, A., S. Lee, K.M. Lonergan, and R.D. Klausner. 1998. The von Hippel-Lindau tumor suppressor gene is required for cell cycle exit upon serum withdrawal. *Proc. Natl. Acad. Sci. USA.* 95:993-998.

Pause, A., S. Lee, R.A. Worrell, D.Y. Chen, W.H. Burgess, W.M. Linehan, and R.D. Klausner. 1997. The von Hippel-Lindau tumor-suppressor gene product forms a stable complex with human CUL-2, a member of the Cdc53 family of proteins. *Proc. Natl. Acad. Sci. USA.* 94:2156-2161.

Pause, A., B. Peterson, G. Schaffar, R. Stearman, and R.D. Klausner. 1999. Studying interactions of four proteins in the yeast two-hybrid system: structural resemblance of the pVHL/elongin BC/hCUL-2 complex with the ubiquitin ligase complex SKP1/cullin/F-box protein. *Proc. Natl. Acad. Sci. USA.* 96:9533-9538.

Paushkin, S.V., M. Patel, B.S. Furia, S.W. Peltz, and C.R. Trotta. 2004. Identification of a human endonuclease complex reveals a link between tRNA splicing and pre-mRNA 3' end formation. *Cell.* 117:311-321.

Pavlovich, C.P., and L.S. Schmidt. 2004. Searching for the hereditary causes of renal-cell carcinoma. *Nat Rev Cancer.* 4:381-393.

Penttila, A., and B.F. Trump. 1974. Extracellular acidosis protects Ehrlich ascites tumor cells and rat renal cortex against anoxic injury. *Science.* 185:277-278.

Petroski, M.D., and R.J. Deshaies. 2005. Function and regulation of cullin-RING ubiquitin ligases. *Nat. Rev. Mol. Cell. Biol.* 6:9-20.

Phair, R.D., and T. Misteli. 2000. High mobility of proteins in the mammalian cell nucleus. *Nature*. 404:604.

Politz, J.C., E.S. Browne, D.E. Wolf, and T. Pederson. 1998. Intranuclear diffusion and hybridization state of oligonucleotides measured by fluorescence correlation spectroscopy in living cells. *Proc Natl Acad Sci U S A*. 95:6043-6048.

Politz, J.C., R.A. Tuft, T. Pederson, and R.H. Singer. 1999. Movement of nuclear poly(A) RNA throughout the interchromatin space in living cells. *Curr Biol*. 9:285-291.

Pugh, C.W., C.C. Tan, R.W. Jones, and P.J. Ratcliffe. 1991. Functional analysis of an oxygen-regulated transcriptional enhancer lying 3' to the mouse erythropoietin gene. *Proc Natl Acad Sci U S A*. 88:10553-10557.

Rabut, G., V. Doye, and J. Ellenberg. 2004. Mapping the dynamic organization of the nuclear pore complex inside single living cells. *Nat. Cell Biol.* 6:1114-1121.

Reeder, R.H. 1984. Enhancers and ribosomal gene spacers. *Cell*. 38:349.

Reeder, R.H., J.G. Roan, and M. Dunaway. 1983. Spacer regulation of Xenopus ribosomal gene transcription: competition in oocytes. *Cell*. 35:449-456.

Richard, D.E., E. Berra, and J. Pouyssegur. 2000. Nonhypoxic pathway mediates the induction of hypoxia-inducible factor 1alpha in vascular smooth muscle cells. *J. Biol. Chem.* 275:26765-26771.

Roth, J., M. Dobbelstein, D.A. Freedman, T. Shenk, and A.J. Levine. 1998. Nucleo-cytoplasmic shuttling of the hdm2 oncoprotein regulates the levels of the p53 protein via a pathway used by the human immunodeficiency virus rev protein. *EMBO J.* 17:554-564.

Ruoslahti, E. 1984. Fibronectin in cell adhesion and invasion. *Cancer Metastasis Rev.* 3:43-51.

Russell, S.J., S.H. Reed, W. Huang, E.C. Friedberg, and S.A. Johnston. 1999. The 19S regulatory complex of the proteasome functions independently of proteolysis in nucleotide excision repair. *Mol. Cell.* 3:687-695.

Salceda, S., and J. Caro. 1997. Hypoxia-inducible factor 1alpha (HIF-1alpha) protein is rapidly degraded by the ubiquitin-proteasome system under normoxic conditions. Its stabilization by hypoxia depends on redox-induced changes. *J Biol Chem.* 272:22642-22647.

Scheffner, M., B.A. Werness, J.M. Huibregtse, A.J. Levine, and P.M. Howley. 1990. The E6 oncoprotein encoded by human papillomavirus types 16 and 18 promotes the degradation of p53. *Cell.* 63:1129-1136.

Schmidt, E.V. 1999. The role of c-myc in cellular growth control. *Oncogene.* 18:2988-2996.

Schoenfeld, A., E.J. Davidowitz, and R.D. Burk. 1998. A second major native von Hippel-Lindau gene product, initiated from an internal translation start site, functions as a tumor suppressor. *Proc. Natl. Acad. Sci. U.S.A.* 95:8817-8822.

Schofield, C.J., and Z. Zhang. 1999. Structural and mechanistic studies on 2-oxoglutarate-dependent oxygenases and related enzymes. *Curr. Opin. Struct. Biol.* 9:722-731.

Seagroves, T.N., H.E. Ryan, H. Lu, B.G. Wouters, M. Knapp, P. Thibault, K. Laderoute, and R.S. Johnson. 2001. Transcription factor HIF-1 is a necessary mediator of the pasteur effect in mammalian cells. *Mol. Cell. Biol.* 21:3436-3444.

Semenza, G.L. 1998. Hypoxia-inducible factor 1: master regulator of O2 homeostasis. *Curr. Opin. Genet. Dev.* 8:588-594.

Semenza, G.L. 1999. Regulation of mammalian O2 homeostasis by hypoxia-inducible factor 1. *Annu Rev Cell Dev Biol.* 15:551-578.

Semenza, G.L. 2000a. HIF-1 and human disease: one highly involved factor. *Genes Dev.* 14:1983-1991.

Semenza, G.L. 2000b. HIF-1: mediator of physiological and pathophysiological responses to hypoxia. *J Appl Physiol.* 88:1474-1480.

Semenza, G.L. 2003. Targeting HIF-1 for cancer therapy. *Nature Rev. Cancer.* 3:721-732.

Semenza, G.L., M.K. Nejfelt, S.M. Chi, and S.E. Antonarakis. 1991. Hypoxia-inducible nuclear factors bind to an enhancer element located 3' to the human erythropoietin gene. *Proc Natl Acad Sci U S A.* 88:5680-5684.

Semenza, G.L., P.H. Roth, H.M. Fang, and G.L. Wang. 1994. Transcriptional regulation of genes encoding glycolytic enzymes by hypoxia-inducible factor 1. *J. Biol. Chem.* 269:23757-23763.

Semenza, G.L., and G.L. Wang. 1992. A nuclear factor induced by hypoxia via de novo protein synthesis binds to the human erythropoietin gene enhancer at a site required for transcriptional activation. *Mol Cell Biol.* 12:5447-5454.

Shav-Tal, Y., X. Darzacq, S.M. Shenoy, D. Fusco, S.M. Janicki, D.L. Spector, and R.H. Singer. 2004a. Dynamics of single mRNPs in nuclei of living cells. *Science.* 304:1797-1800.

Shav-Tal, Y., R.H. Singer, and X. Darzacq. 2004b. Imaging gene expression in single living cells. *Nat. Rev. Mol. Cell Biol.* 5:855-861.

Shou, W., K.M. Sakamoto, J. Keener, K.W. Morimoto, E.E. Traverso, R. Azzam, G.J. Hoppe, R.M. Feldman, J. DeModena, D. Moazed, H. Charbonneau, M. Nomura, and R.J. Deshaies. 2001. Net1 stimulates RNA polymerase I transcription and regulates nucleolar structure independently of controlling mitotic exit. *Mol. Cell.* 8:45-55.

Shou, W., J.H. Seol, A. Shevchenko, C. Baskerville, D. Moazed, Z.W. Chen, J. Jang, H. Charbonneau, and R.J. Deshaies. 1999. Exit from mitosis is triggered by Tem1-dependent release of the protein phosphatase Cdc14 from nucleolar RENT complex. *Cell.* 97:233-244.

Siemeister, G., K. Weindel, K. Mohrs, B. Barleon, G. Martiny-Baron, and D. Marme. 1996. Reversion of deregulated expression of vascular endothelial growth factor in human renal carcinoma cells by von Hippel-Lindau tumor suppressor protein. *Cancer Res.* 56:2299-2301.

Simon, M.C. 2006. Coming up for air: HIF-1 and mitochondrial oxygen consumption. *Cell Metab.* 3:150-151.

Sinclair, D.A., and L. Guarente. 1997. Extrachromosomal rDNA circles: a cause of aging in yeast. *Cell.* 91:1033-1042.

Sinclair, D.A., K. Mills, and L. Guarente. 1997. Accelerated aging and nucleolar fragmentation in yeast sgs1 mutants. *Science.* 277:1313-1316.

Smith, K., L. Gunaratnam, M. Morley, A. Franovic, K. Mekhail, and S. Lee. 2005. Silencing of epidermal growth factor receptor suppresses hypoxia-inducible factor-2-driven VHL-/- renal cancer. *Cancer Res.* 65:5221-5230.

Sporbert, A., A. Gahl, R. Ankerhold, H. Leonhardt, and M.C. Cardoso. 2002. DNA polymerase clamp shows little turnover at established replication sites but sequential de novo assembly at adjacent origin clusters. *Mol. Cell.* 10:1355-1365.

Stade, K., C.S. Ford, C. Guthrie, and K. Weis. 1997. Exportin 1 (Crm1p) is an essential nuclear export factor. *Cell.* 90:1041-1050.

Stauber, R., G.A. Gaitanaris, and G.N. Pavlakis. 1995. Analysis of trafficking of Rev and transdominant Rev proteins in living cells using green fluorescent protein fusions: transdominant Rev blocks the export of Rev from the nucleus to the cytoplasm. *Virology.* 213:439-449.

Stebbins, C.E., W.G. Kaelin, Jr., and N.P. Pavletich. 1999. Structure of the VHL-ElonginC-ElonginB complex: implications for VHL tumor suppressor function. *Science.* 284:455-461.

Stickle, N.H., J. Chung, J.M. Klco, R.P. Hill, W.G. Kaelin, Jr., and M. Ohh. 2004. pVHL modification by NEDD8 is required for fibronectin matrix assembly and suppression of tumor development. *Mol Cell Biol.* 24:3251-3261.

Straight, A.F., W. Shou, G.J. Dowd, C.W. Turck, R.J. Deshaies, A.D. Johnson, and D. Moazed. 1999. Net1, a Sir2-associated nucleolar protein required for rDNA silencing and nucleolar integrity. *Cell.* 97:245-256.

Sun, Y., K. Jin, L. Xie, J. Childs, X.O. Mao, A. Logvinova, and D.A. Greenberg. 2003. VEGF-induced neuroprotection, neurogenesis, and angiogenesis after focal cerebral ischemia. *J. Clin. Invest.* 111:1843-1851.

Sutherland, R.M. 1988. Cell and environment interactions in tumor microregions: the multicell spheroid model. *Science*. 240:177-184.

Tanimoto, K., Y. Makino, T. Pereira, and L. Poellinger. 2000. Mechanism of regulation of the hypoxia-inducible factor-1 alpha by the von Hippel-Lindau tumor suppressor protein. *EMBO J.* 19:4298-4309.

Tao, W., and A.J. Levine. 1999. P19(ARF) stabilizes p53 by blocking nucleo-cytoplasmic shuttling of Mdm2. *Proc. Natl. Acad. Sci. USA*. 96:6937-6941.

Terrell, J., S. Shih, R. Dunn, and L. Hicke. 1998. A function for monoubiquitination in the internalization of a G protein-coupled receptor. *Mol. Cell*. 1:193-202.

Thiry, M., T. Cheutin, M.F. O'Donohue, H. Kaplan, and D. Ploton. 2000. Dynamics and three-dimensional localization of ribosomal RNA within the nucleolus. *RNA*. 6:1750-1761.

Thiry, M., and D.L. Lafontaine. 2005. Birth of a nucleolus: the evolution of nucleolar compartments. *Trends Cell Biol.* 15:194-199.

Thomas, G. 2000. An encore for ribosome biogenesis in the control of cell proliferation. *Nat. Cell Biol.* 2:E71-72.

Thompson, M., R.A. Haeusler, P.D. Good, and D.R. Engelke. 2003. Nucleolar clustering of dispersed tRNA genes. *Science*. 302:1399-1401.

Tian, H., R.E. Hammer, A.M. Matsumoto, D.W. Russell, and S.L. McKnight. 1998. The hypoxia-responsive transcription factor EPAS1 is essential for catecholamine

homeostasis and protection against heart failure during embryonic development. *Genes Dev.* 12:3320-3324.

Tomoda, K., Y. Kubota, and J. Kato. 1999. Degradation of the cyclin-dependent-kinase inhibitor p27Kip1 is instigated by Jab1. *Nature*. 398:160-165.

Tory, K., H. Brauch, M. Linehan, D. Barba, E. Oldfield, M. Filling-Katz, B. Seizinger, Y. Nakamura, R. White, F.F. Marshall, and et al. 1989. Specific genetic change in tumors associated with von Hippel-Lindau disease. *J Natl Cancer Inst.* 81:1097-1101.

Tsai, R.Y., and R.D. McKay. 2002. A nucleolar mechanism controlling cell proliferation in stem cells and cancer cells. *Genes Dev.* 16:2991-3003.

Tsai, R.Y., and R.D. McKay. 2005. A multistep, GTP-driven mechanism controlling the dynamic cycling of nucleostemin. *J. Cell Biol.* 168:179-184.

van den Boom, V., E. Citterio, D. Hoogstraten, A. Zotter, J.M. Egly, W.A. van Cappellen, J.H. Hoeijmakers, A.B. Houtsmuller, and W. Vermeulen. 2004. DNA damage stabilizes interaction of CSB with the transcription elongation machinery. *J. Cell Biol.* 166:27-36.

Verschure, P.J., I. van der Kraan, E.M. Manders, D. Hoogstraten, A.B. Houtsmuller, and R. van Driel. 2003. Condensed chromatin domains in the mammalian nucleus are accessible to large macromolecules. *EMBO Rep.* 4:861-866.

Visintin, R., E.S. Hwang, and A. Amon. 1999. Cfi1 prevents premature exit from mitosis by anchoring Cdc14 phosphatase in the nucleolus. *Nature*. 398:818-823.

von Dohlen, C.D., S. Kohler, S.T. Alsop, and W.R. McManus. 2001. Mealybug beta-proteobacterial endosymbionts contain gamma-proteobacterial symbionts. *Nature*. 412:433-436.

von Hippel, E. 1904. Ueber eine sehr seltene Erkrankung der Nethaut. *Graefe Arch. Ophthalmol.* 59:83-106.

Wada, H., E.T. Yeh, and T. Kamitani. 1999a. Identification of NEDD8-conjugation site in human cullin-2. *Biochem Biophys Res Commun*. 257:100-105.

Wada, H., E.T. Yeh, and T. Kamitani. 1999b. The von Hippel-Lindau tumor suppressor gene product promotes, but is not essential for, NEDD8 conjugation to cullin-2. *J Biol Chem*. 274:36025-36029.

Wagner, P.D. 2001. Skeletal muscle angiogenesis. A possible role for hypoxia. *Adv. Exp. Med. Biol.* 502:21-38.

Walther, R.F., C. Lamprecht, A. Ridsdale, I. Groulx, S. Lee, Y.A. Lefebvre, and R.J. Hache. 2003. Nuclear export of the glucocorticoid receptor is accelerated by cell fusion-dependent release of calreticulin. *J Biol Chem*. 278:37858-37864.

Wang, G.L., and G.L. Semenza. 1995. Purification and characterization of hypoxia-inducible factor 1. *J Biol Chem*. 270:1230-1237.

Wang, H., L. Zhai, J. Xu, H.Y. Joo, S. Jackson, H. Erdjument-Bromage, P. Tempst, Y. Xiong, and Y. Zhang. 2006. Histone H3 and H4 ubiquitylation by the CUL4-DDB-ROC1 ubiquitin ligase facilitates cellular response to DNA damage. *Mol Cell*. 22:383-394.

Warburg, O. 1931. The metabolism of tumors. R. R. Smith, New York. 129-163 pp.

Warburg, O. 1956. On the origin of cancer cells. *Science*. 123:309-314.

Waxman, L., J.M. Fagan, and A.L. Goldberg. 1987. Demonstration of two distinct high molecular weight proteases in rabbit reticulocytes, one of which degrades ubiquitin conjugates. *J Biol Chem.* 262:2451-2457.

Webb, S.D., J.A. Sherratt, and R.G. Fish. 1999. Alterations in proteolytic activity at low pH and its association with invasion: a theoretical model. *Clin Exp Metastasis.* 17:397-407.

Weber, J.D., M.L. Kuo, B. Bothner, E.L. DiGiammarino, R.W. Kriwacki, M.F. Roussel, and C.J. Sherr. 2000. Cooperative signals governing ARF-mdm2 interaction and nucleolar localization of the complex. *Mol. Cell. Biol.* 20:2517-2528.

Weber, J.D., L.J. Taylor, M.F. Roussel, C.J. Sherr, and D. Bar-Sagi. 1999. Nucleolar Arf sequesters Mdm2 and activates p53. *Nat. Cell Biol.* 1:20-26.

Weissman, A.M. 2001. Themes and variations on ubiquitylation. *Nat. Rev. Mol. Cell. Biol.* 2:169-178.

Wenger, R.H. 2002. Cellular adaptation to hypoxia: O2-sensing protein hydroxylases, hypoxia-inducible transcription factors, and O2-regulated gene expression. *FASEB J.* 16:1151-1162.

Wenger, R.H., I. Kvietikova, A. Rolfs, M. Gassmann, and H.H. Marti. 1997. Hypoxia-inducible factor-1 alpha is regulated at the post-mRNA level. *Kidney Int.* 51:560-563.

Wike-Hooley, J.L., J. Haveman, and H.S. Reinhold. 1984. The relevance of tumour pH to the treatment of malignant disease. *Radiother. Oncol.* 2:343-366.

Winter, A.G., G. Sourvinos, S.J. Allison, K. Tosh, P.H. Scott, D.A. Spandidos, and R.J. White. 2000. RNA polymerase III transcription factor TFIIIC2 is overexpressed in ovarian tumors. *Proc. Natl. Acad. Sci. USA*. 97:12619-12624.

Wizigmann-Voos, S., G. Breier, W. Risau, and K.H. Plate. 1995. Up-regulation of vascular endothelial growth factor and its receptors in von Hippel-Lindau disease-associated and sporadic hemangioblastomas. *Cancer Res*. 55:1358-1364.

Wykoff, C.C., C.W. Pugh, P.H. Maxwell, A.L. Harris, and P.J. Ratcliffe. 2000. Identification of novel hypoxia dependent and independent target genes of the von Hippel-Lindau (VHL) tumour suppressor by mRNA differential expression profiling. *Oncogene*. 19:6297-6305.

Xie, Y., and A. Varshavsky. 1999. The E2-E3 interaction in the N-end rule pathway: the RING-H2 finger of E3 is required for the synthesis of multiubiquitin chain. *Embo J.* 18:6832-6844.

Yamamoto, K., M. Yamamoto, K. Hanada, Y. Nogi, T. Matsuyama, and M. Muramatsu. 2004. Multiple protein-protein interactions by RNA polymerase I-associated factor PAF49 and role of PAF49 in rRNA transcription. *Mol. Cell. Biol.* 24:6338-6349.

Yu, F., S.B. White, Q. Zhao, and F.S. Lee. 2001. HIF-1alpha binding to VHL is regulated by stimulus-sensitive proline hydroxylation. *Proc. Natl. Acad. Sci. USA*. 98:9630-9635.

Appendix B – Published Highlights Discussing First-Author Papers

RESEARCH HIGHLIGHTS

Skeleton clocks

Cell **122,** 803-815 (2005)

The genes that make the body's circadian clock tick are also involved in controlling bone formation, according to a team led by Gerard Karsenty at Baylor College of Medicine in Houston, Texas. The findings offer avenues for tackling bone diseases such as osteoporosis in which bone density (pictured) decreases.

Bone formation has a daily rhythm, so Karsenty's team studied mice that had been genetically engineered to lack key clock genes. They found that such mice had heavier bones because they had more bone-building cells. The clock-gene proteins respond to signals from the hormone leptin and control the proliferation of these cells. Intriguingly, bone seems to be the only tissue where leptin acts through this pathway, suggesting this is an evolutionarily ancient and important aspect of leptin biology.

IMAGE UNAVAILABLE FOR COPYRIGHT REASONS

C. MUNOZ-YAGUE/EURELIOS/SPL

CHEMICAL BIOLOGY

Genomic miners

Nature Chem. Biol. doi:10.1038/nchembio731 (2005)

Finding natural compounds that have important medicinal properties has always been a laborious process of searching and purification.

Now, chemists have a powerful tool to speed up their hunts. A team at the University of Warwick, UK, has used the genome sequence of a bacterium to predict that it makes a particular molecule.

The team, led by Gregory Challis, studied DNA sequences from *Streptomyces coelicolor* (pictured below) and identified clusters of genes involved in biosynthesis. Using these, the group predicted the existence of an unknown molecule, which it then isolated from the bacteria and named coelichelin. This technique, which has been dubbed 'genome mining', could be used to discover other natural products.

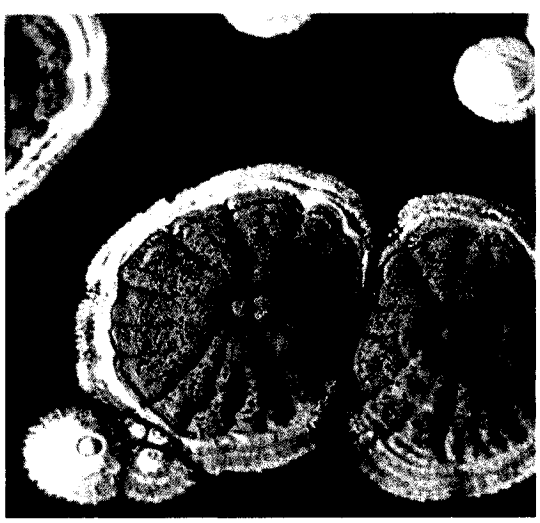

GENETICS

BRCA2 risk for men

J. Med. Gen. **42,** 711-719 (2005)

The *BRCA2* gene, which has been linked to hereditary breast cancer in women, is associated with an increased risk of prostate and pancreatic cancers in men, says a Dutch study.

Flora van Leeuwen of the Netherlands Cancer Institute in Amsterdam and her colleagues investigated 139 families with 66 different mutations of the *BRCA2* gene. They studied the incidence of cancers among family members who had a 50% chance of carrying the mutant gene. The team compared these incidences with those expected in the general population and found increased risks of pancreatic and prostate cancers in men under the age of 65. Male *BRCA2* carriers may also have a greater risk of bone and throat cancers.

CELL BIOLOGY

Bound and gagged

J. Cell Biol. **170,** 733-744 (2005)

Cells can control the activity of enzymes by locking them up in a nuclear structure called the nucleolus, say researchers in Canada.

Stephen Lee and colleagues from the University of Ottawa, Ontario, studied two enzymes called ubiquitin ligases. When active, these attach a molecule called ubiquitin to proteins. This alters a protein's destiny, often signalling its destruction.

The enzymes studied are normally mobile and control the addition of ubiquitin to HIF (hypoxia-inducible factor) and p53, a tumour-suppressor protein. But when temporarily captured in the nucleolus, the enzymes are denied access to these molecules. The researchers propose that cells have evolved a mechanism to regulate the function of proteins by switching the enzymes between mobile and static states.

NEUROBIOLOGY

Wrap artist

Neuron **47,** 681-694 (2005)

A gene known as *neuregulin* helps to provide the insulating coat that certain nerve cells require. James Salzer of the New York University School of Medicine and his co-workers show that switching on this gene triggers the production of myelin. This fatty material envelopes some neurons and allows them to send signals up to 100 times faster than their bare counterparts. The team studied mouse neurons that are normally myelinated but had been engineered to lack both copies of the *neuregulin-1 type III* gene; these cells remained bare. The researchers also discovered that neurons that are usually unmyelinated acquire the protective layer when altered to express the gene.

STEM CELLS

Keep your options open

Cell **122,** 1-10 (2005)

One big question about embryonic stem cells is how they maintain their potential to form

any cell type in the body — an ability known as pluripotency. Now, a team headed by Richard Young at the Massachusetts Institute of Technology sheds light on the cellular control circuits involved.

The researchers studied three proteins called OCT4, SOX2 and NANOG, which control gene activity and are known to be important for pluripotency. Working with human stem cells, the team scanned the whole genome and identified the genes controlled by these proteins.

In many cases, the three proteins acted together on the same genes, activating those involved in pluripotency and division, and repressing those that direct embryonic development.

IMMUNOLOGY

Barrier method

Nature Immunol. **6,** 995-1001 (2005)

A newly discovered 'firewall' that protects our cells against viral invasion could be exploited to develop antiviral drugs, say US researchers.

Roughly half of the viruses that cause human disease are surrounded by a membrane. These invaders, which include flu viruses and HIV, need to fuse their membranes with those of their host cells to enter them.

A team led by Leonid Chernomordik at the National Institutes of Health in Bethesda, Maryland, has found that a set of peptides called defensins, which form part of our innate immune system, can block this fusion. In tests on cultured human cells, they showed that defensins reversibly link cell surface proteins together, forming a barrier that stops the membranes getting close enough to fuse.

CANCER

A sticky situation

Nature Genet. doi:10.1038/ng1635 (2005)

A variant of a gene called *Sipa1* seems to play a key role in helping tumours to spread. Kent Hunter of the National Cancer Institute in Bethesda, Maryland, and his colleagues have found that damping the expression of *Sipa1* significantly slows tumour spread in mice. And engineering tumour cells to make extra Sipa1 protein doubles the chance that they grow and disperse. The team shows this extra protein can cause a cell to lose its adhesive properties, perhaps freeing it to colonize other organs. Tumours that have spread from human prostate cancers also express abnormally high levels of *Sipa1*.

PLANETARY SCIENCE

Dust buster

Science doi:10.1126/science.1118923 (2005)

On 4 July 2005, NASA's Deep Impact mission slammed a probe into Tempel 1 to find out what lies in a comet's interior. The resulting series of papers reveal detailed quantitative data on the comet's composition and structure. In an overview paper, Michael A'Hearn of the University of Maryland, College Park, and his colleagues describe how Tempel 1 is covered in impact craters, which have never been seen before on comets. The surface of Tempel 1 has surprising features, with both old- and young-looking terrains, and signs of past geological processes. The comet consists of very fine, loose particles, and its interior contains organic compounds.

M. VAN WOERT/NOAA NESDIS/ORA

GEOMORPHOLOGY

Chillout dunes

Geology **33,** 753-756 (2005)

The last place most people would look for an ice sheet, such as the one pictured above, is the Sahara Desert. But that is where Julien Moreau of the School and Observatory of Earth Sciences in Strasbourg and his colleagues have found one. It isn't there any more, naturally; it existed about 440 million years ago, when Africa was part of the supercontinent of Gondwana situated over the South Pole.

Moreau and his team have found signatures of glaciation — scratches and ridges in rocks and elongated deposits called drumlins — near the town of Ghat on the border of Algeria and Libya.

These features were made by an ice stream, a fast-flowing section of an ice sheet, and they are the oldest clear evidence of such streams yet found.

JOURNAL CLUB

Frank Wilczek
Massachusetts Institute of Technology, Cambridge, USA

The promise that anyon particles hold for quantum computing excites the physicist who named them.

When I first worked on — and named — anyons in the early 1980s, I thought these particles, whose quantum behaviour goes beyond the familiar categories of bosons and fermions, were an interesting theoretical curiosity.

To my amazement, anyons soon appeared in the theory of the quantum Hall effect, which describes the odd modifications of electronics that occur at low temperatures in strong magnetic fields. But relevant experiments are difficult, and have been a long time coming.

Now Fernando Camino of Stony Brook University in New York and colleagues report observations of peculiarities in the quantum Hall effect that they interpret as the first experimental indication of anyon behaviour (http://www.arxiv.org/cond-mat/0504341; 2005). In a separate paper (http://www.arxiv.org/cond-mat/0412343; 2005), Sankar Das Sarma from the University of Maryland and his colleagues propose a refined experimental arrangement, which could be used both to clarify this behaviour and to make it useful for quantum computing.

Anyons become useful for quantum computing when they wind around each other, so that their world lines form tangles in space-time. The different tangles represent states in Hilbert space, the vast arena of quantum mechanics, and can be used to store information. Hilbert space is big enough to accommodate very complicated tangles, so huge storage and bandwidth could be in the offing.

The theory of anyons has spawned some beautiful but specialized and difficult mathematics, hitherto pursued only by a small cult. I suspect that many of my colleagues have, like me, been waiting for a pretext to dive back in. With these two papers, we have it.

In This Issue

Hiding proteins in the nucleolus

Cells regulate metabolic pathways by rigidly locking enzymes in the nucleolus, report Mekhail et al. on page 733. Two ubiquitin ligase enzymes bind in the nucleolus in response to signals that block their activity.

Ubiquitin tagging alters protein fates, often marking substrates for degradation. Regulation of the process occurs at the level of the ubiquitin ligases, called E3s, which facilitate the transfer of ubiquitin from a conjugating enzyme to the target protein. Several E3 proteins aggregate in the nucleolus in response to inhibitory signals. The new results show that two different E3 enzymes, MDM2 and von Hippel-Lindau tumor suppressor (VHL), become immobilized in the structure and probably bind nucleolar scaffold proteins.

In the presence of oxygen, VHL tags the hypoxia-inducible factor (HIFα), causing its degradation. The authors identified a domain within VHL that detects increased acidity, such as occurs during hypoxia, and somehow induces VHL to move to the nucleolus from the cytoplasm and nucleoplasm, where it normally resides.

Although nucleolar proteins involved in ribosome synthesis move in and out of the structure constantly, the authors saw that VHL was static in the nucleolus, based on FRAP, FLIP, and heterokaryon experiments. Upon neutralization of the culture medium, VHL was released from the nucleolus and resumed its dynamic lifestyle.

MDM2, an E3 that induces the degradation of the p53 tumor suppressor protein, also became fixed in the nucleolus in response to actinomycin-D treatment, which is known to block p53 ubiquitylation.

The authors propose that such nucleolar sequestration, and more generally the concept of switching proteins between a mobile and static state, is likely to be a commonly used mechanism for regulating enzyme reactions. The hypothesis is boosted by preliminary experiments, which indicate that numerous proteins have domains similar to the one that directs VHL's nucleolar targeting. JCB

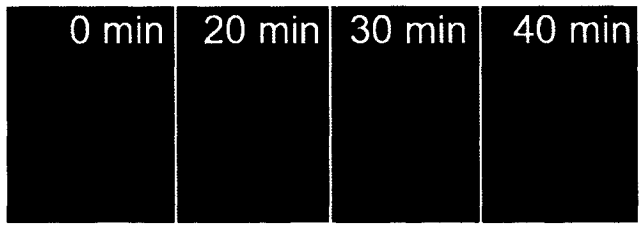

Acidity, as during hypoxia, targets VHL (green) to the nucleous (right).

Immortal DNA

Karpowicz et al. (page 721) report evidence for asymmetric segregation of the oldest DNA during neural stem cell proliferation.

According to the immortal strand hypothesis, which was first proposed in the mid-1970s, stem cells actively retain the oldest DNA during asymmetric cell divisions. That DNA should, statistically speaking, contain fewer replication-induced errors than DNA resulting from more rounds of replication. While tantalizing for its logic, the hypothesis has been controversial, and numerous studies have failed to find evidence for it.

Working with mouse neural stem cells, the authors labeled cells with BrdU and then looked at how the DNA segregated. When populations of cells were labeled, dispersed into single cells, and allowed to proliferate, they gave rise to neurospheres that frequently contained a few BrdU-labeled cells. The retention of the label after numerous divisions suggested that labeled DNA was asymmetrically segregated to just a limited number of cells, rather than evenly distributed as would be expected if the chromosomes were randomly sorted.

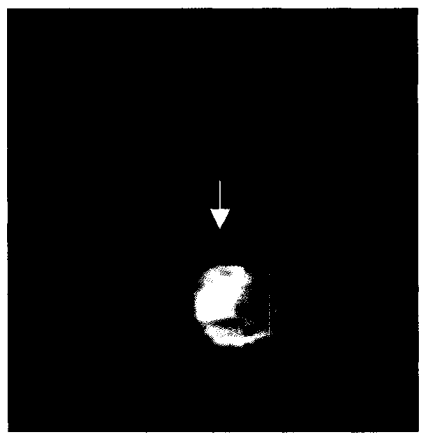

BrdU (green) localizes to only one of two nuclei (red) in a dividing neural stem cell.

To see whether this interpretation was correct, the team watched clones form under the microscope. A single cell was labeled with BrdU during one division. Subsequent imaging showed evidence of asymmetric segregation of the BrdU-labeled DNA in 6 out of 15 lines.

Similar experiments failed to show evidence for asymmetric retention of older DNA in mouse embryonic stem cells or a fibroblast cell line derived from mouse embryos. Thus, neural stem cells may be particularly fussy about their DNA relative to other stem cell types. If it is true that only some stem cells follow the immortal strand hypothesis, that might explain why previous experiments did not find evidence supporting the hypothesis.

The authors are now turning to other stem cell systems in mice and other metazoans to see whether they can replicate their findings in different contexts—and try to convince still-skeptical colleagues that the immortal strand hypothesis holds value. JCB

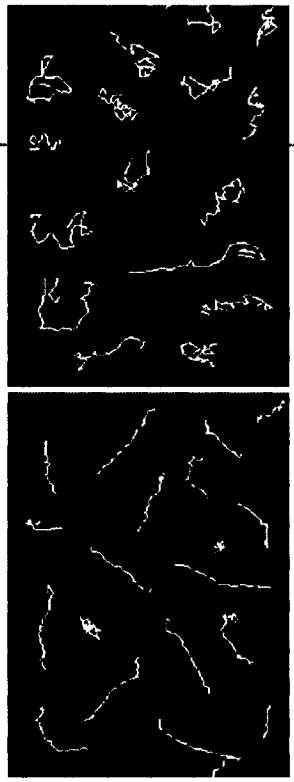

Reduced Rac activation (bottom) leads to more persistent migration.

Text by Rabiya S. Tuma
rabiya@nasw.org

A little Rac goes a long way

A slight reduction in the amount of Rac allows cells to move in a more persistent direction, report Pankov et al. on page 793.

The small GTPases Rac and Rho modulate migration speed and chemotaxis, with increased expression of Rac in lamellipodia correlating with increased velocity. In the current study, Pankov et al. found that reducing the total amount of Rac1 in a cell by 30% to 50% induced persistent movement and limited random walking. The reduction in Rac reduced the number of lamellae, leaving such structures only at the cell ends. By contrast, knocking down RhoA reduced the rate of migration but did not alter migration style.

Unlike chemotaxis, which also induces persistent movement, the newly identified Rac function did not require phosphatidylinositol 3′ kinase activity, indicating that the two methods of migration control are distinct. Rac activity was affected by the cell environment, however. Cells grown in two-dimensional tissue culture had more Rac and moved in a more random fashion than those grown in a three-dimensional matrix, even when the molecular composition of the two substrates was identical. Rac activity was also dependent on β1 integrin, as expected from previous studies.

Given the strength of Rac's influence, the authors speculate that such internal control of migration style might allow cells to switch between exploring their environment through random migration to moving as a group in one direction, as they do during wound healing and development. Now the trick will be to find tools that are sensitive enough to see such small changes in Rac levels in vivo, so that the hypothesis can be tested. JCB

When it comes to cadherin regulation, it is not all about α- and β-catenins. *Drosophila* epithelial cadherin requires a novel regulatory region for cell migration in developing ovaries, according to Pacquelet and Rørth (page 803).

Cadherins are used in cell–cell adhesion and migration in a variety of tissues. The cytoplasmic tail of cadherin contacts the actin cytoskeleton through α- and β-catenin. Studies in tissue culture cells suggested that modulating the interaction between cadherin and the catenins would alter the adhesion strength of cadherin and facilitate migration.

To test whether such mechanisms work in vivo, the authors fused the full-length cadherin or just its transmembrane domain to α- or β-catenin. The full-length cadherin–α-catenin fusion rescued cell–cell interactions and migration in tissues lacking wild-type DE-cadherin or β-catenin. Thus no modulation is required between DE-cadherin and α-catenin for normal migration. If the link between DE-cadherin and the actin cytoskeleton needs to be tempered in vivo, the tempering must happen downstream of α-catenin.

Removing the cytoplasmic tail of cadherin in the α-catenin fusion protein blocked migration in the ovary, though adhesion was normal. Although the specific mechanisms are not yet known, the authors think that this cadherin cytoplasmic domain is required to maximize adhesion force during migration. JCB

Sticky interactions

Upon infection with *Neisseria gonorrhoeae*, human epithelial cells typically float off the underlying extracellular matrix, reducing the bacterial burden for the host. Now, Muenzner et al. (page 825) show that variants of *N. gonorrhoeae* and other bacterial pathogens that bind to certain cell–cell adhesion molecules can inhibit this shedding, thus increasing the bacteria's ability to colonize their hosts.

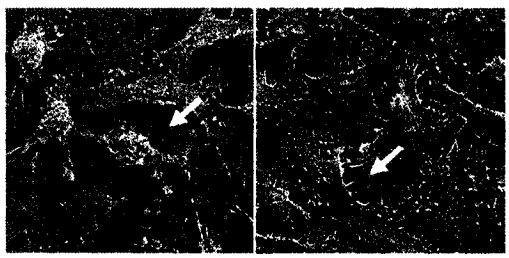

***Neisseria gonorrhoeae* that bind CEACAMs induce greater cell–cell adhesion (right) and less cell shedding.**

The adhesion molecules under study are carcinoembryonic antigen-related cell adhesion molecules (CEACAMs), which are thought to be involved in microbial infection. CEACAM engagement by the bacteria triggered expression of CD105, a TGFβ-like receptor that helps organize focal adhesions. In turn, CD105 expression increased host cell adhesion by activating integrins.

No physical association was detected between CEACAMs and CD105 or between CD105 and integrins, so the molecular mechanisms of the pathway are unclear. However, it is apparent that CEACAMs induce CD105 transcription without direct cytoplasmic signaling. CEACAM-6 naturally lacks a cytoplasmic domain and can trigger the response, as can a CEACAM-1 mutant lacking its cytoplasmic tail.

N. gonorrhoeae isolated from patient samples often contain a disproportionate fraction of bacteria that bind CEACAMs, even in controlled experiments where the infection started with bacterial cells that did not bind CEACAMs. The next question is whether bacteria that are beneficial to humans hosts also use CEACAMs. If not, blocking the reaction may be a viable antibacterial strategy. JCB

Meeting Report

Driven together by entropy

The tendency of large complexes to congregate drives the organization of the genome and other cellular structures, according to Peter Cook (University of Oxford, UK).

In a crowded, enclosed space (such as the cell), the aggregation of two large spheres increases the system's entropy by giving lots of little molecules more room to move around. In physics, this effect is known as depletion attraction. Using mathematical modeling, Cook and colleagues found that this attraction explains the looping of DNA found naturally in cells.

The model is based on transcription and replication complexes that are spaced along DNA like beads on a string. Measurements of the attraction between the "beads" suggest that the entropy gained by their clustering is enough to cover the energy costs of looping the DNA string between them.

In vivo, the effects are seen as the clustering of active genes and the looping of highly transcribed genomes. As predicted, in slow-growing cells, which have little replication and transcription, polymerases did not cluster.

According to Cook, other large cellular structures are always trying to congregate. The cell must therefore fight the depletion attraction. "Otherwise, everything would become one big blob," he says.

This entropic effect might explain why the size of stable complexes is limited to that of a ribosome. It also explains why larger structures, such as the cytoskeleton, are made by loosely associated subunits that constantly turn over. "The cell is spending energy," says Cook, "to maintain the structure." Energy is similarly expended to keep pools of vesicles from fusing into one by turning over their surfaces. Cook explains, "if the vesicles are continually being broken up into smaller pieces that quickly diffuse away, the attraction becomes smaller." JCB

Reference: Marenduzzo, D., et al. 2006. *Biophys. J.* 90:3712–3721.

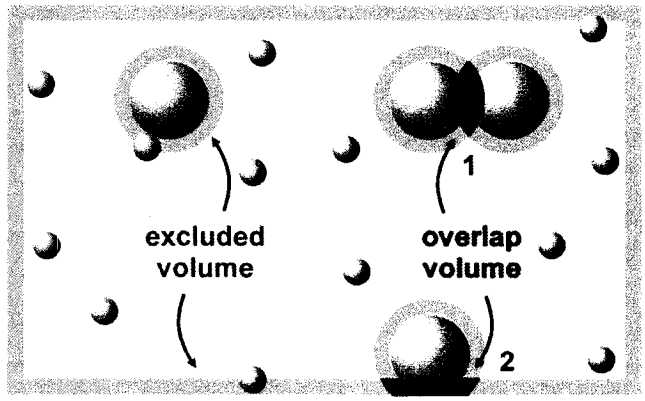

COOK/BIOPHYSICAL SOCIETY

Clustering of large complexes gives smaller ones more room to move.

Genetic postal codes

Transcriptional control elements are like zip codes for genes, based on new findings presented by Barbara Sollner-Webb (Johns Hopkins University, Baltimore, MD). Thousands of copies of transfected plasmids find a common area to inhabit if they share the same zip code, sorted away from plasmids with different zip codes.

"That endogenous genes have specific locations is not so surprising," said Sollner-Webb. "But why are ribosomal genes [for instance] inside the nucleolus? What gets them there?" Her group's findings, although using exogenous DNA, may offer the best explanation so far.

During transient transfection experiments, the group noticed that tens of thousands of copies of a plasmid went to the same location in the mammalian nucleus. The locale was promoter specific. Plasmids containing RNA polymerase (RNAP) I promoter sequences were found only in nucleoli, whereas those with RNAP III promoter sequences formed perinucleolar foci. RNAP II promoters took the plasmid DNA to nucleoplasmic foci, but different promoter sequences resulted in different foci.

The zip codes seem to be read by transcription factors. As even untranscribed plasmids localized in this manner, polymerase activity is not necessary. The perinucleolar localization required just an 18- or 26-base-pair region that binds to TFIIIA or TFIIIC, respectively. These RNAP III factors are found throughout the nucleus, but Sollner-Webb hypothesizes that the subset in these perinuclear foci is special, either because it is bound to DNA or because it is modified (by phosphorylation, for example) to favor DNA binding. Most RNAP I transcription factors are already concentrated in the nucleoli.

RNAP I transcription factors are probably abundant enough, based on published estimates, for each plasmid to have its own copy. Life might be more complicated for less abundant RNAP II factors. The modularity of RNAP II promoters suggests that multiple sequence elements and transcription factors might be necessary. JCB

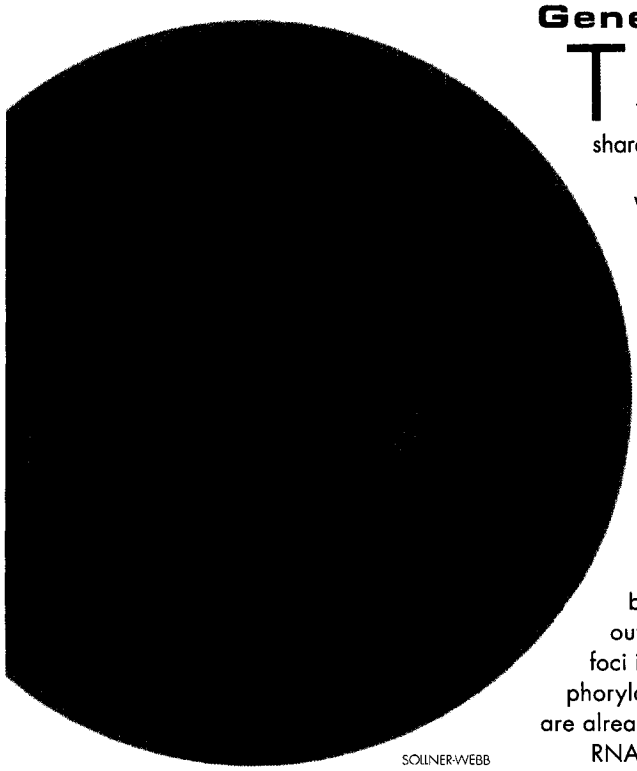

SOLLNER-WEBB

Plasmids with an RNAP I promoter (red) sort to nucleoli, away from plasmids with an RNAP II promoter (green).

Text by Nicole LeBrasseur
lebrasn@rockefeller.edu

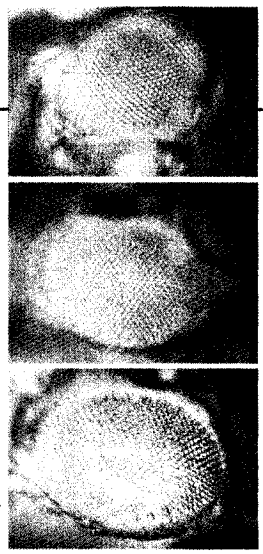

CAVALLI/ELSEVIER

The silencing of eye color (top) is lost in RNAi mutants (bottom two panels).

RNAi and Polycombs cooperate

The RNA interference (RNAi) machinery holds together copies of silencing elements from multiple genes, as described by Giacomo Cavalli (CNRS, Montpellier, France). This group hug reinforces developmental gene silencing.

The silenced state of a developmentally regulated homeotic gene is maintained by chromatin-modifying Polycomb group (PcG) proteins. PcG response elements (PREs), the DNA sequences that recruit PcG proteins, are self locating: PRE-containing sequences from multiple genes travel long distances to cluster with each other, and this association enhances the transcriptional silencing.

The silencing that accompanies heterochromatin formation in yeast requires RNAi components. Cavalli's group has found that PcG-mediated euchromatin silencing also depends on RNAi proteins. Silencing of multiple PRE-containing genes was relieved in fly mutants lacking RNAi proteins such as AGO1 and Dicer-2. PcG proteins were still recruited to their targets, but clustering was lost.

The glue for the PRE clusters seems to be small RNAs. Several species of small RNAs were found that matched the PRE region, and their production depended on the RNAi machinery. Clustering correlates with the presence of small RNAs, but Cavalli has not yet ruled out protein–protein interactions as the cause.

The physical properties of a nanocompartment such as a PRE cluster might help to reinforce silencing. Chromatin rearrangements might be more difficult, or PcG proteins less mobile. Cavalli plans to test the latter theory using GFP-tagged PcG proteins. JCB

Reference: Grimaud, C., et al. 2006. *Cell.* 124:957–971.

RNAs regulate rRNAs

RNAs transcribed from between ribosomal genes alter the chromatin structure and thus silence their rRNA-coding neighbors, as discussed by Ingrid Grummt (German Cancer Research Center, Heidelberg, Germany).

Ribosomal genes are in vast excess in the mammalian genome. Of 400 or so copies of rRNA genes, about half are permanently silenced after embryogenesis. Their heterochromatic state is induced by a complex called NoRC, which recruits histone-modifying enzymes to rDNA. When Grummt and colleagues noticed that RNase treatments dispersed NoRC from the nucleoli, they began searching for an RNA component.

The group has since found that the RNAs responsible for targeting NoRC to chromatin originate from spacer regions that separate individual rRNA genes. Like the rRNA genes, the spacer RNAs are transcribed by RNA polymerase I. The RNAs bind to a subunit of NoRC, and this association is necessary for NoRC to grab onto the rRNA chromatin.

The intergenic RNAs are a few hundred base pairs long and are complementary to the rRNA gene promoter. They have the potential to base-pair with the promoter as well as bind to NoRC, with the latter association depending more on RNA secondary structure than on specific sequence. JCB

Reference: Mayer, C., et al. 2006. *Mol. Cell.* 22:351–361.

Static for silencing

Oxygen-starved cells conserve their limited energy by shutting down ribosome production. In his talk, Stephen Lee (University of Ottawa, Ottawa, Canada) suggested that cells silence ribosomal genes during hypoxia by locking a ubiquitin ligase in the nucleolus.

In abundant oxygen, this ubiquitin ligase, called VHL, is a free-moving protein that keeps hypoxia-induced factor α (HIFα) levels low. But when cells are using anaerobic metabolism pathways, the resulting decrease in pH somehow causes VHL to stick in the nucleolus, where it cannot curb HIFα.

Until this immobile form of VHL was identified, the only other known static protein was histone H2B, which silences chromatin. All other tested proteins exchange dynamically. Based on a supposed need for protein exchange during chromatin remodeling, Tom Misteli (NIH, Bethesda, MD) proposed in 2001 that static proteins in general might induce transcriptional silencing.

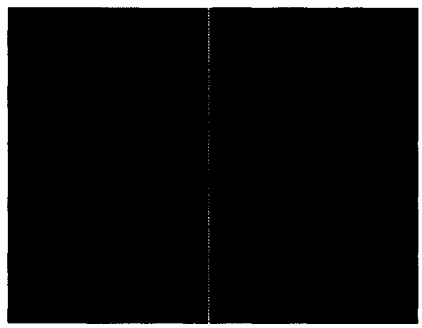

At low pH, the locking of VHL (green) in nucleoli (right) silences rDNA.

Now with VHL in hand as a second immobile protein, Lee's group has put Misteli's hypothesis to the test. They found that VHL is indeed required to silence rRNA genes and thereby protect cells from hypoxia-induced death. The return of oxygen is expected to free VHL from the chromatin and restore rRNA synthesis. Lee was still unclear, however, how a ubiquitin ligase—or degradation of its substrate—is able to remodel chromatin to bring about silencing. JCB

References: Mekhail, K., et al. 2005. *J. Cell Biol.* 170:733–744.
Misteli, T. 2001. *Science.* 291:843–847.

Appendix C – Additional Publications

THE JOURNAL OF BIOLOGICAL CHEMISTRY
Vol. 278, No. 45, Issue of November 7, pp. 44966–44974, 2003
Printed in U.S.A.

Hypoxia Inducible Factor Activates the Transforming Growth Factor-α/Epidermal Growth Factor Receptor Growth Stimulatory Pathway in VHL$^{-/-}$ Renal Cell Carcinoma Cells*

Received for publication, May 27, 2003, and in revised form, August 12, 2003
Published, JBC Papers in Press, August 27, 2003, DOI 10.1074/jbc.M305502200

Lakshman Gunaratnam‡§, Melissa Morley‡¶, Aleksandra Franovic‡, Natalie de Paulsen‡, Karim Mekhail‡, Doris A. E. Parolin‖, Eijiro Nakamura, Ian A. J. Lorimer‖, and Stephen Lee‡ ‡‡**

*From the ‡Department of Cellular and Molecular Medicine and Kidney Research Center, the §Department of Internal Medicine, and the ‖Ottawa Regional Cancer Center and Department of Biochemistry and Immunology, Faculty of Medicine, University of Ottawa, Ottawa, Ontario K1H 8M5, Canada, and the **Howard Hughes Medical Institute, Dana-Farber Institute, Harvard University, Boston, Massachusetts 02115*

Bi-allelic-inactivating mutations of the VHL tumor suppressor gene are found in the majority of clear cell renal cell carcinomas (VHL$^{-/-}$ RCC). VHL$^{-/-}$ RCC cells overproduce hypoxia-inducible genes as a consequence of constitutive, oxygen-independent activation of hypoxia inducible factor (HIF). While HIF activation explains the highly vascularized nature of VHL loss lesions, the relative role of HIF in oncogenesis and loss of growth control remains unknown. Here, we report that HIF plays a central role in promoting unregulated growth of VHL$^{-/-}$ RCC cells by activating the transforming growth factor-α (TGF-α)/epidermal growth factor receptor (EGF-R) pathway. Dominant-negative HIF and enzymatic inhibition of EGF-R were equally efficient at abolishing EGF-R activation and serum-independent growth of VHL$^{-/-}$ RCC cells. TGF-α is the only known EGF-R ligand that has a VHL-dependent expression profile and its overexpression by VHL$^{-/-}$ RCC cells is a direct consequence of HIF activation. In contrast to TGF-α, other HIF targets, including vascular endothelial growth factor (VEGF), were unable to stimulate serum-independent growth of VHL$^{-/-}$ RCC cells. VHL$^{-/-}$ RCC cells expressing reintroduced type 2C mutants of VHL, and which retain the ability to degrade HIF, fail to overproduce TGF-α and proliferate in serum-free media. These data link HIF with the overproduction of a *bona fide* renal cell mitogen leading to activation of a pathway involved in growth of renal cancer cells. Moreover, our results suggest that HIF might be involved in oncogenesis to a much higher extent than previously appreciated.

von Hippel-Lindau (VHL)[1] disease is a hereditary cancer syndrome, which predisposes patients to a variety of highly vascularized tumors including retinal angioma, central nervous system hemangioblastoma, pheochromocytoma, endolymphatic sac tumors, and clear cell renal carcinoma (RCC) (1, 2). VHL syndrome is caused by the inheritance of germ-line mutations of the VHL tumor suppressor gene. Although VHL follows an autosomal dominant pattern of inheritance (3), tumor formation arises only when the remaining wild-type allele acquires a somatic inactivating mutation as predicted by Knudson's two-hit hypothesis (4). Bi-allelic-inactivating mutations of the VHL gene are also found in the majority of sporadic clear cell renal cell carcinomas, the most common malignancy of the human kidney (VHL$^{-/-}$ RCC) (5, 6). Reintroduction of the VHL gene into VHL$^{-/-}$ RCC cells (hereafter referred to as "VHL(+)" cells) abolishes their ability to form tumors in nude mice, suggesting that loss of VHL function is a prerequisite for tumor formation (7). Furthermore, VHL$^{-/-}$ RCC cells display several key features of transformed cells, including the inability to form an extracellular fibronectin matrix (8) and the loss of dependence on exogenous growth factors for proliferation in culture (9, 10). These features can be corrected by the reintroduction of VHL.

VHL forms a complex with several proteins including elongin B, elongin C, cullin-2, and Rbx1 to form a multiprotein complex referred to as VBC/Cul-2 (11). VBC/Cul-2 displays E3-ubiquitin ligase activity *in vivo* and *in vitro* (12–17). VHL acts as the recognition particle of this complex recruiting the α-subunit of hypoxia-inducible factor (HIFα) for cullin-2-mediated ubiquitination and subsequent proteasomal degradation (8, 18–21). The HIF transcription factor assembles as a heterodimer containing one of three different α-subunits and a β-subunit, and together, regulates the expression of several genes involved in the cellular response to hypoxia (22). These genes include the glucose transporter-1 (Glut-1), erythropoeitin, and the angiogenic factor, vascular endothelial growth factor (VEGF) (22). While the HIFβ subunit is constitutively expressed (21), the HIFα subunits accumulate only under conditions of low oxygen tension. HIFα regulation is mediated by oxygen-dependent hydroxylation of a conserved proline residue on its oxygen-dependent degradation domain (23 ,24–28). This post-translational modification increases HIFα affinity toward VHL, leading to its ubiquitination and subsequent degradation. VHL-deficient RCC cell lines fail to degrade HIFα irrespective of ambient oxygen tension (21, 29–32). HIF activation is an

* This work was supported by a grant from the Kidney Foundation of Canada and grant from the Canadian Institute of Health Research (CIHR). The costs of publication of this article were defrayed in part by the payment of page charges. This article must therefore be hereby marked "*advertisement*" in accordance with 18 U.S.C. Section 1734 solely to indicate this fact.

¶ Supported by a studentship from the Natural Science and Engineering Research Council of Canada.

‡‡ Recipient of the Harold E. Johns Research Scientist Award of the National Cancer Institute of Canada. To whom correspondence should be addressed: Dept. of Cellular and Molecular Medicine, Faculty of Medicine, University of Ottawa, 451 Smyth Rd., Ottawa, Ontario K1H 8M5, Canada. Tel.: 613-562-5800 (ext. 8385); Fax: 613-562-5636; E-mail: slee@uottawa.ca.

[1] The abbreviations used are: VHL, von Hippel-Lindau; DMEM, Dulbecco's modified Eagle's medium; FCS, fetal calf serum; PBS, phosphate-buffered saline; GFP, green fluorescent protein; ELISA, enzyme-linked immunosorbent assay; BrdUrd, bromodeoxyuridine.

immediate event upon VHL loss in early multicellular foci in the distal nephron associated with expression of its target genes including Glut-1 and VEGF (33). Angiogenesis is considered a key step in tumor progression (34) implying a fundamental role for HIF in the later stages of tumor progression. However, the link between VHL loss, HIF activation, and how this relates to loss of growth control remains a key unanswered question.

Cancer cells are generally capable of engaging in autonomous growth as reflected by their ability to proliferate in serum-free conditions (35–38). We previously reported that VHL$^{-/-}$ RCC cells are also able to proliferate in the absence of exogenous growth factors and that this defect is correctable by the reintroduction of VHL (10). Transforming growth factor-α (TGF-α) was identified as a potential agent responsible for serum-independent growth of VHL$^{-/-}$ RCC cells. Several pieces of evidence point toward an oncogenic role for TGF-α in VHL$^{-/-}$ RCC cells. First, overproduction of TGF-α and its cognate epidermal growth factor receptor (EGF-R) has been described in overt sporadic RCC tumors *in vivo* (39–44). Second, antisense oligonucleotides directed against TGF-α mRNA abolished serum-independent growth of VHL$^{-/-}$ RCC cells (10). Third, treatment with inhibitors of EGF-R is as efficient as reintroducing VHL at abolishing the ability of RCC cells to form tumors in nude mice (7, 45, 46). However, the mechanism linking VHL loss-of-function to TGF-α overexpression, including the relative contribution of HIF activation to proliferation of VHL$^{-/-}$ RCC cells, remains unknown. In this report, we show that HIF activation is required for serum-independent growth of VHL$^{-/-}$ RCC cells, and this is a consequence of the activation of the EGF-R. We also show that HIF activation is required for overproduction of a TGF-α, an EGF-R ligand and *bona fide* renal cell mitogen. We thus provide the first direct evidence for a mechanism linking HIF activation with its postulated role in oncogenesis in VHL$^{-/-}$ RCC cells.

EXPERIMENTAL PROCEDURES

Cells and Cell Culture—The human sporadic RCC cell line 786-0 contains a single mutated VHL allele predicted to encode a truncated VHL protein. The 786-0 (VHL$^{-/-}$) renal clear cell line (*i.e.* the RCC cells) and the A498 cells were obtained from the American Type Culture Collection (Manassas, VA). The WT-7 (VHL(+)) cell line is derived from 786-0 cells stably transfected with hemagglutinin (HA)-tagged VHL, a kind gift from William Kaelin, Harvard University. The Type 2C VHL cell lines (stable transfectants of 786-0 cells with pVHL L188V, pVHL R64P, and pVHL F119S) were a kind gift from Dr. W. Kaelin (47). Cells were maintained in Dulbecco's modified Eagle's medium (DMEM) supplemented with 10% (v/v) fetal calf serum (FCS) in a 37 °C, humidified 5% CO_2 atmosphere incubator. Hypoxia treatment was performed in a hypoxic chamber with 1% O_2 atmosphere and tempered at 37 °C.

Viral Expression Vectors—The wild-type HIF-2α cDNA in pcDNA3.1 was PCR-amplified with primerEPAS-1-DN 5′*Bam*HI(AGCTGGATCCGCATGGACTACAAAGACGATGACGATAAAACAGCTGACAAGGAGAAGAAAAGGAGTAGC) and primer EPAS-1-DN-3′*Not*I (ACGTGCGGCCGCTCAAGGGCTATTGGGCGTGGAGCAGCTGCTGCTGC) to yield a truncated HIF-2α (amino acids 1–485), restricted with *Bam*HI and *Not*I, and ligated into pAdlox-GFP (kind gift from Dr. David Park, University of Ottawa, Ottawa, Ontario, Canada) to produce an adenovirus that expresses DNHIF. Other adenoviruses were generated as described elsewhere (29, 48). All constructs were authenticated by DNA sequencing.

Construction of Adenovirus through Cre-Lox Recombination—CRE8 and 293 cells were obtained from Dr. David Park and cultured in DMEM with 10% FCS. The properties of CRE8 cells are described elsewhere (49). Transfections were done according to Graham and van der Eb (50). Typically, a confluent 10-cm diameter dish of CRE8 cells (1.6×10^7) was split into 5–6-cm diameter dishes for transfection 2–4 h later. Each dish received 3 μg of pAdlox vector (containing the foreign VHL/HIF construct) and 3 μg of 5 viral DNA in a final volume of 0.5 ml of $CaPO_4$, which was applied to the cells for 16 h. The 10% fetal calf serum DMEM was changed for 2% fetal calf serum DMEM 16 h following the transfection. Cells were fed with fresh 2% DMEM after 64 h. Between day 8 and 10, we had a sizable infection in each dish, almost all of the cells were rounded up or floating. Cells were harvested and subjected to freeze/thaw three times with an alternating liquid N_2/37 °C water bath. Finally, a plaque purification assay was performed in order to isolate the recombinant viruses, which were amplified in CRE8 cells to a higher titer.

Measurement of TGF-α Expression in Cell Lysates—VHL$^{-/-}$ and VHL-positive RCC cells were plated approaching confluence, in DMEM and 10% FCS. After 48–60 h incubation at normoxic conditions (5% CO_2 plus room air) cells were washed, trypsinized, and lysed according to ELISA kit instructions (Oncogene). TGF-α levels were normalized to total cellular protein content (μg) as determined by the BCA method (Pierce).

Tyrosine Kinase Inhibition Experiments—PD153035 (Calbiochem, San Diego, CA), an EGFR tyrosine kinase inhibitor (51), AG1296 (Calbiochem), a platelet-derived growth factor receptor inhibitor, FGF receptor tyrosine kinase inhibitor (52), and Tranilast (53), a vascular endothelial factor inhibitor (Calbiochem) were resuspended in Me_2SO and added to cells maintained in DMEM or ITS to achieve concentrations of 1–10 μM (PD153035), 50 μM (AG1296), and 80 μM Tranilast. Neutralizing antibody to TGF-α was purchased from Calbiochem and used at a concentration suggested by the manufacturer.

Western Blot Analysis—Cells were washed with PBS and lysed in 4% SDS in PBS, and the DNA was sheared with a 20-gauge needle. Protein concentration was quantified with a bicinchoninic acid assay (Pierce), and 20–50 μg of protein was analyzed on an SDS/8% polyacrylamide gel. Proteins were transferred to a polyvinylidene difluoride membrane (PerkinElmer Life Sciences, Boston, MA). Before immunodetection, membranes were blocked in 5% (w/v) skim milk powder (Carnation, Glendale, CA) in a 0.2% Tween PBS solution for 1 h. Subsequently, membranes were incubated with a monoclonal anti-HIF-1α (1:500; Novus, Littleton, CO), a polyclonal anti-Glut1 (1:1000; Alpha Diagnostic International, San Antonio, TX), a monoclonal antibody against EGF-R (1:200; Ab-12 LabVision; Fremont, CA), a rabbit polyclonal anti-pYEGFR (Tyr-1173) (sc-12351, Santa Cruz Biotechnology. Santa Cruz, CA) and anti-actin (1:4000; Sigma) antibody. After washing with 0.2% Tween PBS solution, membranes were incubated for 1 h with an anti-rabbit secondary antibody conjugated to horseradish peroxidase (1:5,000; Jackson ImmunoResearch, West Grove, PA) and detected by enhanced chemiluminescence (Pierce).

BrdUrd Labeling—Cells were plated at low density on coverslips and incubated for at least 16 h in DMEM plus 10% FBS. Cells were washed in PBS and incubated under various growth conditions, as indicated for the indicated time. Cells incubated in the presence of 10 μM BrdUrd (Jackson ImmunoResearch, West Grove, PA) for 3 h prior to labeling. Cells were then fixed in 70% ethanol in 50 mM glycine (pH 2.0) for at least 30 min at 20 °C. Cells were washed and incubated with a solution containing an anti-BrdUrd antibody for 30 min at 37 °C and washed and incubated with an anti-mouse fluorescein isothiocyanate (FITC)-conjugated secondary antibody. All coverslips were counterstained with Hoechst reagent to identify nuclei and the percentage of BrdUrd-labeled cells (FITC-stained cells/Hoechst-stained cells) was determined with a Zeiss fluorescence microscope and digital imaging.

RT-PCR and Real-time RT-PCR—Total RNA was isolated using TRIPURE isolation reagent (Roche Applied Science) according to the manufacturer's protocol. RT-PCR was performed on 500 ng of RNA using the One-Step Superscript RT Platinum *Taq*RT-PCR kit (Invitrogen) and 0.6 μM of each primer (Table I). Cycling conditions were 30 min at 50 °C, 2 min at 94 °C, 25 or 30 cycles of 20 s at 94 °C, 20 s at 60 °C, 40 s at 72 °C, with a final extension of 10 min at 72 °C. RT-PCR products were electrophoresed in 1.2% agarose gels and ethidium bromide staining visualized using a Kodak digital science IC440 system. The sequences of the primers used in this study are as follows: TGF-α forward: 5′-TCGCTCTGGGTATTGTGTTG-3′; TGF-α reverse: 5′-GACCTGGCAGCAGTGTATCA-3′; EGF forward: 5′-CGCAGGAAATGGGAATTCTA-3′; EGF reverse: 5′-CCTTCCTGTTGATTTGACCA-3′; Amphiregulin forward: 5′-TGGATTGGACCTCAATGACA-3′; Amphiregulinreverse: 5′-CCATTTTTGCCTCCCTTTTT-3′; Betacellulin forward: 5′-TGGGAATTCCACCAGAAGTC-3′; Betacellulin reverse: 5′-TTACGACGTTTCCGAAGAGG-3′; Epiregulin forward: 5′-AGGATGGAGATGCTCTGTGC-3′; Epiregulin reverse: 5′-GTGTTCACATCGGACACCAG-3′; HB-EGF forward: 5′-GGTGGTGCTGAAGCTCTTTC-3′; HB-EGF reverse: 5′-CCCATGACACCTCTCTCCAT-3′; Glut-1forward: 5′-CTGTCTGGCATCAACGCTGTCTTC-3′; Glut-1 reverse: TCCTCGGGTGTCTTATCACTTTGG; β-actin forward: 5′-CGTACCACTGGCATCGTGAT-3′; β-actin reverse: 5′-GTGTTGGCGTACAGGTCTTTG-3′.

For real time RT-RCR, triplicates of 25-μl multiplex PCR reactions

were performed on 50 ng of total RNA using TaqMan One-Step RT-PCR master mix reagents (Applied Biosystems) and 0.2 μM 5′-VIC of TGF-α– and 5′-6FAM β-actin-modified probes. Cycling conditions were 30 min at 48 °C, 10 min at 95 °C, then 40 cycles of 15 s at 95°, 1 min at 60 °C. Amplification and analysis were performed using ABI PRISM 7000 Sequence Detection System (Applied Biosystems) and data normalized to the β-actin endogenous control. Primers for the real time RT-PCR experiments were designed as follows: Real time TGF-α forward: 5′-GCACGTCCCCGCTGAGT-3′; Real time TGF-α probe: 5′-TTTTAATGACTGCCCAGATTCCCACACTCA-3′; Real time TGF-α reverse: 5′-CAGGTTCCATGGAAGCAGAA-3′; Real time β-actin forward: 5′-AGCCTCGCCTTTGCCGA-3′; Real time β-actin probe: 5′-CCGCCGCCCGTCCACACCCGCC-3′; Real time β-actin reverse: 5′-CTGGTGCCTGGGGCG-3′.

RESULTS

HIF Activation Is Required for EGF-R-dependent Growth of VHL$^{-/-}$ RCC Cells in Serum-free Media—Cancer cells are generally capable of engaging in autonomous growth reflected by their ability to proliferate in serum-free medium (35–37). We recently reported that VHL$^{-/-}$ RCC cells share this defect, which is correctable by the reintroduction of VHL (10). To determine the role of HIF activation in the ability of VHL$^{-/-}$ RCC cells to engage in serum-independent growth, we produced an adenovirus that expresses a truncated version of HIF-2α, which acts as a dominant-negative molecule repressing HIF-mediated gene expression (DNHIF) (54) as well as an adenovirus that expresses a green fluorescent protein (GFP) fusion to HIF-1α (48). We also engineered adenoviruses that express GFP alone and GFP fused to VHL (VHL), and a naturally occurring C-terminal truncation mutant of VHL (Δ157-VHL) that fails to mediate oxygen-dependent degradation of HIFα (Fig. 1*A*). Infection efficiency was more than 90% in all cell lines used in this study, and production of the recombinant proteins was monitored by Western blots (data not shown and see Refs. 29 and 45). Normoxic VHL$^{-/-}$ RCC cells overproduce Glut-1 as a consequence of HIF activation, which is correctable by the reintroduction of VHL (55). DNHIF was as efficient as VHL at down-regulating Glut-1 levels in normoxic VHL$^{-/-}$ RCC cells incubated in the presence or absence of serum compared with controls (uninfected cells), or cells expressing Δ157-VHL, or GFP alone (Fig. 1*A*). Furthermore, overproduction of HIF-1α led to Glut-1 accumulation in normoxic VHL(+) cells, regardless of serum conditions (Fig. 1*A*). These results demonstrate that DNHIF and HIF-1α can be used as tools to inhibit or activate HIF-targets in normoxic VHL$^{-/-}$ RCC or VHL(+) cells, respectively.

We then examined whether the serum-independent growth phenotype observed in VHL$^{-/-}$ RCC cells is a consequence of HIF activation. DNHIF was as efficient as VHL at abolishing serum-independent growth of VHL$^{-/-}$ RCC cells, as measured by a marked reduction in the ability of these cells to incorporate BrdUrd (Fig. 1*B*). In contrast, VHL$^{-/-}$ RCC cells expressing GFP or Δ157-GFP incorporated BrdUrd to levels similar to those of uninfected cells. Addition of 5% serum abolished the growth inhibitory effect of DNHIF and VHL. Likewise, overproduction of HIF-1α was sufficient to enable VHL(+) cells to proliferate in serum-free medium (ITS), in contrast to uninfected VHL(+) cells or cells expressing GFP alone (Fig. 1*B*). These results indicate that the ability of VHL$^{-/-}$ RCC cells to engage in serum-independent growth is a consequence of HIF activation.

We previously reported that overexpression of TGF-α and activation of EGF-R were involved in serum-independent growth of VHL$^{-/-}$ RCC cells (10). Based on data shown in Fig. 1, we next asked whether HIF activation promoted serum-independent growth of VHL$^{-/-}$ RCC cells through EGF-R-dependent or -independent pathways. To do so, we first compared the effect of DNHIF and reintroducing VHL on EGF-R levels

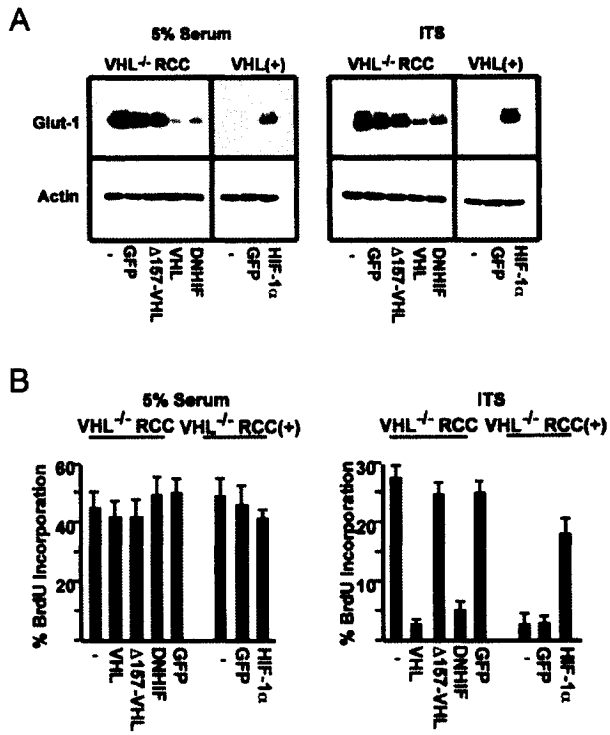

FIG. 1. **HIF activation is required for serum-independent proliferation of VHL$^{-/-}$ RCC cells.** *A*, DNHIF down-regulates levels of Glut-1 in VHL$^{-/-}$ RCC cells. Western blot analysis of Glut-1 levels in uninfected (–) or infected VHL$^{-/-}$ RCC cells with adenoviruses expressing GFP, Δ157-VHL, VHL, DNHIF, and uninfected VHL(+) cells or VHL(+) cells infected with GFP or HIF-1α. Cell lysates were prepared 60 h after infections in cells plated in DMEM supplemented with 5% serum or DMEM supplemented with ITS (serum-free media). Western blots were carried out to detect Glut-1 and actin as a loading control. *B*, effect of HIF activation on growth of VHL$^{-/-}$ RCC and VHL(+) cells in serum-free media. VHL$^{-/-}$ RCC or VHL(+) cells were either uninfected, or infected with the indicated adenoviruses. Cells were incubated for 48–60 h in DMEM supplemented with ITS or 5% serum prior to 3 h labeling with BrdUrd. Cells were subsequently fixed and stained. Shown is the percentage of BrdUrd-positive cells in relation to Hoechst-stained nuclei. Data shown are the mean average of at least three independent experiments with S.E.

and phosphorylation state in VHL$^{-/-}$ RCC cells. Levels of EGF-R remained essentially unchanged regardless of growth conditions, VHL/HIF activity or incubation with PD153035, a membrane permeable inhibitor of EGF-R tyrosine kinase activity (referred to as EGF-Ri). The specificity of EGF-Ri at abolishing EGF-R activation has been reported elsewhere (51) and controls are shown in Fig. 2*B* and Fig 5*A*. DNHIF and VHL did not affect the phosphorylation status of VHL$^{-/-}$ RCC cells in 10% serum (Fig. 2*A*). In contrast, DNHIF and VHL were essentially as efficient as EGF-Ri in reducing EGF-R phosphorylation in serum-free media. Therefore, abolishing HIF activation as essentially the same effect as reintroducing VHL on EGF-R phosphorylation of VHL$^{-/-}$ RCC cells. The data also shows that EGF-R phosphorylation is dependent upon HIF activation.

We next tested whether serum-independent growth of VHL$^{-/-}$ RCC cells was solely the consequence of HIF-dependent activation of EGF-R that occurs upon VHL loss. We reasoned that, if EGF-R-independent signaling existed, the EGF-Ri-treated VHL$^{-/-}$ RCC cells would display measurable differences in BrdUrd incorporation relative to VHL(+) cells, or VHL$^{-/-}$ RCC cells expressing DNHIF (see Fig. 1*B*) in serum-free media. EGF-Ri treatment had comparable growth suppressive effects to that of reintroduction of VHL on VHL$^{-/-}$ RCC

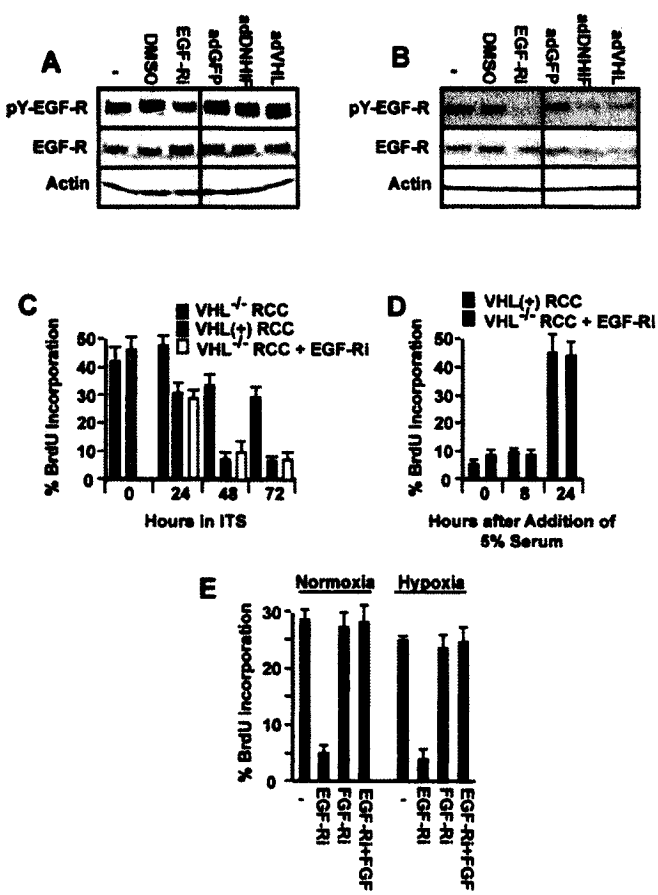

FIG. 2. **HIF-mediated activation of the EGF-R is required for serum-independent growth of VHL$^{-/-}$ RCC cells.** *A* and *B*, EGF-R phosphorylation in VHL−/− RCC cells incubated in serum-free media requires HIF activation. VHL−/− RCC 786-0 cells were not treated (−), treated with Me_2SO alone, in the presence of 10 μM PD153035 (EGF-Ri), or infected with adGFP, adDNHIF or adVHL. Cells were incubated for 48 h in the presence (*A*) or absence (*B*) of 10% serum. Lysates were blotted against an anti-phospho-EGF-R antibody (*py-EGF-R*), an anti-EGF-R antibody (*EGF-R*), or an anti-actin antibody (*Actin*). *C*, inhibition of the EGF-R has similar effects on proliferation of VHL$^{-/-}$ RCC cells as reintroducing wild-type VHL. VHL$^{-/-}$ RCC cells were incubated in DMEM supplemented with 5% FCS for 16 h (time 0 h). Cells were transferred to DMEM with ITS and VHL$^{-/-}$ RCC cells were treated with either vehicle alone, Me_2SO (*DMSO*), or PD153035 (1 μM) for the indicated time. VHL$^{-/-}$ RCC cells stably expressing reintroduced VHL (VHL(+) RCC) were incubated in the same growth conditions and in the presence of Me_2SO. BrdUrd was added for the last 3 h before fixing and staining. Shown is the mean of three independent experiments with S.E. *D*, EGF-R inhibitor-treated VHL$^{-/-}$ RCC cells are in a state of quiescence (G_0). VHL$^{-/-}$ RCC were incubated in DMEM supplemented with ITS and in the presence of PD153035 (1 μM) for 72 h. VHL(+) cells were incubated in the same conditions but with Me_2SO. The cells were washed and the medium replaced with DMEM supplemented with 5% serum. BrdUrd was added 3 h prior to fixation and staining at the indicated times. *E*, inhibition of EGF-R activity abolishes serum-free growth of VHL$^{-/-}$ RCC cells in hypoxia to the same levels as in normoxia. VHL$^{-/-}$ RCC 786-0 cells were plated overnight and then washed, and medium was replaced with DMEM supplemented with ITS. The EGF-R inhibitor (PD153035; 1 μM) with or without bFGF (100 ng/ml) or the FGF-R inhibitor (AG1296; 50 μM) were added, and cells were maintained in normoxia for 24 h. Cells were maintained in normoxia or transferred to hypoxia for another 24 h. BrdUrd was added for the last 3 h prior to analysis. Data shown are the mean of three independent experiments with S.E.

cells incubated in ITS for 24–72 h (Fig. 2*C*). Interestingly, the growth inhibitory effects of serum starvation or EGF-Ri treatment was not reversed until about 24 h following serum stimulation of EGF-Ri-treated VHL$^{-/-}$ RCC cells (Fig. 2*D*). This observation suggests that VHL$^{-/-}$ RCC cells are able to enter

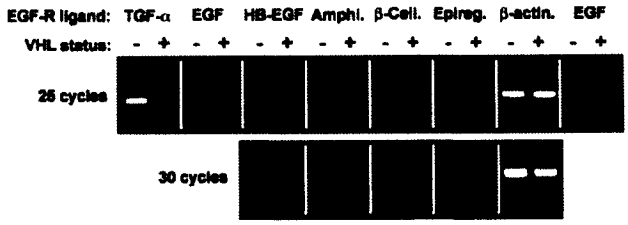

FIG. 3. **TGF-α is the only known EGF-R ligand with an expression profile dependent upon VHL status.** VHL$^{-/-}$ RCC cells were infected with adGFP (VHL status −) or adVHL (VHL status +) and incubated in serum for 48 h prior to isolation of total RNA. RT-PCR was carried out as described under "Experimental Procedures" for 25 cycles (*top panel*) or 30 cycles (*bottom panel*). The *extreme right* of the top panel is a longer exposure of the EGF RT-PCR to show the presence of low amounts of the EGF transcript. *Amphi*, amphiregulin; *Beta*, betacellulin; *Epireg.*, epiregulin. β-Actin is shown as a reaction and loading control.

quiescence when EGF-R activation is abolished in a manner similar to that observed in VHL(+) RCC cells (9). It also shows that EGF-Ri does not block growth non-specifically. EGF-Ri had similar growth inhibitory effect regardless of oxygen tension (Fig. 2*E*) whereas a FGF tyrosine kinase inhibitor (FGF-Ri) failed to alter the ability of VHL$^{-/-}$ RCC cells to incorporate BrdUrd (Fig. 2*E*). Taken together, the findings shown in Figs. 1 and 2 suggest that HIF activation is required for EGF-R phosphorylation and EGF-R-mediated serum-independent growth of VHL$^{-/-}$ RCC cells.

Identification of TGF-α as a Novel HIF-regulated Gene in VHL$^{-/-}$ RCC Cells—Next, we focused on identifying the mechanism(s) by which HIF activation confers EGF-R-dependent serum-free growth characteristics to VHL$^{-/-}$ RCC cells. One potential candidate that we had previously identified is TGF-α. This is based on experiments using antisense oligonucleotides to TGF-α that efficiently abrogated the ability of VHL$^{-/-}$ RCC cells to proliferate in serum-free conditions (10). In addition, TGF-α remains the only identified factor that displays both VHL-regulated expression as well as mitogenic effect on renal epithelial cells, the cell type thought to give rise to VHL$^{-/-}$ RCC (33, 40, 42). However, there are several known EGF-R ligands. We, therefore, decided to analyze their expression profile in RCC cells and furthermore asked if their expression profile was dependent upon VHL status. TGF-α mRNA was the only transcript that was easily detectable at 25 cycle of RT-PCR in VHL$^{-/-}$ RCC cells and negatively regulated by reintroduction of VHL. EGF transcript could also be detected at 25 cycles but its expression profile was unaffected by VHL status. Transcript for epiregulin and heparin-binding EGF (HB-EGF) were detected at cycle 30 but also unaffected by VHL status whereas we failed to detect transcripts for amphiregulin and betacellulin using this approach (Fig. 3). An RT reaction using random hexamers prior to PCR yielded essentially the same results as shown in Fig. 3 though we did detect low abundant amphiregulin product in both VHL-positive and -negative cells (data not shown). We failed to detect products for betacellulin using different conditions in our system though these primers produced a product for betacellulin from RNA isolated from HCT-15 cell line used as a positive control (data not shown). These data indicate that TGF-α is the only known EGF-R ligand tested in our system that displays an expression profile dependent upon VHL status in RCC cells.

Given that HIF activation, EGF-R stimulation and TGF-α overproduction (10) are equally required for serum-independent growth, we hypothesized that TGF-α overproduction by VHL$^{-/-}$ RCC cells might be a consequence of HIF activation. Fig. 4*A* shows that overproduction of TGF-α protein can be detected in two independent VHL$^{-/-}$ RCC cell lines correctable

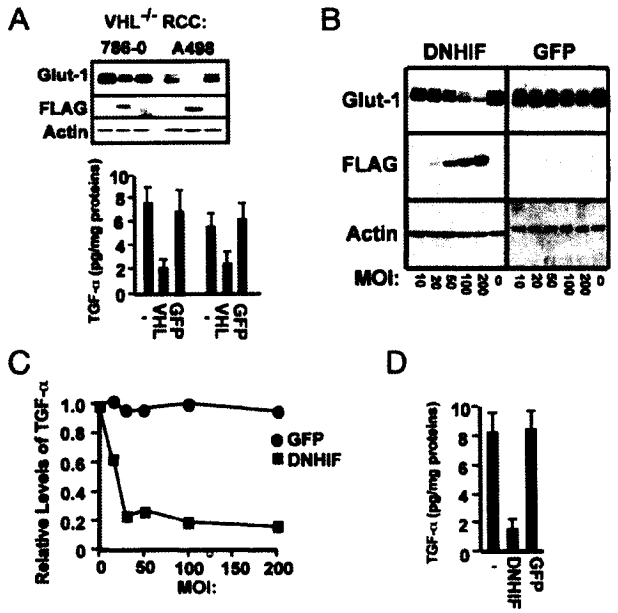

FIG. 4. **Overproduction of TGF-α by VHL$^{-/-}$RCC cells requires HIF activation.** *A*, TGF-α protein level is dependent on VHL status in RCC cells. Two independent VHL$^{-/-}$ RCC cell lines were either uninfected or infected with VHL or GFP as a control. Cell lysates were prepared 60 h after infection, and Western blots were carried out to detect Glut-1 and actin as a loading control (*top panel*) or ELISA was performed to measure levels of TGF-α normalized per microgram of total cellular protein with data showing the mean average of at least three independent experiments with S.E. *B*, Western blot analysis of Glut-1 levels in VHL$^{-/-}$ cells expressing increasing MOI (multiplicity of infection) of DNHIF. VHL$^{-/-}$ RCC cells were infected with increasing amounts of DNHIF, and lysates were prepared for Western blots 60 h post-infection to detect Glut-1 or actin as a loading control. *C* and *D*, DNHIF down-regulates TGF-α levels in VHL$^{-/-}$ RCC cells. VHL$^{-/-}$ RCC cells were treated as described in *B* but lysates were prepared as suggested by the manufacturer. Levels of TGF-α were normalized per microgram of total cellular protein. Data shown in *panel D* are the mean average of three independent experiments with S.E. at a multiplicity of infection (*MOI*) of 200.

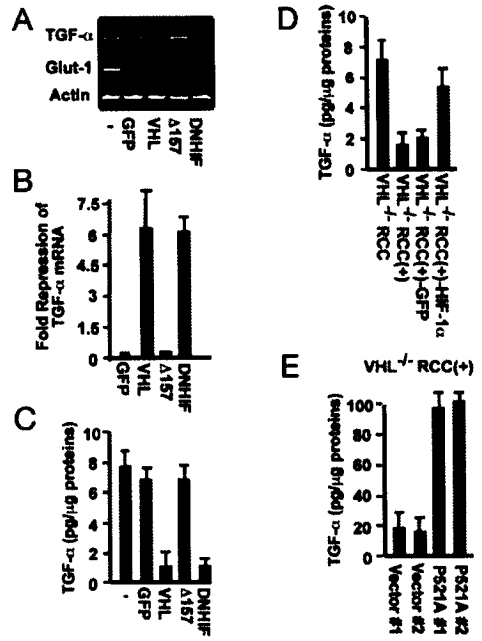

FIG. 5. **HIF activation is sufficient to increase TGF-α mRNA and protein levels in VHL$^{-/-}$ RCC cells.** *A* and *B*, DNHIF is as efficient as reintroducing VHL at abolishing overexpression of TGF-α mRNA by VHL$^{-/-}$ RCC cells. RT-PCR analysis of TGF-α and Glut-1 mRNA levels in VHL$^{-/-}$ RCC cells infected with adenoviruses expressing DNHIF or VHL. VHL$^{-/-}$ RCC cells were either uninfected (−) or infected with adenoviruses expressing GFP, VHL, Δ157-VHL, or DNHIF. Total RNA was isolated 60 h post-infection and RT-PCR was preformed using primers specific to TGF-α, Glut-1, or β-actin mRNA (*A*). The same samples were also analyzed by real-time RT-PCR and plotted as fold reduction as compared with uninfected VHL$^{-/-}$ RCC cells (*B*). Mean average of three independent experiments with S.E. is shown. *C*, cells were treated as described in *A* but lysates were prepared to analyze TGF-α protein levels by ELISA. Levels of TGF-α were normalized per μg of total cellular protein assessed by the BCA method. Data shown are the mean average of three independent experiments with S.E. *D*, effect of HIF-1α overexpression on levels of TGF-α in normoxic VHL(+) cells. VHL(+) cells were either uninfected or infected with adenoviruses expressing GFP or HIF-1α and lysates were prepared 60 h post-infection. Lysates were also prepared from uninfected VHL$^{-/-}$ RCC cells. TGF-α protein levels were assessed by ELISA and normalized per microgram of total cellular protein assessed by the BCA method. Data shown are the mean average of at least three independent experiments with S.E. *E*, ELISA analysis of TGF-α levels in VHL(+) cells expressing HIF-2α P521A mutant. Lysates of two independent VHL(+) cell line expressing HIF-2α P531A mutant or vector alone (VHL(+) vector) were analyzed for TGF-α content by ELISA and normalized per μg of total cellular protein. Data shown are the mean average of at least three independent experiments with S.E.

by the reintroduction of VHL. DNHIF was as efficient at reducing TGF-α levels in VHL$^{-/-}$ RCC 786-0 as it was at reducing levels of the well known HIF-target, Glut-1 (Fig. 4, *B* and *C*). Maximal DNHIF-mediated inhibition of TGF-α production was attained at 100–200 MOI and was ~6-fold compared with uninfected or GFP-infected cells (Fig. 4*D*). These results demonstrate that TGF-α overproduction is a general phenomenon observed in many VHL$^{-/-}$ RCC cells and requires HIF activation.

We next decided to further examine the relative role of HIF activation in the overexpression of TGF-α in comparison to that of loss of VHL function. We reasoned that, if HIF activation was the sole cause of TGF-α overexpression, DNHIF would have essentially the same effect at down-regulating TGF-α levels in VHL$^{-/-}$ RCC cells as reintroduction of VHL function. VHL$^{-/-}$ RCC 786-0 cells were infected with DNHIF and VHL, Δ157-VHL, and GFP. DNHIF was as efficient as VHL at down-regulating mRNA levels of Glut-1 and TGF-α in VHL$^{-/-}$ RCC cells (Fig. 5*A*). Real time RT-PCR (Fig. 5*B*) and ELISA (Fig. 5*C*) revealed a similar decrease of TGF-α mRNA and protein levels (about 6-fold) in VHL$^{-/-}$ RCC cells expressing DNHIF or reintroduced VHL. As expected, controls GFP and Δ157-GFP had essentially no effects on Glut-1 and TGF-α mRNA and protein levels (Fig. 5, *B* and *C*). Similar data were obtained with VHL$^{-/-}$ RCC A498 cells (data not shown). We next asked if HIF activation was sufficient to promote TGF-α overproduction even in a VHL-positive environment. Accumulation of HIF-α by adenovirus-mediated infection of normoxic VHL(+) cells was sufficient to induce overproduction of TGF-α to levels comparable to those observed in VHL$^{-/-}$ RCC cells (Fig. 5*D*). Furthermore, VHL(+) cells expressing an ODD mutant of HIF-2α, which fails to assemble to VHL, also displayed increased levels of TGF-α protein compared with VHL(+) transfected with vector alone (Fig. 5*E*). Therefore, TGF-α overproduction by VHL$^{-/-}$ RCC cells is solely dependent upon HIF activation, as observed with other known HIF targets and does not require VHL loss of function. Furthermore, data shown in Figs. 4 and 5 identify TGF-α as a novel HIF-regulated gene.

TGF-α-mediated Activation of EGF-R Is a Major Mitogenic Event in VHL$^{-/-}$ RCC Cells—The next step consisted of examining the mechanisms involved in TGF-α-mediated proliferation of VHL$^{-/-}$ RCC cells. It is generally thought that TGF-α stimulates proliferation through the activation of the EGF-R although this has yet to be formally shown in renal cancer cells (56, 57). To test this, we analyzed the ability of EGF-Ri to

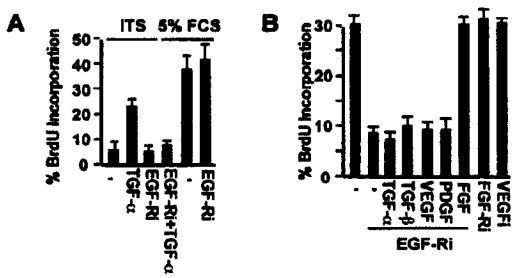

FIG. 6. **TGF-α, but not other cytokines associated with HIF activation, promotes serum-independent growth through the activation of the EGF-R.** *A*, growth stimulatory effect of exogenous TGF-α on VHL(+) cells is abolished by treatment with EGF-Ri. VHL(+) RCC cells were incubated in the absence or presence of PD153035 (1 μM), in ITS alone or ITS with TGF-α (10 ng/ml), or 5% serum for 48 h. Cells were incubated in the presence of BrdUrd 3 h prior to fixing and staining. Shown are the means of at least three independent experiments with S.E. *B*, growth factors associated with VHL loss-of-function fail to rescue the growth inhibitory effect of an EGF-R inhibitor on VHL$^{-/-}$ RCC cells in culture. VHL$^{-/-}$ RCC cells were incubated in ITS without or with PD153035 (1 μM) or with PD153035 plus TGF-α (10 ng/ml), TGF-β1 (5 ng/ml), VEGF (50 ng/ml), PDGF (25 ng/ml), or bFGF (10 ng/ml). VHL$^{-/-}$ RCC cells were also incubated in DMEM supplemented with ITS and in the presence of the FGF-R inhibitor (AG1296; 50 μM) or the VEGF inhibitor (tranilast; 80 μM). Cells were incubated for 48–60 h prior to the addition of BrdUrd for the last 3 h before fixing and staining. Shown is the mean of three independent experiments with S.E.

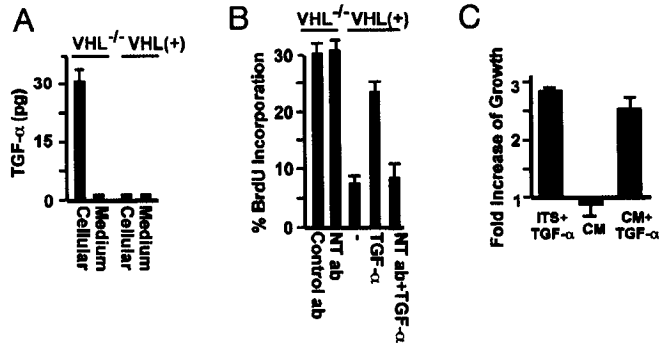

FIG. 7. **TGF-α is not secreted by VHL$^{-/-}$ RCC cells.** *A*, TGF-α accumulates in intracellular compartments of VHL$^{-/-}$ RCC cells. VHL$^{-/-}$ RCC and VHL(+) cells were plated overnight, washed and maintained in 2 ml of DMEM supplemented with ITS for 48 prior to measuring TGF-α protein from cellular lysates and media by ELISA. TGF-α concentration is reported from an equal number of cells or from 50 μl of medium collected from the same number of cells. Results shown are from at least three independent experiments with S.E. The *asterisk* indicates that TGF-α levels were essentially below the detection limit of the ELISA assay. *B*, a neutralizing antibody to TGF-α fails to prevent serum-independent growth of VHL$^{-/-}$ RCC cells. VHL$^{-/-}$ RCC and VHL(+) cells were treated with a TGF-α neutralizing antibody (10 ng/ml) or a control antibody (M2 anti-FLAG; 10 ng/ml) for 48 h in DMEM supplemented with ITS or ITS with TGF-α (50 pg/ml). BrdUrd was added in the last 3 h prior to fixation and staining. Shown is the mean of at least two independent experiments. *C*, conditioned media from VHL$^{-/-}$ RCC cells fails to stimulate proliferation of VHL(+) cells. VHL$^{-/-}$ RCC cells were incubated in DMEM supplemented with ITS for 48 h. The conditioned medium was decanted, filtered, and placed immediately in quiescent VHL(+) cells that were maintained in DMEM supplemented with ITS for 72 h. Alternatively, the medium was replaced from quiescent VHL(+) cells with DMEM supplemented with ITS with exogenous TGF-α (10 ng/ml) or conditioned medium with exogenous TGF-α (10 ng/ml). BrdUrd was added at the moment of the media switch for 24 h prior to fixation and staining. The fold increase in growth is as compared with quiescent VHL(+) whose medium was replaced with DMEM supplemented with ITS alone. Data shown are the mean average of three independent experiments with S.E.

abolish exogenous TGF-α growth stimulatory effect on VHL(+) cells grown in serum-free media. VHL(+) cells do not incorporate BrdUrd in serum-free media (Fig. 6*A*). Addition of exogenous TGF-α stimulated BrdUrd incorporation, which was abolished by treatment with EGF-Ri (Fig. 6*A*). In contrast, addition of 5% serum abolished the growth inhibitory effect of EGF-Ri, a consequence of EGF-R-independent stimulation of other receptors again demonstrating that EGF-Ri does not block growth nonspecifically (Fig. 6*A*). These data further confirm that TGF-α promotes proliferation through the activation of EGF-R in our cell culture system and not through a yet unappreciated alternative pathway.

We had previously demonstrated that other growth factors overproduced by VHL$^{-/-}$ RCC cells, such as VEGF and PDGF, do not display mitogenic activity on VHL(+) cells in culture (10). However, it could be argued that mitogenic sensitivity to these cytokines is acquired upon VHL loss. To further investigate this, several factors that are overproduced by VHL$^{-/-}$ RCC cells were tested for their ability to stimulate proliferation of EGF-Ri-treated VHL$^{-/-}$ RCC 786-0 cells. VHL$^{-/-}$ RCC 786-0 cells continued to incorporate BrdUrd in the absence of exogenous growth factors (Fig. 6*B*). Treatment with EGF-Ri reduced the ability of VHL$^{-/-}$ RCC cells to incorporate BrdUrd by 3–4-fold after 48 h in serum-free media (10) (Fig. 6*B*). Addition of TGF-α did not stimulate the proliferation of VHL$^{-/-}$ RCC cells in the presence of EGF-Ri, suggesting that TGF-α was not able to stimulate growth through an independent receptor in VHL loss RCC cells (Fig. 6*B* and see Fig. 6*A*). Growth factors overproduced by VHL$^{-/-}$ RCC cells and under HIF regulation, such as TGF-β, VEGF, and PDGF, were unable to promote BrdUrd incorporation of EGF-Ri-treated VHL$^{-/-}$ RCC 786-0 cells (Fig. 6*B*). As expected, addition of FGF stimulated the incorporation of BrdUrd in VHL$^{-/-}$ RCC cells grown in ITS and in the presence of an EGF-Ri though it should be noted that VHL$^{-/-}$ RCC cells do not overproduce FGF. Likewise, treatment with an inhibitor of FGF receptor, as well as a VEGF inhibitor, failed to abolish the ability of VHL$^{-/-}$ RCC 786-0 cells to incorporate BrdUrd in ITS (Fig. 6*B*). These results indicate that VHL$^{-/-}$ RCC cells are not sensitive to other growth factors overproduced by VHL$^{-/-}$ RCC cells except for TGF-α.

TGF-α can either be retained in cells or secreted in the medium (58–60). We failed to detect TGF-α in the media of VHL$^{-/-}$ RCC 786-0 cells implying that TGF-α is retained within cellular compartments (Fig. 7*A*). Likewise, neutralizing antibodies to TGF-α had no measurable effect on proliferation on VHL$^{-/-}$ RCC cells in serum-free media (Fig. 7*B*). In contrast, neutralizing antibodies abolished the mitogenic effect of exogenous TGF-α on VHL(+) in serum free media demonstrating that the antibody could efficiently prevent exogenous TGF-α signaling. Furthermore, conditioned media obtained from VHL$^{-/-}$ RCC cells in serum-free media failed to stimulate proliferation of VHL(+) although the addition of exogenous TGF-α to the conditioned media, or ITS, stimulated proliferation (Fig. 7*C*). These results demonstrate that TGF-α is retained in VHL$^{-/-}$ RCC cells and not secreted into the media, as observed with VEGF (61).

Type 2C Mutants Negatively Regulate TGF-α and Restore Serum-dependent Growth of VHL$^{-/-}$ RCC Cells—Individuals afflicted with type 2C VHL syndrome develop pheochromocytoma, but not RCC or hemangioblastomas (62, 63). VHL$^{-/-}$ RCC cells expressing reintroduced VHL mutants harboring missense mutations associated with type 2C disease failed to form tumors in nude mice and were able to mediate oxygen-dependent ubiquitination and degradation of HIF (31, 47). Type 2C mutants were able to negatively regulate Glut-1 and TGF-α levels, albeit to a different extent compared with VHL(+) cells (Fig. 8, *A* and *B*). Type 2C mutants that were most efficient at down-regulating Glut-1 and TGF-α levels were also able to

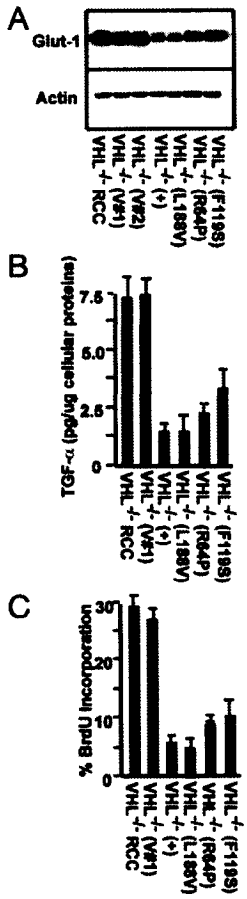

FIG. 8. **VHL harboring type 2C mutations down-regulate TGF-α and restore serum-dependent growth to levels similar to those of wild-type VHL.** *A*, Western blot analysis of Glut-1 levels. Cells were plated 24 h prior to Western blots being carried out to detect Glut-1 and actin as a loading control. *B*, ELISA analysis of TGF-α levels. Cells were treated as described in *A* but lysates were prepared as suggested by the manufacturer. Levels of TGF-α were normalized per microgram of total cellular protein assessed by the BCA method. Data shown are the mean average of at least three independent experiments with S.E. *C*, effect of different type 2C mutants of VHL on the ability of VHL$^{-/-}$ RCC cells to incorporate BrdUrd in serum-free media. Cells were incubated for 48–60 h in ITS prior to 3 h labeling with BrdUrd. Cells were subsequently fixed and stained. Shown is the percentage of BrdUrd-positive cells in relation to Hoechst-stained nuclei. Data shown are the mean average of at least three independent experiments with S.E.

abolish the ability of VHL$^{-/-}$ RCC cells to incorporate BrdUrd in the absence of exogenous growth factors to levels similar to those of VHL (+) cells (Fig. 8*C*). This data suggest that VHL$^{-/-}$ RCC cells expressing reintroduced type 2C mutants of VHL do not engage in an HIF-dependent TGF-α/EGF-R autonomous growth stimulatory pathway in culture.

DISCUSSION

In this report, we link HIF activation to oncogenesis and loss of growth control of VHL$^{-/-}$ RCC cells in addition to its reported role in adaptation to hypoxia, angiogenesis, and tumor progression. Data presented here link HIF with a *bona fide* renal mitogen and identifies TGF-α as a novel HIF-regulated gene. We suggest that VHL-null cells engage in an HIF-dependent constitutive activation of the TGF-α/EGF-R growth stimulatory pathway and that this constitutes the postulated gatekeeper function of VHL in renal epithelial cells (9, 10, 64, 65). This model is founded on experiments focusing on the ability of VHL$^{-/-}$ RCC cells to proliferate in the absence of exogenous growth factors, whereas primary cultures of renal epithelial cells require addition of exogenous growth factors, or serum, to proliferate in culture (66, 67). The ability of transformed cells to engage in an autonomous growth stimulatory pathway has been appreciated in several types of cancers and is one of the accepted hallmarks of cellular transformation (35–38, 68–70) Our model of HIF-mediated activation of the TGF-α/EGF-R pathway as a major oncogenic pathway in VHL$^{-/-}$ RCC cells is supported by the following: First, we show in this report that inhibition of EGF-R phosphorylation and of serum-independent growth of VHL$^{-/-}$ RCC can be achieved to a similar extent by either reintroducing VHL function, by abolishing HIF activation or by inhibiting EGF-R activity. Second, antisense oligonucleotides to TGF-α mRNA efficiently abolished serum-independent growth of VHL$^{-/-}$ RCC cells (10). Third, TGF-α overproduction is a consequence of HIF activation. While it remains possible that other, as yet unidentified, EGF-R ligands might be overproduced upon HIF activation, the antisense data in addition to results shown here do argue for a crucial role for TGF-α in activating the EGF-R. Finally, and in agreement with our data, are reports that have shown that the reintroduction of VHL, or treatment with an EGF-R inhibitor, are both equally efficient at suppressing RCC tumor formation in nude mice assays (7, 45, 46, 71, 72). We argue that obvious differences would have been observed in growth inhibitory activity among these very different approaches if VHL$^{-/-}$ RCC cells had evolved other intrinsic mechanisms of unregulated growth. These finding provide the first evidence linking HIF activation with autonomous and aberrant proliferation of fully transformed VHL$^{-/-}$ RCC cells. It remains to be determined if other HIF-dependent cytokines, including unidentified EGF-R ligands, are also involved in addition to TGF-α. However, based on our data, we propose that the HIF-mediated activation of the TGF-α/EGF-R pathway serves as a common oncogenic event in RCC cells upon the loss of VHL function thereby explaining serum-free growth and tumorigenesis.

Recently, Mandriota *et al.* (33) elegantly showed that VHL loss-of-function and HIF activation are early events in the development of multicellular neoplastic foci of the distal nephron (33). It will obviously be difficult to formally prove that HIF activation, by way of TGF-α overproduction, provides the initial growth advantage to renal epithelial cells upon the loss of VHL function. However, our interpretation is that HIF-dependent constitutive overproduction of TGF-α would provide a very strong initial oncogenic signal for renal epithelial cells (70). Consistent with this argument is the observation that transgenic expression of TGF-α in mice leads to the formation of multiple renal cysts (73) reminiscent of pre-neoplastic lesions of the human kidney (11, 74). This mouse model provides evidence suggesting that TGF-α overproduction is sufficient to initiate unregulated growth of renal epithelial cells in intact kidneys. Furthermore, renal epithelial cells are particularly sensitive to the growth promoting effect of TGF-α in culture (75). An autocrine TGF-α model has also been proposed for other models of epithelial cancers (70, 76). We find that HIF-mediated constitutive activation of the TGF-α/EGF-R pathway provides an adequate explanation for tumor initiation upon the loss of VHL function in the distal nephron. Nonetheless, data shown in this report establishe an unappreciated link between HIF activation and a potent growth factor of renal epithelial cells suggesting a possible role for HIF in tumorigenesis.

Complex genotype-phenotype correlations have emerged from the study of different families with VHL disease. Patients with type 2C VHL mutations carry an increased risk of pheochromocytoma but not hemangioblastoma or RCC (62, 63, 77–79). Products of type 2C VHL mutations retain the ability to down regulate HIF and HIF responsive genes (47, 80). As

The Journal of Biological Chemistry jbc

expected, all three type 2C VHL mutants that we tested (L188V, F119S, and R64P) failed to overproduce TGF-α to the same extent as VHL$^{-/-}$ 786-0 cells. We did, however, note different TGF-α levels among the three type 2C mutants, two of which produced higher levels than WT VHL(+) cells. Specifically, F119S exhibited the highest level of TGF-α of all the cell lines tested in correlation to an equivalently increased level of Glut-1. Consistent with our hypothesis that TGF-α drives the proliferation of RCC cells, the levels of TGF-α produced in the three Type 2C mutants correlated with their growth profiles in serum-free medium. It is interesting that both F119S and R64P were less efficient at polyubiquitinating HIFα compared with L188V (47) and it would be interesting to test if these mutants are able to suppress RCC tumor growth *in vivo*. Thus, our observation that TGF-α is a HIF-regulated gene responsible for growth in VHL$^{-/-}$ RCC may help in delineating genotype/phenotype correlation in VHL disease.

Taken together, our study links HIF activation with the aberrant production of a *bona fide* mitogen of renal epithelial cells and provides evidence for a role of HIF in the initiation of tumorigenesis. We propose that HIF activation-mediated overproduction of TGF-α and subsequent activation of the EGF-R is the dominant pathway driving proliferation of fully transformed VHL$^{-/-}$ RCC cells. Our observations suggest that contributions from other putative HIF-dependent or -independent growth pathways that might occur upon VHL loss-of-function are relatively minor, at least in culture and in nude mice tumor assays. RCC is the most frequent malignant neoplasm arising from the kidney (3). Standard management for stage I or stage II disease is radical nephrectomy, with advanced disease carrying a poor prognosis. Since HIF activation is an early event in RCC development, blocking the EGF-R pathway has the potential to restore at least some of the normal growth characteristics of fully transformed VHL$^{-/-}$ RCC cells. Based on these data, we suggest that VHL$^{-/-}$ RCC tumors would provide an ideal neoplastic disease for treatment with one of the many inhibitors of EGF-R, especially enzymatic inhibitors of tyrosine kinase activity.

Acknowledgments—We thank Martine Whissel and Erika Sanger for technical expertise and Dr. W. Kaelin for the Type 2C VHL mutant cell lines.

REFERENCES

1. Linehan, W. M., Lerman, M. I., and Zbar, B. (1995) *J. Am. Med. Assoc.* **273,** 564–570
2. Kaelin, W. G., Iliopoulos, O., Lonergan, K. M., and Ohh, M. (1998) *J. Intern. Med.* **243,** 535–539
3. Maher, E. R., and Kaelin, W. G., Jr. (1997) *Medicine (Baltimore)* **76,** 381–391
4. Knudson, A. G., Jr. (1971) *Proc. Natl. Acad. Sci. U. S. A.* **68,** 820–823
5. Zbar, B., Kishida, T., Chen, F., Schmidt, L., Maher, E. R., Richards, F. M., Crossey, P. A., Webster, A. R., Affara, N. A., Ferguson-Smith, M. A., Brauch, H., Glavac, D., Neumann, H. P., Tisherman, S., Mulvihill, J. J., Gross, D. J., Shuin, T., Whaley, J., Seizinger, B., Kley, N., Olschwang, S., Boisson, C., Richard, S., Lips, C. H., Linehan, W. M., and Lerman, M. (1996) *Hum. Mutat.* **8,** 348–357
6. Chen, F., Slife, L., Kishida, T., Mulvihill, J., Tisherman, S. E., and Zbar, B. (1996) *J. Med. Genet.* **33,** 716–717
7. Iliopoulos, O., Kibel, A., Gray, S., and Kaelin, W. G., Jr. (1995) *Nat. Med.* **1,** 822–826
8. Ohh, M., Park, C. W., Ivan, M., Hoffman, M. A., Kim, T. Y., Huang, L. E., Pavletich, N., Chau, V., and Kaelin, W. G. (2000) *Nat. Cell Biol.* **2,** 423–427
9. Pause, A., Lee, S., Lonergan, K. M., and Klausner, R. D. (1998) *Proc. Natl. Acad. Sci. U. S. A.* **95,** 993–998
10. de Paulsen, N., Brychzy, A., Fournier, M. C., Klausner, R. D., Gnarra, J. R., Pause, A., and Lee, S. (2001) *Proc. Natl. Acad. Sci. U. S. A.* **98,** 1387–1392
11. Kaelin, W. G. (2002) *Nat. Rev. Cancer* **2,** 673–682
12. Lisztwan, J., Imbert, G., Wirbelauer, C., Gstaiger, M., and Krek, W. (1999) *Genes Dev.* **13,** 1822–1833
13. Iwai, K., Yamanaka, K., Kamura, T., Minato, N., Conaway, R. C., Conaway, J. W., Klausner, R. D., and Pause, A. (1999) *Proc. Natl. Acad. Sci. U. S. A.* **96,** 12436–12441
14. Kamura, T., Koepp, D. M., Conrad, M. N., Skowyra, D., Moreland, R. J., Iliopoulos, O., Lane, W. S., Kaelin, W. G., Jr., Elledge, S. J., Conaway, R. C., Harper, J. W., and Conaway, J. W. (1999) *Science* **284,** 657–661
15. Kibel, A., Iliopoulos, O., DeCaprio, J. A., and Kaelin, W. G., Jr. (1995) *Science* **269,** 1444–1446
16. Iliopoulos, O., Ohh, M., and Kaelin, W. G., Jr. (1998) *Proc. Natl. Acad. Sci. U. S. A.* **95,** 11661–11666
17. Duan, D. R., Humphrey, J. S., Chen, D. Y., Weng, Y., Sukegawa, J., Lee, S., Gnarra, J. R., Linehan, W. M., and Klausner, R. D. (1995) *Proc. Natl. Acad. Sci. U. S. A.* **92,** 6459–6463
18. Cockman, M. E., Masson, N., Mole, D. R., Jaakkola, P., Chang, G. W., Clifford, S. C., Maher, E. R., Pugh, C. W., Ratcliffe, P. J., and Maxwell, P. H. (2000) *J. Biol. Chem.* **275,** 25733–25741
19. Tanimoto, K., Makino, Y., Pereira, T., and Poellinger, L. (2000) *EMBO J.* **19,** 4298–4309
20. Kamura, T., Sato, S., Iwai, K., Czyzyk-Krzeska, M., Conaway, R. C., and Conaway, J. W. (2000) *Proc. Natl. Acad. Sci. U. S. A.* **97,** 10430–10435
21. Maxwell, P. H., Wiesener, M. S., Chang, G. W., Clifford, S. C., Vaux, E. C., Cockman, M. E., Wykoff, C. C., Pugh, C. W., Maher, E. R., and Ratcliffe, P. J. (1999) *Nature* **399,** 271–275
22. Semenza, G. L. (1999) *Annu. Rev. Cell Dev. Biol.* **15,** 551–578
23. Ivan, M., Kondo, K., Yang, H., Kim, W., Valiando, J., Ohh, M., Salic, A., Asara, J. M., Lane, W. S., and Kaelin, W. G., Jr. (2001) *Science* **292,** 464–468
24. Bruick, R. K., and McKnight, S. L. (2001) *Science* **294,** 1337–1340
25. Epstein, A. C., Gleadle, J. M., McNeill, L. A., Hewitson, K. S., O'Rourke, J., Mole, D. R., Mukherji, M., Metzen, E., Wilson, M. I., Dhanda, A., Tian, Y. M., Masson, N., Hamilton, D. L., Jaakkola, P., Barstead, R., Hodgkin, J., Maxwell, P. H., Pugh, C. W., Schofield, C. J., and Ratcliffe, P. J. (2001) *Cell* **107,** 43–54
26. Jaakkola, P., Mole, D. R., Tian, Y. M., Wilson, M. I., Gielbert, J., Gaskell, S. J., Kriegsheim, A., Hebestreit, H. F., Mukherji, M., Schofield, C. J., Maxwell, P. H., Pugh, C. W., and Ratcliffe, P. J. (2001) *Science* **292,** 468–472
27. Masson, N., Willam, C., Maxwell, P. H., Pugh, C. W., and Ratcliffe, P. J. (2001) *EMBO J.* **20,** 5197–5206
28. Yu, F., White, S. B., Zhao, Q., and Lee, F. S. (2001) *Proc. Natl. Acad. Sci. U. S. A.* **98,** 9630–9635
29. Bonicalzi, M. E., Groulx, I., de Paulsen, N., and Lee, S. (2001) *J. Biol. Chem.* **276,** 1407–1416
30. Krieg, M., Haas, R., Brauch, H., Acker, T., Flamme, I., and Plate, K. H. (2000) *Oncogene* **19,** 5435–5443
31. Clifford, S. C., Cockman, M. E., Smallwood, A. C., Mole, D. R., Woodward, E. R., Maxwell, P. H., Ratcliffe, P. J., and Maher, E. R. (2001) *Hum. Mol. Genet.* **10,** 1029–1038
32. Wiesener, M. S., Munchenhagen, P. M., Berger, I., Morgan, N. V., Roigas, J., Schwiertz, A., Jurgensen, J. S., Gruber, G., Maxwell, P. H., Loning, S. A., Frei, U., Maher, E. R., Grone, H. J., and Eckardt, K. U. (2001) *Cancer Res.* **61,** 5215–5222
33. Mandriota, S. J., Turner, K. J., Davies, D. R., Murray, P. G., Morgan, N. V., Sowter, H. M., Wykoff, C. C., Maher, E. R., Harris, A. L., Ratcliffe, P. J., and Maxwell, P. H. (2002) *Cancer Cell* **1,** 459–468
34. Hanahan, D., and Folkman, J. (1996) *Cell* **86,** 353–364
35. Hanahan, D., and Weinberg, R. A. (2000) *Cell* **100,** 57–70
36. Weinberg, R. A. (1996) *Sci. Am.* **275,** 62–70
37. Pardee, A. B. (1989) *Science* **246,** 603–608
38. Sporn, M. B., and Roberts, A. B. (1985) *Nature* **313,** 745–747
39. Atlas, I., Mendelsohn, J., Baselga, J., Fair, W. R., Masui, H., and Kumar, R. (1992) *Cancer Res.* **52,** 3335–3339
40. Knebelmann, B., Ananth, S., Cohen, H. T., and Sukhatme, V. P. (1998) *Cancer Res.* **58,** 226–231
41. Lager, D. J., Slagel, D. D., and Palechek, P. L. (1994) *Mod. Pathol.* **7,** 544–548
42. Mydlo, J. H., Michaeli, J., Cordon-Cardo, C., Goldenberg, A. S., Heston, W. D., and Fair, W. R. (1989) *Cancer Res.* **49,** 3407–3411
43. Petrides, P. E., Bock, S., Bovens, J., Hofmann, R., and Jakse, G. (1990) *Cancer Res.* **50,** 3934–3939
44. Reifenberger, G., Reifenberger, J., Bilzer, T., Wechsler, W., and Collins, V. P. (1995) *Am. J. Pathol.* **147,** 245–250
45. Prewett, M., Rothman, M., Waksal, H., Feldman, M., Bander, N. H., and Hicklin, D. J. (1998) *Clin. Cancer Res.* **4,** 2957–2966
46. Ciardiello, F., Caputo, R., Bianco, R., Damiano, V., Pomatico, G., Pepe, S., Bianco, A. R., Agrawal, S., Mendelsohn, J., and Tortora, G. (1998) *J. Natl. Cancer Inst.* **90,** 1087–1094
47. Hoffman, M. A., Ohh, M., Yang, H., Klco, J. M., Ivan, M., and Kaelin, W. G., Jr. (2001) *Hum. Mol. Genet.* **10,** 1019–1027
48. Groulx, I., and Lee, S. (2002) *Mol. Cell. Biol.* **22,** 5319–5336
49. Chen, L., Anton, M., and Graham, F. L. (1996) *Somat. Cell Mol. Genet.* **22,** 477–488
50. Graham, F. L., and van der Eb, A. J. (1973) *Virology* **54,** 536–539
51. Fry, D. W., Kraker, A. J., McMichael, A., Ambroso, L. A., Nelson, J. M., Leopold, W. R., Connors, R. W., and Bridges, A. J. (1994) *Science* **265,** 1093–1095
52. Kovalenko, M., Gazit, A., Bohmer, A., Rorsman, C., Ronnstrand, L., Heldin, C. H., Waltenberger, J., Bohmer, F. D., and Levitzki, A. (1994) *Cancer Res.* **54,** 6106–6114
53. Koyama, S., Takagi, H., Otani, A., Suzuma, K., Nishimura, K., and Honda, Y. (1999) *Br. J. Pharmacol.* **127,** 537–545
54. Maemura, K., Hsieh, C. M., Jain, M. K., Fukumoto, S., Layne, M. D., Liu, Y., Kourembanas, S., Yet, S. F., Perrella, M. A., and Lee, M. E. (1999) *J. Biol. Chem.* **274,** 31565–31570
55. Iliopoulos, O., Levy, A. P., Jiang, C., Kaelin, W. G., Jr., and Goldberg, M. A. (1996) *Proc. Natl. Acad. Sci. U. S. A.* **93,** 10595–10599
56. Reynolds, F. H., Jr., Todaro, G. J., Fryling, C., and Stephenson, J. R. (1981) *Nature* **292,** 259–262
57. Lee, D. C., Fenton, S. E., Berkowitz, E. A., and Hissong, M. A. (1995) *Pharmacol. Rev.* **47,** 51–85
58. Harris, R. C., Chung, E., and Coffey, R. J. (2003) *Exp. Cell Res.* **284,** 2–13
59. Lee, D. C., Sunnarborg, S. W., Hinkle, C. L., Myers, T. J., Stevenson, M. Y., Russell, W. E., Castner, B. J., Gerhart, M. J., Paxton, R. J., Black, R. A., Chang, A., and Jackson, L. F. (2003) *Ann. N. Y. Acad. Sci.* **995,** 22–38

60. Luetteke, N. C., and Lee, D. C. (1990) *Semin. Cancer Biol.* **1,** 265–275
61. Siemeister, G., Weindel, K., Mohrs, K., Barleon, B., Martiny-Baron, G., and Marme, D. (1996) *Cancer Res.* **56,** 2299–2301
62. Ritter, M. M., Frilling, A., Crossey, P. A., Hoppner, W., Maher, E. R., Mulligan, L., Ponder, B. A., and Engelhardt, D. (1996) *J. Clin. Endocrinol. Metab.* **81,** 1035–1037
63. van der Harst, E., de Krijger, R. R., Dinjens, W. N., Weeks, L. E., Bonjer, H. J., Bruining, H. A., Lamberts, S. W., and Koper, J. W. (1998) *Int. J. Cancer* **77,** 337–340
64. Kondo, K., and Kaelin, W. G., Jr. (2001) *Exp. Cell Res.* **264,** 117–125
65. Kinzler, K. W., and Vogelstein, B. (1997) *Nature* **386,** 761–763
66. Humes, H. D., Beals, T. F., Cieslinski, D. A., Sanchez, I. O., and Page, T. P. (1991) *Lab. Invest.* **64,** 538–545
67. Gomella, L. G., Sargent, E. R., Wade, T. P., Anglard, P., Linehan, W. M., and Kasid, A. (1989) *Cancer Res.* **49,** 6972–6975
68. Rosenthal, A., Lindquist, P. B., Bringman, T. S., Goeddel, D. V., and Derynck, R. (1986) *Cell* **46,** 301–309
69. Watanabe, S., Lazar, E., and Sporn, M. B. (1987) *Proc. Natl. Acad. Sci. U. S. A.* **84,** 1258–1262
70. Sporn, M. B., and Todaro, G. J. (1980) *N. Engl. J. Med.* **303,** 878–880
71. Bos, M., Mendelsohn, J., Kim, Y. M., Albanell, J., Fry, D. W., and Baselga, J. (1997) *Clin. Cancer Res.* **3,** 2099–2106
72. Weber, K. L., Doucet, M., Price, J. E., Baker, C., Kim, S. J., and Fidler, I. J. (2003) *Cancer Res.* **63,** 2940–2947
73. Lowden, D. A., Lindemann, G. W., Merlino, G., Barash, B. D., Calvet, J. P., and Gattone, V. H., 2nd. (1994) *J. Lab. Clin. Med.* **124,** 386–394
74. Everitt, J. I., Walker, C. L., Goldsworthy, T. W., and Wolf, D. C. (1997) *Mol. Carcinog.* **19,** 213–219
75. Neufeld, T. K., Douglass, D., Grant, M., Ye, M., Silva, F., Nadasdy, T., and Grantham, J. J. (1992) *Kidney Int.* **41,** 1222–1236
76. Smith, J. J., Derynck, R., and Korc, M. (1987) *Proc. Natl. Acad. Sci. U. S. A.* **84,** 7567–7570
77. Neumann, H. P., Lips, C. J., Hsia, Y. E., and Zbar, B. (1995) *Brain Pathol.* **5,** 181–193
78. Crossey, P. A., Eng, C., Ginalska-Malinowska, M., Lennard, T. W., Wheeler, D. C., Ponder, B. A., and Maher, E. R. (1995) *J. Med. Genet.* **32,** 885–886
79. Eng, C., Crossey, P. A., Mulligan, L. M., Healey, C. S., Houghton, C., Prowse, A., Chew, S. L., Dahia, P. L., O'Riordan, J. L., and Toledo, S. P. (1995) *J. Med. Genet.* **32,** 934–937
80. Clifford, S. C., Astuti, D., Hooper, L., Maxwell, P. H., Ratcliffe, P. J., and Maher, E. R. (2001) *Oncogene* **20,** 5067–5074

Silencing of Epidermal Growth Factor Receptor Suppresses Hypoxia-Inducible Factor-2–Driven *VHL*$^{-/-}$ Renal Cancer

Karlene Smith, Lakshman Gunaratnam, Melissa Morley, Aleksandra Franovic, Karim Mekhail, and Stephen Lee

Department of Cellular and Molecular Medicine, Faculty of Medicine, University of Ottawa, Ottawa, Ontario, Canada

Abstract

Inactivating mutations in the von Hippel-Lindau (*VHL*) tumor suppressor gene are associated with clear cell renal cell carcinoma (VHL$^{-/-}$ RCC), the most frequent malignancy of the human kidney. The VHL protein targets the α subunits of hypoxia-inducible factor (HIF) transcription factor for ubiquitination and degradation. VHL$^{-/-}$ RCC cells fail to degrade HIF resulting in the constitutive activation of its target genes, a process that is required for tumorigenesis. We recently reported that HIF activates the transforming growth factor-α/epidermal growth factor receptor (TGF-α/EGFR) pathway in VHL-defective RCC cells. Here, we show that short hairpin RNA (shRNA)–mediated inhibition of EGFR is sufficient to abolish HIF-dependent tumorigenesis in multiple VHL$^{-/-}$ RCC cell lines. The 2α form of HIF (HIF-2α), but not HIF-1α, drives *in vitro* and *in vivo* tumorigenesis of VHL$^{-/-}$ RCC cells by specifically activating the TGF-α/EGFR pathway. Transient incubation of VHL$^{-/-}$ RCC cell lines with small interfering RNA directed against EGFR prevents autonomous growth in two-dimensional culture as well as the ability of these cells to form dense spheroids in a three-dimensional *in vitro* tumor assay. Stable expression of shRNA against EGFR does not alter characteristics associated with VHL loss including constitutive production of HIF targets and defects in fibronectin deposition. In spite of this, silencing of EGFR efficiently abolishes *in vivo* tumor growth of VHL loss RCC cells. These data identify EGFR as a critical determinant of HIF-2α-dependent tumorigenesis and show at the molecular level that EGFR remains a credible target for therapeutic strategies against VHL$^{-/-}$ renal carcinoma. (Cancer Res 2005; 65(12): 5221-30)

Introduction

Inactivating mutations of the von Hippel-Lindau (VHL) tumor suppressor genes are associated with inherited VHL syndrome, of which afflicted individuals are at increased risk to develop a wide variety of neoplasms, including central nervous system hemangioblastoma and clear cell renal cell carcinoma (RCC; ref. 1). Mutations in the *VHL* gene are also found in the vast majority of sporadic clear cell RCC, the most frequent malignancy of the human kidney (2). Surgery remains the mainstay of treatment for kidney cancer as an incomplete understanding of the molecular mechanisms underlying this disease has limited the development of successful nonsurgical therapies (3). Consequently, the prognosis for patients with recurrent or metastasic renal cancer is often bleak with a mortality rate of 20% within 1 year of diagnosis. Hence, novel clinically relevant therapeutic approaches will directly alter the prognosis of patients with metastatic RCC.

Recent studies have yielded important clues as to the function of the VHL protein. Reintroduction of wild-type VHL in VHL-defective RCC cells prevents tumor formation in nude mice confirming the tumor suppressive function of VHL (4). VHL assembles with elongin B, C, rbx1, and cullin-2 to form and E3 ubiquitin ligase. VHL recruits the α subunits of hypoxia-inducible factor (HIFα) for cullin-2-mediated ubiquitination and subsequent degradation by the 26s proteasome (5–9). HIF is a transcription factor that activates an array of genes involved in cellular adaptation to hypoxia including the angiogenic vascular endothelial growth factor (*VEGF*; refs. 10, 11). The interaction between VHL and HIFα is regulated by oxygen tension. In the presence of oxygen (normoxia), HIF prolyl hydroxylases (PHD) hydroxylate key proline residues in the oxygen-dependent degradation domains of HIFα (12–15). This post-translational modification enables recruitment of HIF by VHL to the VBC/Cul-2 complex subsequently leading to ubiquitination and degradation. The HIF PHDs are inhibited by low oxygen tension resulting in the accumulation of HIFα, assembly with the constitutively expressed HIFβ and activation of HIF target genes such as *VEGF* and glucose transporter-1 (*Glut-1*). VHL-defective RCC cells fail to degrade HIFα regardless of oxygen tension leading to the constitutive activation of its targets. Silencing of HIFα by short hairpin RNA (shRNA) prevents VHL$^{-/-}$ RCC tumor formation in a nude mice xenograft assay showing that the constitutive activation of HIF targets is required for VHL-defective RCC tumorigenesis (16). VHL$^{-/-}$ RCC cells are also unable to form an extracellular fibronectin matrix, which is thought to play an important role in RCC development (17, 18).

Whereas the role of HIF in promoting the highly vascularized phenotype of VHL loss RCC tumors is well characterized, the mechanisms by which this transcription factor can promote tumorigenesis remain debatable (19, 20). There are two active forms of HIFα called HIF-1α and HIF-2α, which activate common as well as distinct targets (21). Recent reports have led to the suggestion that HIF-2α is the oncogenic form of HIFα, at least in human RCC (22–24). This would imply that HIF-2α differs from HIF-1α in its ability to activate a specific target(s) that is involved in oncogenic growth of RCC cells. We recently reported that HIF activates the transforming growth factor-α/epidermal growth factor (TGF-α/EGFR) pathway in VHL$^{-/-}$ RCC cells (25). We suggested that HIF-mediated constitutive EGFR activation provides permanent self-sufficiency in growth signaling that drives the growth autonomy of VHL-defective RCC cells, a hallmark of cancer (26). In this report, we put forward an explanation for the differential oncogenic potential of HIF-2α in RCC cells by

Note: Supplementary data for this article are available at Cancer Research Online (http://cancerres.aacrjournals.org/).

K. Smith and L. Gunaratnam contributed equally to this work.

Requests for reprints: Stephen Lee, Department of Cellular and Molecular Medicine, Faculty of Medicine, University of Ottawa, 451 Smyth Road, Ottawa, Ontario, Canada K1H 8M5. Phone: 613-562-5800 ext. 8385; Fax: 613-562-5636; E-mail: slee@uottawa.ca.

identifying TGF-α as a HIF-2α-specific target. We show that HIF-2α, but not HIF-1α, is able to promote *in vitro* and *in vivo* tumorigenesis of $VHL^{-/-}$ RCC cells by constitutively activating the TGF-α/EGFR oncogenic pathway. Transient and stable silencing of EGFR is sufficient to prevent HIF-2α-dependent tumorigenesis in multiple $VHL^{-/-}$ RCC cell lines. These data reaffirm EGFR as a crucial therapeutic target for VHL-defective renal cancer treatment.

Materials and Methods

Cell culture and reagents. Normoxic cells were incubated at 37°C under a 5% CO_2 environment. Hypoxia was achieved by incubation in a hypoxic chamber at 37°C under 1% O_2, 5% CO_2, and N_2-balanced atmosphere. VHL-deficient, 786-0 and A498 RCC cells, and HCT116 colon carcinoma cells were purchased from the American Type Culture Collection (Rockville, MD). HOP62, MCF7, SKMEL, and PC3 cells were a kind gift from John Bell (Ottawa Regional Cancer Center, Ottawa, Ontario, Canada) and U87MG cells a kind gift from Ian Lorimer (Ottawa Regional Cancer Center, Ottawa, Ontario, Canada). 786-0 and A498 cells stably transfected with HA-VHL (786-0 + VHL and A498 + VHL, respectively) were a kind from Dr. W.G. Kaelin (Harvard University, Boston, MA). KTCL140 cell line was a kind gift from Dr. Peter Ratcliffe (University of Oxford, Oxford, United Kingdom). Primary cultures of human renal cortical epithelial cells were purchased from Clonetics (San Diego, CA). Serum containing medium consisted of DMEM or McCoys 5A (HCT116) medium with 10% fetal bovine serum (FBS). Serum-free medium consisted of DMEM supplemented with 1% insulin-transferrin-selenium (Invitrogen, Burlington, Ontario, Canada). PD153035 (Calbiochem, San Diego, CA) was used as indicated. Treatment of VHL-deficient cells with antisense targeting TGF-α was carried out as previously described (27).

Adenovirus construction. Adenoviruses encoding the HIF-α mutants, VHL, GFP, and DN-HIF were generated through Cre-lox recombination as described elsewhere (25, 28). Vectors encoding HIF-α subunits mutated at proline hydroxylation sites encoding HA-HIF-2α (P405A and P531α) and HA-HIF1α (P402A and P564A) were a kind gift from Dr. W.G. Kaelin. cDNA encoding the constitutively active variants of HIFα were released by *Bam*HI/*Not*I restriction digest from their original pcDNA 3.0 vector and subcloned, in-frame, downstream of a Flag-GFP moiety previously cloned into the *Hin*dIII and *Bam*HI sites of a pAdlox adenoviral vector. DNA sequencing analysis confirmed the alanine substitutions of the targeted proline residues. Experiments used approximately equal multiplicity of infection.

RNA isolation and reverse transcription-PCR analysis. One microgram of total RNA collected using TRIPURE isolation reagent (Roche, Indianapolis, IN) was used. All primers and cycle details for reverse transcription-PCR (RT-PCR) for TGF-α, Glut-1, and actin are described elsewhere (25). Semiquantitative RT-PCR was done by taking samples after 30 amplification cycles. Products were analyzed with gel electrophoresis and ethidium bromide staining, and visualized using a Kodak Digital Science IC440 system.

For real-time RT-PCR, triplicate (25 μL) multiplex RT-PCR reactions were done on 50 ng of total RNA using Taqman One-Step RT-PCR master mix reagents (Applied Biosystems, Streetville, Ontario, Canada) and 0.25 μmol/L 5′-VIC TGF-α and 5′-6FAM actin modified probes. Cycling conditions were 30 minutes at 48°C, 10 minutes at 95°C, then 40 cycles of alternating 15 seconds at 95°C and 1 minutes at 60°C. Amplification and analysis of real-time data was done using ABI PRISM 7000 Sequence Detection System (Applied Biosystems). The quantity of TGF-α detected in each reaction tube was normalized to the level of coamplified actin endogenous control. Each RNA sample was analyzed in triplicate to obtain an average normalized quantity of TGF-α transcript (arbitrary units). TGF-α forward GCACGTCCCCGCTGAGT and TGF-α reverse CAGGTTCCATGGAAGCAGAA; TGF-α probe TTTTAATGACTGCCCAGATTCCCACACTCA; β-actin probe CCGCCGCCCGTCCACACCCGCC. The sequences all other primers used are described elsewhere (25).

Bromodeoxyuridine labeling. Cells were plated at low density on coverslips and incubated overnight in DMEM supplemented with 10% FBS. At the start of the experiment, cells were washed and supplemented with fresh serum-containing or serum-free medium. The cells were infected with adenoviruses as indicated. After the indicated time cells were fixed and stained with an anti-bromodeoxyuridine (BrdUrd) antibody according to instructions of manufacturer (Roche). Nuclei were stained (Hoechst 33258; Sigma, St. Louis, MO) and assessed for BrdUrd incorporation using a Ziess Axiovert S100TV microscope (Thornwood, NY). Data is presented as proportion of nuclei incorporating BrdUrd.

Transforming growth factor-α ELISA. An equal number of cells were seeded approaching confluence and allowed to settle overnight in DMEM supplemented with 5% FBS. The appropriate cells were infected with adenovirus after addition of fresh culture medium. Medium and total cell lysates were collected and analyzed for TGF-α protein according to instructions of manufacturer (Oncogene, Boston, MA). Total protein concentration was determined using the bicinchoninic acid protein assay reagent (Pierce, Rockford, IL) to ensure equivalence between samples. Antisense to TGF-α experiments were as described previously (27).

Western blot. Cells were washed with PBS and harvested in 4% SDS in PBS. Samples (20-100 μg of each) were separated on denaturing polyacrylamide gels containing SDS and transferred to methanol-activated polyvinylidene difluoride membrane (NEN, Boston, MA). Membranes were blocked in skimmed milk before incubation with Flag (Sigma) or EGFR (Ab-12; LabVision, Fremont, CA) monoclonal antibodies. Polyclonal antibodies were used to detect py-EGFR (sc-12351; Santa Cruz Biotechnology, Santa Cruz, CA), HIF-2α (Novus, Littleton, CO), Glut-1 (Alpha Diagnostic International, San Antonio, TX), and actin (Sigma). After washing with 0.2% Tween-PBS solution, membranes were blotted with secondary antibodies conjugated to horseradish peroxidase (Jackson ImmunoResearch, West Grove, PA) and detected by enhanced chemiluminescence (Pierce).

Immunofluorescence. Cells were grown to confluence for 6 days on glass coverslips, washed thrice with PBS, and fixed/permeabilized in prechilled 95% ethanol at −20°C for 30 minutes. Ethanol was aspirated and residual was allowed to air dry at 4°C. Cells were stained for 1 hour at room temperature with anti-fibronectin antibody as described in (29). Staining was visualized with a Ziess Axiovert S100TV microscope.

Epidermal growth factor receptor RNA interference. For transient inhibition of EGFR mRNA production, VHL-deficient RCC cells were transfected with commercially available double-stranded 21-nucleotide-long small interfering RNA (siRNA) targeting the EGFR or a control siRNA (Ambion, Austin, TX). VHL-deficient RCC cells were also stably transfected to express one of two different shRNA sequences targeting the EGFR (30). For each sequence, two ssDNA oligonucleotides were synthesized (Invitrogen) and subsequently annealed by incubation for 3 minutes at 90°C followed by 1 hour at 50°C. ssDNA were designed with overhangs encoding restriction sites for *Bam*HI/*Hin*dIII, and the annealed products were ligated directly into the pSilencer 3.1-H1 neo vector (Ambion). Sequence 1 (5′-3′): shRNA EGFR-1 forward GATCCAACTCTGGAGGAAAAGAAAGTTTCAAGAGAACTTTCTTTTCCTCCAGAGTTTTTTTTGGAAA and shRNA EGFR-1 reverse AGCTTTTCCAAAAAAAACTCTGGAGGAAAAGAAAGTTCTCTTGAAACTTTCTTTTCCTCCAGAGTTG. Sequence 2 (5′-3′): shRNA EGFR-2 forward GATCCAACACAGTGGAGCGAATTCCTTTCAAGAGAAGGAATTCGCTCCACTGTGTTTTTTTTGGAAA and shRNA EGFR-2 reverse AGCTTTTCCAAAAAAAACACAGTGGAGCGAATTCCTTCTCTTGAAAGGAATTCGCTCCACTGTGTTG. A pSilencer 3.1-H1 neo vector encoding random control shRNA was also purchased from Ambion. Stable clones were selected in neomycin containing medium. All transfections were conducted with Effectene transfection reagent (Qiagen, Valencia, CA). All constructs were verified by standard DNA sequencing.

***In vitro* tumor spheroid.** Multicellular spheroids were prepared by the liquid overlay technique (31–33) and as described by our group elsewhere (34). Briefly, 24-well plates were coated with 250 μL of preheated 1% Seaplaque agarose (Cambrex, Rockland, ME) in serum-free medium; 10^5 of indicated cells were plated per 1 mL of DMEM per well. To promote cell-cell adhesion, the plates were gently swirled (32 times) 30 minutes after plating. Spheroids were grown for 6 days at 37°C under 5% CO_2 in serum-containing medium. Spheroids were harvested in lysis buffer (4% SDS in PBS) before

immunoblotting. Alternatively, spheroids were fixed in 10% formaldehyde, embedded in paraffin, sectioned, mounted on slides, and stained with H&E.

Nude mouse xenograft assays. Nude mouse xenograft assays were done as described elsewhere (4). In brief, 10^7 viable cells (trypan dye exclusion method) were injected s.c. in the flanks of female nude mice (Charles River, Wilmington, MA). Mice injected with both control and EGFR shRNA were sacrificed 9 weeks post-injection according to facility protocol (University of Ottawa). In keeping with the Animal Facility Guidelines to examine latent tumor formation, a subset of mice was only injected with cells expressing shRNA targeting EGFR. These mice were sacrificed 16 weeks post-injection and did not exhibit any latent tumor formation. Tumor size was measured weekly, and at the time of sacrifice tumors were excised and weighed. Experiments were done blinded.

Results

Hypoxia-inducible factor-2α specifically promotes growth autonomy of renal cell carcinoma cells. VHL loss RCC cells constitutively overproduce HIF-regulated genes as a consequence of the inability of these cells to degrade HIFα in normoxia (8). Constitutive HIF activation is required for serum-independent growth of $VHL^{-/-}$ RCC cells in culture as well as for tumor formation in a xenograft nude mice tumor assay (16, 25). In addition, constitutive expression of HIF-2α, but not HIF-1α, overrides VHL-mediated RCC tumor suppression (22, 24). To further investigate the role of the two HIFα forms in RCC tumorigenesis, we produced adenoviruses that express HIF-1α and HIF-2α variants that evade VHL recognition in the presence of oxygen (henceforth called HIF-1α and HIF-2α; Fig. 1*A* schematic). To do so, key proline residues in the ODD domain of HIFα were substituted to alanine, which prevents recognition and degradation by VHL in normoxic cells (Fig. 1*A*; see ref. 22). HIFα variants were expressed to similar levels and were functional as they equally promoted the accumulation of *Glut-1* mRNA, a well-characterized HIF-regulated gene, in normoxic VHL-competent cells (Fig. 1*A*). In the absence of exogenous growth factors or serum, VHL-deficient cells are able to engage in autonomous growth, a hallmark of cellular transformation (26). Reintroduction of VHL in VHL-defective cells enables these cells to respond like primary renal epithelial cells and quiesce, a process measured by a decrease in BrdUrd incorporation (Fig. 1*B*; refs. 25, 35). As previously shown, dominant-negative HIF (DNHIF) abolished BrdUrd incorporation by VHL-deficient RCC cells in serum-free medium, thereby demonstrating that the observed autonomous proliferation of these RCC cells is a consequence of HIF activation (Fig. 1*B*; ref. 25). Addition of serum restored BrdUrd incorporation in all conditions showing that RCC cells are equally sensitive to exogenous growth factors, regardless of VHL status or HIF activation (Fig. 1*B*). We asked whether HIF-1α or HIF-2α activation could promote growth autonomy of RCC cells by overriding the effect of reintroduction of VHL in VHL-defective RCC cells. Expression of HIF-1α had no discernable effect on growth of VHL-competent cells in the presence or absence of serum nor did it promote cell death or dominant cell cycle arrest in the presence of serum, as reported for other cell lines (Fig. 1*C*; data not shown; see ref. 36). In contrast, expression of HIF-2α was sufficient to promote autonomous growth of RCC cell lines overriding the effect of stable expression of VHL (Fig. 1*C*). These experiments show that HIF-2α-specific transcriptional activity differs from HIF-1α and enables VHL-competent cells to engage in autonomous growth consistent with its ability to promote tumorigenesis *in vivo* (22).

Transforming growth factor-α is a hypoxia-inducible factor-2α–specific target. Next, we wanted to uncover the

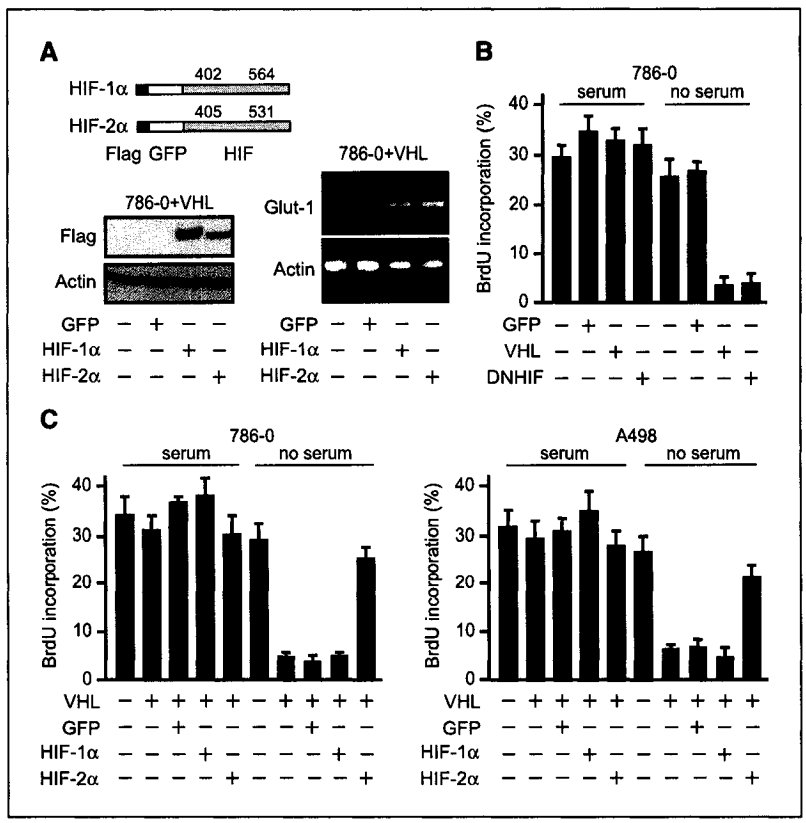

Figure 1. HIF-2α promotes autonomous growth of RCC cells. *A*, HIF-1α and HIF-2α variants carrying P-to-A mutations at prolyl hydroxylation sites (schematic) are both able to activate HIF target genes. VHL-deficient 786-0 cells were stably transfected to express HA-VHL and infected with adenoviruses expressing flag-tagged HIF-1α, HIF-2α, or GFP. After 48 hours post-infection immunoblotting or RT-PCR was done to detect flag protein or Glut-1 mRNA, respectively. *B*, HIF activation is required for serum independent growth of VHL-deficient RCCs. 786-0 cells infected to express GFP, VHL, or dominant-negative HIF were incubated for 72 hours in the absence or presence of serum and assessed for BrdUrd incorporation. *Columns*, average mean of at least three independent experiments in triplicates; *bars*, SE. *C*, HIF-2α but not HIF-1α is able to promote serum-independent growth in VHL-competent cells. Growth was measured in 786-0 or A498 cells deficient or competent for VHL expression (786-0 + VHL or A498 + VHL, respectively) following infection with an adenovirus encoding GFP, HIF-1α, or HIF-2α. *Columns*, average mean of at least three independent experiments in triplicates; *bars*, SE.

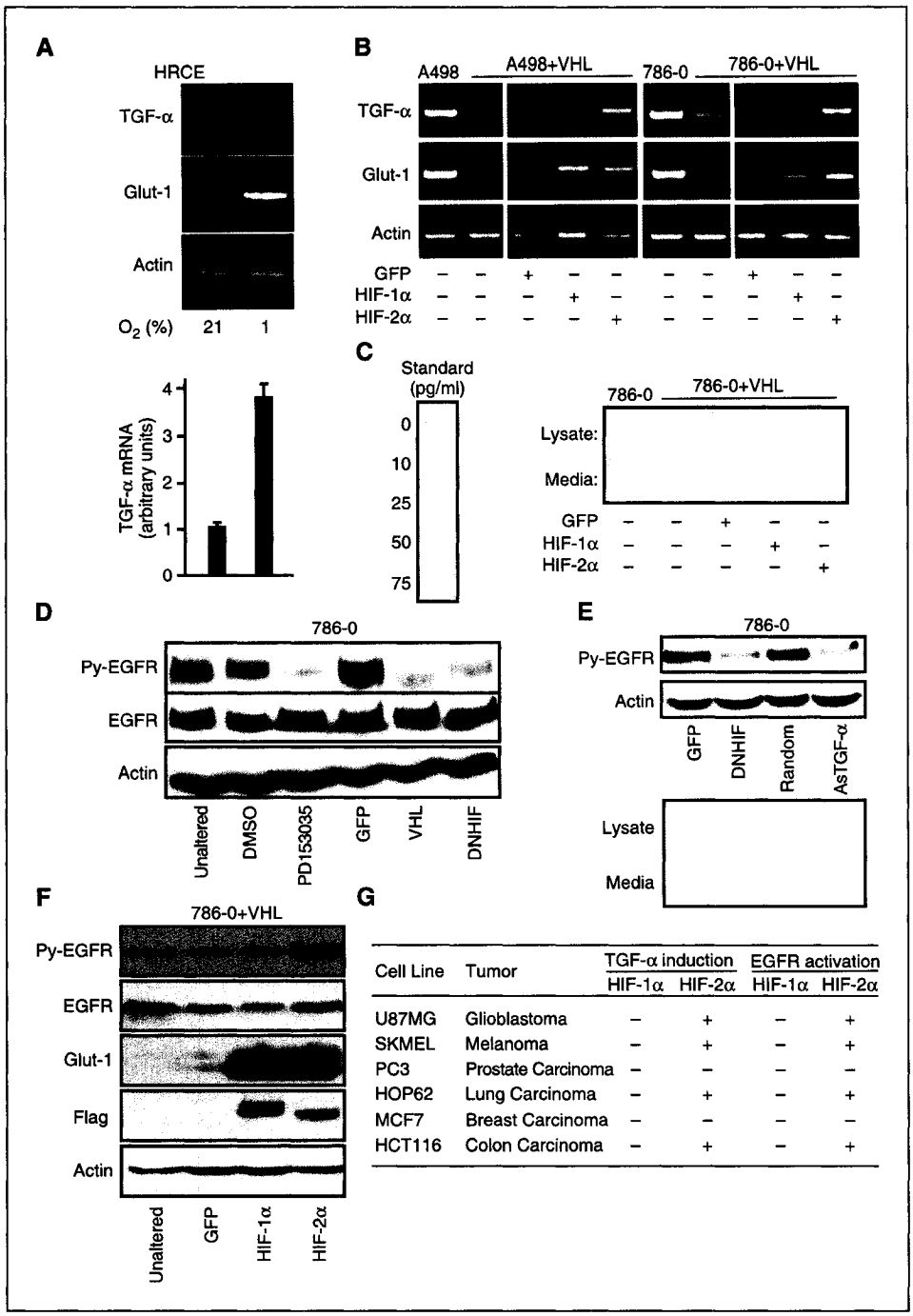

Cell Line	Tumor	TGF-α induction		EGFR activation	
		HIF-1α	HIF-2α	HIF-1α	HIF-2α
U87MG	Glioblastoma	–	+	–	+
SKMEL	Melanoma	–	+	–	+
PC3	Prostate Carcinoma	–	–	–	–
HOP62	Lung Carcinoma	–	+	–	+
MCF7	Breast Carcinoma	–	–	–	–
HCT116	Colon Carcinoma	–	+	–	+

Figure 2. Specific induction of TGF-α by HIF-2α activates the EGFR. *A*, hypoxic induction of TGF-α mRNA as measured by RT-PCR in primary human renal cortical epithelial cells. Real-time PCR results (*bottom inset*). *Columns*, average mean of three independent experiments in triplicates; *bars*, SE. *B*, HIF-2α but not HIF-1α induces TGF-α mRNA synthesis in VHL-competent cells. RT-PCR was used to detect TGF-α and Glut-1 in VHL-deficient A498 and 786-0 cells and in A498 and 786-0 cells that stably express reintroduced VHL (A498 + VHL and 786-0 + VHL). Cells were infected to express indicated proteins. *C*, HIF-2α but not HIF-1α induces TGF-α protein in VHL-competent cells. ELISA was done to detect TGF-α protein in cellular lysates and media. VHL-deficient 786-0 cells and VHL-competent 786-0 + VHL cells were infected to express the indicated proteins. *D*, immunoblotting detecting EGFR and phosphorylated, activated EGFR in 786-0 cells treated with PD153035, or infected to express GFP, VHL or DNHIF. Cells were incubated for 48 hours in serum-free conditions before collection of lysates. *E*, blockade of HIF activation or silencing of its target TGF-α reduces EGFR activation. 786-0 cells were infected to express GFP or DNHIF, or were treated with TGF-α antisense or random oligomers. Total cell lysates were submitted to anti-Py-EGFR immunoblotting. In parallel, ELISA was used to detect TGF-α. Cells were incubated for 48 hours in serum-free conditions before collection of lysates. *F*, HIF-2α but not HIF-1α induces EGFR activation in VHL-competent 786-0 cells. Cells were infected to express the indicated proteins and lysates were submitted to immunoblotting to detect the indicated proteins. Cells were incubated for 48 hours in serum-free conditions before collection of lysates. *G*, HIF-2α induces TGF-α mRNA/protein production and EGF-R activation in cancer cells from various tissue origin. Cells were infected to express HIF-1α or HIF-2α and submitted to RT-PCR analysis to detect TGF-α mRNA and to immunoblotting to detect increased phosphorylation of EGFR as described in (*B*), (*C*), and (*F*). Data is presented as a table for the sake of simplicity.

mechanism by which HIF-2α differs from HIF-1α and promotes autonomous proliferation. We recently reported that overproduction of TGF-α, a bona fide epithelial cell mitogen, by RCC cells is triggered by HIF activation (25). Thus, we suspected that TGF-α might play a key oncogenic role in HIF-2α-mediated autonomous growth. As shown in Fig. 2*A*, TGF-α mRNA is hypoxia-inducible in primary cultures of renal epithelial cells, the cell type from which VHL loss RCC arises (1, 37–39). VHL loss RCC cells overproduce TGF-α mRNA in normoxia, which can be down-regulated by the reintroduction of VHL (Fig. 2*B*; refs. 27, 40). Whereas HIF-1α and HIF-2α equally promoted Glut-1 transcription in normoxic VHL-competent cells, TGF-α mRNA induction was observed only in cells expressing HIF-2α (Fig. 2*B*). TGF-α protein was present in cellular lysates of HIF-2α-, but not HIF-1α-infected, VHL-competent cells (Fig. 2*C*). In addition, quantitative RT-PCR experiments showed that TGF-α is a target of endogenous, wild-type HIF-2α in hypoxic VHL-competent cells or VHL-defective RCC 786-0 cells (Supplementary Fig. S1). An RT-PCR screen revealed that TGF-α is the only known EGFR ligand to be activated by HIF-2α or by VHL loss (data not shown; see ref. 25 for the screen in VHL loss RCC cells).

We next asked if HIF-2α was able to activate EGFR through production of TGF-α ligand. VHL-deficient 786-0 RCC cells

expressing endogenous HIF-2α displayed strong EGFR phosphorylation, in the absence of exogenous growth factors (Fig. 2*D*). Expression of VHL or DNHIF was essentially as efficient as PD15035 at abolishing EGFR phosphorylation in VHL-deficient RCC cells. In addition, antisense-mediated inhibition of TGF-α production blocks autonomous growth of VHL-deficient cells (27) and abrogates EGFR phosphorylation (Fig. 2*E*). Expression of HIF-2α resulted in a marked activation of the EGFR in VHL-competent 786-0 (Fig. 2*F*) and A498 cells (data not shown). In contrast, HIF-1α did not activate the EGFR, further supporting the notion that HIF-1α is unable to drive the production of active EGFR ligands (Fig. 2*F*). HIF-2α-specific induction of TGF-α mRNA was observed in the majority of tested cancer cell lines maintained in normal oxygen tension (Fig. 2*G*). No significant TGF-α transcript or protein was detected in HIF-1α-expressing cells, although HIF-1α was as efficient as HIF-2α at promoting Glut-1 mRNA accumulation (Fig. 2*G*; data not shown). Furthermore, activation of the EGFR was observed only in cancer cell lines where HIF-2α induced TGF-α production. These results support the hypothesis that HIF-2α drives autonomous proliferation by activating EGFR through the specific production of TGF-α. The data also suggest that HIF-1α activation alone is insufficient to promote serum-free growth of VHL-competent RCC cells.

Transient silencing of epidermal growth factor receptor by small interfering RNA prevents formation of dense renal cell carcinoma tumors *in vitro*. We next asked whether EGFR activation plays a central role in the ability of HIF-2α to drive VHL loss RCC tumorigenesis. To do so, a panel of VHL-defective

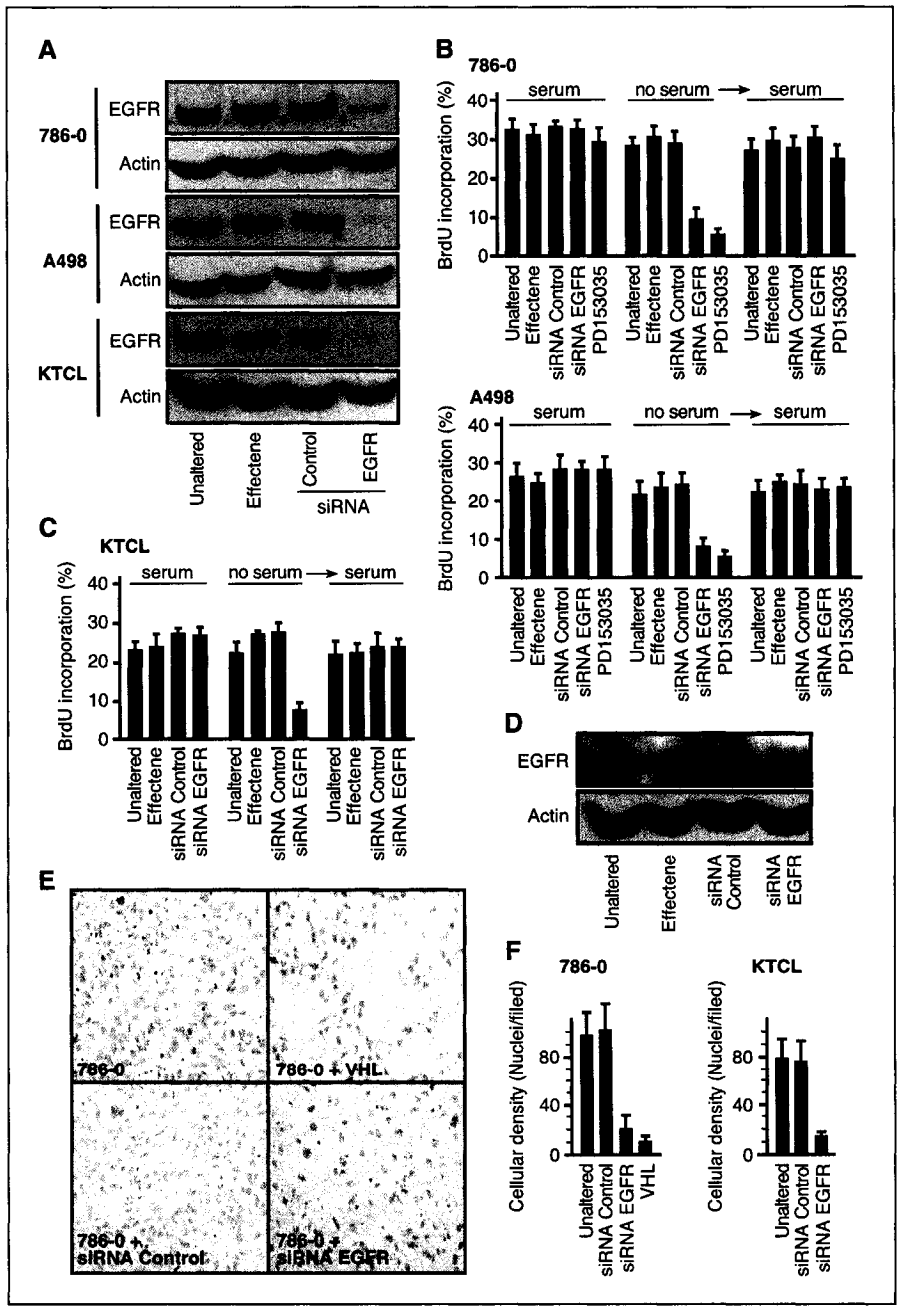

Figure 3. Transient silencing of EGFR with siRNA prevents serum-free growth and formation of dense tumor spheroids. *A*, transient incubation with siRNA directed against EGFR mRNA suppresses EGFR protein production in multiple VHL-defective cells. Immunoblots were done to detect EGFR in untreated cells, cells treated with effectene, control siRNA, or siRNA against EGFR. *B-C*, siRNA directed against EGFR prevents serum-independent growth of multiple $VHL^{-/-}$ RCC cells. Cells were incubated in the presence of 10% serum or in the absence of serum for 72 hours followed by addition of serum for 48 hours. BrdUrd labeling was for 3 hours in all conditions. Transient incubation with siRNA was as described in Materials and Methods. PD153035 was added for the duration of the experiments without noticeable toxic effects. *Columns*, average mean of at least three independent experiments in triplicates; *bars*, SE. *D-E*, siRNA directed against EGFR prevents dense spheroid formation. *In vitro* tumor spheroids were produced as described in Materials and Methods for 6 days in the presence or absence of control siRNA or siRNA directed against EGFR. Histology from spheroids is visualized at a magnification of 400×. Immunoblot detection of EGFR shown in (*D*) was from lysates of spheroids incubated for 6 days to show inhibition of EGFR protein production by siRNA. *F*, density was measured at 400× magnification in four independent spheroids in at least three sections per spheroid and reported as nuclei/field. *Columns*, average mean of at least three independent experiments in triplicates; *bars*, SE.

RCC cell lines was incubated in the presence of a siRNA directed against EGFR mRNA. The cell lines included the widely characterized VHL-defective RCC 786-0 and A498 cell lines. In addition, we used the KTCL140 line reported to harbor VHL inactivating mutations and overexpress HIF-2α and its targets (8). KTCL140 overproduce TGF-α and display strong EGFR phosphorylation that can be repressed by reintroduction of VHL or expression of DNHIF (data not shown; Fig. 5). The siRNA efficiently decreased levels of EGFR protein in $VHL^{-/-}$ RCC cells (Fig. 3*A*) and, importantly, prevented HIF-2α-mediated autonomous growth as efficiently as the EGFR tyrosine kinase inhibitor PD153035 for 786-0 and A498 (Fig. 3*B-C*). The effect of silencing EGFR on growth was restricted to serum-free conditions because addition of fresh serum abolished the growth inhibitory effect of the siRNA, as expected. These data show that the ability of HIF-2α to drive growth autonomy of $VHL^{-/-}$ RCC cells requires activation of EGFR.

VHL-deficient RCC cells, like most tumorigenic cell lines, are able to form dense tumor spheroids *in vitro* (33), an accepted assay that measures the tumorigenic potential of cancer cells (31, 32). This assay has also the advantage of measuring tumorigenicity in the absence of neovascularization, a variable especially important in the case of the highly angiogenic $VHL^{-/-}$ RCC tumors. Tumor density was measured by nuclei/field in several sections of tumor spheroids. As shown in Fig. 3*E*, VHL-deficient RCC cells form highly dense *in vitro* tumors. In contrast, VHL-competent RCC cells are characterized by a loose arrangement of cells and a significant decrease of cell density (Fig. 3*F*). Transient incubation with siRNA against EGFR suppressed EGFR protein levels in the spheroids (Fig. 3*D*) and prevented formation of dense tumors in $VHL^{-/-}$ RCC 786-0 and KTCL140 cell lines to levels similar to those observed with reintroduction of VHL (Fig. 3*E* and *F*). These data show that siRNA to EGFR suppresses autonomous growth and dense tumor spheroid formation as efficiently as reintroduction of VHL.

Stable silencing of epidermal growth factor receptor suppresses tumorigenesis of von Hippel-Lindau–defective renal cell carcinoma. Based on the data obtained in Fig. 3, we decided to engineer $VHL^{-/-}$ RCC cells with stably inactivated EGFR by expression of shRNA. For these experiments, we used the $VHL^{-/-}$ RCC cells 786-0, which has been extensively characterized by several other groups (4, 33, 40, 41). The 786-0 cells form tumors

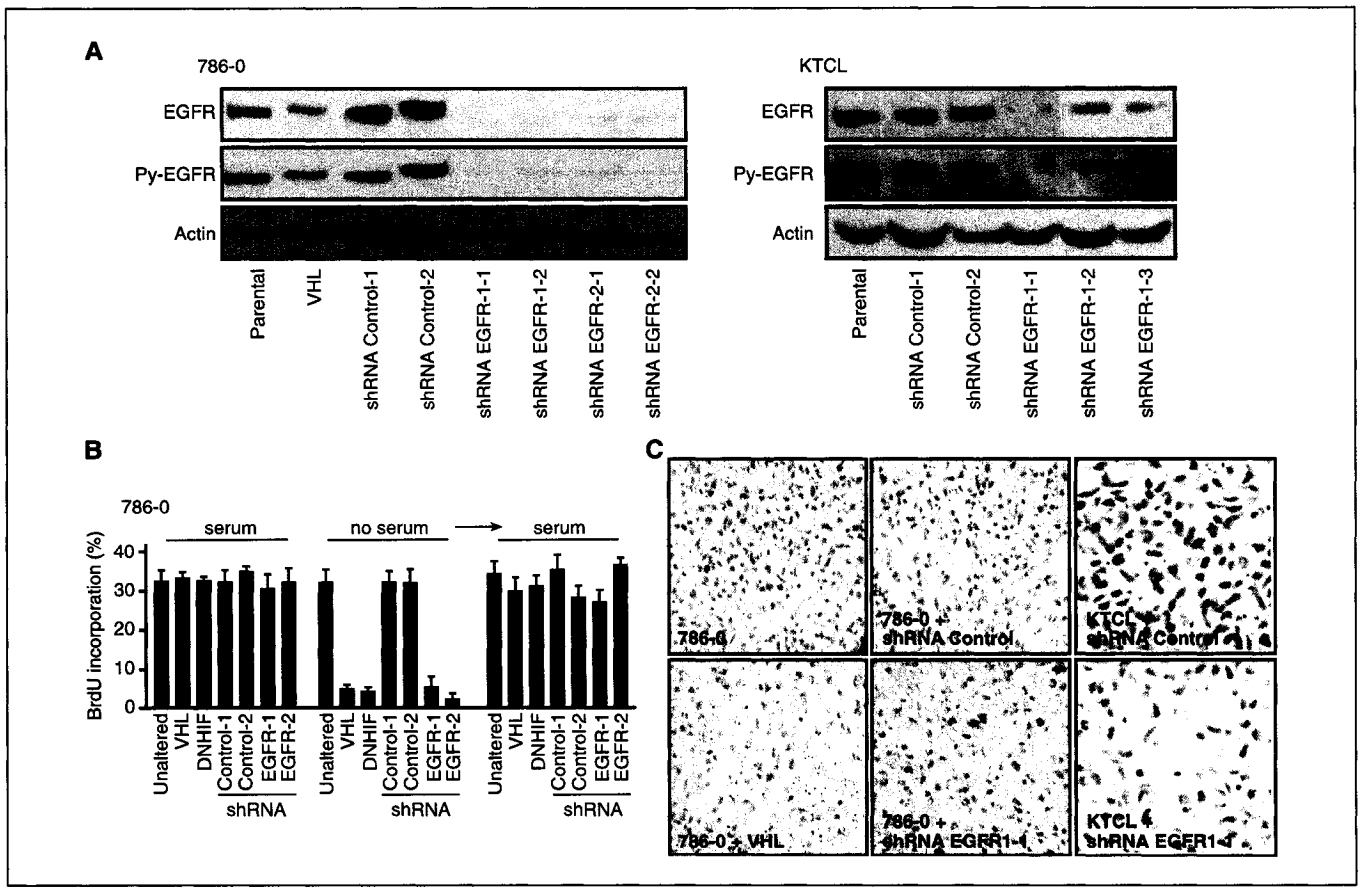

Figure 4. Stable inhibition of EGFR protein and activity by shRNA in $VHL^{-/-}$ RCC cells. *A*, shRNA directed against EGFR mRNA suppresses EGFR protein levels. $VHL^{-/-}$ RCC 786-0 and KTCL140 were stably transfected with pSilencer expressing control shRNA (called shRNA control) or expressing shRNA1 or shRNA2 directed against EGFR mRNA (called shRNA EGFR-1 or shRNA EGFR-2, respectively). Cell lines of 786-0 cells stably expressing reintroduced VHL are denoted VHL. Immunoblots were done to detect EGFR or phosphorylated EGFR. *B*, stable silencing of EGFR by shRNA abolishes growth autonomy of $VHL^{-/-}$ RCC cells as efficiently as expression of VHL or DNHIF. $VHL^{-/-}$ RCC 786-0 cells infected to express GFP, VHL, or DNHIF as well as stably expressing control shRNAs or shRNA EGFR-1 or EGFR-2 were incubated in 10% serum, transferred to serum-free conditions for 72 hours followed by addition of serum for 48 hours. BrdUrd incubation was for 3 hours in each case. Similar data were obtained for KTCL140 cell line but omitted for the sake of clarity. *Columns*, average mean of at least three independent experiments in triplicates; *bars*, SE. *C*, stable silencing of EGFR by shRNA prevents dense tumor formation. *In vitro* tumor spheroids were produced as described in Materials and Methods for 6 days. Histology from spheroids is visualized at a magnification of 400×.

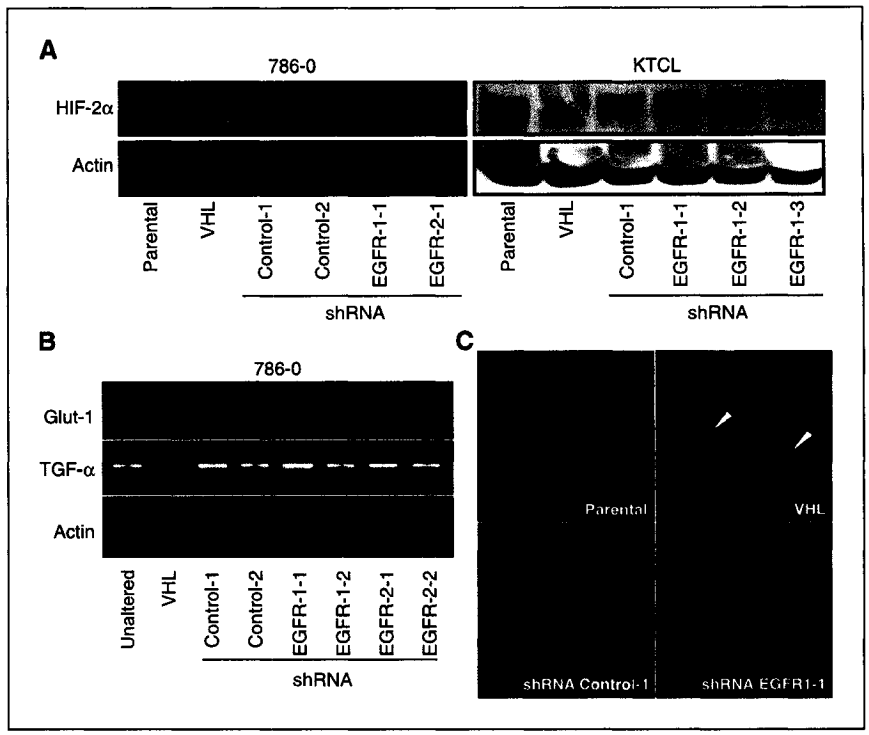

Figure 5. Inhibition of EGFR does not correct other defects associated with VHL loss. *A*, stable inhibition of EGFR does not alter HIF-2α protein levels. Immunoblots were done to monitor HIF-2α protein levels in 786-0 or KTCL140 cells stably expressing shRNA directed against EGFR. *B*, stable silencing of EGFR by shRNA does not prevent activation of HIF-2α-regulated genes. RT-PCR was done from RNA isolated from the indicted clones to detect TGF-α and Glut-1 mRNA as well as actin mRNA for loading comparison. *C*, inhibition of EGFR does not correct defects of $VHL^{-/-}$ RCC cells in fibronectin matrix deposition. Immunofluorescence to detect fibronectin was as described in Material and Methods. Arrows point to fibronectin matrix only found in VHL-expressing cells.

in nude mice, which can be suppressed by reintroduction of VHL or shRNA-mediated inhibition of HIF-2α (4, 16). Several different shRNA targeted against different regions of the EGFR mRNA were tested for their ability to efficiently suppress EGFR protein production. After initial screening of several shRNA-expressing stable clones, two different shRNAs, called shRNA1 and shRNA2, were further characterized because of their ability to mediate a stable and efficient decrease in EGFR protein levels (data not shown). $VHL^{-/-}$ RCC 786-0 cells stably expressing shRNA1 or shRNA2 displayed a significant decrease in EGFR protein levels compared with parental cells and cells stably expressing control scrambled shRNA (Fig. 4*A*). Importantly, loss of phosphorylated EGFR was also observed in shRNA-expressing cells demonstrating a near-complete loss of EGFR function (Fig. 4*A*). As observed with transient inhibition of EGFR, we did not notice a significant difference in two-dimensional growth in the presence of serum between parental 786-0 cells, or 786-0 cells expressing either VHL, control shRNA or shRNA against EGFR mRNA. However, shRNA-mediated inhibition of EGFR restored the ability of VHL-defective RCC cells to withdraw from the cell cycle upon serum withdrawal, a process that could be rescued by the addition of fresh serum. The ability of the shRNA against EGFR to abolish growth autonomy of VHL-defective RCC cells was similar to that observed upon reintroduction of VHL, expression of DNHIF (Fig. 4*B*), transient incubation with siRNA against EGFR, treatment with PD153035 (Fig. 3) or incubation with antisense oligonucleotides against TGF-α mRNA (27). EGFR protein levels and phosphorylation were also significantly diminished in the KTCL140 line stably expressing shRNA1 (Fig. 4*A*). The effects of suppressing EGFR expression in KTCL140 cells were very similar to those shown for 786-0 cells (data not shown). Stable silencing of EGFR by shRNA resulted in low-density spheroids formation in 786-0 and KTCL140 cells (Fig. 4*C*). These experiments confirm that VHL-defective 786-0 clones stably expressing shRNA directed against EGFR mRNA display significant decrease in EGFR protein level, phosphorylation status, and activity without significant dominant effect on the cell cycle in medium supplemented with exogenous growth factors. The data also suggest that observations made in 786-0 can be generalized to other $VHL^{-/-}$ RCC cells.

We next wanted to examine the effect of EGFR knockdown on defects associated with VHL loss. shRNA-mediated silencing of EGFR did not affect HIF-2α protein levels and its ability to activate downstream targets, such as Glut-1 and TGF-α (Fig. 5*A-B*). In addition, EGFR knockdown failed to restore the ability of $VHL^{-/-}$ RCC 786-0 cells to form a fibronectin extracellular matrix (Fig. 5*C*; ref. 17). Similar data were obtained with the KTCL140 cell lines stably expressing shRNA1 against EGFR (Fig. 5*A*; data not shown). These data indicate that RCC cells expressing shRNA against EGFR display all of the cancer-like biochemical characteristics associated with VHL loss including constitutive activation of HIF-2α-regulated genes and loss of fibronectin deposition.

Finally, we examined the effect of EGFR knockdown on the tumorigeneic potential of VHL-deficient RCC cells by injecting clones into nude mice and monitoring tumor formation for a period of 9 weeks. Parental 786-0 cells as well as 786-0 cells expressing vector alone or control shRNA cells produced large tumors detectable after 4 to 5 weeks. $VHL^{-/-}$ RCC cells expressing reintroduced VHL did not form tumors after 9 weeks of incubation (Fig. 6*A-B*). RCC 786-0 cells expressing either shRNA1 or shRNA2 directed against EGFR mRNA failed to form tumors after 9 weeks post-injection (Fig. 6*A-C*). It should be noted that prolong periods of incubation resulted in measurable tumor formation by VHL-competent RCC cells. In contrast, we were unable to detect small tumors in shRNA-expressing cells even after 15 weeks of incubation suggesting that EGFR knockdown abolishes latent tumor formation observed in VHL-competent RCC cells (data not shown). Similar data were obtained with $VHL^{-/-}$ RCC KTCL140 cells expressing shRNA1, although tumor size observed with KTCL140 cells

expressing control shRNA was smaller than that observed with the 786-0 cells (Fig. 6*C*). These results show that shRNA-mediated silencing of EGFR phenocopies the effect of reintroduction of VHL, or silencing of HIF-2α, suggesting that EGFR is a central downstream target of HIF-dependent tumorigenesis.

Discussion

We report that oncogenic EGFR signaling is involved in HIF-2α-dependent tumorigenesis in VHL loss RCC cells because silencing of EGFR prevents tumor formation *in vivo*, phenocopying the effect of HIF-2α silencing or reintroduction of VHL (4, 16). Kaelin et al. originally proposed that HIF-2α might act as an oncogene based on the ability of this transcription factor to override tumor suppression by VHL and drive tumorigenesis of human renal cancer cells (16, 22). Here, we provide a mechanistic explanation for HIF-2α-dependent tumorigenesis. We show that HIF-2α is able to promote autonomous growth of RCC cells by specifically activating the TGF-α/EGFR pathway. Silencing of EGFR is sufficient to block the oncogenic activity of HIF-2α and to prevent HIF-2α-driven tumor formation of VHL-defective RCC cells *in vitro* and in a xenograft nude mice assay. In stark contrast, HIF-1α fails to promote autonomous growth of RCC cells and is unable to activate the *TGF-α* gene or the EGFR pathway. Our previous observation that overexpression of wild-type HIF-1α induced expression of TGF-α in VHL-competent 786-0 cells is explained by accumulation of endogenous HIF-2α, likely the result of saturation of the β-domain of VHL by overproduced wild-type HIF-1α (23). Our studies provide an explanation for the inability of this particular HIFα form to drive tumorigenesis of renal cancer cells. Inactivating mutations of the *VHL* gene confer a number of molecular defects to cells including improper assembly of a fibronectin matrix and constitutive HIFα activation. Despite these cellular flaws, silencing of EGFR was sufficient to block tumorigenesis overriding the effect of VHL loss, HIF-2α activation, and failed fibronectin deposition. The observation that transient or stable inactivation of EGFR prevented dense spheroids formation in the avascular *in vitro* tumor assay argues that suppression of tumorigenesis is not an indirect outcome of failed angiogenesis. Likewise, we showed that silencing of EGFR prevents autonomous growth of VHL-defective RCC cells providing further evidence that HIF-2α acts as an oncogene through activation of the TGF-α/EGFR pathway. It is also noteworthy that TGF-α expression can be induced by hypoxia in primary cultures of human renal epithelial cells, the cell type thought to give rise to RCC. We thus propose that VHL loss and subsequent HIF-2α activation, observed in early multicellular lesions of the distal nephrons, results in aberrant growth by eliciting permanent EGFR signaling by way of TGF-α activation (37). These data also explain why HIF-1α is not tumorigenic in RCC, which is most likely the consequence of the inability of this HIFα subunit to activate TGF-α/EGFR pathway. Immunohistochemical studies have shown expression of HIF-2α, but not HIF-1α, in premalignant multicellular foci in nephrons upon VHL loss, which is consistent with the inability of HIF-1α to drive EGFR activation and proliferation (24, 37). We therefore suggest that the oncogenic activity of HIF-2α is linked to its ability to activate TGF-α/EGFR pathway.

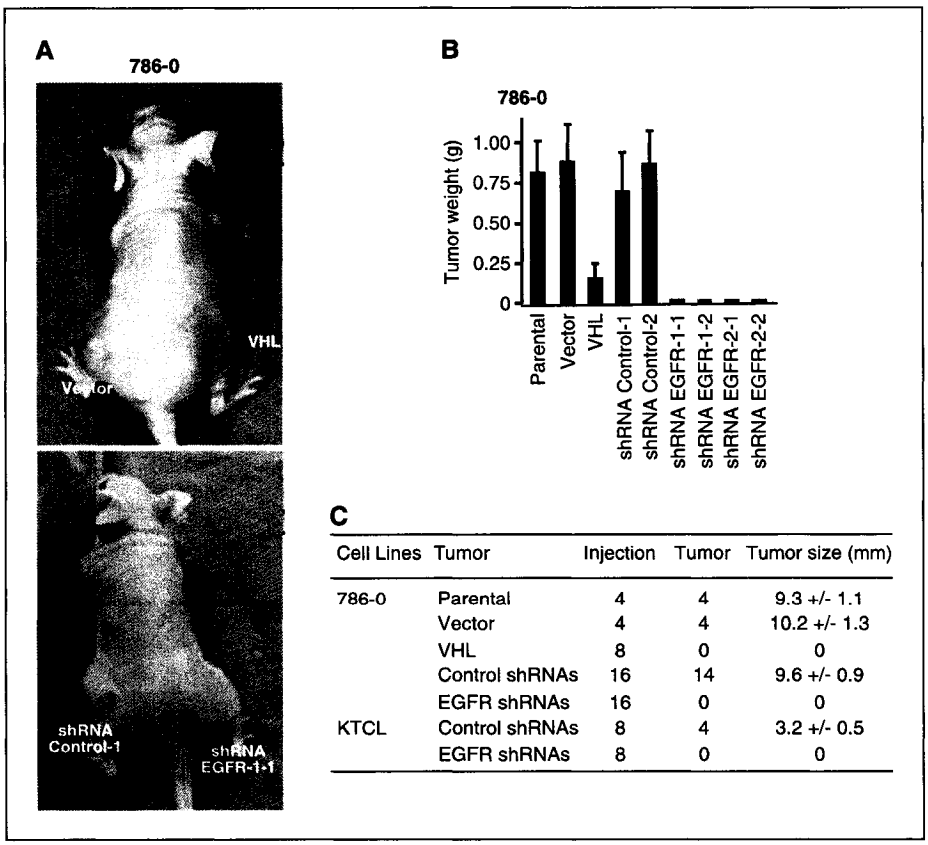

C

Cell Lines	Tumor	Injection	Tumor	Tumor size (mm)
786-0	Parental	4	4	9.3 +/- 1.1
	Vector	4	4	10.2 +/- 1.3
	VHL	8	0	0
	Control shRNAs	16	14	9.6 +/- 0.9
	EGFR shRNAs	16	0	0
KTCL	Control shRNAs	8	4	3.2 +/- 0.5
	EGFR shRNAs	8	0	0

Figure 6. Silencing of EGFR suppresses $VHL^{-/-}$ RCC tumor formation. *A*, representative nude mice injected with $VHL^{-/-}$ RCC 786-0 cells expressing vector alone, reintroduced VHL (*VHL*), control shRNA and shRNA-1 directed against EGFR. *B*, average of tumor mass 9 weeks post-injection of at least four injections per cell line. In all cases, we failed to detect a tumor even after 15 weeks following injection of shRNA to EGFR-expressing $VHL^{-/-}$ RCC cells; thus, no statistical analysis is shown. Small tumors were detected after ~12 weeks in the cases of 786-0 cells expressing reintroduced VHL. Notice that the tumor mass is lower in the KTCL140 cells compared with 786-0. *Columns*, average mean of tumor weight; *bars*, SE. *C*, cell line used in this study, number of injections, number of tumors observed after 9 weeks of incubation, and average size of tumors (±SE) when detectable. Experiments were blinded.

Hanahan and Weinberg proposed that the malignant phenotype is the manifestation of six essential alterations in cell physiology called hallmarks of cancer (26). Oncogenic dysregulation or environmental activation of HIF-2α may play a central role in at least two of these hallmarks. First, HIF-2α activation provides an environment of continued production of endogenous growth factor (TGF-α) and permanent EGFR signaling reducing the dependence of cancer cells on exogenous growth factors to maintain proliferation. Therefore, HIF-2α-expressing cells acquire the ability to engage in permanent EGFR signaling, which provides the necessary cellular milieu for growth autonomy. Whereas these data were obtained from renal cancer cells, we suggest that HIF-2α activation and subsequent EGFR signaling may have a broad implication in human malignancies. HIF-2α is induced in the vast majority of human cancer as a consequence of altered microenvironment conditions (e.g., hypoxia and acidosis) found in the core of tumors (34, 42). TGF-α overexpression and oncogenic dysregulation of EGFR activity are common features of human malignancies and are thought to provide permanent self-sufficiency in growth signaling that drives growth autonomy of cancer cells. Whereas still unproven, TGF-α/EGFR activation found in many tumors may be rationalized by HIF-2α activation and may explain why the hypoxic core of tumors is associated with increased probability of metastasis and poor prognosis. This hypothesis is supported by data shown in this report, which suggest that HIF-2α activation drives TGF-α production and EGFR activation in human cancer cell lines from different tissue origins. Second, although the data presented here focuses on the oncogenic potential of HIF-2α, its role in tumor angiogenesis has been previously well documented. HIF-2α, in cooperation with HIF-1α, activates genes such as *VEGF* and *TGF-β* to sustain proper tumor vascularization required for growth and metastasis, another hallmark of tumorigenesis.

Lastly, the data shown here supports the hypothesis that HIF-2α acts as an oncogene in VHL loss RCC by promoting EGFR signaling. VHL loss is associated with several cancer-like defects and HIF-2α activates an array of genes in RCC, some of which have generated interest as potential therapeutic targets to treat patients afflicted with RCC (43–45). The results shown here argue that the EGFR should remain a prime and bona fide therapeutic target for nonsurgical treatment of VHL-defective RCC. Consistent with our data, preclinical trials testing the effect of EGFR inhibitors in RCC have yielded encouraging results (46, 47). Whereas there have not been any large-scale randomized trials monitoring the effect of multiple EGFR inhibitors specifically targeting VHL loss RCC, a recent phase II trial of Gefitinib (Iressa) in stage IV or recurrent renal carcinoma did not alter outcome in those patients (48). One obvious explanation is that blocking EGFR phosphorylation is insufficient to prevent tumor growth of advance primary or metastasic RCC, which tumor cells may use alternative growth stimulatory pathways. Another possibility is that HIF-2α-mediated activation of the EGFR confers altered biochemical properties to receptor rendering it refractory to the inhibitory effect of these small molecules. Nonetheless, given that all cell lines used in this study were derived from patients with RCC, our findings support the search for effective therapies that target the EGFR pathway in RCC.

Acknowledgments

Received 1/18/2005; revised 3/29/2005; accepted 4/6/2005.

Grant support: Cancer Research Society of Canada (S. Lee), Canadian Institute of Health Research (S. Lee), National Cancer Institute of Canada Harold. E. Johns award (S. Lee), Natural Science and Engineering Research Council of Canada studentships (M. Morley, A. Franovic, and K. Mekhail), and Ontario Graduate Scholarship program (K. Smith).

The costs of publication of this article were defrayed in part by the payment of page charges. This article must therefore be hereby marked *advertisement* in accordance with 18 U.S.C. Section 1734 solely to indicate this fact.

We thank Christine Lavigne and Erika Sanger for their expert technical help.

References

1. Kaelin WG. Molecular basis of the VHL hereditary cancer syndrome. Nat Rev Cancer 2002;2:673–82.
2. Gnarra JR, Tory K, Weng Y, et al. Mutations of the VHL tumour suppressor gene in renal carcinoma. Nat Genet 1994;7:85–90.
3. Bukowski RM, Novick AC. Renal cell carcinoma: molecular biology, immunology, and clinical management. 1st ed. New Jersey: Humana Press Inc.; 2000.
4. Iliopoulos O, Kibel A, Gray S, Kaelin WG Jr. Tumour suppression by the human von Hippel-Lindau gene product. Nat Med 1995;1:822–6.
5. Clifford SC, Astuti D, Hooper L, Maxwell PH, Ratcliffe PJ, Maher ER. The pVHL-associated SCF ubiquitin ligase complex: molecular genetic analysis of elongin B and C, Rbx1 and HIF-1α in renal cell carcinoma. Oncogene 2001;20:5067–74.
6. Iwai K, Yamanaka K, Kamura T, et al. Identification of the von Hippel-Lindau tumor-suppressor protein as part of an active E3 ubiquitin ligase complex. Proc Natl Acad Sci U S A 1999;96:12436–41.
7. Kamura T, Koepp DM, Conrad MN, et al. Rbx1, a component of the VHL tumor suppressor complex and SCF ubiquitin ligase. Science 1999;284:657–61.
8. Maxwell PH, Wiesener MS, Chang GW, et al. The tumour suppressor protein VHL targets hypoxia-inducible factors for oxygen-dependent proteolysis. Nature 1999;399:271–5.
9. Ohh M, Park CW, Ivan M, et al. Ubiquitination of hypoxia-inducible factor requires direct binding to the β-domain of the von Hippel-Lindau protein. Nat Cell Biol 2000;2:423–7.
10. Pugh CW, Ratcliffe PJ. Regulation of angiogenesis by hypoxia: role of the HIF system. Nat Med 2003;9:677–84.
11. Semenza GL. HIF-1 and mechanisms of hypoxia sensing. Curr Opin Cell Biol 2001;13:167–71.
12. Epstein AC, Gleadle JM, McNeill LA, et al. C. elegans EGL-9 and mammalian homologs define a family of dioxygenases that regulate HIF by prolyl hydroxylation. Cell 2001;107:43–54.
13. Ivan M, Kondo K, Yang H, et al. HIFα targeted for VHL-mediated destruction by proline hydroxylation: implications for O_2 sensing. Science 2001;292:464–8.
14. Bruick RK, McKnight SL. A conserved family of prolyl-4-hydroxylases that modify HIF. Science 2001;294: 1337–40.
15. Jaakkola P, Mole DR, Tian YM, et al. Targeting of HIF-α to the von Hippel-Lindau ubiquitylation complex by O_2-regulated prolyl hydroxylation. Science 2001; 292:468–72.
16. Kondo K, Kim WY, Lechpammer M, Kaelin WG Jr. Inhibition of HIF2α is sufficient to suppress pVHL-defective tumor growth. PLoS Biol 2003;1:E83.
17. Ohh M, Yauch RL, Lonergan KM, et al. The von Hippel-Lindau tumor suppressor protein is required for proper assembly of an extracellular fibronectin matrix. Mol Cell 1998;1:959–68.
18. Stickle NH, Chung J, Klco JM, Hill RP, Kaelin WG Jr, Ohh M. pVHL modification by NEDD8 is required for fibronectin matrix assembly and suppression of tumor development. Mol Cell Biol 2004;24:3251–61.
19. Rathmell WK, Hickey MM, Bezman NA, Chmielecki CA, Carraway NC, Simon MC. *In vitro* and *in vivo* models analyzing von Hippel-Lindau disease-specific mutations. Cancer Res 2004;64:8595–603.
20. Mack FA, Rathmell WK, Arsham AM, Gnarra J, Keith B, Simon MC. Loss of pVHL is sufficient to cause HIF dysregulation in primary cells but does not promote tumor growth. Cancer Cell 2003;3:75–88.
21. Sowter HM, Raval R, Moore J, Ratcliffe PJ, Harris AL. Predominant role of hypoxia-inducible transcription factor (Hif)-1α versus Hif-2α in regulation of the transcriptional response to hypoxia. Cancer Res 2003; 63:6130–4.
22. Kondo K, Klco J, Nakamura E, Lechpammer M, Kaelin WG Jr. Inhibition of HIF is necessary for tumor suppression by the von Hippel-Lindau protein. Cancer Cell 2002;1:237–46.
23. Seagroves T, Johnson RS. Two HIFs may be better than one. Cancer Cell 2002;1:211–3.
24. Maranchie JK, Vasselli JR, Riss J, Bonifacino JS, Linehan WM, Klausner RD. The contribution of VHL substrate binding and HIF1-α to the phenotype of VHL loss in renal cell carcinoma. Cancer Cell 2002; 1:247–55.
25. Gunaratnam L, Morley M, Franovic A, et al. Hypoxia inducible factor activates the transforming growth factor-α/epidermal growth factor receptor growth stimulatory pathway in VHL(−/−) renal cell carcinoma cells. J Biol Chem 2003;278:44966–74.
26. Hanahan D, Weinberg RA. The hallmarks of cancer. Cell 2000;100:57–70.
27. de Paulsen N, Brychzy A, Fournier MC, et al. Role of transforming growth factor-α in von Hippel-Lindau (VHL)(−/−) clear cell renal carcinoma cell proliferation: a possible mechanism coupling VHL tumor suppressor inactivation and tumorigenesis. Proc Natl Acad Sci U S A 2001;98:1387–92.

28. Groulx I, Lee S. Oxygen-dependent ubiquitination and degradation of hypoxia-inducible factor requires nuclear-cytoplasmic trafficking of the von Hippel-Lindau tumor suppressor protein. Mol Cell Biol 2002; 22:5319–36.
29. Bonicalzi ME, Groulx I, de Paulsen N, Lee S. Role of exon 2-encoded β-domain of the von Hippel-Lindau tumor suppressor protein. J Biol Chem 2001;276:1407–16.
30. Nagy P, Arndt-Jovin DJ, Jovin TM. Small interfering RNAs suppress the expression of endogenous and GFP-fused epidermal growth factor receptor (erbB1) and induce apoptosis in erbB1-overexpressing cells. Exp Cell Res 2003;285:39–49.
31. Sutherland RM. Cell and environment interactions in tumor microregions: the multicell spheroid model. Science 1988;240:177–84.
32. Kunz-Schughart LA, Kreutz M, Knuechel R. Multicellular spheroids: a three-dimensional *in vitro* culture system to study tumour biology. Int J Exp Pathol 1998; 79:1–23.
33. Lieubeau-Teillet B, Rak J, Jothy S, Iliopoulos O, Kaelin W, Kerbel RS. von Hippel-Lindau gene-mediated growth suppression and induction of differentiation in renal cell carcinoma cells grown as multicellular tumor spheroids. Cancer Res 1998;58:4957–62.
34. Mekhail K, Gunaratnam L, Bonicalzi ME, Lee S. HIF activation by pH-dependent nucleolar sequestration of VHL. Nat Cell Biol 2004;6:642–7.
35. Pause A, Lee S, Lonergan KM, Klausner RD. The von Hippel-Lindau tumor suppressor gene is required for cell cycle exit upon serum withdrawal. Proc Natl Acad Sci U S A 1998;95:993–8.
36. Koshiji M, Kageyama Y, Pete EA, Horikawa I, Barrett JC, Huang LE. HIF-1α induces cell cycle arrest by functionally counteracting Myc. EMBO J 2004;23: 1949–56.
37. Mandriota SJ, Turner KJ, Davies DR, et al. HIF activation identifies early lesions in VHL kidneys: evidence for site-specific tumor suppressor function in the nephron. Cancer Cell 2002;1:459–68.
38. Everitt JI, Walker CL, Goldsworthy TW, Wolf DC. Altered expression of transforming growth factor-α: an early event in renal cell carcinoma development. Mol Carcinog 1997;19:213–9.
39. Gomella LG, Sargent ER, Wade TP, Anglard P, Linehan WM, Kasid A. Expression of transforming growth factor α in normal human adult kidney and enhanced expression of transforming growth factors α and β 1 in renal cell carcinoma. Cancer Res 1989;49: 6972–5.
40. Knebelmann B, Ananth S, Cohen HT, Sukhatme VP. Transforming growth factor α is a target for the von Hippel-Lindau tumor suppressor. Cancer Res 1998;58: 226–31.
41. Koochekpour S, Jeffers M, Wang PH, et al. The von Hippel-Lindau tumor suppressor gene inhibits hepatocyte growth factor/scatter factor-induced invasion and branching morphogenesis in renal carcinoma cells. Mol Cell Biol 1999;19:5902–12.
42. Talks KL, Turley H, Gatter KC, et al. The expression and distribution of the hypoxia-inducible factors HIF-1α and HIF-2α in normal human tissues, cancers, and tumor-associated macrophages. Am J Pathol 2000;157: 411–21.
43. Ratcliffe PJ, Pugh CW, Maxwell PH. Targeting tumors through the HIF system. Nat Med 2000;6: 1315–6.
44. Semenza GL. Targeting HIF-1 for cancer therapy. Nat Rev Cancer 2003;3:721–32.
45. Giaccia A, Siim BG, Johnson RS. HIF-1 as a target for drug development. Nat Rev Drug Discov 2003; 2:803–11.
46. Weber KL, Doucet M, Price JE, Baker C, Kim SJ, Fidler IJ. Blockade of epidermal growth factor receptor signaling leads to inhibition of renal cell carcinoma growth in the bone of nude mice. Cancer Res 2003;63: 2940–7.
47. Dancey JE. Epidermal growth factor receptor and epidermal growth factor receptor therapies in renal cell carcinoma: do we need a better mouse trap? J Clin Oncol 2004;22:2975–7.
48. Drucker B, Bacik J, Ginsberg M, et al. Phase II trial of ZD1839 (IRESSA) in patients with advanced renal cell carcinoma. Invest New Drugs 2003;21:341–5.